Influence of Ultrasonic Mixing on Enzyme Catalyzed Biodiesel Production from Waste Animal Fats

By

Peter Adewale

Department of Bioresource Engineering
McGill University, Montreal
April, 2015

A thesis submitted to the Office of Graduate and Postdoctoral Studies in partial fulfillment of the requirements for the degree of

Doctor of Philosophy

Copyright © Peter O. Adewale, 2015

Dedication

This thesis is dedicated to my dearest wife Mary Taiwo Adewale, for her devotion, boundless love, and support all along this journey and my beautiful daughter Grace Ayomide Adewale, who is a miraculous blessing from God few weeks to the end of this journey.

Abstract

This study investigated the influence of ultrasonic mixing on enzyme catalyzed biodiesel production from waste animal fats. Non-edible feedstocks such as animal fat wastes (AFW) have recently increased in popularity as alternatives to vegetable oils in the production of biodiesel. They are low cost, mitigate environmental damage and increase the quality of the resultant biodiesel fuel (low NO_x emissions, high cetane number and oxidative stability). But the presence of a high content in free fatty acid (FFA) in AFW has been seen as a challenge, especially when synthesized by alkaline-catalyzed transesterification.

A comprehensive investigation of the rheological, thermal and physicochemical properties of AFW (tallow, lard, choice white grease and yellow grease) were studied. The physicochemical properties of animal fat waste samples and the correlation of these properties to their thermal and rheological behaviors were elucidated. Pure lard was used to monitor the effects of impurities on the rheological and thermal properties of the animal fat waste. It was established that the presence of impurities had effects on the rheological and thermal properties of fats. Additionally, due to the high level of FFA present in the wastes, transesterification cannot be applied directly. It will be necessary to reduce the FFA level by using acid pretreatment or enzyme catalyzed transesterification

Further study was conducted to develop a non-destructive technique to determine iodine value (IV) and free fatty acids (FFA) content of four different animal fat waste and their blends using Fourier transform near-infrared spectroscopy (FT-NIR). Chemometric analysis by Partial Least Squares (PLS) regression was used to correlate spectral data with IV and FFA reference values of the samples. The effects of four spectra pre-processing (first derivative (FD), second derivative (SD), multiplicative scatter correction (MSC) and vector normalization (VN)) methods were investigated to predict the reproducibility and robustness of the PLS-NIR model developed. PLS-NIR models developed using first derivative and second derivative spectral preprocessing methods were the best for both IV and FFA content analysis.

The use of ultrasonic processing was evaluated for its ability to achieve adequate mixing while providing sufficient activation energy for the enzymatic transesterification of waste tallow, lard, and choice white grease (CWG). The investigation was carried out to study the effects of ultrasonic parameters (amplitude, cycle and pulse) and major reaction factors (molar ratio and enzyme concentration) on the reaction kinetics of biodiesel production by immobilized lipase [*Candida antarctica* Lipase B (CALB)]. A Ping Pong Bi Bi kinetic model approach was employed to study the effect of ultrasonic amplitude on the enzymatic transesterification. A yield of 85.6, 96.8, and 98.2 % was attained in 20 min at an ultrasonic amplitude (40%) at 5 kHz, fat:methanol molar ratio (1:4) and catalyst level 6% (w/w of fat) for tallow, lard, and CWG, respectively. The fitted curves of the kinetic mechanism showed a sigmoidal curve due to mass transfer limitations which controlled the process at the beginning of the reaction. The kinetic model results revealed interesting features of ultrasound assisted enzyme-catalyzed transesterification (as compared to conventional system): at ultrasonic amplitude 40%, the reaction activities within the system seemed to be steady after 20 min which means the reaction could proceed with or without ultrasonic mixing.

The results of this study give a better understanding of the reaction rates with respect to individual reactants and system parameters which is a great advantage for design and construction of the biodiesel reactors using ultrasonic mixing.

Résumé

L’objet de cette thèse était d’étudier la production de biodiésel à partir de déchets de gras animaux (DAGx). Une enzyme fut utilisée comme catalyseur et l'influence de la combinaison des ultrasons ainsi que de la vitesse de malaxage sur la production de biodiesel a été déterminée.

Les DAGx ont gagné en popularité comme alternatives aux huiles végétales pour la production de biodiesel. Ils sont de faible coût, atténuent les dommages environnementaux et peuvent améliorer la qualité du biodiesel (faibles émissions de NOx, indice de cétane élevé et résistance à l'oxydation). Mais la présence d'une forte teneur en acides gras libres (AGLs) dans les DAGx est perçue comme un défi lors de la transestérification en milieu alcalin.

Une étude sur les propriétés rhéologiques, thermiques et physico-chimique des DAGx (suif, graisse blanche et graisse jaune) a été effectuée. Les propriétés physico-chimiques des graisses ainsi que leurs corrélations sur les propriétés thermiques et rhéologiques ont été élucidées. Du saindoux commercial a été utilisé comme standard. Il a été établi que la présence d'impuretés avait des effets néfastes sur les propriétés des graisses. En raison du niveau élevé des AGLs présent dans les DAGx, la réaction de transestérification ne peut être appliquée directement. Il est nécessaire de réduire le niveau de AGLs en appliquant un prétraitement à l’acide ou en performant une transestérification enzymatique.

Une étude plus approfondie a été menée pour développer une technique non destructive pour déterminer l'indice d'iode (II) ainsi que les AGLs contenus dans les DAGx. La spectroscopie dans le proche infrarouge à transformée de Fourier (FT-NIR) fut utilisée comme instrument de caractérisation. Les analyses chimiométriques par régression des moindres carrés partiels (PLS) ont été utilisées pour corréler les données spectrales avec les valeurs de références II et AGLs des échantillons. Les effets de quatre méthodes de prétraitement des spectres (dérivée première (DP), la dérivée seconde (DS), correction de l'atténuation multiplicative (CAM) et normalisation de vecteur (NV)) ont été étudiés afin de prédire la reproductibilité et la robustesse du modèle PLS-NIR développé. Les modèles PLS-NIR développés à l'aide de la DP et de la DS étaient les meilleurs pour l'analyse de II ainsi que des AGLs.

Les ultrasons furent utilisés afin de réaliser un mélange adéquat tout en offrant suffisamment d'énergie d'activation lors de la transestérification enzymatique des DAGx. Les effets des paramètres ultrasons (amplitude, cycle et le rythme) et les principaux facteurs de réaction (ratio molaire et concentration d'enzyme) sur la cinétique de la production de biodiesel par la lipase immobilisée [Candida antarctica Lipase B (CALB)] furent étudiés. Le modèle cinétique Ping Pong Bi Bi a été utilisé pour étudier l'effet de l'amplitude des ultrasons sur la transestérification. Un rendement de 85.6, 96.8, et 96,8% a été atteint en 20 min à une amplitude ultrasonique (40 %) à 5 kHz, rapport molaire de graisse : méthanol (1:4) ainsi qu'un niveau de catalyseur de 6 % (poids/poids de graisse) pour le suif, de saindoux et graisse blanche, respectivement. Une courbe sigmoïdale a été obtenue en raison des limites du transfert de masse qui contrôlait le processus au début de la réaction. Les résultats du modèle ont révélés des caractéristiques intéressantes de la transestérification enzymatique assistée par les ultrasons: à une amplitude d'ultrasons de 40 %, les activités de la réaction au sein du système semblent être stable après 20 min, ce qui signifie que la réaction pourrait aller de l'avant avec ou sans ultrasons.

Les résultats de cette étude donnent une meilleure compréhension des vitesses de réaction en rapport aux différents réactants et paramètres du système. Ceci est un avantage pour la conception et la construction des réacteurs combinant des ultrasons au système de malaxage pour la production de biodiesel.

Acknowledgement

To God Almighty be all praise, honor and glory for giving me the ability and strength to start and finish this Ph.D. research. My profound gratitude goes to my primary thesis supervisor, Prof. Michael O. Ngadi, for giving me the opportunity to undertake this project under his tutelage, and for the dedication, encouragement, and financial support during my stay at McGill. Constructive criticisms, untiring devotion to work and push for excellence were the indelible impressions he left on me. Very special thanks to my thesis co-supervisor (Messiah of this thesis), Dr. Marie-Josée Dumont for her expertise, guidance and constructive critiques on this work and manuscripts, financial support, and for providing me unlimited access to her laboratory.

I gratefully acknowledged members of my Ph.D. committee; Dr. Benjamin Simpson (Food Science and Agricultural Chemistry, McGill), Dr. Grant Clark (Bioresource Engineering, McGill), and Dr. Jeff Bergthorson (Mechanical Engineering, McGill), for their constructive critiques and suggestions for the improvement of my thesis proposal.

My fellow graduate students; Jamshid Rahimi, Ogan Mba, Hernan rey sanchez Solano, Adeyemi Adegbenjo, Ebenezer Kwofie, Patrick Cortbaoui, Chijioke Ejebe, Audrey Yank, Chijioke Nwankpa, Wathsala Tennakoon, and Nnedimma Nnebe, are appreciatively acknowledged for their helpful comments on my research and for their encouragement and consolation during difficult times. Also worth mentioning and appreciated is the technical supports and suggestions of; Dr. Kebba Sabally.

Rothsay Biodiesel, Canada is thankfully acknowledged for the provision of animal fat waste samples for this work.

I am very thankful to Mr. Luciano Germani of IT Customer Services (ICS), Macdonald Campus of McGill University, for his encouragement, moral support and consolation during difficult times and when things were going tough in this journey. Exceptional handling and wonderful administrative support from the Bioresource Engineering Department non-academic staff; Ms. Susan Gregus, Ms. Patricia Singleton, and Ms. Abida Subhan are equally indebted to.

I remain eternally indebted to my mom, siblings, and friends for their unconditional love, support, and encouragement, most especially during the dark moments. To all those who in one way or another helped make this dream come true, I pray you accept this general appreciation.

TABLE OF CONTENTS

CHAPTER 4: DETERMINATION OF THE IODINE VALUE AND THE FREE FATTY ACID CONTENT OF WASTE ANIMAL FAT BLENDS USING FT-NIR

Contributions of authors

The following are the manuscripts prepared from this thesis for publication.

I. Adewale, P., Dumont, M.-J., and Ngadi, M., (2014). Rheological, thermal, and physicochemical characterization of animal fat wastes for use in biodiesel production. Energy Technology, 2, 634-642; dx.doi.org/10.1002/ente.201402001.

II. Adewale, P., Mba, O., Dumont, M.-J., Ngadi, M., and Cocciardi, R., (2014). Determination of the iodine value and the free fatty acid contents of waste animal fat blends using FT-NIR. Vibrational Spectroscopy, 72, 72-78; dx.doi.org/10.1016/j.vibspec.2014.02.016

III. Adewale, P., Dumont, M.-J., and Ngadi, M., 2015. Recent Trends of Biodiesel Production from Animal Fat Wastes and Associated Production Techniques. Renewable and Sustainable Energy Reviews, 45, 574-588; doi:10.1016/j.rser.2015.02.039

IV. Adewale, P., Dumont, M.-J., and Ngadi, M., 2015. Enzyme-catalyzed synthesis of biodiesel from waste tallow assisted by ultrasonication. Ultrasonic Sonochemistry Journal, 27, 1-9; doi:10.1016/j.ultsonch.2015.04.032.

V. Adewale, P., Dumont, M.-J., and Ngadi, M. Enzyme-catalyzed synthesis and kinetics of ultrasonic-assisted biodiesel production from waste lard. Revised paper submitted to Chemical Engineering Journal for publication.

VI. Adewale, P., Dumont, M.-J., and Ngadi, M., Enzyme-catalyzed synthesis and kinetics of ultrasonic-assisted biodiesel production from waste choice white grease. Revised paper submitted to Energy and Fuel Journal for publication.

The following are the roles and contributions made by different authors involved in this research: The research work reported here was performed and completed by Peter Olusola Adewale. He was a PhD candidate responsible for the experimental setup, design of experiment, analytical work in the laboratory, data analysis, modeling, and manuscript preparing and revision for scientific publications and the thesis thereof. Professor Michael O. Ngadi is the primary thesis supervisor, providing scientific advice and technical supervision during the entire program. He was directly involved with editing, correcting, and reviewing the manuscripts.

Dr. Marie-Josée Dumont is the thesis co-supervisor, providing scientific advice and technical supervision during the entire program. She was passionately involved with editing, correcting, and reviewing the manuscripts.

Dr. Robert Cocciardi is a Regional Sales Manager, Montreal, Canada Area, Bruker Cooperation, who has provided us with multipurpose analyzer (MPA FT-NIR) machine and technical suggestions on the analysis of spectral data.

Mr Ogan Mba is a PhD candidate in Bioresource Engineering Department, McGill University, Canada and he collaborated technically on the use of MPA FT-NIR and helped in experimental and data analysis.

List of tables

List of figures

Nomenclature

ACS	American chemical society
AFW	animal fat wastes
ANOVA	analysis of variance
AOAC	the association of analytical communities
AOCS	American oil chemists’ society
ASTM	American standard of testing material
ATT	assisted transesterification techniques
B100	100% biodiesel
Bd	biodiesel
BG	brown grease
C_2H_5ONa	sodium ethoxide
CALB	*Candida Antarctica* lipase B
CF	chicken fat
CFPP	cold filter plugging point
CH_3CH_2OH	ethanol
CH_3OH	methanol
CLEA	cross linked enzyme aggregate
CO	carbon monoxide
CO_2	carbon dioxide
CWG	choice white grease
DAG	diacylglyceride

DG	diglyceride
DSC	differential scanning calorimeter
E	enzyme
E′	intermediate enzyme
E′Bd	intermediate enzyme and biodiesel complex
EG	enzyme and glycerol complex
E′M	intermediate enzyme and methanol complex
ETG	enzyme triglyceride complex
FA	fatty acid
FAEE	fatty acid ethyl ester
FAME	fatty acid methyl ester
FD	first derivative
FFA	free fatty acid
FO	fish oil
FT-IR	Fourier transform infrared
FT-MIR	Fourier transform mid infrared
FT-NIR	Fourier transform near infrared
G	glycerol
G″	loss modulus
G′	storage modulus
GC	gas chromatography
GC-FID	gas chromatography flame ionized detector
H_2SO_4	sulphuric acid

HPLC	high performance (or pressure) liquid chromatography
HSD	honest significant difference
IS	internal standard
IV	iodine value
JMP	graphical user interface statistical software
$K_1 – K_6$	reaction kinetic constants
KI	potassium iodide
KOH	potassium hydroxide
M	methanol
MA	microwave assisted
MAG	monoacylglyceride
ME	methyl ester
MG	monoglyceride
MgO	magnesium oxide
MPA	multipurpose analyzer
MSC	multiple scattering correction
N	normality
NaOH	sodium hydroxide
NDsolve	ordinary differential equations solver
NO_x	nitrogen oxides
OD	optical density
OLF	organic liquid fraction
P_c	critical pressure

PCA	principal components analysis
PL	pure lard
PLS	partial least square
PLS-NIR	partial least square near infrared
PROC ANOVA	procedure of analysis of variance
PROC BOXPLOT	procedure of box-and-whisker plots
PROC GLM	procedure of general linear model
PROC GPLOT	procedure of graphical plot
PV	peroxide value
QUANT2	Bruker optic’s opus software program
R^2	coefficient of determination
RI	refractive index
RMSEE	root mean square error of estimation
RMSEP	root mean square error of prediction
RP	reverse phase
RPD	residual prediction deviation
RRT	relative retention time
RT	retention time
SAS	statistical analysis software
SCF	super critical fluid
SD	second derivative
SEP	standard error of prediction
SFA	saturated fatty acid

SO_2	sulphur IV oxide
TAG	triacylglyceride
T_c	critical temperature
TG	triglyceride
T_{onset}	onset temperature
T_{peak}	peak temperature
UA	ultrasonic assisted
UFA	unsaturated fatty acid
VN	vector normalization
WCO	waste cooking oil
WFO	waste frying oil
WIJS	iodine solution
YG	yellow grease
ΔH	enthalpy
ΔH_f	enthalpy of formation

THESIS FORMAT

This thesis is submitted in the format of papers suitable for journal publication. This thesis format has been approved by the Faculty of Graduate and Postdoctoral Studies, McGill University, and follows the conditions outlined in the Guidelines: Concerning Thesis Preparation, which are as follows:

“As an alternative to the traditional thesis format, the dissertation can consist of a collection of papers of which the student is an author or co-author. These papers must have a cohesive, unitary character making them a report of a single program of research”. The structure for the manuscript based thesis must conform to the following:

1. Candidates have the option of including, as part of the thesis, the text of one or more papers submitted, or to be submitted, for publication, or the clearly duplicated text (not the reprints) of one or more published papers. These texts must conform to the "Guidelines for Thesis Preparation" with respect to font size, line spacing and margin sizes and must be bound together as an integral part of the thesis. (Reprints of published papers can be included in the appendices at the end of the thesis).

2. The thesis must be more than a collection of manuscripts. All components must be integrated into a cohesive unit with a logical progression from one chapter to the next. In order to ensure that the thesis has continuity, connecting texts that provide logical bridges between the different papers are mandatory.

3. The thesis must conform to all other requirements of the "Guidelines for Thesis Preparation" in addition to the manuscripts. The thesis must include the following:

(a) A table of contents;

(b) An abstract in English and French;

(c) An introduction which clearly states the rational and objectives of the research;

(d) A comprehensive review of the literature (in addition to that covered in the introduction to each paper);

(e) A final conclusion and summary;

4. As manuscripts for publication are frequently very concise documents, where appropriate, additional material must be provided (e.g., in appendices) in sufficient detail to allow a clear and precise judgment to be made of the importance and originality of the research reported in the thesis.

5. In general, when co-authored papers are included in a thesis the candidate must have made a substantial contribution to all papers included in the thesis. In addition, the candidate is required to make an explicit statement in the thesis as to who contributed to such work and to what extent. This statement should appear in a single section entitled "Contributions of Authors" as a preface to the thesis. The supervisor must attest to the accuracy of this statement at the doctoral oral defense. Since the task of the examiners is made more difficult in these cases, it is in the candidate's interest to clearly specify the responsibilities of all the authors of the co-authored papers”.

Thesis organization

Chapter 1: Introduction to the project, including a scope and research objectives

Chapter 2: Literature review on recent trends of biodiesel production from animal fat waste and associated production techniques

Chapter 3: A comprehensive investigation of rheological, thermal, and physicochemical characterization of animal fat waste for use in biodiesel production

Chapter 4: Development of a non-destructive technique to determine the iodine value and the free fatty acid content of waste animal fat blends by FT-NIR

Chapter 5: Enzyme-catalyzed synthesis and reaction kinetic modeling of biodiesel production from waste tallow assisted by ultrasonication

Chapter 6: Enzyme-catalyzed synthesis and reaction kinetic modeling of biodiesel production from waste lard assisted by ultrasonication

Chapter 7: Enzyme-catalyzed synthesis and reaction kinetic modeling of biodiesel production from waste choice white grease assisted by ultrasonication

Chapter 8: General summary and conclusions

Chapter 9: Contributions to knowledge and future research

Chapter 10: Bibliography

CHAPTER 1 GENERAL INTRODUCTION

1.1 Background

Biodiesel production and use have enticed many countries to invest in the technologies and equipment involved in its production. The European Biodiesel Board (2011) reported that the European Union produced over 24.7×10^9 L yr^{-1} in 2011, while the US produced 4.16×10^9 L yr^{-1} of biodiesel in 2011(Nurfitri et al., 2013). Due to new production capacities, projected Canadian biodiesel production for 2013 (0.471×10^9 L yr^{-1}) was more than twice the estimates for 2012 (0.210×10^9 L yr^{-1}). A forecasted rise to biodiesel production of 0.65×10^9 L in 2014 was partly attributed to the expected completion of a plant producing 2.65×10^8 L yr^{-1} (Evans and Gray, 2013). The major biodiesel feedstock in Europe, United States, and Canada is rapeseed (*Brassica napus L.*), soybean (*Glyine max* (L.) Merr.), and canola (low erucic acid varieties of *Brassica napus L.*) oil, respectively. There has been a strong drive for the use of rendered animal fat waste (AFW), rendered oils, as well as palm (*Elaeis guineensis* Jacq.) oil in order to increase biodiesel production and meet biodiesel demand in some countries such as the United States, Europe, China, Malaysia and Canada (Evans and Gray, 2013). Therefore, AFW could drastically lower the cost of biodiesel production and make biodiesel competitive with petro-diesel. Biodiesel from AFW feedstocks such as tallow, lard, yellow grease (YG), and choice white grease (CWG) has high cetane number, an important quality parameter for diesel fuels (Bamgboye and Hansen, 2008; Ramírez-Verduzco et al., 2012; Tong et al., 2011). The AFW comprise of a high ratio of saturated fatty acids (Canakci and Van Gerpen, 2001; 2003), which are the reason behind high cetane number (>60) as compared to most vegetable oils. Similarly, the saturated fatty acids in AFW contribute to better oxidative stability for biodiesel (Knothe, 2007; Wyatt et al., 2005). But the presence of a high content in free fatty acid (FFA) in AFW has been seen as a challenge, especially when synthesized by alkaline-catalyzed transesterification.

In terms of chemical composition, biodiesel is a mixture of fatty acid alkyl esters, produced from reacting triglyceride with an alcohol usually methanol by catalyzed (alkali, acid or enzyme) transesterification. The reaction is affected by a number of factors such as: the type of alcohol used in the reaction, the molar ratio of alcohol to vegetable oil or animal fats, the type and concentration of catalyst, the moisture and the agitation intensity (Stamenković et al., 2007). The chemical composition and rheological properties of biodiesel depends on the type of feedstock used for its production (Knothe, 2005). Therefore, knowing the rheological properties of the starting materials used for the production of biodiesel will provide information on their response to shear stress and strain rate, a typical phenomenon in mixing. Ross et al. (2006) examined the effects of mixing on the rheological properties of an agar gel and found that mixing resulted in stronger gels. They reported that mixing affected the degree of porosity induced in the system by incorporation of air bubbles, but these bubbles did not weaken the gel macrostructure. Thermal and physicochemical properties phenomena in oils and fats are essential in order to understand their thermal related processing and can be used to clarify their physical and chemical properties (Abdul Azis et al., 2011; Anand et al., 2011). Many studies have been conducted to investigate the thermal profile of various edible oils and fats. For example, Tan and Che Man (2000, 2002) studied thermal properties of edible oils, palm oil, palm oil based products and coconut oil: comparison of thermal properties and chemical composition and effects of scanning rate variation, Graboski and McCormick (1998) showed wide variations in the measured properties of the same biodiesel fuel, because of changes in its fatty acid composition, and Anand et al. (2011) also reported a comprehensive study on thermo-physical properties of biodiesel fuels. Despite the extensive studies on the effects of rheological properties of different materials on their mixing phenomena in the literature, limited reports are available on the effects of rheological behavior of AFW on their mixing.

Biodiesel production techniques which lead to production efficiency are very important to be considered in the development of a biodiesel plant. Two major production techniques currently exist to synthesize biodiesel from animal fats or vegetable oils: chemical synthesis and biological synthesis. Well recognized and widely used in the industrial scale production of biodiesel, chemical-based production techniques have limitations: high pollution emission, a complex downstream purification process, and high equipment, energy, and alcohol requirements. Enzyme-based production techniques are suitable for overcoming the limitations of chemical-based production techniques (Gog et al., 2012; Kumar et al., 2011a; Kumari et al., 2009; Lam et al., 2010; Nielsen et al., 2008) and have the advantages of overcoming the specific limitations of base or acid transesterification technology (e.g. need for feedstock extremely low in FFA content and moisture) through an enzyme-catalyzed transesterification process. Compared to chemical-based catalysis, biodiesel production by enzymatic catalysis limits the risk of soap formation and the need to use a high molar ratio of alcohol to animal fat in the process (Rodrigues and Fernandez-Lafuente, 2010). High cost and easy inactivation of lipases by methanol are the main shortcomings of enzyme-catalyzed technology; however, enzyme immobilization techniques have generated more alcohol-tolerant lipases, thus providing a cost-efficient and reusable enzyme (Luković et al., 2011).

Some of the new and emerging techniques involve the use of treatments to reduce reactor operation time while achieving the highest yield possible. Ultrasound-assisted (UA) and microwave-assisted (MA) transesterification are examples of the emerging techniques for the production of biodiesel.

UA technique is of interest to many researchers due to its shorter reaction times, cheap reagents and the non-complexity of the process reactors. Similarly, application of MA technique has gained positive attention due to its rapid reaction rates, the high purity of products, the improved yields, and the greater energy efficiency. Hsiao et al. (2010) studied ultrasonic mixing and closed microwave irradiation-assisted transesterification of soybean oil. Veljković et al. (2012) studied biodiesel production by ultrasonic-assisted transesterification: State of the art and the perspectives on different edible oils by acid, alkali and enzyme catalyzed methods. They reported that low frequency ultrasound has shown to be a valuable tool in biodiesel synthesis, regarding to short reaction time. Jadhav and Gogate (2014a, 2014b) examined the feasibility of ultrasound assisted enzymatic conversion of non-edible oil to methyl esters and intensification in the activity of lipase enzyme using ultrasonic power. The authors concluded that ultrasound assisted process showed considerable reduction in reaction time for getting the same amount of yield as compared to the conventional method. Due to the complexity of AFW physical properties and intricacy of possible flow patterns within a stirred vessel because of their compositions, AFW will require a productive ways to mix them in order to enhance biodiesel production.

Another important aspect of this study is the investigation of the effects of ultrasound assisted mixing on the reaction kinetics of enzyme-catalyzed transesterification of waste animal fats for the production of biodiesel. Darnoko and Cheryan (2000); Kumar et al. (2011e); Noureddini and Zhu (1997); Poljanšek and Likozar (2011); Stamenković et al. (2008) reported that transesterification reaction compose of three step-wise series of reversible decompositions in which triglyceride (TG) reacts with alcohol to produce diglycerides (DG), diglyceride yields monoglycerides (MG) and finally monoglyceride with methanol (M) to produce biodiesel (Bd) and glycerol (G) as shown in equations (1.1 – 1.3).

$$\mathbf{TG + M \overset{E}{\leftrightarrow} DG + Bd} \qquad \mathbf{1.1}$$

$$\mathbf{DG + M \overset{E}{\leftrightarrow} MG + Bd} \qquad \mathbf{1.2}$$

$$\mathbf{MG + M \overset{E}{\leftrightarrow} Bd + G} \qquad \mathbf{1.3}$$

The study of the reaction kinetics of biodiesel production from waste animal fats provides parameters that can be used to predict the extent of the reaction at any time under particular conditions. Despite the extensive literature on reaction kinetics of biodiesel production from edible oils such as soybean (Izida et al., 2015), palmitic acid (Raita et al., 2015) and sunflower (Stamenković et al., 2008), there is limited information in the literature on the reaction kinetics of ultrasound assisted enzyme-catalyzed transesterification of waste animal fats for the production of biodiesel.

1.2 Hypothesis

Based on the foregoing discussions, it was hypothesized that the use of ultrasonic waves as a mixing technique for enzyme-catalyzed transesterification of AWFs would have significant effect on the reaction time, reaction kinetics, and yield of biodiesel.

1.3 Overall objective

The overall objective of this research is to investigate the impact of ultrasonic mixing processes on the enhancement of biodiesel production from waste animal fats.

1.4 Specific objectives

The following specific objectives are drawn in order to dig deep into the overall objective of this study:

1. To evaluate the physicochemical and thermal properties of waste animal fats destined for the production of biodiesel

2. To develop a non-destructive method to determine the physicochemical properties of waste animal fats destined for the production of biodiesel

3. To determine parametric effects of ultrasonic mixing on the yield of biodiesel produced from animal fat waste

4. To model the reaction kinetics of ultrasonic mixing processes on transesterification of animal fat waste for the production of biodiesel

CHAPTER 2 LITERATURE REVIEW

Biodiesel can be made from different varieties of feedstocks, but price and availability are important factors in determining the optimal feedstock and result in feedstock differences from one region of the world to another (Badday et al., 2013; Balat, 2011; Kumar et al., 2011a; Ramadhas et al., 2005; Sanli et al., 2013). Despite the current growth, sustainability of the biodiesel industries may be limited due to the industry's inability to secure cheap feedstock (Evans and Gray, 2013). Most of the current and forecasted biodiesel production in Canada comes from canola (Figure 2.1). Similarly, other biodiesel producing countries (US and Europe) depend on edible vegetable oils as feedstocks. This trend also implies the need for a large supply of vegetable oils, which if they are drawn from neat edible oil sources, may lead to food security and ethical issues. Food security issues such as diversion of food crops to biofuel production have engendered heated arguments worldwide (Birur et al., 2007; Gui et al., 2008; Hill, 2007; Pinzi et al., 2014; Srinivasan, 2009).

2.1 Non-edible Feedstocks

With an increasing world population, the rising demand for edible oils and animal fats has led to price increase on the world markets and has limited their use as fuel, particularly in developing countries (Silitonga et al., 2013). Several studies have shown greases and AFW are viable, reliable and environmental friendly feedstocks for biodiesel production (Ghazavi et al., 2013; Gürü et al., 2009; Ito et al., 2012; Mata et al., 2013). These materials are available on the order of millions of tons in most developed countries. Similarly, non-edible oil plants are naturally accessible worldwide (Atabani et al., 2013; Demirbas, 2009c). Although, there has not been any direct food *vs*. fuel competition reported, indirect competition for land between food *vs.* non-edible oil crops might become a strong controversial debate.

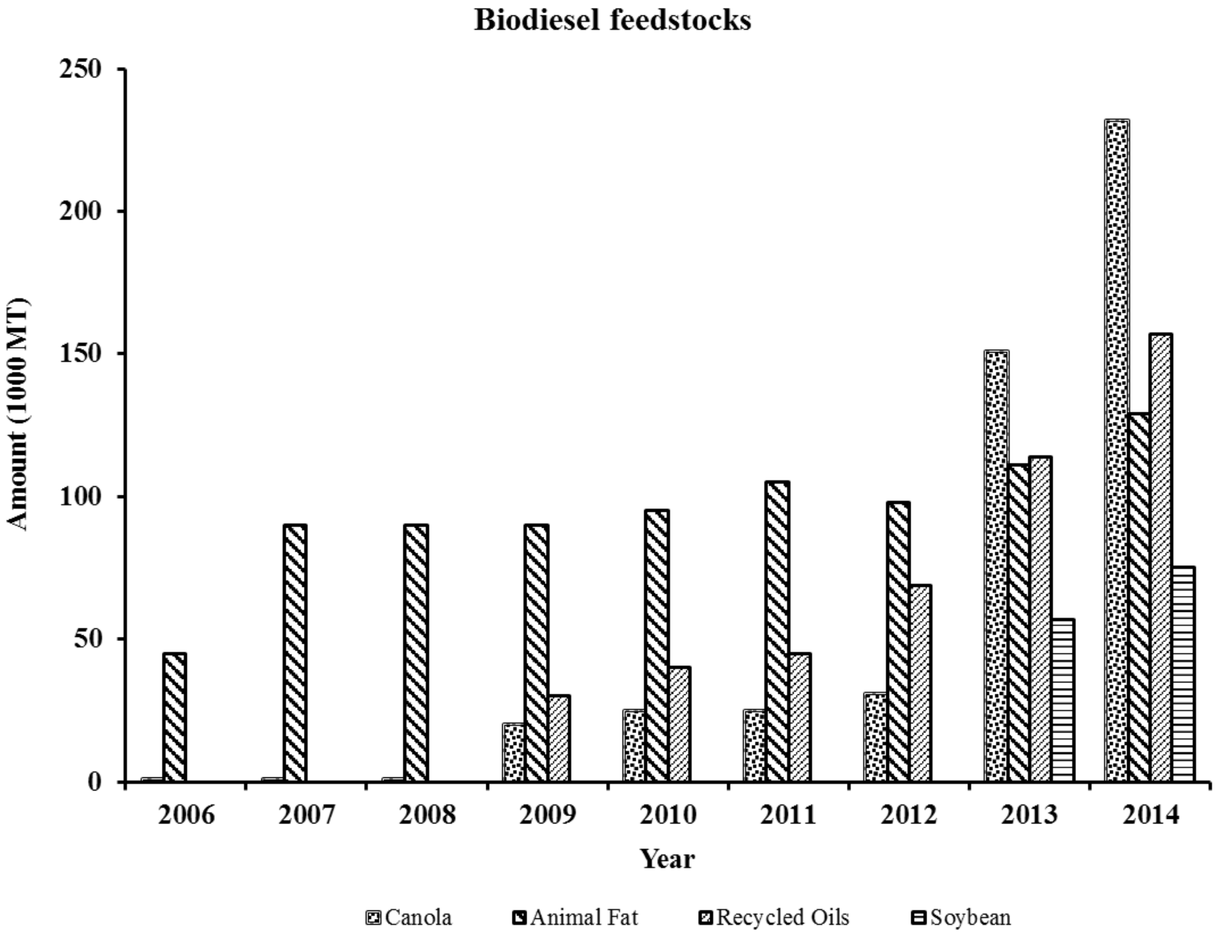

Figure 2.1: The current and forecasted biodiesel production feedstocks in Canada (Data source: Evans and Gray, 2013)

2.2 Non-edible vegetable oils

In recent years, several investigations have been conducted on the suitability of non-edible oilseed plants such as Oleaginous, Leguminosae, Brassicaceae and Euphorbiaceae to produce biodiesel (Atabani et al., 2013; Badday et al., 2013; Kumar et al., 2012; Kumar et al., 2011e; Kumari et al., 2009; Shah and Gupta, 2007; Taufiq-Yap et al., 2011; Zou and Lei, 2012). The mature seeds of these oilseed plants bear high oil content, but these oils are unsuitable for human consumption or animal feed given their high FFA content and the presence of toxic substances. As in case of edible oils, the use of non-edible oils can actually polarize direct competition in terms of food availability and safety. Some of the non-edible crops used in biodiesel production, include: physic nut (*Jatropha curcas* L.), karanja (*Pongamia pinnata* (L.) *Pierre*), rubber seed (*Hevea brasiliensis* (Willd. ex A.Juss.) Müll.Arg.), castor bean (*Ricinus communis* L.), yellow oleander (*Thevettia peruviana* (Pers.) K.Schum), tobacco (*Nicotiana tabacum* L), chinese tallow (*Sapium sebiferum* (L.) Dum.Cours.), Rice (*Oryza sativa* L.) bran, sea mango (*Cerbera odollam* Gaertn), cotton (*Gossypium hirsutum* L.), mahua (*Madhuca indica* (J.Koenig ex L.) J.F.Macbr.) and Ethiopian mustard (*Brassica carinata* A.Braun) (Pinzi et al., 2009; Pinzi et al., 2014; Ramadhas et al., 2005; Wang et al., 2011). The research performed on non-edible plant oils and their cultivations differs from region to region around the world. For example, in the USA, Canada, and the EU, research on lipid-based feedstocks focuses on oleaginous microorganisms (Bowling et al., 2014; Franklin et al., 2014; Zhang et al., 2014). The highly fertilized cultivation of non-edible oil crops on arable areas for use as biofuel feedstocks may decrease their price advantage and contribute to conflicting land usage.

2.3 Waste cooking oils

The use of waste oils as biodiesel feedstock offers no direct conflict with food availability and land usage. Waste cooking or frying oils (WFO) can be categorized into yellow grease and brown grease. Used cooking oil contains vegetable oil or animal fat that has been heated and used for cooking a wide variety of food such as meat, fish, or vegetable products and may therefore include grease rendered from hamburger, bacon or cooked meat entrees. With FFA contents of less than 15%, yellow grease, generated from used cooking oil, fats, and oils collected from restaurant or industrial cooking operations, offers a considerable potential as a low-cost raw material for biodiesel production (Canakci and Van Gerpen, 2001).

Brown grease (*i.e.* trap grease) is collected from grease traps installed in restaurant, industrial, or municipal sewage facilities to separate grease and oil from waste water. Grease traps are sealed containers installed in sewer lines in such a manner as to allow the lighter grease and oil that is flushed down a drain to float to the top of the trap. These traps allow the water to flow under the grease and through to the main sewer or water treatment area. Brown grease is high in FFA (>15%) and water content (Canakci and Van Gerpen, 2001), which negatively affects its potential conversion to biodiesel (Kulkarni and Dalai, 2006; Mandolesi de Araújo et al., 2013).

Alkaline catalyzed transesterification (Chesterfield et al., 2012; De Paola et al., 2009; Demirbas, 2009a), acid catalyzed transesterification (Canakci and Van Gerpen, 1999; Jacobson et al., 2008; Lotero et al., 2005; Zheng et al., 2006), two-step transesterification (Çaylı and Küsefoğlu, 2008; Wang et al., 2007b), enzymatic catalysis (Chen et al., 2006; Lam et al., 2010; Yagiz et al., 2007) and supercritical temperature processing (Demirbas, 2009a; Ghoreishi and Moein, 2013) are all techniques for converting waste cooking oils to biodiesel. Prolonged heating of initially virgin oil leads to waste cooking oil accumulating FFA, which interferes with the alkaline transesterification process since the alkaline catalyst acts on the FFA to produce soap (saponification reaction). The saponification reaction reduces biodiesel yield and requires a more complex downstream separation of biodiesel, glycerol, and washing water (Canakci and Van Gerpen, 2001; 2003).

2.4 Animal fats

Animal fats are primarily derived as by-products from meat animal processing facilities and by the rendering process. The main animal fats include tallow from processing cattle, lard and CWG from swine processing, and poultry fat from the processing of chicken, turkey, or other birds. The fats/oils generated by fish processing plant and leather industry fleshing wastes have also been found to be viable biodiesel feedstocks (Alptekin et al., 2012; Jayasinghe and Hawboldt, 2012; Ong et al., 2013). Some animal fat based feedstocks are already in used at the industrial scale (e.g. chicken, tallow, lard fats) for biodiesel production (Bender, 1999; Da Cunha et al., 2009; Schörken and Kempers, 2009). The use of AFW as biodiesel feedstocks offers economic, environmental, and food security advantages over the more commonly used edible vegetable oils. AFW contain high levels of saturated fatty acids and FFA (Table 2.1), requiring more complex production techniques, and this result in biodiesel with a lower physical and chemical quality; however low unsaturation of AFW's fatty acids has several advantages (e.g. high calorific value, high cetane number and high oxidation stability) (Alptekin et al., 2012; Ramírez-Verduzco et al., 2012; Tong et al., 2011).

Table 2.1: Fatty acid compositions (%) of animal fat waste

Fatty acids	Carbon number	Animal Fat Wastes						
		YG[1]	BG[2]	CWG[3]	Lard	Tallow	CF[4]	FO[5]
Reference		[a]	[b][c]	[a]	[a]	[a]	[b]	[d]
Lauric	C12:0	-	-	-	-	-	-	0.14
Myristic	C14:0	1.02	1.7	1.60	1.41	2.76	-	5.77
Palmitic	C16:0	14.83	23.8	22.39	25.69	25.95	22.20	16.94
Palmitioleic	C16:1	1.50	3.1	3.40	2.82	2.84	8.40	5.42
Stearic	C18:0	8.41	12.5	9.15	14.50	17.54	5.10	4.31
Oleic	C18:1	47.88	42.4	44.14	40.88	41.67	42.50	19.20
Linoleic	C18:2	19.11	12.1	11.90	12.93	6.91	19.30	16.05
Linolenic	C18:3	4.68	0.8	-	-	-	1.00	2.82
Arachidic	C20:0	2.56	-	7.43	0.50	0.44	-	-
Eicosenoic	C20:1	-	-	-	1.34	1.88	-	-
Eicosadienoic	C20:2	-	-	-	-	-	-	-
Eicosapentaenoic	C20:5	-	-	-	-	-	-	15.55
Docosapentaenoic	C22:5	-	-	-	-	-	-	2.45
Docosahexanoic	C22:6	-	-	-	-	-	-	11.36

[1]Yellow grease [2]Brown grease [3]Choice white grease [4]Chicken fat [5]Fish oil [a = (Adewale et al., 2014a)] [b = (Lotero et al., 2005)] [c = (Canakci and Van Gerpen, 2003)] [d = (Aryee et al., 2011)]

2.4.1. Chicken fat

Chicken fat is generated during rendering of chicken feathers and poultry by-products to produce feather meal (Figure 2.2). Poultry by-products consists of ground dry- or wet-rendered portion of the clean carcass (e.g. heads, feet, undeveloped eggs, and intestines, exclusive of feathers) (Kondamudi et al., 2009). The amount of fat extracted from the feather meal varies from 2% to 12%, depending on feather type (Dale, 1992; Moritz and Latshaw, 2001). Gürü et al. (2010) produced biodiesel from chicken fat through a two-step catalytic process, using methanol (CH_3OH), sulphuric acid (H_2SO_4) and sodium hydroxide (NaOH) catalysts. The authors studied the effects of a synthetic Mg additive to chicken fat biodiesel in a single-cylinder, direct injection diesel engine and its effects on engine performance and exhaust emissions. It was also reported that an increase in the magnesium concentration from 0 to 16 mmol/L led to a decrease in viscosity and flash point from 5.184 to 4.812°C and 129 to 122°C, respectively. More so, a dosage of 16 mmol/L Mg into the chicken fat methyl ester caused a 7 °C pour point decrease. Optimum pre-treatment and methyl ester production conditions for chicken fat investigation were reported to be 20% sulfuric acid and 40:1 methanol molar ratio based on the amount of FFA (13.45%) in the chicken fat for 80 min at 60 °C, and the methyl ester yield was 87.4% (Alptekin and Canakci, 2010, 2011).

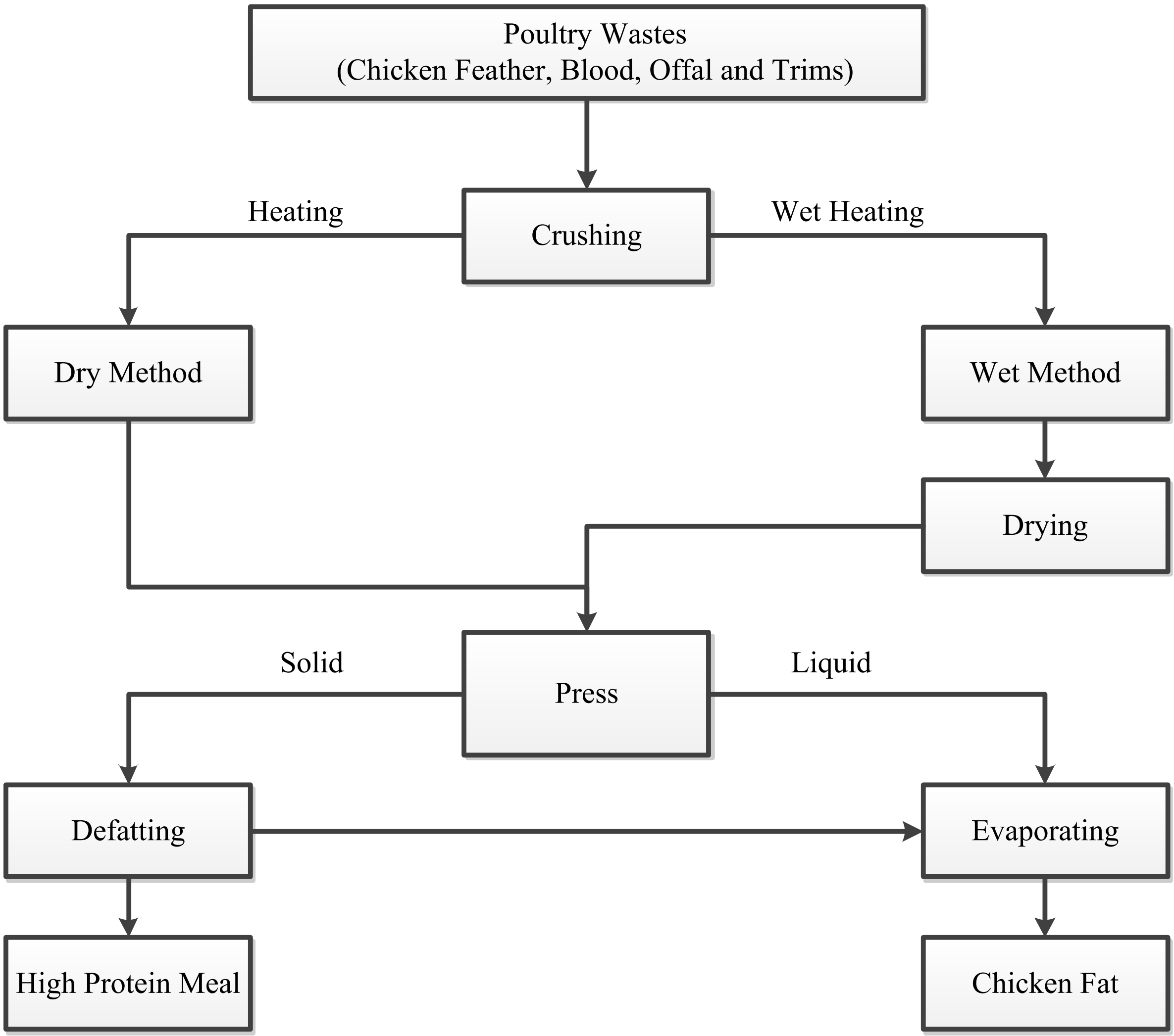

Figure 2.2: Poultry wastes rendering process

Supercritical CH_3OH transesterification method for converting chicken fat to biodiesel was investigated at various temperatures (e.g. 350, 375, and 400 °C), pressures (e.g. 100, 200, and 300 bar), molar ratios (3:1 to 12:1), and reaction times (3-10 min), in which the best triglycerides conversion and decomposition of glycerol were obtained at temperature, pressure, molar ratio, and reaction time: 400 °C, 300 bar, 9:1, and 6 min, respectively (Marulanda et al., 2009, 2010).

2.4.2 Lard

Lard is basically pig fat in its rendered form. Pig fat can be rendered by a wet or dry process. In wet rendering (Figure 2.3), pig fat is boiled in water or steamed at a high temperature and the lard, which is insoluble in water, is skimmed off the surface of the mixture, or separated in an industrial centrifuge (AOCS, 2013). In dry rendering (Figure 2.4), the fat is exposed to high heat in a pan or oven without the presence of water (AOCS, 2013). The two processes yield different products. Wet-rendered lard has a more neutral flavor, a lighter color, and a high smoke point. Dry-rendered lard is browner in color and has lower smoke point. Edible lard is commonly used in many cuisines such as cooking fat or shortening, or as a spread similar to butter.

Dias et al. (2009), studying the acid transesterification generation of biodiesel from acid waste lard pretreated with up to 14.57 mg KOH per g of FFA reported that the pre-treatment adopted effectively enable acid waste lard to serve as a single raw material for biodiesel production with acceptable quality, but a low yield (65 % by weight). Mixtures of waste frying oil and pork lard were investigated for the production of biodiesel which was reported to have biodiesel yields varied from 81.7 to 88.0 (wt%) with the lowest yields obtained by waste frying oil and lard alone as raw materials (Dias et al., 2008c). The application of biocatalyst transesterification of lard using Candida sp. 99-125 was studied by investigating the effect of temperature, water content, enzyme amount, solvent, and three-step methanolysis on the yield of biodiesel from lard and the optimal reaction conditions for processing 1 g of lard were: 0.2 g immobilized lipase, 8 ml n-hexane as solvent, 20% water based on the fat weight, temperature 40 °C, and three-step addition of methanol which yielded 87.4% fatty acid methyl esters (Lu et al., 2007).

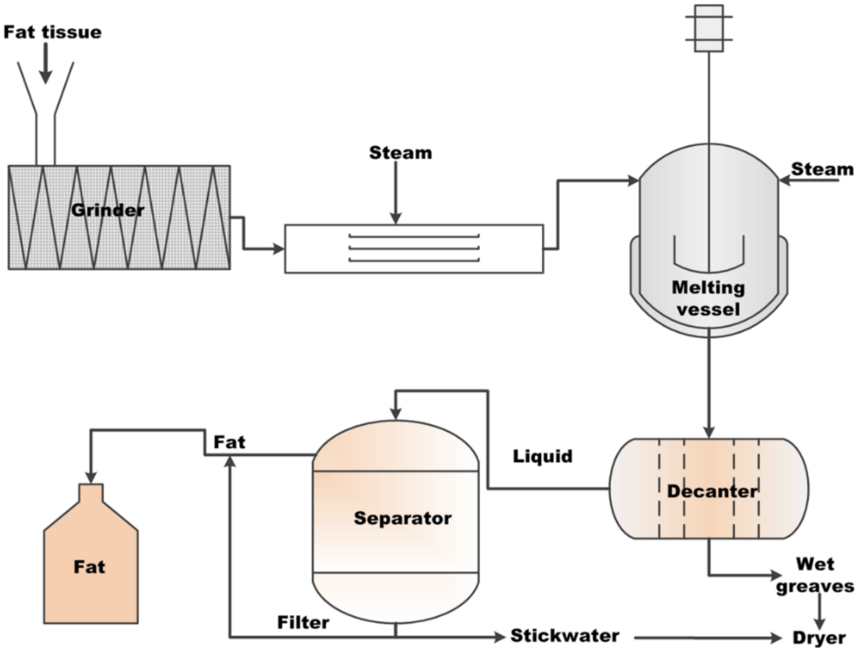

Figure 2.3: Flow diagram of wet rendering (Adapted from AOCS, 2013)

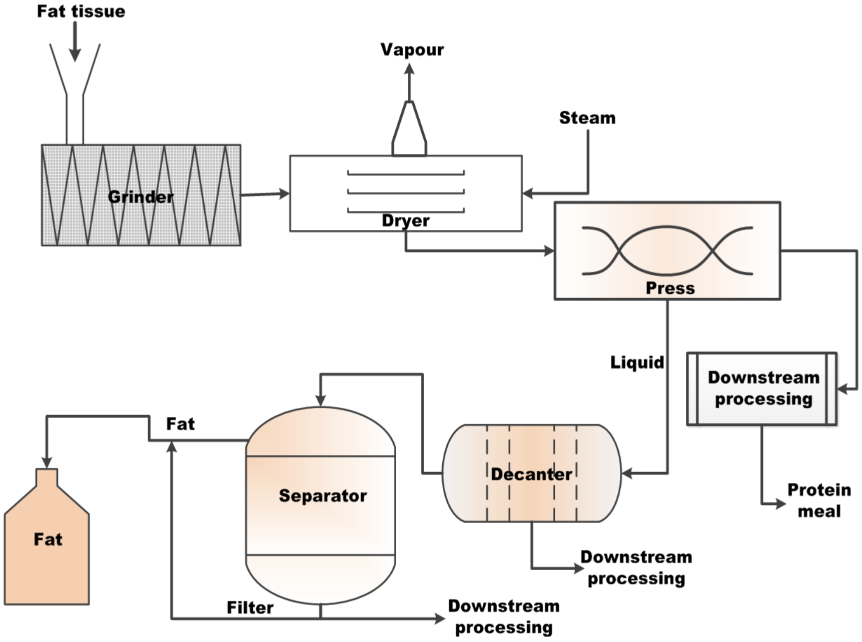

Figure 2.4: Flow diagram of dry rendering (Adapted from AOCS, 2013)

Similarly, process optimization of biodiesel production from lard was reported on the effect of agitation speed (most suitable 600 rpm) and catalyst concentration (most suitable 0.9 wt.%) by developing a regression model to predict the methyl ester concentration which adequately described the experimental parameters range (Berrios et al., 2009). Shin et al. (2012a) reported the production of biodiesel from waste lard by a supercritical temperature method in the absence of catalyst and found that biodiesel produced from waste lard under the optimal reaction conditions without pre-treatment was comparable to that produced from refined lard, even though waste lard samples contained various free fatty acid contents and water.

2.4.3 Tallow

The rendering process converts slaughter house animal by-products to a fat and protein meal (Figure 2.5). In most tallows, 50% of the total fatty acids are saturated (Adewale et al., 2014a; Da Cunha et al., 2009). Tallow has higher stearic and palmitic acid contents which leads to high melting point and viscosity (Bhatti et al., 2008; Da Cunha et al., 2009; Grompone and Moyna, 1983), causing it to be solid at room temperature (Ma and Hanna, 1999). One of the most commonly used animal fats employed as substrate for biodiesel production is derived from beef or mutton in the form of edible or non-edible tallow. The edible form is relatively expensive and has a low FFA content, making it a viable substrate for an alkaline transesterification reaction. Resource availability, energetic efficiency, and economic feasibility of converting edible and inedible beef tallow into biodiesel has previously been investigated [86]. The authors concluded that beef tallow generated from the slaughter of cattle could provide a historically cheap feedstock, which if converted to biodiesel, would offer a wide range of energy, environmental, and economic advantages. Ma et al. (1999); Ma and Hanna (1999) studied the effects of catalysts, FFA content, water content and mixing intensities on the yield of biodiesel from edible tallow and reported that no reaction occurred without mixing, but when a mixture of NaOH and CH_3OH was added to the melted beef tallow in the reactor only very limited stirring was required for the process to occur. They further found that adding NaOH and CH_3OH solution to melted beef tallow before stirring would require higher stirring speeds and longer stirring times to mix the two phases.

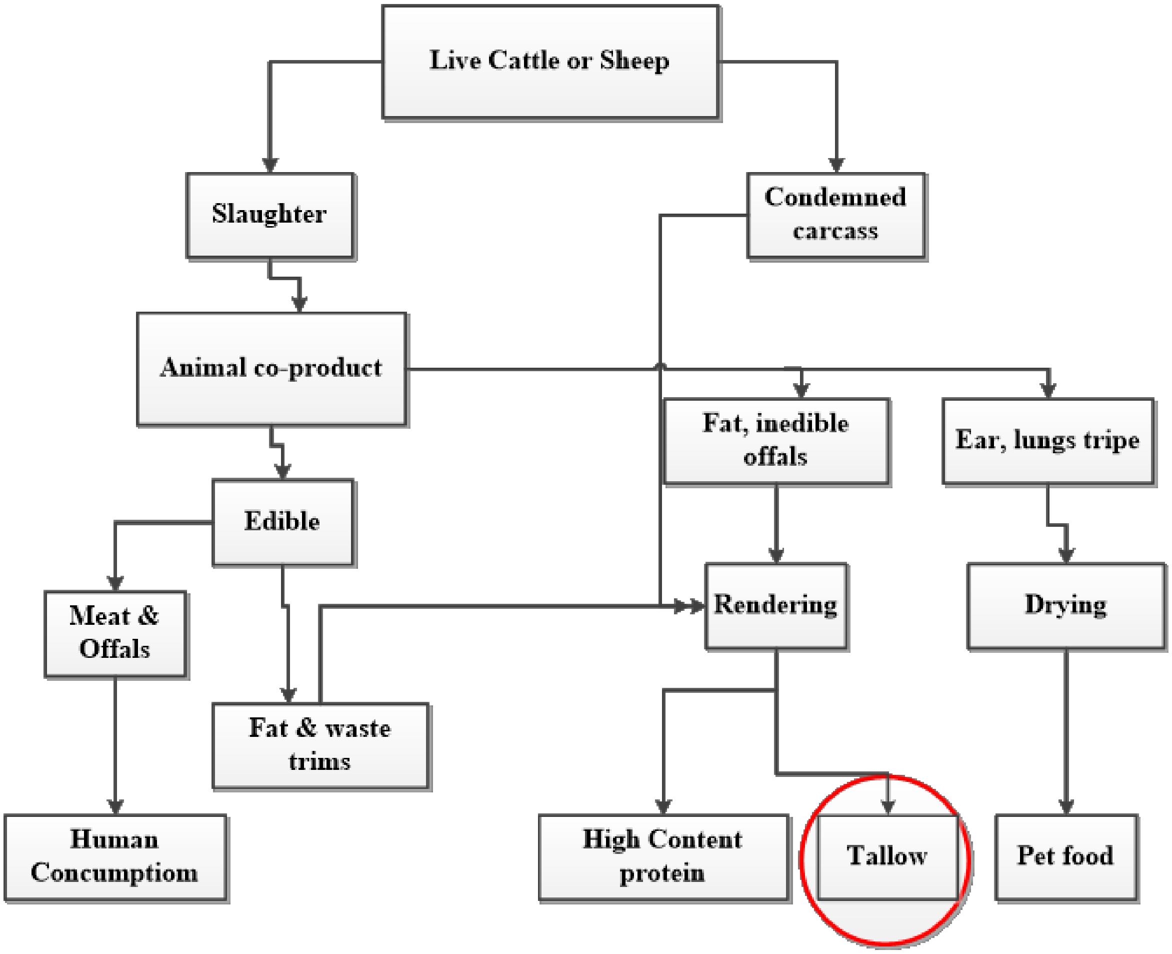

Figure 2.5: Flow chart of waste tallow production (Adapted from AOCS, 2013)

Non-edible tallow is high in FFAs content, therefore a more expensive processing method will be needed for its conversion to biodiesel. Feasibility studies of biodiesel production from low grade or inedible tallow have been reported. Bhatti et al. (2008) studied the effect of process parameters on biodiesel production from waste tallow by acid catalyzed transesterification. They reported that under optimal processing conditions (60°C, oil/ CH_3OH molar ratio of 1:30, and 2.5 g of H_2SO_4)

5 g of mutton tallow yielded a 93.21 % of biodiesel after 24 h. Öner and Altun (2009) studied injection of biodiesel synthesized from inedible animal tallow and its blends directly into diesel engines. The authors observed a decrease in the effective efficiency of the engine and an increase in the specific fuel consumption (Moraes et al., 2008) but significant reduction in emissions of carbon monoxide (CO), NO_x, sulphur dioxide (SO_2), and smoke opacity were reported to be around 15%, 38.5%, 72.7% and 56.8%, respectively, for tallow methyl esters (B100) as compared to petro-diesel. Teixeira et al. (2009) compared conventional and ultrasonic-assisted production of biodiesel from beef tallow and found that the reaction rate and biodiesel quality were similar in both cases but the use of ultrasonic power decreased the reaction time. However the authors did not account for the effects of ultrasonication parameters and optimization of these parameters. The effectiveness of enzymatic transesterification of beef tallow using experimental enzyme ns88001 with methanol and n-hexane as a solvent was reported by Kumar et al. (2013). The authors showed that using n-hexane in the reaction stabilized the enzyme and minimized toxicity of alcohol and the activity of experimental enzyme catalyst (ns88001) in the presence n-hexane was found to slightly reduce after 10 cycles of reusability. Hsu et al. (2001) investigated the effects of the presence of alcohol and the amount of enzyme used for production of alkyl esters from tallow and grease using lipase immobilized in a phyllosilicate sol-gel. The authors reported that transesterification of tallow with primary alcohols (e.g. methanol) was effective using immobilized PS-30 lipase with good conversions from 82 to 94%, while free lipase under the same reaction conditions gave lower conversions from 47 to 89% and the poorest yields were found in methyl esters.

2.4.4 Leather industry solid waste fat

In the leather industry, solid waste fat is obtained from the waste generated during the pre-fleshing, lime fleshing, shaving, buffing and trimming processes (Ozgunay et al., 2007). The fat is in solid state at room temperature and bears a high water content. It is subjected to a heating at 110°C for one hour to remove water and then filtered to remove the insoluble materials (Alptekin et al., 2012). The Turkish research group of Colak et al. (2005; 2006) were the first to investigate the use of leather industry pre-fleshing in biodiesel production. They proved that the fat generated from tanneries fleshing wastes could be utilized in the production of an environmentally friendly fuel that could work with petrodiesel engine without a need for a major adjustment. In the study of the effects of biodiesel production parameters (e.g. catalyst weight percentage, temperature and oil/alcohol molar ratio) on base-catalyzed transesterification of raw fleshing oil, İşler et al. (2010) reported optimum reaction conditions for efficient biodiesel yield to consist of molar ratio of a 1:6 oil/alcohol; a reaction temperature of 50°C; a catalyst weight percentage of 0.75% and reaction period of 15 min.

Alptekin et al. (2012) evaluated leather industry wastes as a feedstock for biodiesel production by alkaline catalyzed transesterification. The authors studied the effects of catalyst type, catalyst quantity and the alcohol molar ratio on the fuel properties of methyl esters generated. The fuel properties was reported to fit the biodiesel standards except for cold filter plugging point (CFPP), ester and sulfur content and improvement of CFPP was recommended by adding cold flow enhancers or mixed with petroleum diesel fuel which has better cold flow properties. Ong et al. (2013) applied a supercritical methanol approach to the transesterification of leather tanning waste to produce biodiesel. The authors modeled the kinetic reactions of fatty acid methyl esters (FAMEs) formation from leather tanning waste, encompassing reversible esterification, non-reversible and first-order esterification single-step, pseudo-first order, and irreversible transesterification.

2.4.5 Fish oil

The fish processing industry generates significant amount of oil-rich wastes appropriate for biodiesel production (Jayasinghe and Hawboldt, 2013). Before disposal, the effluents from the fish processing industry contain heads, viscera, bones, trimmings, tails, fins and skin mixed with wastewater. A substantial portion (6–11 w %) of the effluent is oil and a good yield is achieved with physical separation technique (Jayasinghe and Hawboldt, 2013). The fish oil is recovered from the effluent by grinding/ homogenizing the waste, heating it to 95–100 °C for 15–20 min, screw pressing to remove the liquid from the solids, centrifuging the liquid to remove the water from the oil, and polishing the oil by water washing (Guadixz and Guadix, 2013). A two-step transesterification method for biodiesel production using oil from fish canning industry waste was investigated by Costa et al. (2013). The authors found that the catalyst concentration during esterification had the greatest influence on product yield and quality. The best conditions were 1 w % catalyst and 60 vol.% of methanolic solution. Recently, Tanwar et al. (2013) and Jayasinghe and Hawboldt (2013) investigated biodiesel production from fish processing plant effluents, which included waste characterization and quality assessments. The feedstock quality and type are the major factors in determining the transesterification technique to adopt for biodiesel production. Similar studies were carried out on the engine performance, emission and combustion of biodiesel synthesized from fish processing industry effluent (Behçet, 2011; Lin and Li, 2009; Sakthivel et al., 2013).

2.5 Biodiesel production techniques

Four main techniques exist to reduce the potentially high viscosity of biofuels made from animal fats and vegetable oils and eliminate any operational problems from its use in a common diesel engine: direct use and blending, microemulsions (cosolvent blending), thermal cracking (pyrolysis) and transesterification (alcoholysis) (Harold, 1997; Knothe et al., 2005). Leading to the products commonly known as biodiesel (alkyl esters of oils and fats), transesterification is the most commonly used method to reduce viscosity associated with animal fats and vegetable oils. Methodologies such as microemulsions and pyrolysis of animal fats and vegetable oils can produce compounds that are smaller than their triglyceride (TG) source, resulting in lesser viscosity and making them suitable for use as a fuel. However, they cannot be used for biodiesel production (Ma and Hanna, 1999).

2.5.1 Direct use and blending

The main issues of direct use of animal fats as fuel in diesel engines are their high viscosity and poor volatility. Some investigators have attempted to directly inject animal fats into an unmodified diesel engine. Senthil Kumar et al. (2005) preheated animal fat at different temperatures before injection into a single-cylinder direct injection diesel engine with a rated power of 2.8 kW at 1500 rpm. The preheated animal fat showed a reduced ignition delay, reduced combustion duration, a rise in peak pressure and lower smoke emissions than diesel. In a comparative study of different methods of using animal fat as a fuel in a compression ignition engine, Kumar et al. (2005) used a single-cylinder air-cooled, direct injection diesel engine to test fuels at 100% and 60% of the engine's maximum power output. The authors reported a drop in cylinder peak pressure, a longer ignition delay, and a lower premixed combustion rate with neat animal fat as compared to neat diesel at normal temperature. Numerically investigating a compression ignition engine's operation using animal fats and vegetable oils as fuels, Bousbaa et al. (2012) reported slightly different combustion characteristics when comparing neat diesel to biofuels. Fuel derived from AFW decreased the total unburned fuel as well as the nitrogen oxides (NO_x) emissions as compared to neat diesel. They concluded that numerical results concurred with those obtained experimentally.

Blends of animal fats with petrodiesel has been used to reduce the latter's viscosity. Diesel engines have been reported to use the resulting animal fats blends efficiently. The major advantages of the blending are the absence of technical modifications and the ease of implementation. Blending of animal fats with alcohols results in a significant improvement in their physical properties (Bousbaa et al., 2012; Kumar et al., 2005; Mrad et al., 2012). Storage stability of poultry fat and diesel fuel mixtures in terms of specific gravity and viscosity were studied and slight changes in viscosity and specific gravity of the biofuels blends over the course of one year storage period was found (Geller et al., 2008). In a comprehensive review of the direct use of vegetable oil and animal fat as an alternative fuel in internal combustion engines, Mondal et al. (2008) reported that the effects of the high viscosity of animal fats and their blends as a major cause of poor atomization and difficulty in handling by conventional fuel injection system of compression ignition engines. Micro-emulsifications permit a greater atomization of fuel, improved brake thermal efficiency, and decrease smoke, particulate and nitric oxide emissions due to micro-explosion (Schwab et al., 1983).

2.5.2 Microemulsions

Microemulsification is a process used to formulate hybrid diesel fuels by solubilisation of vegetable oil/alcohol mixtures through the addition of amphiphiles. Alcohols such as CH_3OH or ethanol (CH_3CH_2OH) have limited solubility in nonpolar animal fats and vegetable oils; therefore, amphiphilic compounds such as phospholipids, sorbitan sesquiolate (span83), n-butanol, 2-octanol, carboxylate surfactants and the like, are added to increase solubility, dilute the oil, and reduce viscosity. An equilibrium dispersion of optically isotropic fluid microstructures with an average diameter less than one quarter the wavelength of visible light that spontaneously form upon the addition of amphiphiles to a mixture of otherwise nearly immiscible liquids is known as a microemulsion (Schwab et al., 1983). Microemulsions do not require agitation to remain in a single-phase, translucent solution at constant temperature and pressure because they are thermodynamically stable (Ivanov and Kralchevsky, 1997).

Investigating the use of animal fats as compression-ignition (CI) engine fuel by making stable emulsion with water and CH_3OH, Kerihuel et al. (2005) used Span 83 (sorbitan sesquiolate) and span 80 (sorbitan monooleate) as surfactants to prepare and stabilize animal fat-water emulsions. They concluded that animal fats can be transformed into a stable biofuel emulsions with improved physical and chemical properties and can be used as a viable fuel in diesel engines. Kerihuel et al. (2006) studied the effects of formulation and other influential parameters on the CH_3CH_2OH animal fat emulsions as a diesel engine fuel based on stability, structure, viscosity, fat content and economic aspects. They determined optimum emulsions conditions to be 36.4% CH_3CH_2OH, 3.6% of SPAN 83, 10% of water and 50% animal fat by volume. Kumar et al. (2006), performed diesel engine test on CH_3CH_2OH-animal fat emulsions based fuels, and reported an improvement in the heat release pattern during the premixed combustion phase with animal fat emulsion *vs.* neat animal fat. At high power outputs they found the fuel emulsion to show a drastic reduction in smoke, nitric oxide, hydrocarbon and carbon monoxide emissions compared to neat fat and neat diesel.

2.5.3 Pyrolysis

Pyrolysis or cracking involves the thermal decomposition of organic material to smaller molecules through the application of heat without the addition of supplemental air or oxygen. Thermal cracking of triglyceride materials (animal fats and vegetable oils) represents an alternative method of producing renewable bio-based products suitable for use in fuel and chemical applications. Considerable investigations have been done on the pyrolysis of different varieties of vegetable oils to produce chemicals and diesel-like fuel (Alencar et al., 1983; Demirbas, 2008; Lima et al., 2004; Schwab et al., 1987). Animal fat pyrolysis has received much less interest as compared to vegetable oils. Adebanjo et al. (2005), pioneers in the study of lard pyrolysis, investigated the production of diesel-like fuel and other value-added chemicals from the pyrolysis of lard and reported the potential for producing a diesel-like liquid and a high calorific-value (68-165 MJ/m^3) gaseous fuel through lard pyrolysis. The authors reported diesel-like liquid product maximum yield from lard as 37 g/100 g at reaction conditions: temperature, residence time, and packing particle size to be 600 °C, 1.2 s, and 1.7 - 2.4 mm, respectively.

In recent years, pyrolysis of animal fats has been reported by a number of investigators. Wiggers et al. (2009) and Wisniewski Jr et al. (2010) investigated the pyrolysis of waste fish oil at a pilot plant scale and studied the chemical compositions of the pyrolysates. The authors reported the compositional yields to be: liquid (72.83%), bio-gas (15.85%), and coke (11.32%) at the operation conditions: average reaction temperature, residence time, and water content to be 525 °C, 17 s, and 5%, respectively. Ben Hassen-Trabelsi et al. (2014) reported the production of bio-oil and bio-char by pyrolysis of lamb, poultry and swine AFW in a fixed-bed reactor. They concluded that pyrolysis was a viable method of converting AFW to high yield liquid products (hydrocarbons). However, bio-oils generated still required an enhancement in composition and fuel properties before their use as engine fuels. Asomaning et al. (2014) used a two-stage thermal conversion approach to produce renewable chemicals and fuels from inedible lipid feedstocks e.g. beef tallow, yellow grease, brown grease and cold pressed camelina (*Camelina sativa* (L.) Crantz) oil were first hydrolyzed and the fatty acids produced were recovered and pyrolyzed in batch reactors. The authors reported similar product yield for all the feedstocks used with the organic liquid fraction (OLF) accounting for 76–80% of the product. They concluded that the research demonstrated the viability of a novel two-stage thermal hydrolysis–pyrolysis conversion method for producing OLF from inedible feedstocks and low-value lipids.

2.5.4 Transesterification reaction techniques

Transesterification is the most commonly used method to reduce viscosity of animal fats and vegetable oils. It generates products commonly known as biodiesel (alkyl esters of fats or oils) (Gerpen, 2005; Knothe et al., 2005). This biodiesel production technique has been reported to have particular advantages over other processes: 1. reaction conditions are mild, 2. the process is environmentally friendly and 3. a wide variety of feedstocks can be processed through this technique. Transesterification of TAGs can be classified into two types: catalyzed or non-catalyzed. Catalyzed transesterification can be further grouped according to the type of catalyst employed (e.g. homogeneous, heterogeneous and enzymatically-catalyzed). Supercritical process (a non-catalyzed transesterification reaction) has been employed to mitigate critical issues in the production process and lower cost of production (Ong et al., 2013; Shin et al., 2012c). Conventionally, homogeneous base or acid catalysts are the most commonly used transesterification processes. In recent years, enzymes immobilized or in their free-forms have been reported as very promising reaction agents for biodiesel production (Kumar et al., 2013; Nielsen et al., 2008). While the process commercialization is still limited by enzyme production costs, enzyme reusability and the lack of complex downstream products and associated separation problems have overshadowed the enzyme shortcomings. AFW transesterification for biodiesel production had been investigated by researchers using all four transesterification methods (Table 2.2).

2.5.4.1 Homogeneous catalytic conversion of AFW

Homogeneous catalytic transesterification is the most commonly used commercial transesterification process for the production of biodiesel. It can be divided into two types: homogeneous base catalytic transesterification and homogeneous acid catalytic transesterification. In most cases, AFW require pre-heating and preprocessing steps prior to transesterification through homogeneous catalytic conversion by one- or two-step catalytic processes. Biodiesel production from AFW under homogeneous catalysis and process parameters (e.g. molar (alcohol:fat) ratio, catalyst concentration, reaction temperature, and time) effects on the yield and the purity of biodiesel have been the subject of numerous critical investigations.

Homogeneous base catalytic transesterification is mostly a one-step catalytic process in which sodium or potassium hydroxide serve as catalyst for the transesterification of AFW (Balat, 2011). Bhatti et al. (2008) investigated biodiesel production from waste mutton tallow and chicken fat by a homogeneous base and acid (H_2SO_4 and KOH) catalyzed transesterification. They reported high biodiesel yield in a one-step acid transesterification reaction as compared to the one-step KOH method which was attributed to soap formation under the KOH process. Encinar et al. (2011), studied the effects of homogeneous base and acid catalysts at different concentrations on the biodiesel yield from beef tallow and concluded that NaOH was a more efficient base catalyst than sodium methoxide for the transesterification of beef tallow. They obtained optimum yield of

Table 2.2: Animal fats transesterification process parameters and techniques for biodiesel production

Feedback	Production technique	Catalyst (wt/wt of fat)	Molar ratio	T (°C)	Time (h)	Conversion (%)	Reference
Chicken fat	Homogeneous						
	Acid	H_2SO_4 25%	1:30	50	24	99.01	(Bhatti et al., 2008)
	Base	KOH 1%	-	30	1	88.10	
Mutton fat	Homogeneous						
	Acid	H_2SO_4 25%	1:30	60	24	93.21	(Bhatti et al., 2008)
	Base	KOH 1%	-	30	1	79.70	
Beef tallow	Heterogeneous Acid	Surfonated polystyrene 20 mol%	-	64	18	75.00	(Soldi et al., 2009)
Waste animal fat	Homogeneous two steps	Step 1: H_2SO_4 0.08% Step 2: NaOH 0.001%	-	62	2	89.00	(Gürü et al., 2009)
Lard	Enzymatic	Immobilized-lipase (*candida* sp. 99-125) 20 %	1:1	40	30	87.40	(Lu et al., 2007)
Beef tallow	Homogeneous Base	KOH 2%	-	60	1.5	95.00	(Moraes et al., 2008)
Feather meal fat	Homogeneous Base	KOH 1%	1:9	70	1/4	7-11 (dry basis)	(Kondamudi et al., 2009)
(Beef tallow:sunflower oil) blends	Homogeneous Base	NaOH 1%	1:6	60	1	-	(Taravus et al., 2009)
(Lard:soybean oil) blend	Homogeneous two steps	NaOH 0.8%	1:6	65	3	81.7-88.6	(Dias et al., 2008a)
Beef tallow	Homogeneous Base	KOH 1.5%	1:6	65	3	-	(Da Cunha et al., 2009)
Poultry fat	Heterogeneous Base	Mg-Al hydrocalcite 10%	1:30	120	8	93.00	(Liu et al., 2007)
Mutton tallow	Heterogeneous Base	MgO-KOH	1:22	65	1/3	98.00	(Mutreja et al., 2011)
Acid waste lard	Homogeneous two steps	Step 1: H_2SO_4 2% Step 2: NaOH 1%	1:6	65	Step 1:5 Step 2:1	66.20	(Dias et al., 2009)
Lard	Enzymatic	(Novozym435 and Lipozyme TLIM) combine 4%	1:2	50	20	97.20	(Huang et al., 2010)
Animal fats and fish oil	Enzymatic	Lipozyme-IM	1:4	25	96	50.00	(Aryee et al., 2011)
Chicken fat	Supercritical methanol	-	1:6	400	1/10	88.00	(Marulanda et al., 2010)
Waste lard	Supercritical methanol	-	1:45	335	1/4	89.91	(Shin et al., 2012a)

biodiesel at a 9% catalyst concentration. Several other studies have employed this method for the production of biodiesel either as a one-step or two-step homogeneous catalytic transesterification process. Some of the different feedstocks were animal fats and their blends, especially chicken-swine fat blends, sunflower oil-beef tallow blends, duck oil, lard etc. The process was monitored under different reaction conditions reflecting catalyst load, molar ratio, temperature and time (Dias et al., 2008a; Dias et al., 2008c; Kondamudi et al., 2009; Taravus et al., 2009).

2.5.4.2 Heterogeneous catalytic conversion of AFW

In the quest to solve the issue of high FFA biodiesel feedstocks, many recent studies have reported the application of heterogeneous catalysis for biodiesel production from animal fats. The shortcomings of homogeneous catalytic transesterification are reported to be considerably minimized through the application of heterogeneous catalysts such as solid and enzymatic catalysts (Semwal et al., 2011). Most researchers prefer using heterogeneous over homogeneous catalysts to produce biodiesel because of their inherent advantages: catalyst regeneration and reusability, simple downstream separation and purification, and production of less hazardous wastewater (Borges and Díaz, 2012; Lam et al., 2010; Semwal et al., 2011). Heterogeneous catalysis can be classified according to the types of catalysts used: heterogeneous base catalytic transesterification and heterogeneous acid catalytic transesterification. Heterogeneous catalysis using various solid catalysts can be further grouped according to the number of reaction steps (e.g. one- and two-step processes).

Liu et al. (2007) investigated the use of heterogeneous base catalysts derived from Mg–Al hydrotalcite in a one-step processing approach for the conversion of poultry fat to biodiesel. They reported that a 94% biodiesel yield was achieved at 120 °C when a fixed catalyst added at a rate of 0.04 g/mL and a 60:1 molar ratio. They also found the mixed Mg–Al oxide to be thermally and mechanically stable after operation with no significant difference in particle size or morphology occurring. The use of nanocrystalline calcium oxide as a heterogeneous base catalyst for the transesterification of poultry fat (fat to methanol ratio 3:10) at room temperature was investigated by Venkat Reddy et al. (2006), who reported that the maximum conversion of the poultry fat to biodiesel under the reaction conditions would require 6 hr. Mutreja et al. (2011) investigated the production of biodiesel from mutton fat using KOH impregnated MgO as a heterogeneous base catalyst, where the KOH impregnation level was 5-20 wt%, the catalyst/fat ratio 1.5-4 wt%, the reaction temperature ranged from 45 to 65 °C, the fat:methanol molar ratio ranged from 1:11-1:22. They also investigated the effect of adding up to 1 wt% of water/oleic acid/palmitic acid to the reaction mix. The authors concluded that impregnation with 20 wt% KOH of MgO increased the biodiesel yield (>98%) in the transesterification of mutton fat under operating conditions of: 20 min reaction time at 65 ^{o}C, fat:methanol molar ratio of 1:22 and use of MgO-KOH catalyst. Many other solid catalysts have been investigated by researchers for the production of biodiesel from AFW under different reactions conditions. These have generally shown reasonable results, highlighting the greater feasibility of heterogeneous over homogeneous catalysis (Bianchi et al., 2010; Di Serio et al., 2007; Huong et al., 2011; Melero et al., 2012).

Heterogeneous acid catalytic transesterification of AFW has been reported to have a slower reaction rate than heterogeneous base catalytic transesterification (Bianchi et al., 2010; Dias et al., 2012; Kim et al., 2004; Soldi et al., 2009). Bianchi et al. (2010) studied direct esterification of FFA in animal fat using solid acid resins as heterogeneous catalysts. The FFA (>90%) in the lard samples were converted such that the FFA concentration in the lard were lowered below 0.5%, a practical value suitable for direct biodiesel production. Investigating the Zr-SBA-15 acid catalyst:

optimization and reaction conditions for biodiesel production from low-grade oils and fats, Melero et al. (2012) found this catalyst to be highly active in the simultaneous esterification of FFAs and transesterification of TAGs from low-grade AFW in the presence of methanol, completely independently of their acid value or unsaponifiable matter content. While few reports of two-step transesterification of AFW using heterogeneous catalysts have appeared in the literature, heterogeneous catalysts have been used to pre-treat high FFA AFW, thus reducing their FFA levels below certain threshold thereby allowing direct transesterification (Melero et al., 2012). Kim M (2011) developed a heterogeneous ZrO_2 supported metal-oxide catalysts for brown grease esterification and sulfur removal. These catalysts were claimed to achieve high yields through esterification of FFA and simultaneously desulfurization and de-metallization. The authors further noted that methanolysis with the zirconia supported catalysts, was more effective for desulfurization than an acid washing process. Ngo (2008, 2010) and Ngo et al. (2013) presented different heterogeneous catalysts capable of reducing greases FFA content to below 1% under mild reaction conditions and thereafter achieve a high conversion. However, the major drawbacks of using heterogeneous catalysts include: 1. complexity in preparation; 2. a requirement of high selectivity for the desired product formation; 3. difficulty in reuse in some cases; 4. high molar ratio of alcohol:fat as compared to homogeneous catalysts; and 5. long reaction time.

2.5.4.3 Enzyme catalytic conversion of AFW

Biodiesel production using an enzymatic transesterification process could solve problems associated with AFW physicochemical properties as well as be more environmental friendly than conventional catalytic processes (Akoh et al., 2007; Lee et al., 2002; Lu et al., 2007). The advantages of using enzyme-catalyzed transesterification include: ease of enzyme recovery, reusability and thermal stability of enzyme under mild reaction conditions (pH, temperature, and pressure), and the easy downstream recovery of products etc. Lipases from different organisms *Mucor miehei, Candida rugosa, Penicillium camembertii, Penicillium roqueforti, Pseudomonas fluorescens, Pseudomonas cepacia, Candida lypolytica, Candida Antarctica, and Bacillus subtilis* have been effectively employed in transesterification of high FFA feedstocks as free-form or immobilized enzymes (Kaieda et al., 2001; Kaieda et al., 1999; Noureddini et al., 2005). While the higher cost of enzymes compared to chemical catalysts and the risk of product contamination by enzyme residues are cited as drawbacks (Christopher et al., 2014). Enzyme immobilization techniques which have enabled reuse and easy recovery of enzyme have been found to remediate these problems (Nielsen et al., 2008). Likewise, tailored derivatives with minimum undesirable side reactions are also positive elements of enzyme-catalyzed process (Christopher et al., 2014). Figure 2.6 shows a typical enzymatic transesterification process.

Several studies have been carried out on enzyme-catalyzed transesterification (free-form and immobilized form) of vegetable oils in solvent free and solvent media (Dizge and Keskinler, 2008; Kaieda et al., 1999; Kumar et al., 2011a; Samukawa et al., 2000). However, in depth studies of enzymatic transesterification of AFW have been sparsely reported in the literature. So far, the most commonly used lipases for AFW transesterification are: *Burkholderia cepacia* (Da Rós et al., 2010; Da Rós et al., 2012; Nelson et al., 1996), *Candida antarctica* (Huang et al., 2010; Lu et al., 2007) and *Rhizomucor miehei* (Nelson et al., 1996). Aryee et al. (2011) investigated ethanolysis of enzymatic transesterification of three feedstocks: salmon skin oil, Rothsay composite (blend of yellow grease and rendered animal fats), and olive oil with Lipozyme-IM as catalyst. The authors assessed the effects of operational parameters (e.g. temperature, oil: alcohol molar ratio, and reaction time) on the yield of biodiesel and reported a generally moderate oil to fatty acid ethyl ester conversion rate of 50% at the optimal operation parameters. Assessing the reusability of immobilized lipases during methanolysis of lard, Lu et al. (2007) reused the enzymes over seven consecutive cycles with no significant decrease in lipase activity, while maintaining a biodiesel yield exceeding 80%. Huang et al. (2010) optimized lipase-catalyzed transesterification of lard for biodiesel production using a response surface methodology. In their study, two enzymes (Novozyme 435 and Lipozyme TLIM) were combined to catalyze biodiesel production from lard and process optimization. The response surface methodology identified the optimal reaction conditions for biodiesel yield (97.2% methyl ester yield) as a lipase:fat ratio of 0.04:1, a Novozyme435/total lipases (w/w) ratio of 0.49:1, a tert-butanol/fat (v/v) ratio of 0.55:1, a 5.12:1 methanol/fat (mol/mol) ratio, for 20 h reaction time. The optimum temperature for enzymatic AFW transesterification lies in the range between 30 °C and 50 °C (Lee et al., 2002; Lu et al., 2007), outside of which enzyme denaturation and solvent volatilization may occur (Aryee et al., 2011; Huang et al., 2010).

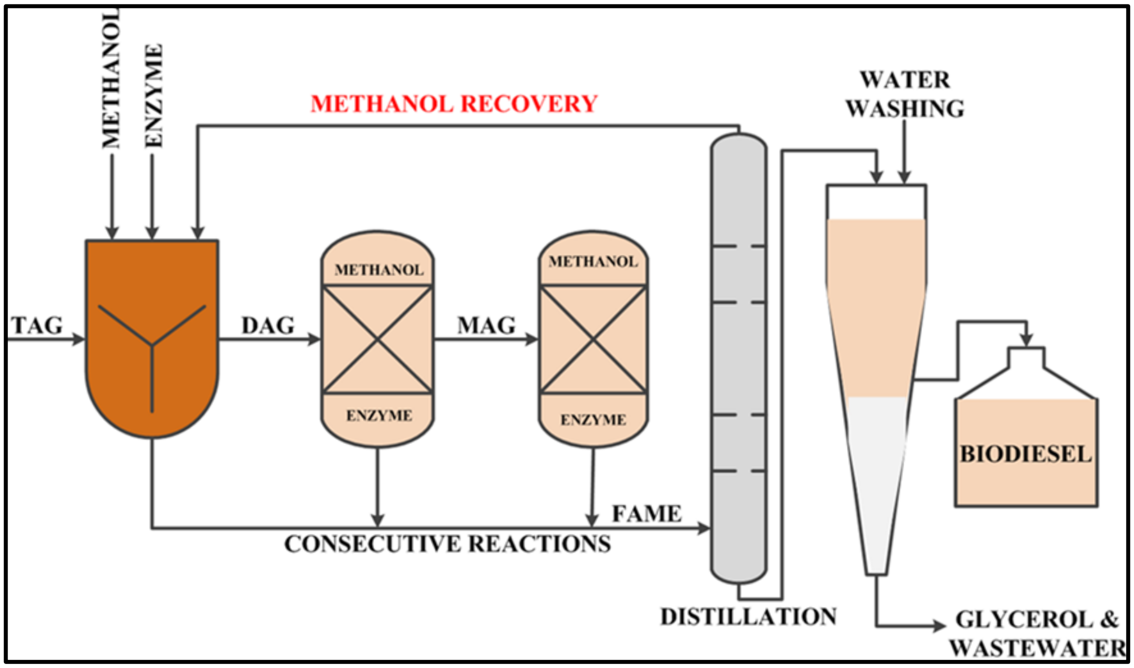

Figure 2.6: Enzyme catalyzed transesterification of triglycerides flow chart. TAG = triacylglyceride; DAG = diacylglyceride; MAG = monoacylglyceride; FAME = fatty acid methyl ester

2.5.4.4 Supercritical non-catalytic conversion of AFW

A supercritical fluid (SCF) is any substance (compound, mixture or element) above its critical pressure (P_c) and critical temperature (T_c), where distinct liquid and gas phases do not exist. SCFs can diffuse through solids like a gas, and dissolve materials like a liquid. The properties of SCFs can be classified as an intermediate between a gas and a liquid. Table 2.3 shows the properties of commonly used SCFs. Decaffeination of coffee with supercritical carbon dioxide (CO_2) was one of the first applications of SCFs (Bernal et al., 2012). In the literature, different SCFs techniques have been employed for the production of biodiesel from vegetable oils feedstocks. The SCF transesterification of rapeseed oil was reported by Kusdiana and Saka (2001), Saka et al. (2010), and Wang et al. (2007a). SCF transesterification of soybean oil was reported by Wang and Yang (2007); Yin et al. (2012), and Anitescu and Bruno (2012a, 2012b). Similarly, SCF transesterification of sunflower (*Helianthus annuus* L.) oil was reported by Madras et al. (2004), and Tateno and Sasaki (2004). Few studies have been reported in the literature about the SCF transesterification of AFW.

Table 2.3: Commonly used supercritical fluids

Fluid	**T_c (°C)**	**P_c (MPa)**	**Density(g/L)**
Methanol (CH_4O)	239.6	8.09	272
Ethanol (C_2H_6O)	240.9	6.14	276
Acetone (C_3H_6O)	235.1	4.70	278
Water (H_2O)	374.3	22.12	348
Carbon dioxide (CO_2)	31.3	7.29	469
Methane (CH_4)	−82.6	4.60	162
Fluoroform (CHF_3)	26.2	4.85	516
Ethane (C_2H_6)	32.3	4.88	203

Marulanda et al. (2010) investigated the effect of reaction parameters under supercritical conditions: temperature (350, 375, and 400 °C), pressure (10, 20, and 30 MPa), alcohol:fat molar ratio (3:1 to 12:1) and residence time (3-10 min) on the yield and quality of biodiesel derived from chicken fat, low-cost lipid feedstocks. The optimum reaction conditions for the conversion of triglycerides and the decomposition of glycerol to fuel components were: 400 °C, 30 MPa, 9:1 alcohol:fat ratio, and residence time 6 min. Taher et al. (2011), and Al-Zuhair et al. (2012), studied the production of biodiesel from fat extracted from lamb meat in supercritical CO_2 media. They assessed the effects of reaction parameters (e.g. enzyme concentration, reaction temperature and methanol:fat molar ratio) on the biodiesel yield. In a continuous extraction of fat from lamb meat and biodiesel synthesis using supercritical CO_2, the authors observed a decrease in enzymatic activity in the third cycle of meat replacement. They concluded that biodiesel yield increased with both the quantity of enzyme and the length of the reaction time. Shin et al. (2012c) investigated the production of biodiesel from waste lard using supercritical methanol. They reported that biodiesel obtained from waste lard without pre-treatment was of equal quality to biodiesel from refined lard, even though waste lard samples contained high FFA and a high water contents. This confirmed that water content and high FFA have no effect on the SCF transesterification of animal fats for the production of biodiesel.

2.6 Assisted transesterification techniques

The aim of assisted transesterification techniques (ATT) is to reduce reactor operation time while achieving the highest yield possible. Apart from benefits in terms of reaction time, ATT employs low reaction reagent levels (i.e. low catalyst concentrations and lower alcohol to fat ratio), thus reducing the overall cost of production. Two types of ATTs are commonly used in biodiesel production from vegetable oils and animal fats. These include ultrasound assisted (UA) and microwave assisted (MA).

2.6.1 Ultrasound-assisted technique

Ultrasound is the process of propagating an oscillating sound pressure wave with a frequency greater than the upper limit of the human hearing range. Ultrasound frequencies range between 20 kHz and l0 MHz, with associated acoustic wavelengths in liquids of roughly 100-0.15 mm. Application of ultrasound in the chemical processing enhances both mass transfer and chemical reactions, leading to shorter reaction times, and cheaper reagents. Acoustic cavitation which is the most important element of ultra-sonication is the formation, growth, and implosive collapse of bubbles in a liquid irradiated with sound or ultrasound. The propagation of sound through the liquid causes expansion waves and compression waves, which forms an aerosol of solvent, solute vapor and previously dissolved gases. This phenomena causes bubbles to grow and recompress due to the high mass transfer rates arising from the formation of a microemulsion through ultrasonic cavitation (Singh et al., 2007).

The application of UA to the transesterification of different vegetable oils has been widely investigated and reported (Kumar et al., 2012; Kumar et al., 2010; Singh et al., 2007; Veljković et al., 2012). This technique has been proven to enhance reaction rates. Its implementation has been shown to overcome the inherent issues of slow batch reaction rates and time-consuming phase separation of conventional transesterification process (Boffito et al., 2013; Kalva et al., 2008; Parkar et al., 2012). Compared to vegetable oils, few reports of UA transesterification of AFW appear in the literature. Comparing conventional and UA transesterification of beef tallow to produce biodiesel, Teixeira et al. (2009) showed that the ultra-sonication process led to similar yields of alkyl esters as the conventional procedure, while significantly decreasing the reaction time. They concluded that methanolysis of triglycerides using ultrasonic power was an efficient, time saving and economical method of producing biodiesel fuel, but the effects of reaction parameters and ultrasound conditions were not reported.

Armenta et al. (2007a), evaluated the ethanolysis production of biodiesel from fish oil using ultrasound energy. They examined the effects of different parameters such as: ultrasonic device (bath *vs.* probe), catalyst type (KOH *vs.* C_2H_5ONa), catalyst concentration (0.5 *vs.* 1%), temperature (20 *vs.* 60 °C), and duration of exposure (10–90 min) on the production process. The authors reported that sodium ethoxide was a more efficient catalyst than KOH. The best reaction conditions for the ethanolysis of fish oil were reported as a reaction time of 30 min, a temperature of 60 °C, a catalyst concentration of 0.8% C_2H_5ONa. Through this conditions, a yield of over 98% can be expected.

2.6.2 Microwave-assisted technique

The microwave radiation region is located between infrared radiation and radio-waves in the electromagnetic spectrum. Microwaves have wavelengths of 1 mm – 1 m, corresponding to frequencies between 0.3 and 300 GHz (Lidström et al., 2001; Varma, 2001). The band frequencies in this region are occupied by telecommunication and microwave radar equipment. In order to avoid interference with these systems, the household and industrial microwave ovens operate at a fixed frequency of 2.45 GHz (Gedye et al., 1988; Smith and Arsenault, 1996). Microwave irradiation has been employed in different applications including organic synthesis (Aydın et al., 2014; Khattab et al., 2014), where chemical reactions are accelerated because of selective absorption of microwave energy by polar molecules, nonpolar molecules being inert to the microwave dielectric loss (Lidström et al., 2001; Varma, 2001). Other benefits of microwave-assisted chemical syntheses are rapid reactions, the high purity of products, improved yields and greater energy efficiency. The application of the MA transesterification process to the production of biodiesel from vegetable oils has been well investigated (Hsiao et al., 2011; Kumar et al., 2011g; Patil et al., 2009). These studies have reported the feasibilities of using MA for the production of biodiesel from different varieties of vegetable oils, but have only paid limited attention to the use of AFW as feedstocks. However, Da Rós et al. (2012) have reported optimal conditions for the MA enzymatic synthesis of biodiesel from beef tallow. They noted an almost total conversion of the fatty acid original beef tallow's fatty acids optimum conditions of: beef tallow:ethanol molar ratio of 1:6, a temperature of 50 °C and a reaction time of 8 h. This represented a six-fold increase in the rate of the process carried out under conventional heating. They concluded that MA process promises to be energy efficient, limit destructive effects to enzymes and delivered higher biodiesel production compared to conventional heating.

2.7 Conclusion

In terms of availability and low cost, compared to virgin vegetable oils, AFW have been proven to be very good potential feedstocks for high quality biodiesel production. The use of AFW as biodiesel feedstock represents one of the possible ways biodiesel production's impact on food security can be limited, while reducing production costs and environmental damage. The combustion of animal fat based biodiesel has been shown to produce lesser NO_x emission than vegetable oil based biodiesel. The former have high cetane number, which is an important quality parameter for diesel fuels. Seen as a challenge to good biodiesel yield by homogeneous base catalyzed reaction due to formation of soap, the significant quantity of FFAs in AFW and their elevated water contents have proved problematic. The application of non-catalytic (SCFs) as well as two-step homogeneous (acid/base), heterogeneous, enzymatically catalyzed transesterification processes have shown a tremendous success compared to one-step homogeneous base catalyzed transesterification of AFW for the production of biodiesel. Although, the enzymatic transesterification process is usually time consuming as compared to the conventional methods, this technique offers advantages in processing high FFA feedstocks without chemical pre-treatment. Assisted transesterification techniques such as ultrasonic power and microwave heating have been applied as novel processes to enhance biodiesel production from AFW. The overall energy-consumption and production cost to biodiesel synthesis can be drastically reduced through the application of these techniques given their capability to reduce reaction time, temperature and pressure required during biodiesel production. In conclusion, further intensive research on assisted transesterification techniques (ultrasound power and microwaves heating) for the production of biodiesel should be carried out on AFW. Similarly, SFCs processes for AFW should be well researched.

CONNECTING TEXT TO CHAPTER 3

Chapter two of this dissertation reviewed the recent trends of biodiesel production from AFW and associated production techniques, as well as assisted transesterification approaches for biodiesel production. The need to enhance enzyme-catalyzed transesterification of AFW by assisted and intensified techniques was identified and further investigated in this study. The review manuscript was published online in February, 2015 in Renewable and Sustainable Energy Reviews. This review manuscript is co-authored by Drs. Dumont, M.-J., and Ngadi, M. All literature cited in chapter 2 is listed in the reference section at the end of this thesis.

Adewale, P., Dumont, M.-J., Ngadi, M. Recent trends of biodiesel production from animal fat wastes and associated production techniques. Renewable and Sustainable Energy Reviews. 2015; 45:574–588. dx.doi.org/10.1016/j.rser.2015.02.039

Chapter three of this thesis addressed rheological, thermal and physicochemical characterization of AWFs. This part of the dissertation gave us possible behavioral pattern of AWFs to mixing and transesterification processes due to their basic properties. The manuscript from this study, which addressed objective one of this dissertation, was published in Energy Technology in February, 2014. The manuscript is co-authored by Drs. Dumont, M.-J., and Michael, M. The format of the manuscript has been altered to be consistent with this thesis. All literature cited in chapter 3 is listed in the references section at the end of this thesis.

Adewale, P., Dumont, M.-J., Ngadi, M. Rheological, thermal and physicochemical characterization of animal fat wastes destined for biodiesel production. Energy Technology. 2014; 2:634–642. dx.doi.org/10.1002/ente.201402001

Chapter 3

Rheological, Thermal, and Physicochemical Characterization of Animal Fat Wastes for use in Biodiesel Production

Abstract

The rheological, thermal and physicochemical properties of AFW (tallow, lard, choice white grease and yellow grease) are important parameters for an efficient design of equipment and to optimize the processing procedures of biodiesel production. In this study, the physicochemical properties of animal fat waste samples and the correlation of these properties to their thermal and rheological behaviors were elucidated. Pure lard was equally investigated to monitor the effects of impurities on the rheological and thermal properties of the AFW. It was established that the presence of impurities had effects on the rheological and thermal properties of fats. Additionally, due to the high level of free fatty acid (FFA) present in the wastes, transesterification cannot be applied directly. It will be necessary to reduce the FFA level by using acid pretreatment or enzyme catalyzed transesterification.

3.1 Introduction

The physical and chemical properties of animal fats and vegetable oils such as viscosity, melting and crystallization are essential engineering parameters for the design of processing equipment and optimization of their processing procedures. The fatty acid (FA) composition, including the saturated fatty acids (SFA) fraction of animal fats and vegetable oils determines the hardness, viscoelasticity and plasticity of the samples (Aguirre-Mandujano et al., 2009; Goodrum et al., 2003). The analysis and quantification of these properties can be used to predict the optimal processing variations or to modify the processing equipment for more efficient operation. Ma et al. (1998) studied the effects of catalysts, free fatty acids (FFA), and water on transesterification of edible beef tallow. They reported that FFA and water should be kept within 0.06% w/w and 0.5% w/w in order to obtain a good biodiesel yield. Karmakar et al. (2010) reviewed the properties of various plants and animals feedstocks used for biodiesel production. They reported that animal fats have chemical structures similar to vegetable oils, but the only difference is in the distribution of FA. They equally reported animal fats as excellent feedstock sources for biodiesel production, although they are not studied as extensively as vegetable oils.

Several studies have been carried out on the rheological, thermal and physicochemical properties of many vegetable oils and their modified forms such as blends, shortening etc. (Aguirre-Mandujano et al., 2009; Lai et al., 2000; Liu et al., 2012; Tan and Che Man, 2002; Wang and Briggs, 2002). However, limited attention has been given to the rheological, thermal and physicochemical properties of AFW in the literature. Goodrum et al. (2003) investigated the rheological characteristics of animal fats and their mixtures with diesel fuel using a Brookfield Synchro-metric LVT viscometer equipped with a UL adapter. The authors reported a significant correlation between the FA composition and their rheological behaviour. They equally reported that the mixture of yellow grease (YG) and diesel fuel had a higher viscosity as compared to other samples investigated.

Animal fats and vegetable oils are transesterified mainly to reduce their viscosity (Chesterfield et al., 2012; Leung et al., 2010; Meher et al., 2006) in order to meet up with the American Society for Testing and Materials (ASTM) standard for biodiesel. Canoira et al. (2008) assessed different production processes and characterized biodiesel produced from low-grade animal fat. They reported that the viscosity of biodiesel was approximately an order of magnitude lower than that of the starting animal fat, leading to better atomization of the fuel in the combustion chamber of the engine. Hence, selection of suitable feedstocks to synthesize biodiesel of desired properties require systematic study of the influence of each of the chemical structure in FA composition on thermal and physicochemical properties such as melting, crystallization and viscosity of the selected feedstock.

Tang and Marangoni (2006) reported that viscoelastic properties of fat products can be categorized into elastic and viscous. The storage modulus (G′) revealed the solid-like characteristic of fats, particularly the strength of the links between the clusters of fat crystals while the loss modulus (G″) showed the liquid-like characteristic of fat (Cullen, 2009). Bell et al. (2007) reported that fully melted fats (hardened rapeseed oil and palm olein) showed a weak viscoelastic liquid structure when the loss modulus (G″) higher than the storage modulus (G′) throughout the measured frequency range used in their study while during crystallization, the rheology of the fats changed from a weak viscoelastic solid system to a weak viscoelastic liquid. In the study of Liu et al. (2008) on full-fat and low-fat cheese analogues with or without pectin gel through microstructure, texture, rheology, thermal and sensory analysis, they reported that fat is a viscoelastic material at small deformations and when subjected to external forces (such as strain, stress, etc.), solid crystals would deform and liquid would flow. The study of rheological properties of AFW would provide good knowledge and useful information of their behaviors when subjected to external forces during transesterification processes.

AFW have been used as a liquid fuel in large-scale heating boilers (Knothe et al., 2005). Recent studies have shown AFW as potential biodiesel feedstocks (Bhatti et al., 2008; Ghazavi et al., 2013; Gürü et al., 2010). These fats have been used in mixtures with petroleum-based heating oils and fuel additives for diesel engines. To optimize biodiesel production and maximize AFW potential as biodiesel feedstock on a large scale, it is paramount to determine comprehensive thermal and rheological behavior of these substances to guide the design of systems and the biodiesel production process. This study was aimed to determine the rheological, thermal and physicochemical properties of four AFW (YG, Choice white grease (CWG), Lard and Tallow) and pure lard (PL). PL was used as a standard to monitor effects of impurities on the rheological, thermal and physicochemical properties of the AFW.

3.2 Materials and methods

3.2.1 Materials

This study investigated four AFW: Tallow, Lard, CWG and YG (Rothsay Canada, Sainte-Catherine, QC, Canada) and PL obtained from a local grocery store in Montreal, Canada. The fat samples were kept in a deep freezer at a temperature below –10 °C before analysis. All chemicals and solvents used were analytical and GC grades purchased from Sigma and Fischer scientific. Hexane (ACS grade), sodium methoxide (pure anhydrous powder), and sulfuric acid (99.9%) were purchased from Fisher Scientific (Nepean, ON, Canada). Saturated fatty acid standards: hexanoic (6:0), octanoic (8:0), decanoic (10:0), dodecanoic (12:0), tetradecanoic (14:0), palmitic (16:0), octadecanoic (18:0), eicosanoic (20:0), docosanoic (22:0) and tetracosanoic acid (24:0), and the unsaturated fatty acid standards: docosahexaenoic (16:1), oleic (18:1, n-9), linoleic (18:2, n-6), linolenic (18:3, n-3), erucic, cis-5,8,11,14-eicosatetraenoic, elaidic, nervonic and petroselinic were purchased from Sigma Aldrich, (Oakville, ON, Canada). Analytical grade chloroform, acetone, sodium thiosulphate, potassium iodide, sodium hydroxide, WIJS solution, internal standard (IS); methyl nonadecanoate were purchased from Sigma Aldrich (Oakville, ON, Canada).

3.2.2 Iodine value analysis

Iodine value (IV) of the animal fats was determined by using AOAC 993.20 (AOAC, 1999). The animal fats (0.5 g) were dissolved in 10 mL of chloroform. WIJS solution (25 mL) was added with vigorous mixing and the solution was allowed to stand in the dark for 30 min with occasional shaking. Then, 10 mL of 15% potassium iodide (KI) and 100 mL of freshly boiled and cooled water were added with thorough shaking, and then titrated against 0.1 N sodium thiosulphate until the yellow solution turns almost colorless. Then, few drops of starch as indicator were added and titrate until the blue color completely disappears. The IV formula is as shown in equation 1. IV of each sample was determined in triplicate.

$$IV = \frac{(B-S) \times N \times 12.69}{weight\ of\ sample(g)} \qquad [3.1]$$

where, IV is the iodine value, B is mL thiosulphate for blank, S is mL thiosulphate for sample, and N is the normality of thiosulphate solution.

3.2.3 Free Fatty Acid Content Analysis

The FFA content of the animal fat samples was determined using the AOCS official method Ca 5a-40 (AOCS, 2009). Animal fat (7.05 g) was weighed and dissolved in 75 mL of 95% ethanol, and then titrated against a standardized sodium hydroxide solution (0.25 M) with phenolphthalein as indicator (1% in 95% ethanol). FFA was expressed as mg (NaOH)/g. The percentage of FFA content of the AFW was calculated as oleic acid. The FFA content of each sample was determined in triplicate.

3.2.4 Fatty acid composition by GC-FID

3.2.4.1 Methylation of animal fats

The samples were vigorously mixed for homogeneity before sampling. The water content of the animal fats was determined by freeze drying them at -50 ºC for 48 hours. The following methylation procedure was followed to derivatize the AFW: dried sample (10 mg) was weighed into a screw-capped derivatization vial; the sample was solubilized by adding 0.8 mL of hexane; then 0.2 mL of 2 M of sodium methoxide (in 20 % methanol) was added as catalyst. The mixture was vortexed and then shook in water bath at 65 °C for 20 minutes. The sample was taken out of the water-bath and 1 mL of 10% sulfuric acid in methanol was added; the sample was transferred to the water-bath at 85 °C for 30 minutes. Hexane (4 mL) was added to recover the fatty acids. The mixture was centrifuged at 5000 x g, 5 minutes to separate the biodiesel phase from the glycerol phase; the upper layer (biodiesel phase) was collected (repeated twice); the solvent was dried out by nitrogen gas; the fatty acid was diluted to an appropriate concentration while 50 ml of the internal standard (IS) was added before GC injection. The samples were analyzed by GC on the same day of their preparation and each sample was injected in triplicate.

3.2.4.2 Preparation of Standard Solutions

Standard solutions were prepared by dissolving the standards in hexane. Fatty acid standards were methylated as described under the section entitled “methylation of animal fats”. All the standard solutions were injected with the internal standard. The choice of methyl nonadecanoate as internal standard was justified by its absence in animal fat samples. There is no interference of retention time of the internal standard with the fatty acids in the samples, this further justified the choice of internal standard. Standard calibration curves were developed by the analysis of standard solutions over appropriate concentration ranges. For the calibration curves, fatty acid standards were injected within the concentration range of 0.1– 2.5 mg/mL. All calibration concentration points were ran in triplicate. The values reported are the averages of the measured values of different runs and their standard deviations.

3.2.4.3 Fatty acid analysis

Hewlett-Packard model HP 5890 series II Gas Chromatography equipped with an auto sampler and flame ionization detector (FID) with a range of 0-10 V was used to analyze the fatty acid composition of the animal fats. Helium was used as the carrier gas at a flow rate of 40 mL/min. The initial oven temperature was held at 80 ºC for 3 min, rising to 150 ºC at 10 ºC/min, and then to 250 ºC at 10 ºC/min where it was held for 20 min. A Zebron ZB-WAX column (Phenomenex, USA) (30 m, 0.25 mm i.d, 0.25 µm film thickness) was used. A split injection 1:100 was used for 1 µL of the methylated samples. Identification and quantitative fatty acid compositions were calculated as percentage of the total fatty acids present in the sample determined from the peak areas using methyl nonadecanoate as internal standard.

3.2.5 Thermal analysis by DSC

Melting and crystallization curves of the AFW and pure lard were determined using DSC (Q100, TA Instrument, New Castle, DE, USA). Purge gas was nitrogen (99.99% purity) with a flow rate of 50 ml/min. The instrument was calibrated using indium (melting point 156.6°C, ΔH_f = 28.45 J/g). Animal fat samples (6-12 mg) were weighed into aluminum hermetic pans and the covers were hermetically sealed into place. An empty, hermetically sealed aluminum pan was used as reference. The baseline was optimized using two empty pans (one placed at the reference oven compartment and the other at the sample oven compartment) prior to sample analysis. The animal fat samples were subjected to the following temperature program: for crystallization characteristics, samples in pan was; (a) heated to 80°C to destroy the crystal structure; (b) equilibrated at 80°C for 3 minutes (c) held isothermally for 10 minutes (d) ramped at a rate of 10°C/min from 80 to –35°C. A new sample set was used for the melting characteristics and were; (a) cooled to –35°C; (b) equilibrated at –35°C for 3 minutes (c) held isothermally for 10 minutes (d) ramped at a rate of 10°C/min from –35 to 80°C. The crystallization and melting characteristics of each sample, i.e. extrapolated onset temperature (T_{onset}), maximum peak temperature (T_{peak}) and enthalpy (ΔH), were obtained using TA Universal Analysis 2000 software. Data were collected in triplicate.

3.2.6 Rheological analysis

AR 2000 controlled-stress and rate rheometer (TA Instruments, New Castle, DE, USA) was used to measure the viscosity and viscoelasticity behaviors of the animal fat waste and pure lard samples. A 40 mm diameter 2° steel cone geometry was used with a gap of 1 mm. The instrument was set at zero-gap before actual measurement. Oscillatory temperature ramps were carried out to determine the temperature dependency of viscosity and insight of the samples melting strength and viscoelastic behavior while a controlled stress-rotation shear rate ramp method was used to investigate the viscosity. The temperature of the samples was equilibrated at 30 °C for 5 minutes before the test. An initial pre-shear stress of 0.5968 Pa was found to produce response within the linear viscoelastic region of each test sample at a fix frequency of 1 Hz. The temperature ramp was performed from 30 – 60 °C, ramp rate of 5 °C by loading sample onto the rheometer plate to fill up the space between the geometry and the plate. Viscosity analysis was carried out on different sample sets. The instrument was programmed to a fix temperature and equilibrated for 10 min followed by one-cycle shear rate ramping from 50 to 250 s^{-1}. Viscosity behaviors over the shear rate ramping of each sample was investigated at four different temperatures (30, 40, 50 and 60 °C). These temperature values were chosen in order to understand AFW behaviour within the temperature range that favors enzymatic transesterification. The storage modulus (G′) and loss modulus (G″) were determined as a function of temperature for each sample. The viscosity and viscoelastic measurements were acquired by Rheology Advantage, TA version 5.7 at each step and each sample was tested in triplicate.

3.2.7 Statistical analysis

Statistical analysis was carried out by the general linear model procedure (PROC GLM) using SAS (Statistical Analysis Systems, Version 9.3, SAS Institute Inc., Cary, NC, USA). Mean comparison of viscosity and significant differences between the fat samples were further analyzed by Tukey’s studentized range test (SAS, 2013). Tukey's HSD (honest significant difference) test is a single-step multiple comparison procedure that compares the means of every treatment to the means of every other treatments.

3.3 Results and Discussion

3.3.1 Physicochemical analysis

Pure lard has the lowest FFA content ($P < 0.05$) out of the samples while CWG has the highest (Table 1). Pure lard is produced for consumption, it is expected to have very low FFA content. However, the FFA content of all the other samples does not meet up with the recommendation for the use of alkaline catalysis (below 1%), a common industrial method of biodiesel production (Alptekin et al., 2012; Canakci, 2007). Enzyme catalyzed transesterification would be an economical biodiesel synthetic pathway for these feedstocks (Gog et al., 2012).

Table 3.1: Fatty acid composition of the animal fat waste samples

Analyses	**Animal Fat Wastes**				
	YG	**CWG**	**Lard**	**Tallow**	**PL**
Physicochemical properties					
FFA (%)	18.40 ± 0.02	19.26 ± 0.06	10.03 ± 0.18	3.19 ± 0.14	0.20 ± 0.01
IV (mg/g)	80.40 ± 0.31	67.30 ± 0.60	63.90 ± 0.36	55.60 ± 0.41	68.30 ± 0.21
Fatty acid composition (%)					
C14:0	1.02 ± 0.12	1.60 ± 0.29	1.41 ± 0.13	2.76 ± 0.10	2.15 ± 0.12
C16:0	14.83 ± 0.26	22.39 ± 0.26	25.69 ± 0.12	25.95 ± 0.21	23.41 ± 0.23
C16:1	1.50 ± 0.04	3.40 ± 0.23	2.82 ± 0.23	2.84 ± 0.06	0.61 ± 0.15
C18:0	8.41 ± 0.07	9.15 ± 0.24	14.50 ± 0.14	17.54 ± 0.18	10.01 ± 0.07
C18:1	47.88 ± 0.39	44.14 ± 0.87	40.88 ± 0.17	41.67 ± 0.53	44.82 ± 0.32
C18:2	19.11 ± 0.11	11.90 ± 0.34	12.93 ± 0.24	6.91 ± 0.42	15.20 ± 0.61
C18:3	4.68 ± 0.15	0.00	0.00	0.00	0.00
C20:0	2.56 ± 0.12	7.43 ± 0.26	0.50 ± 0.06	0.44 ± 0.17	0.27 ± 0.11
C20:1	0.00	0.00	1.34 ± 0.03	1.88 ± 0.37	3.53 ± 0.25
∑SFA	26.83 ± 0.36	40.56 ± 0.74	42.03 ± 0.22	46.69 ± 0.43	35.84 ± 0.35
∑UFA	73.17 ± 0.40	59.44 ± 0.74	57.97 ± 0.22	53.31 ± 0.43	64.16 ± 0.52
UFA/SFA	2.73	1.47	1.38	1.14	1.79

The IV of tallow was found to be the lowest. It contained the highest percentage of SFA. This was expected as the sample is solid at room temperature. Lard, pure lard and CWG had close range IV (63.9, 68.3 and 67.3, respectively) while YG was of the highest IV value. There was no significant difference ($P>0.05$) in IV values of lard and pure lard, which showed that possibility of impurities in lard had no effect on its level of unsaturation. YG was liquid at room temperature while lard, PL and CWG were semisolid. Similar results were reported in the literature (Knothe, 2002; Yılmaz et al., 2010). The high percentage composition of SFA found in CWG, lard and tallow would favor stable oxidative biodiesel synthesis.

3.3.2 Fatty acid composition by GC-FID

The chromatograms of FA composition of YG, CWG, lard, PL and tallow are shown in Figure 3.1. Relative retention time (RRT) to the internal standard of the compound was compared to that of the standard, for the FA identification of the samples. Standard calibration curves were developed for sample components quantification. Linear dynamic range was fitted to a least squares regression line for each FA standard (Table 3.2). The correlation coefficients R^2 were greater than 0.99 for all the identified FA components in the samples. The repeatability (within-run precision) and reproducibility (between-run precision) were carried out on five different standards to validate GC-FID accuracy. YG had higher amounts of C18:1n-9 (48%) as compared to CWG, lard, PL and tallow, while C18:0 was detected at higher concentrations in lard and tallow (15 and 18%, respectively). The concentration of C16:0 (14.83%) was lower in YG as compared to the other samples. Also, YG was the only fat type which contained C18:3n-3. Therefore, the higher concentration in C18:1n-9 combined with the presence of C18:3n-3 in YG was responsible for its liquid state at room temperature.

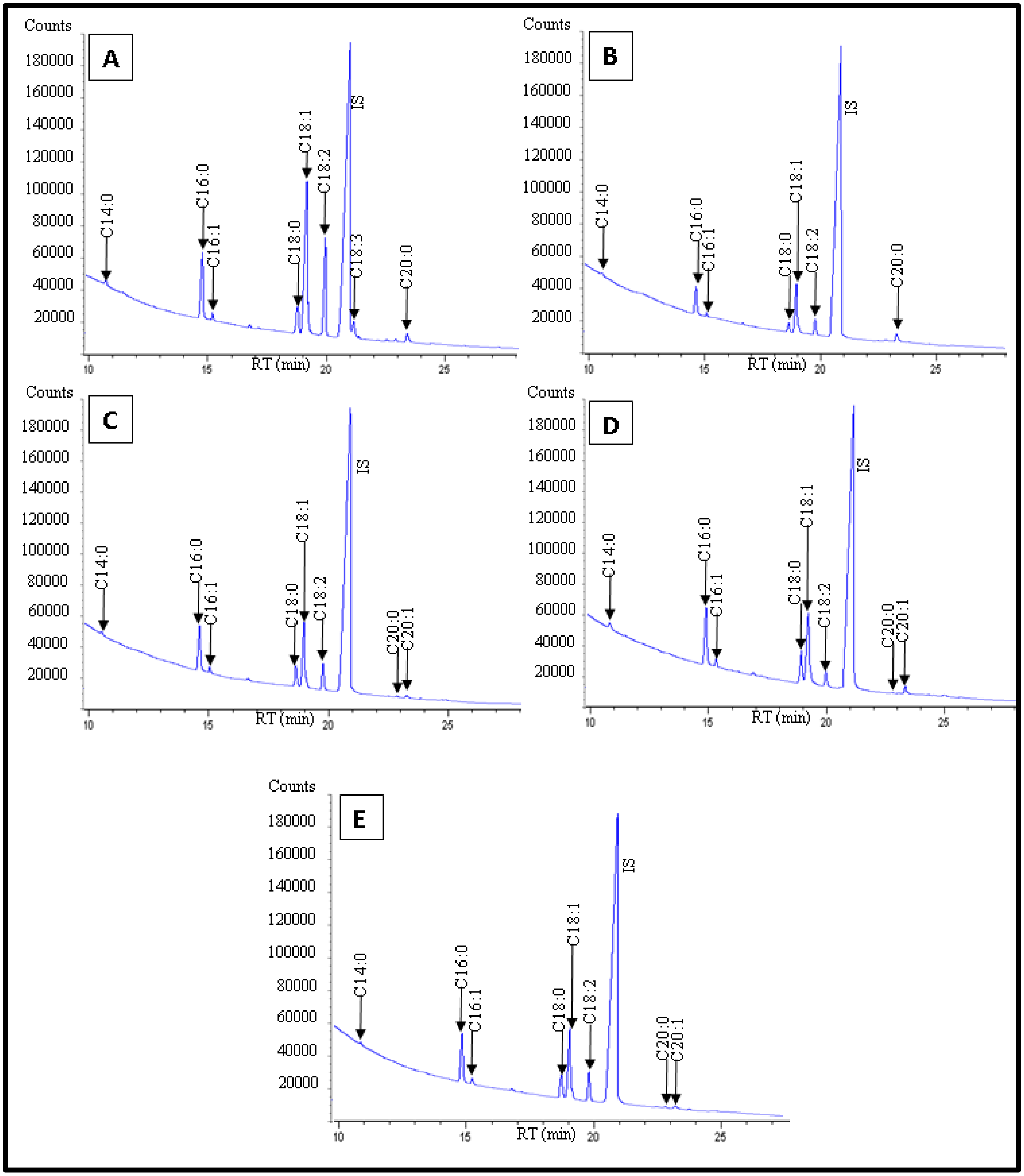

Figure 3.1: Fatty acid chromatograms of YG (A), CWG (B), Lard (C), Tallow (D) and PL (E); RT = Retention Time

Table 3.2: Calibration curves least squares regression line parameters and correlation coefficients (R^2)

FA Component	**m**	**b**	**R^2**
C14:0	1.4E+06	6.2E+04	0.9924
C16:0	1.8E+06	-1.5E+05	0.9977
C16:1	2.4E+06	-3.1E+05	0.9915
C18:0	3.9E+06	-1.2E+05	0.9977
C18:1	1.5E+06	5.9E+04	0.9952
C18:2	1.7E+06	-1.2E+05	0.9953
C18:3	1.3E+06	2.7E+05	0.9937
C20:0	8.8E+05	-1.8E+04	0.9920
C20:1	1.9E+06	-2.5E+05	0.9930

$y = mx + b$ where y is the concentration in mg/mL and x is the peak area of chromatogram

Lard, PL and tallow contained C20:1n-6 in amount of 1.3, 3.5 and 1.9%, respectively while YG and CWG did not contain this compound. The fatty acid profile of lard is similar to that of pure lard but with varying percentage composition. Presence of impurities, animal feeds constituents and production method of lard might cause this varying percentage composition. Total SFA in YG were lower than in CWG, lard and tallow, while total unsaturated fatty acids (UFA) were found in higher amounts in YG as compared to CWG, lard and tallow. The UFA/SFA ratio of YG was higher than other samples. This was expected due to the source of YG which might allow mixture of vegetable oils with the animal fats. YG is produced by rendering companies and is typically comprised of used cooking oil from restaurant and may contain rendered animal fats such as tallow, poultry fat or lard. UFA amount and the UFA/SFA ratio in CWG, lard and PL were higher than tallow. This could be responsible for the solid state at room temperature of tallow. There was no other remarkable difference found among these samples with respect to the remaining fatty acids. These results showed YG as distinct animal fat waste among the samples with respect to percentage composition of UFA to SFA. There were some unknown (unresolved) peaks, before the stearic acid peak and between the internal standard and eicosanoic acid peaks (Figure 3.1). They are likely *trans* fatty acids or impurities in the samples since samples are waste products. Despite the similarities in FA composition of the samples, there were differences in the percentage composition values because FA composition could be affected by nutritional conditions, breed, sex etc. (Couvreur et al., 2006; Prieto et al., 2012; Sato, 2001).

3.3.3 Thermal characteristics by DSC

The melting and crystallization curves of the AFW determined by DSC are presented in Figure 2(a-j). Melting and crystallization curve parameters were as follows: onset temperature (T_{onset}), peak temperatures (T_{peak}), and enthalpy change (ΔH) are presented in Table 3.3. The samples thermal behaviors during the cooling and the heating phases were very different. During cooling, two exothermic peaks were observed (Figure 2(f-j)) while upon heating, multiple endothermic peaks were observed in their thermograms (Figure 2(a-e)). Multiple endothermic peaks of the samples may be caused by solid–solid transition between two different crystalline phases; it may also due to melting of different crystalline phases.

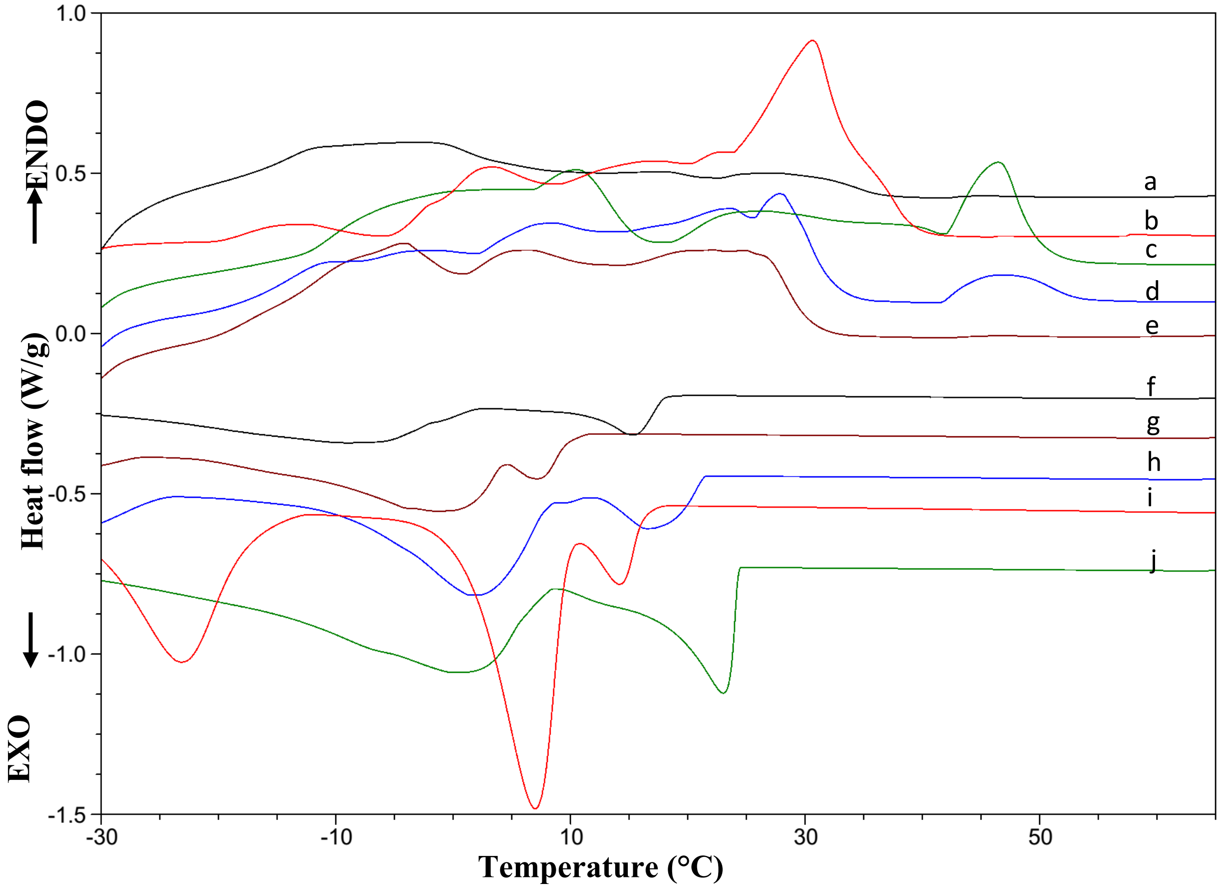

Figure 3.2: DSC melting curves of (a) YG, (b) PL, (c) Tallow, (d) Lard, (e) CWG; and crystallization curves of (f) YG, (g) CWG, (h) Lard, (i) PL, and (j) Tallow

The crystallization curves were more reproducible and simpler than the melting curves. This was due to the fact that crystallization was only influenced by the chemical composition of the sample and not by the initial crystalline stage since all samples started from the liquid state (Tan and Che Man, 2002). The multiple endothermic peaks of the melting curves were due to polymorphism of animal fats. Polymorphism is a property of oils and fats that is recognized as being composition dependent (Tan and Che Man, 2000; Wang and Briggs, 2002). Rapid cooling of vegetable oil and fat samples in the DSC pans might lead to the formation of different crystals lower-melting. During the gradual temperature increase, the less stable crystals may have melted first and recrystallized into higher melting forms to give the melting profiles.

The lowest values for T_{onset} and T_{peak} were found in the YG crystallization profile (Table 3.3). The lowest values of T_{onset} and T_{peak} are due to the highest percentage of oleic acid (18:1n-9, 73.17%) in YG. These differences in T_{onset} and T_{peak} can be attributed to the physical properties of the triglycerides [35]. The lower T_{onset} of YG could also be attributed to the lowest percentage of the saturated stearic acid (C18:0 = 8.41%) and ∑SFA = 26.83%. In contrast, T_{onset} and T_{peak} values in the first crystallization curve of CWG were lower than that of YG. But, T_{onset} and T_{peak} of CWG and pure lard for both first and second melting peaks were similar to that of YG, and differ from that of lard and tallow. Perhaps, this can be attributed to the lower percentage of the saturated stearic acid (C18:0 = 9.15% and 10.01%) and palmitic acid (C16:0 = 22.39% and 23.41%), respectively as compared to that of lard and tallow, and the higher amount of unsaturated fatty acids (∑UFA ≈ 60% and 64%, respectively) as compared to lard and tallow. However, the heating profile of lard and tallow were determined to show high-melting endothermic peaks at 46.44 and 46.36 °C, respectively. When the TAG molecules are more saturated, the molecular interaction is stronger. The TAG molecules interact with each other primarily through Van der Waals interaction. These weak bonds between TAG molecules are broken at the solid-liquid transition. In a saturated fat the acyl chains are able to align perfectly right along their length, which maximizes intermolecular interactions. Thus, more energy is needed to disintegrate the molecular association to cause melting or relative molecular movement. As is shown in Table 3.3, the highest ΔH was determined to be at the second crystallization peaks of lard and tallow. These higher peak values could be used to differentiate the properties of lard and tallow from YG and CWG using melting thermograms from DSC.

Table 3.3: T_{onset}, T_{peak} and ΔH values obtained from melting and crystallization peaks of animal fat samples

Melting

Samples	First melting peak			Second melting peak		
	T_{onset} (°C)	T_{peak} (°C)	ΔH (J/g)	T_{onset} (°C)	T_{peak} (°C)	ΔH (J/g)
YG	13.83 ± 0.84	18.04 ± 0.44	0.23 ± 0.02	23.37 ± 0.65	28.58 ± 0.25	0.94 ± 0.47
CWG	14.83 ± 0.23	17.73 ± 0.45	1.67 ± 0.31	23.74 ± 0.07	25.04 ± 0.13	0.14 ± 0.10
Lard	25.85 ± 0.10	28.22 ± 0.08	1.96 ± 0.40	41.90 ± 0.14	46.44 ± 0.29	3.16 ± 0.32
PL	20.87 ± 0.22	22.41 ± 0.12	0.14 ± 0.05	25.70 ± 0.18	30.85 ± 0.20	9.03 ± 0.54
Tallow	19.40 ± 0.16	24.26 ± 0.12	3.55 ± 0.21	42.27 ± 0.07	46.38 ± 0.12	6.40 ± 0.34

Crystallization

Samples	First crystallization peak			Second crystallization peak		
	T_{onset} (°C)	T_{peak} (°C)	ΔH (J/g)	T_{onset} (°C)	T_{peak} (°C)	ΔH (J/g)
YG	17.19 ± 0.41	15.28 ± 0.20	-2.32 ± 0.08	-1.87 ± 0.06	-8.65 ± 0.15	-4.63 ± 0.37
CWG	10.98 ± 0.20	9.16 ± 0.11	-1.15 ± 0.10	2.18 ± 0.03	-1.43 ± 0.19	-5.81 ± 0.57
Lard	21.22 ± 0.11	17.39 ± 0.34	-4.41 ± 0.30	7.94 ± 0.10	2.45 ± 0.38	-15.70 ± 0.55
PL	15.77 ± 0.11	14.19 ± 0.48	-2.47 ± 0.02	9.56 ± 0.34	6.77 ± 0.28	-26.15 ± 0.51
Tallow	24.23 ± 0.12	23.03 ± 0.16	-10.25 ± 0.78	6.87 ± 0.54	1.11 ± 0.54	-16.93 ± 0.56

3.3.4 Rheological properties

The viscosities of the samples versus shear rate measured at four different temperatures (30, 40, 50, and 60°C) are shown in Figure 3.3. In general, viscosities of all the samples responded in inverse proportionality to shear rate and temperature, but the degree of decrease was dependent on the samples composition (the interaction between sample types and temperature was significant, ($P < 0.05$). All samples had wide difference in viscosity between 30 and 40°C but lard and tallow had significantly higher viscosity than YG and CWG within these temperatures (Figure 3.3). When the temperature was greater than 50 °C, their viscosities became steady throughout the shear rate range. YG had the lowest viscosity. This result was expected because YG has the highest UFA which makes it to be liquid at room temperature (Table 3.1). The viscosity value for CWG was not significantly different from that YG despite its high SFA composition, while lard and tallow had significantly higher viscosity values than the other two AFW. Figure 3.4 shows HSD mean comparison of the viscosity of the four AFW and pure lard. Statistically, tallow was found to have the highest viscosity distribution ($P < 0.05$) as compared to other samples, followed by lard while CWG was found to be lowest ($P < 0.05$) and closely related to that of YG. Pairwise comparison of samples viscosity was significant except for the interaction between YG, CWG and PL. Similar result was observed in ANOVA distribution of samples viscosity where YG, CWG and PL were in the same viscosity distribution range (Figure 3.4).

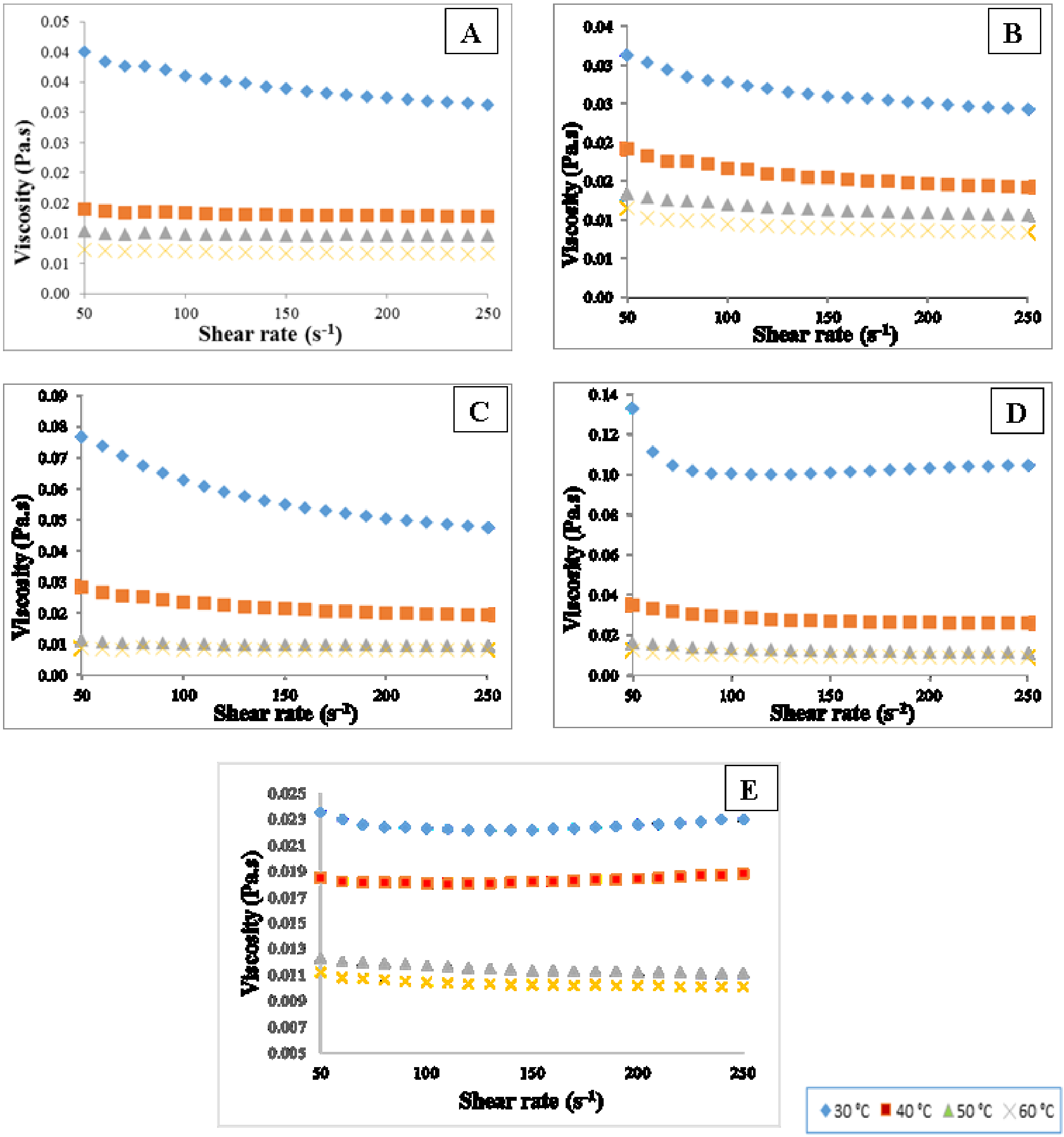

Figure 3.3: Variation in viscosities (Pa.s) at different temperatures for the animal fat waste: (A) YG, (B) CWG, (C) Lard, (D) Tallow, and (E) PL; as a function of shear rate (1/s)

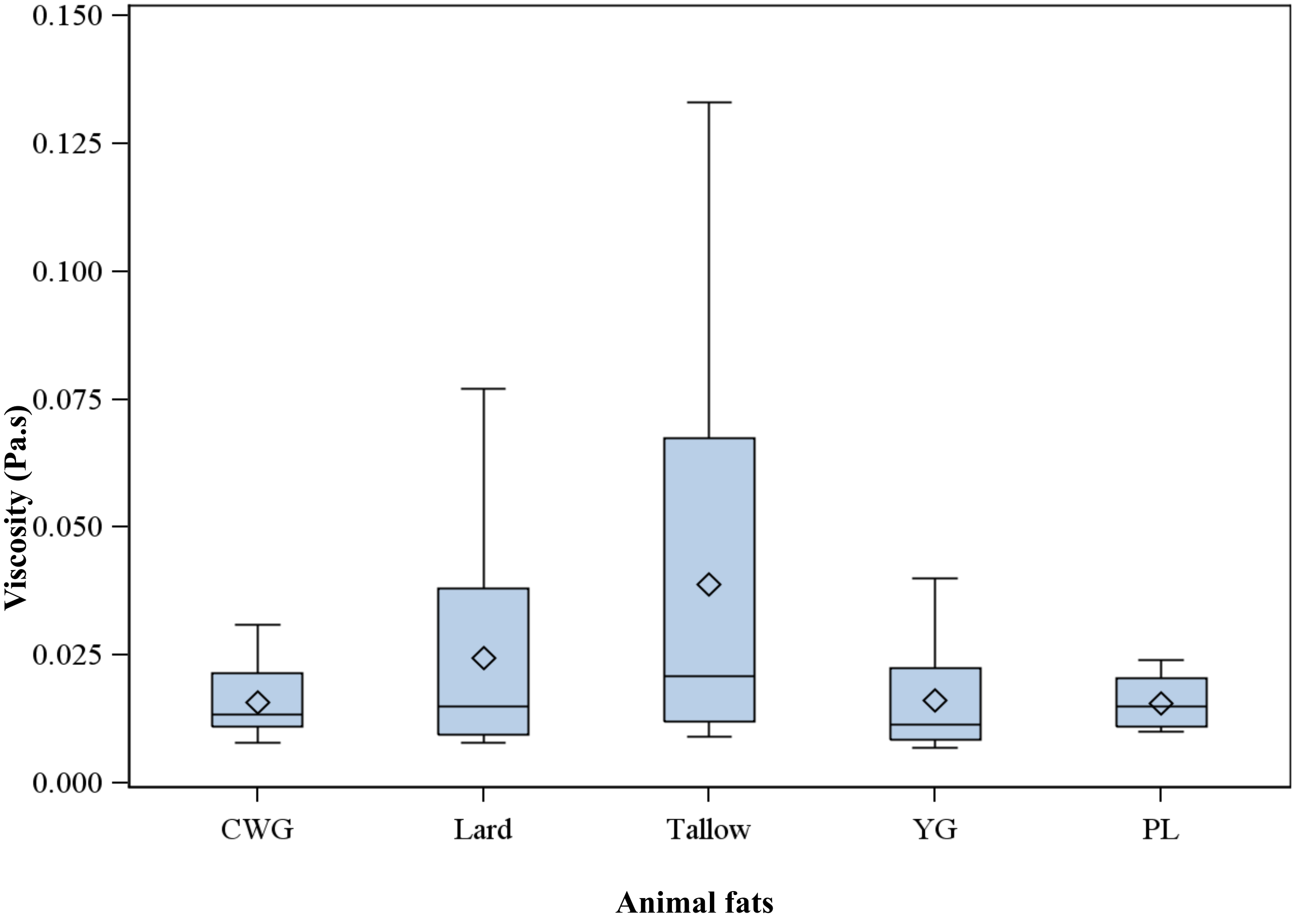

Figure 3.4: ANOVA viscosity distribution of the animal fat sample

Viscoelastic properties of the animal fat samples were evaluated through their storage modulus (G′) and loss modulus (G″), in which G′ relate to elastic or solid behavior of material, while G″ represents the viscous or fluid behavior (Bell et al., 2007; Lee et al., 2008; Tang and Marangoni, 2006). These samples contained a different content of solid fats at different temperatures, and consequently the viscoelastic behavior was affected by the temperature (Lee et al., 2008). In order to investigate the temperature dependency of viscosity, melting strength and viscoelastic behavior of the samples, the G′ and G″ values were obtained as a function of temperature from 30 to 60 °C.

Figure 3.5 shows G′ and G″ values of the samples. Lard, PL and tallow have higher G′ values than G″ values up to 39, 44 and 34 °C, respectively, while CWG has higher G″ values than G′ values up to 48 °C beyond which G′ values are above G″ at a constant value to the end of the run. There was a sharp decline in G′ values for lard, PL and tallow as the temperature increased due to the melting of crystalline fats. The values of G′ and G″ remained constant after 38, 48, 43, 45 and 35 °C for YG, CWG, lard, PL and tallow, respectively (Figure 3.5 A, B, C, D and E). At these temperatures, the samples were showing similar viscous behavioral pattern as shown in Figure 3.3. The results obtained have provided useful information on important parameters for biodiesel production from these samples. We have clearly demonstrated the transition temperatures, viscosity and viscoelastic behaviors of these AFW. The selection of adequate operating temperature and most importantly best agitation intensity to enhance biodiesel production from these samples has been deduced.

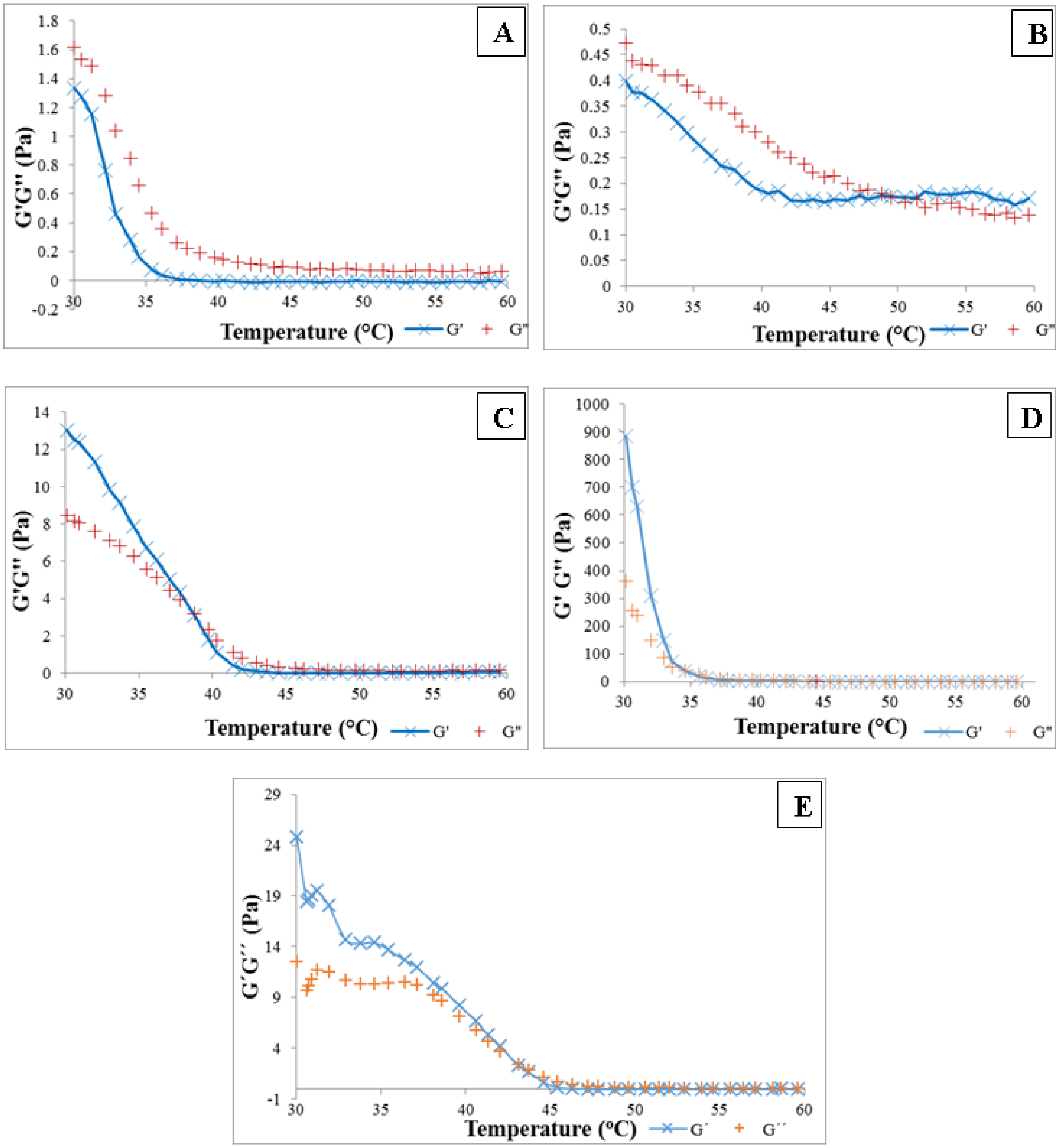

Figure 3.5: Oscillatory rheological characterization changes in storage (G′) and loss (G″) modulus at 1Hz for the animal fat waste samples: (A) YG, (B) CWG, (C) Lard, (D) Tallow, (E) PL; as a function of temperature

3.4 Conclusion

Physicochemical parameters of four AFW including: FA composition, FFA, IV, viscosity, melting and crystallization must be understood for adequate design of equipment and optimum biodiesel production process. Thermal and rheological behavioral pattern at different shear rate and temperature were established for each of the samples. The transesterification operating temperature for each sample must be above the temperature at which the viscosity becomes steady. This parameter differs among the samples. Steady viscosity equally exists at shear rate above which increase in shear rate has no effect on the sample viscosity. If agitation is lowered or stopped when this shear rate is achieved, transesterification reaction will proceed without loss of biodiesel yield. This will reduce wear and tear, more so production cost. Due to the high level of FFA in the AFW, alkaline transesterification cannot be applied directly for biodiesel production. It is necessary to reduce the FFA level of the fats by using acid pretreatment or enzyme catalyzed transesterification. It was established that animal fat waste impurities had effect on their rheological and thermal properties, but did not show any significant effect on fatty acid profile except differ percentage compositions between PL and lard.

CONNECTING TEXT TO CHAPTER 4

Once a firm understanding of the rheological, thermal and physicochemical characterization of AFW was established (Chapter 3), an attempt was made in Chapter 4 to characterize AFW using a non-destructive method. Two important physicochemical parameters (Iodine value and free fatty acids content) were determined using FT-NIR (Fourier Transform Near Infrared) spectroscopy. In Chapter 4, a good correlation between the predicted values of free fatty acids content and iodine values of AFW by FT-NIR spectrometer as compared to the experimental results (chemical based analysis) was determined.

This dissertation chapter was published in a peer-reviewed journal entitled Vibrational Spectroscopy. The manuscript is co-authored by Dr. Dumont, M.-J., Dr. Ngadi, M., Mr. Mba, O., and Dr. Cocciardi, R. The format of the manuscript has been altered to be consistent with this thesis. All literature cited in this chapter is listed in the references section at the end of this thesis.

Adewale, P., Mba, O., Dumont, M.-J., Ngadi, M., Cocciardi, R. Determination of the iodine value and the free fatty acid content of waste animal fat blends using FT-NIR. Vibrational Spectroscopy. 2014; 72:72–78. dx.doi.org/10.1016/j.vibspec.2014.02.016

Chapter 4

Determination of the iodine value and the free fatty acid content of waste animal fat blends using FT-NIR

Abstract

This study determined iodine value (IV) and free fatty acids (FFA) content of four different AFW and their blends using Fourier transform near-infrared spectroscopy (FT-NIR). Chemometric analysis by Partial Least Squares (PLS) regression was used to correlate spectral data with IV and FFA reference values of the samples. The effects of four spectra pre-processing (first derivative (FD), second derivative (SD), multiplicative scatter correction (MSC) and vector normalization (VN)) methods were investigated to predict the reproducibility and robustness of the PLS-NIR model developed. A set of 70% of AFW and their blends were used for developing PLS calibration models for measuring IV and FFA content using the remaining 30% samples as an independent test set validation. The coefficient of determination (R^2), the root mean square error estimation (RMSEE), and the residual prediction deviation (RPD) were used as indicators for the predictability of the PLS models. PLS-NIR models developed using first derivative and second derivative spectral preprocessing methods were the best for both IV and FFA content analysis (For IV, FD; R^2 = 98.70, RMSEE = 1.40 $gI_2/100g$, RPD = 8.76, SD; R^2 = 98.92, RMSEE = 1.28 $gI_2/100g$, RPD = 9.64 while For FFA, FD; R^2 = 99.91, RMSEE = 0.195%, RPD = 34.00, SD; R^2 = 99.93, RMSEE = 0.182%, RPD = 36.8). Overall, the results of this study demonstrate the suitability of FT-NIR spectroscopy for the quality control analysis of feedstocks for biodiesel production.

4.1 Introduction

The chemical and physical properties of biodiesel are correlated to the properties of their corresponding feedstocks. For example, the free fatty acid (FFA) content of feedstocks is frequently quantified to verify their suitability for biodiesel production and to assess the type of transesterification process to be selected. As the feedstocks' FFA content exceeds 0.5%, the use of alkaline transesterification is not suitable due to the formation of soap by the reaction between the FFAs and homogeneous basic catalyst (Canakci and Sanli, 2008; Canakci and Van Gerpen, 2001; Jasen and Marchetti, 2012; Ma et al., 1998). Another parameter which must be verified is the iodine value (IV). Feedstocks with high IV will tend to be less stable and more susceptible to oxidation due to their high degree of unsaturation.

Official methods developed by the American Oil Chemists' Society (AOCS) and the Association of Analytical Communities (AOAC) are available to measure the FFA content and the IV of fats. However, these official methods tend to be laborious and time consuming and further involve the use of toxic chemicals. The use of non-invasive and chemical free methods for the determination of physical and chemical properties of edible oils and fats have been developed such as Fourier Transform Infrared (FT-IR), Fourier Transform Mid Infrared (FT-MIR) and Fourier Transform Near Infrared (FT-NIR) spectroscopy (Cen and He, 2007; Che Man et al., 1999; Hendl et al., 2001; Samyn et al., 2012). Despite that the FT-MIR spectroscopy has gained acceptance as an analytical tool for oils, FT-NIR has been favored by the industry due to instrument ruggedness compared to FT-MIR spectroscopy (Du et al., 2012). FT-NIR has been used to determine both physical and chemical properties of fats and oils and it provides rapid results when compared with the conventional chemical methods (Armenta et al., 2007f; Azizian et al., 2010; Li et al., 1999).

The principle of FT-NIR spectroscopy is based on the absorption of electromagnetic radiation at wavenumbers ranging from 12500 to 4000 cm^{-1} (800 to 2500 nm). The spectra produced by FT-NIR arise from overlapping absorptions corresponding mainly to overtones and combinations of vibrational modes involving C–H, O–H, C=C, C=O and N–H chemical bonds (Azizian et al., 2010; Stefanov et al., 2013). The wide range of overtone bands makes FT-NIR a reliable tool for measurements of organic and biological systems. For the determination of the components in the samples, it is imperative to perform an accurate calibration of the FT-NIR spectrometer either by using appropriate calibration standards of known composition or by using analytical methods known as the reference methods. The main limitation of FT-NIR is its dependence on reference methods, its low sensitivity to minor constituents and its dependency on intricate calibration procedures (Büning-Pfaue, 2003; McClure, 1994).

The application and the use of NIR and chemometrics in foods and agricultural commodities such as lipids, oilseed, cereal, dairy, pharmaceutical and other processing industries to predict chemical composition of biological products with high accuracy had been reported by many researchers. Huang et al. (2008) reviewed the use of on/in-line NIRs reflectance instruments for quick quantitative determination of moisture, lipids, proteins, carbohydrates, and fiber in agricultural and food products. Armenta et al. (2007f) developed a chemometric method for the determination of acidity (FFA) and peroxide value (PV) in edible oils of different types and origins using NIRs. Du et al. (2012) used second derivative pre-processing multivariate partial least square (PLS) analysis for the evaluation of the quality of deep frying oils with FT-NIR and FT-MIR. It was reported that there was no strict linear relationship ($R^2 = 0.457$) between the FFA and PV; indicating the independence of these two parameters for oil quality evaluation. Li et al. (1999), Li et al. (2000)

also reported the use of FT-NIR for rapid determination of *cis* and *trans* content, iodine value, and saponification number of edible oils.

Azizian and Kramer (2005) reported the use of NIR spectroscopy to study the fatty acid composition in mixtures of shortening and lard. Pérez-Juan et al. (2010) reported the prediction of fatty acid composition using a NIRs fibre optics probe at two different locations of ham subcutaneous fat. Also, Pérez-Marín et al. (2007) studied the use of chemometric utilities to achieve robustness in liquid NIRs calibrations: application to pig fat (Iberian pork) analysis. Also, NIRs was used to estimate the concentration of polyunsaturated fatty acids and their bio-hydrogenation products in the subcutaneous fat of beef cows fed flaxseed (Prieto et al., 2012) and for the determination of oxidative stability of animal fats (Baptista et al., 2008). Finally, Cox et al. (2000) used a FT-NIR for determination of the iodine value of different vegetable oils and animal fats. In their study, it was reported that over 1200 samples of processed, blended oil samples and some animal fats (milk-fat, beef tallow, fish and lard) were used for the calibration and validation of the PLS-NIR IV model developed. This study demonstrated the ability to evaluate and predict the IV and FFA of AFW using FT-NIR.

FT-NIR has been proven to be a reliable method of rapidly determining the chemical and physical properties of edible fats (solid and liquid states) and oils. This has provided a responsive alternative to the commonly used chemical methods employed in the industry. The objectives of this study were (1) to develop calibration models based on partial least squares (PLS) regression for quantitatively measuring IV and FFA of AFW and their blends using an FT-NIR spectrometer and (2) to investigate the influence of spectral pre-processing methods on the robustness and predictability of calibration models developed using PLS-NIR.

4.2 Materials and Methods

4.2.1 Materials

Tallow (T), lard (L), choice white grease (CWG) and yellow grease (YG) were obtained from Rothsay (Canada) and pure lard (PL) was purchased from a local grocery store in Montreal. The samples were stored below -10 ^{o}C prior to use. Sodium thiosulphate, potassium iodide, sodium hydroxide, 95% ethyl alcohol, chloroform and WIJS solution used for chemical analysis were of analytical grade and purchased from Sigma Aldrich Canada Co., Ontario.

4.2.2 Methods

4.2.2.1 Samples preparation and determination of reference values*:* A set of 40 samples were prepared by blending two types of animal fats or animal fat blends (tallow, lard, CWG, YG or PL) to obtain a wide range of IV and FFA for calibration and validation of PLS-NIR model. The sample set included tallow, lard, CWG, YG, PL and 35 different blends of two types of the animal fats. For the calibration model development, 70% of AFW and their blends were randomly selected for developing the PLS-NIR calibration models for IV and FFA content of the samples, test set validation was carried out for each calibration by using the remaining 30% of the samples not used in the PLS calibration model. The test set validation samples were prepared by blending pure lard with AFW. Pure lard was also included in the test set validation samples to verify effect of impurities on calibration and validation of the models. The reference values of IV and FFA content of the samples were determined using official standard procedure and analytical chemicals AOAC 993.20 (AOAC, 1999) and the AOCS Ca 5a-40 (AOCS, 2009) methods, respectively: For IV reference value determination, 0.5 g of each sample was dissolved in 10 mL of chloroform. Twenty five (25) mL of WIJS solution was added with vigorous mixing and allowed to stand in dark for exactly 30 min with occasional shaking. An aliquot of 10 mL of 15% potassium iodide

(KI) and 100 mL of freshly boiled and cooled water were added with thorough shaking, and then titrated against 0.1 N sodium thiosulphate until yellow solution turns almost colorless. For FFA content determination, 7.05 g of each sample was dissolved in 75 mL of 95% ethanol, and were then titrated against a standardized sodium hydroxide solution (0.25 M) with phenolphthalein as indicator (1% in 95% ethanol). FFA was expressed in mg (NaOH)/g. The percentage of FFA content of the calibration standards was calculated as oleic acid while IV of the standards was estimated based on the expression of official method for iodine value. Each sample was measured in triplicate and the average value was used for NIR calibration and validation.

4.2.2.2 Chemometric analysis/sample handling: The FT-NIR spectra of tallow, lard, CWG, YG, PL and 35 blends of the animal fats were acquired using a Bruker Optics) Multi-Purpose Analyzer (MPA) FT-NIR spectrometer equipped with a thermoelectrically cooled InGaAs detector and sample compartment for measuring liquid samples in transmittance (Bruker Milton, ON, Canada). Samples of lard, tallow, choice white grease, yellow grease, pure lard and their blends were transferred into 8-mm OD glass vials using a transfer pipettes, capped and then placed into the sample holder of the MPA. The samples were heated in the compartment at 50 °C and held at that temperature for 30 seconds before scanning to ensure that each sample was fully melted, transparent and homogeneous before taking readings. FT-NIR spectral of completely melted samples were collected using 16 co-added scans at a resolution of 8 cm^{-1} between 12500 to 4000 cm^{-1} (or 800 to 2500 nm wavelength). The spectral of each sample was collected in triplicate. A background scan of air was collected without any sample in the compartment before taking measurements and then approximately every 1 hour there afterwards. The single channel spectra of the samples were automatically converted to absorbance spectra by the Bruker Optics OPUS 7.0 software.

4.2.2.3 Development of FT-NIR Quantification Model*:* For developing quantitative calibration models, PLS was used since this method does not require detailed relationships between the concentration and the absorbance measurement at specified frequencies (i.e. peak heights or peak areas), but rather develops a model by compressing the spectral data for a set of calibration samples into a series of mathematical “spectra”, known as loading spectra or factor (Li et al., 1999). The PLS models were developed using Bruker Optics’ OPUS QUANT 2 software program provided with the instrument. The data incorporated to this program included the IV and FFA content obtained from experimental procedures certified by AOAC (993.20) and AOCS (5a Ca-40) as well as the corresponding FT-NIR spectra for each sample. The calibration models for IV and FFA were developed using 70% of the samples and validated using the remaining 30% of the samples as an independent test set. Optimal calibration model for IV and FFA was selected based on the fit between the reference values and the predictions obtained by test set validation. No pre-processing (NP) and four spectral pre-processing options were investigated in the calibration model developments; first derivative (FD), second derivatives (SD), vector normalization (VN) and multiplicative scatter correction (MSC). Models that gave the lowest possible rank (latent variable) with the highest coefficient of determination (R^2), lowest root mean square error of estimation (RMSEE), lowest root mean square error of prediction (RMSEP) and highest value of residual prediction deviation (RPD) were chosen. RMSEE measures the model’s ability to predict new samples. RPD is the ratio of the standard deviation of the reference data divided by standard error of prediction (SEP) and was used to verify the accuracy of the calibration models developed. Ability of the calibration to predict IV and FFA content was assessed using the coefficient of determination and RMSEP of test set validation as well as by comparing the FT-NIR predicted IV and FFA values to the values obtained by the AOAC and AOCS methods.

4.3 Results and Discussion

4.3.1 Chemical data

The percentage blend ratio (weight/weight) of AFW for IV and FFA reference values varied between 25 to 85%. The range of reference IV was 37.56 - 80.70 $gI_2/100g$, while the range for the reference FFA content was 0.20 - 19.09%. These data sets were of good correlation with those in the PLS-NIR test set validation results for IV and FFA pre-processing methods investigated. The IV and FFA reference data for the four AFW were within the normal range of variation reported by other authors (Cox et al., 2000; Knothe, 2002; Olsen et al., 2010). These results showed wide variability, which is important when searching for calibration equations to be used for predictions of new animal fat waste samples.

4.3.2 Spectral information

Figure 4.1 shows the raw absorbance spectra for the five animal fat samples and their blends. The NIR spectral pattern of tallow, lard, CWG, YG, PL and their blends were very similar. There was a slight variation in the baseline of absorbance spectral which could be attributed to the different scattering characteristics of impurities that may be present in the sample mixtures. Therefore, four spectra pre-processing derivatives (FD, SD, MSC and VN) were employed to correct spectra baseline defect due to scattering of blends. FD of the spectrum emphasizes the steep edges of a peak so that small features can be more readily observed over a broad background. Similarly to FD the SD further enhances spectrum increasing resolution between peaks and at the same time enhancing noise. MSC is a spectral pre-processing method which fits each spectrum to the average spectrum as closely as possible using least squares thereby reducing effects of light scattering.

Likewise, VN procedure eliminates scattering effects by mean centering the spectra in the data set and then scaling the sample spectrum by dividing the spectrum by the square root of its sum.

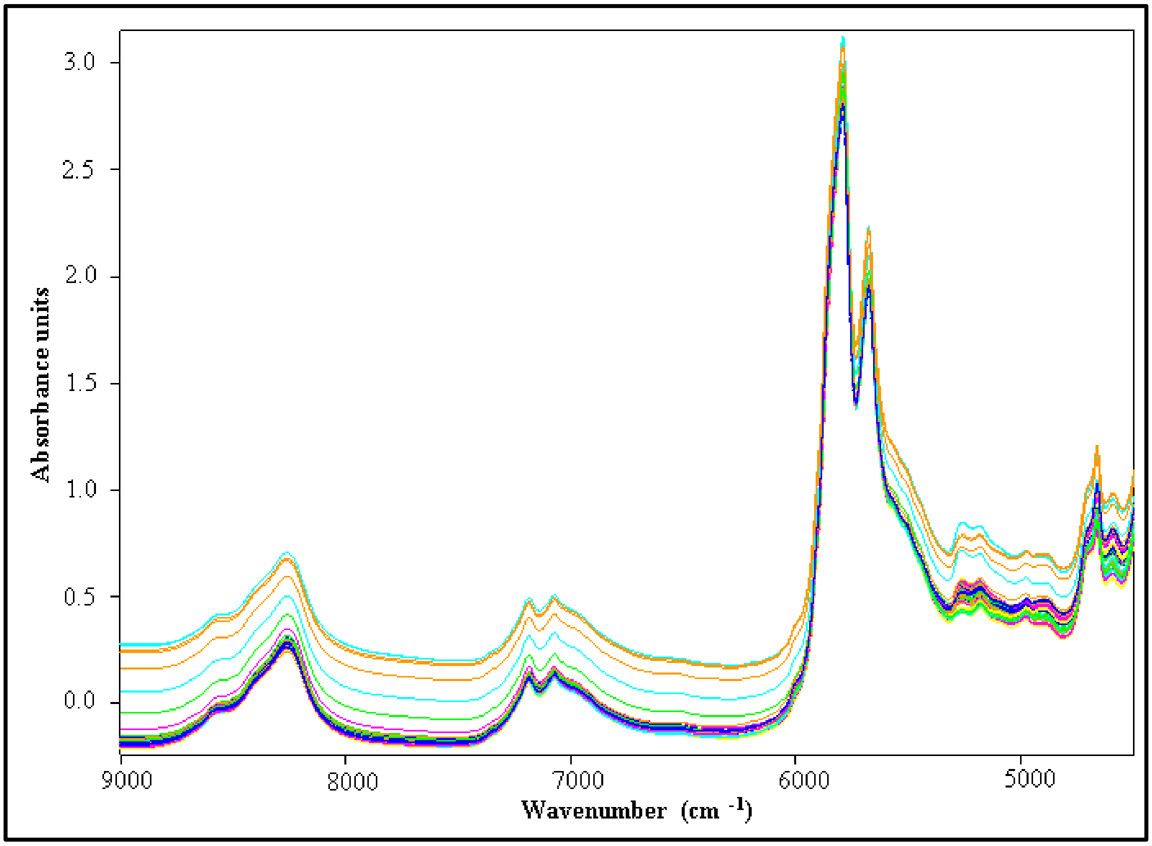

Figure 4.1: Raw FT-NIR spectral of the animal fat and their blends

Li et al. (1999) reported optimized calibration regions for rapid determination of rapid determination of IV of edible oils to be 8975-7189, 6085-5938, and 4698-4553 (cm^{-1}). It was also reported in their results that most strong absorption bands of the calibration samples were observed at CH and CH_2 overtones. These overtones occurred at 8285, 7185, around 7100, 5829 and 5767 cm^{-1} together with minor absorption bands in the range between 4800 and 4540 cm^{-1}. The absorption bands around 8285 cm^{-1} comprised the second overtones of CH, while those between 6200-5500 cm^{-1} are attributed to the first overtones of CH which comprises $–CH_3$, $–CH_2–$ and –HC–CH–. Cox et al. (2000) identified NIR spectral region for unsaturation (IV) in the second overtone to be 7500 to 9100 cm^{-1} (1333–1100 nm). It was subsequently reported that this spectral region is uniform for a wide variety of oils and fats.

The FD, SD, MSC and VN of the average spectrum of animal fats and their blends are shown in Figure 4.2(a-d). The spectral band at 6900 cm^{-1} in the first overtone region is due to the O–H first overtone of carboxylic acids, which is related to the FFA content of the animal fats and their blends. The second overtone region between 7600 – 9000 cm^{-1} corresponds to C–H stretching band, the band most commonly used for NIR iodine value determination (Cox et al., 2000; Li et al., 1999). In general, because the NIR region corresponds to the absorption of overtones and combinations of the fundamental frequency molecular vibrations, NIR spectra features are broad and highly overlap. Therefore, chemometric methods such as principal component analysis (PCA) and PLS need to be employed to detect spectral differences by computing latent variables, also known as loading spectra, that are related to the component of interest.

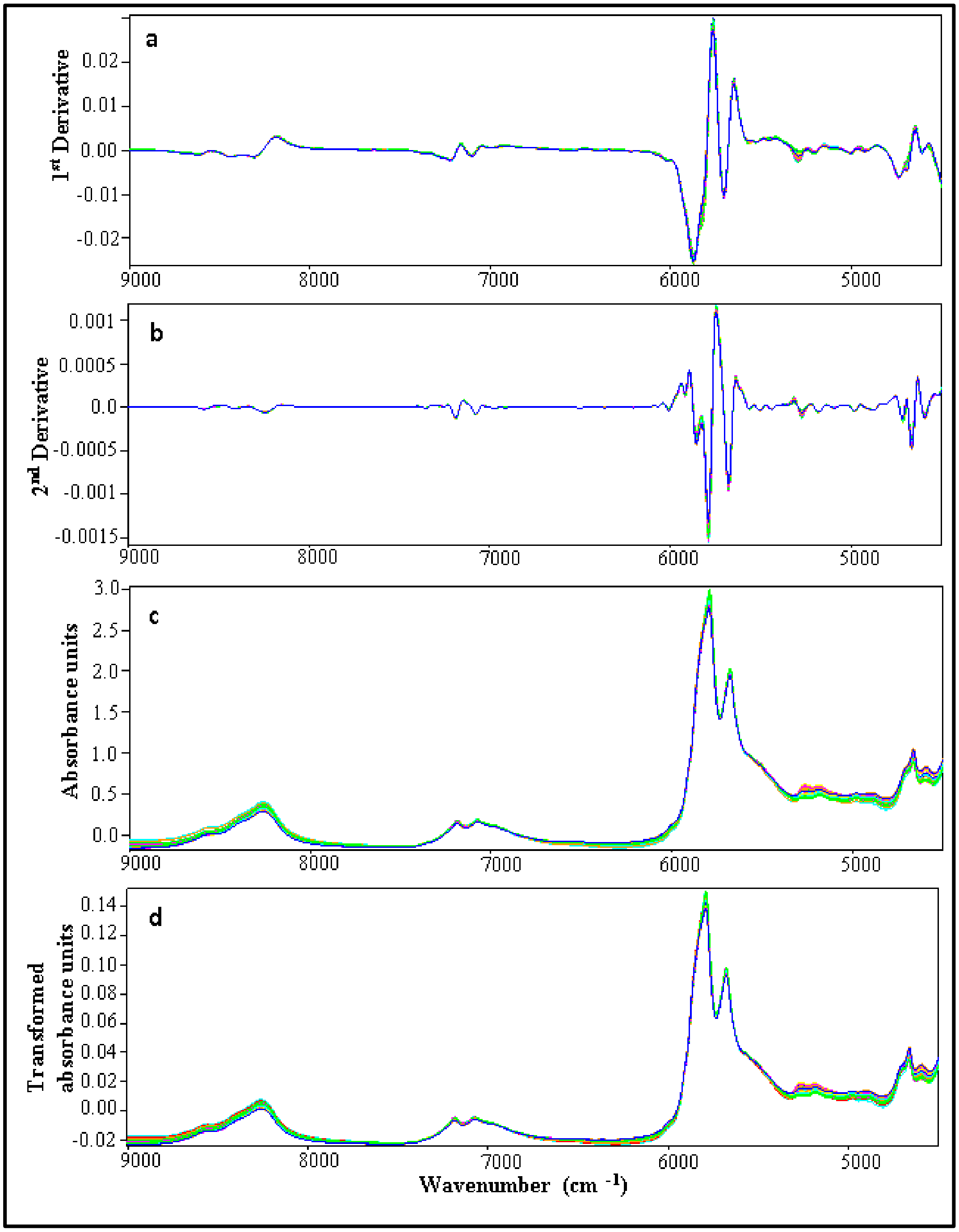

Figure 4.2: Plot of preprocessed spectra of animal fat waste and their blends (a) First derivative (b) Second derivative (c) Multiplicative scatter correction (d) Vector normalization

4.3.3 Calibration Model for Iodine Value and Free Fatty Acid Content

PLS regression was used to develop calibration models for the IV and FFA content of AFW and their blends. The presence of spectral outlier was examined by using PCA and by comparing the Mahalanobis distance of each sample spectrum in the data set relative to the spectra of the other calibration samples. No spectral outlier was found in the calibration data set and this shows that the samples selected for the calibration data set were determined accurately and were not significantly contaminated. PLS regression of the calibration spectral was then carried out using different spectral regions and pre-processing techniques, and each model was evaluated by test set validation. For the calibration model development, 70% of AFW and their blends were randomly selected for developing the PLS-NIR calibration models for IV and FFA content of the samples. For each of the parameters of interest, the regions and preprocessing method selected that gave the lowest prediction error with the lowest rank was chosen as the most robust model.

Table 4.1 shows spectral region, data preprocessing method, rank, coefficient of determination (R^2), root mean square error of estimation (RMSEE), and residual prediction deviation (RPD) for the PLS calibration models developed for IV and FFA content. The spectral regions selected for the calibration models for IV and FFA included the corresponding component observed NIR spectral band intensity changes. Figure 4.3 shows the approximate spectral band (9000-7500 cm^{-1}) related to IV which was used for the model development. Prediction equations developed using each of the spectral preprocessed method for the IV and FFA by using the OPUS Quant 2 PLS algorithm are presented in Figures 4.4 and 4.5.

Table 4.1: Spectral regions, data preprocessing methods and PLS regression models results for iodine value and free fatty acid content in animal fat waste and their blends

Iodine value (9000 – 7502 (cm^{-1}))

Data Pre-processing	**Rank**	**R^2**	**RMSEE (gI_2/100g)**	**RPD**
NP	8	99.00	1.23	10.00
FD	6	98.70	1.40	8.76
SD	8	98.92	1.28	9.64
VN	6	97.58	1.89	6.43
MSC	5	97.88	1.75	6.86

Free fatty acid (7502 – 6098 (cm^{-1}))

Data Pre-processing	**Rank**	**R^2**	**RMSEE (%)**	**RPD**
NP	7	99.67	0.376	17.4
FD	7	99.91	0.195	34.0
SD	9	99.93	0.182	36.8
VN	10	99.94	0.169	40.1
MSC	5	99.00	0.644	9.99

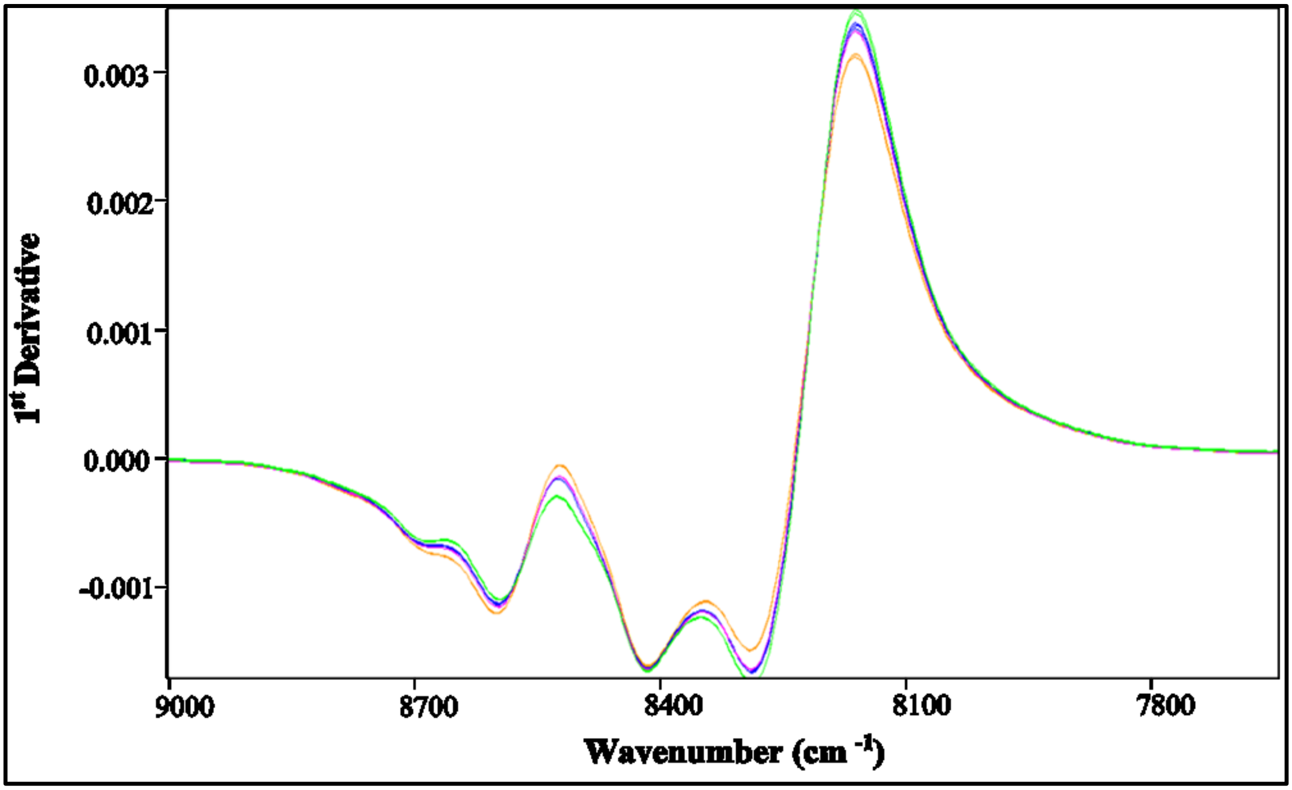

Figure 4.3: First derivative of the spectral of animal fats and their blends for the second overtone region over the spectral range between 9,000 and 7,500 cm^{-1}

The higher the RPD value, the greater the probability of the model to accurately predict the chemical composition of a new sample set. Williams (2001) and Natsuga and Kawamura (2006) reported that RPD ranges: 0.0 to 2.3 as not recommended, 2.4 to 3.0 as very rough screening quality, 3.1 to 4.9 as screening quality, 5.0 to 6.4 as quality control, 6.5 to 8.0 as process control, and > 8.1 suitable for any application. For IV models, RPD of both FD and SD is greater than 8.1. For FFA models, RPD of FD, SD, MSC and VN is greater than 8.1 which make the models suitable to predict IV and FFA content of any animal fat. Both SD and FD pre-processing methods reduced baseline offset due to scattering (Figure 4.2), but FD calibration model is favoured with lower rank (latent variable) compare to SD calibration model. The sample spectral produced by MSC and VN pre-processing methods still contained some baseline shifts dues to scattering. Hence, the calibration model developed by FD pre-processing method has been chosen as the best predicting model for both IV and FFA content of AFW and their blends.

4.3.4 Prediction of the Iodine Value and Free Fatty Acid Contents

A test set validation was carried out for each calibration by using the remaining 30% of samples not used in the PLS calibration model. Table 4.2 details the value for R^2, RMSEP, bias and slope between the actual and the predicted values for the IV and FFA content of the samples. There was a good correlation between the reference values and the PLS-NIR predicted values of both IV and FFA content for the preprocessed spectral methods. Figures 4.4 and 4.5 show the model equations for the predicted and the reference values of IV, FFA content and R^2 for each of the pre-processed and no pre-processing spectral methods investigated. Despite the fact that PLS-NIR results of all the spectral pre-processing methods and no pre-processing (NP) methods showed good predictability qualities, FD and SD show the best correlation between PLS-NIR of both IV and FFA content of the samples and their reference values (Table 4.2).

In the IV and FFA content model equations, the results indicate that there was a comparatively good correlation between the reference values and FT-NIR predictions with little bias between the methods (bias < RMSEP), values for the slope of the regression line > 0.9, and RMSEP values comparable to their respective RMSEE values in Table 4.1. In general, the results showed relatively good predictions for the test set validation indicating that the calibration models are robust. Based on these results, it was determined that the FT-NIR predictions are comparable to their corresponding reference methods for IV and FFA determination and therefore the FT-NIR based method for AFW and their blends analysis is suitable for rapid measurement of IV and FFA content of animal fat waste feedstocks for biodiesel production.

Table 4.2: Validation of reference values and FT-NIR predictions of an independent test set validation for the determination of iodine value and free fatty acid content of animal fat waste and their blends.

Iodine Value

Data Pre-processing	R^2	RMSEP ($gI_2/100g$)	Bias	Slope
NP	97.47	1.36	0.43	1.03
FD	98.24	1.13	0.42	1.03
SD	97.82	1.26	0.51	1.04
VN	96.70	1.55	0.34	1.01
MSC	97.07	1.46	0.43	1.02

Free fatty acid

Data Pre-processing	R^2	RMSEP (%)	Bias	Slope
NP	98.75	0.489	0.18	0.97
FD	98.81	0.477	0.26	0.99
SD	98.80	0.478	0.15	0.98
VN	97.36	0.709	0.59	0.97
MSC	98.11	0.601	0.31	0.96

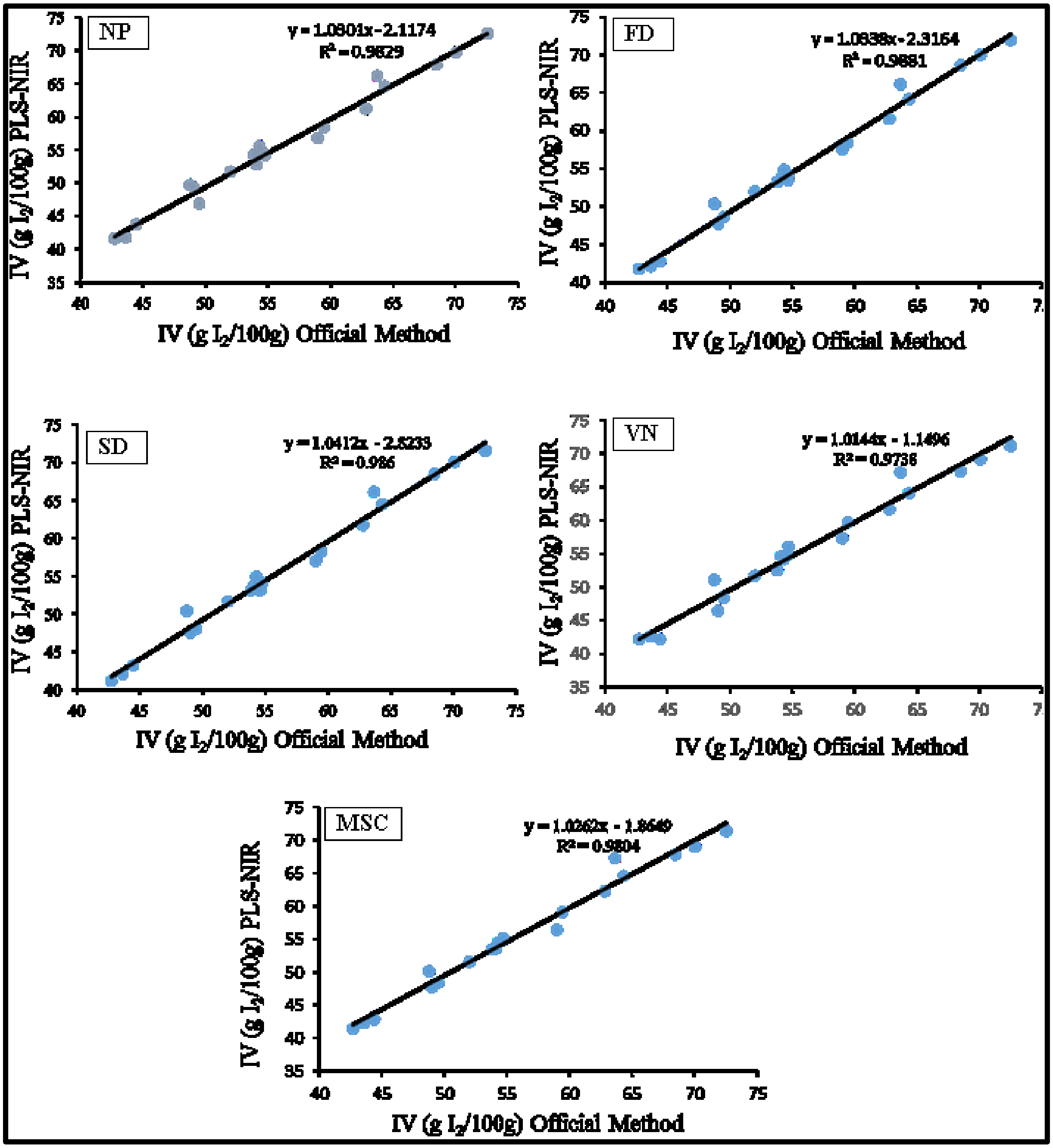

NP - No Preprocessing; FD - First Derivative; SD - Second Derivative; VN - Vector Normalization; MSC - Multiplicative Scatter Correction

Figure 4.4: Plot of predicted vs. true IV values for the test validation samples

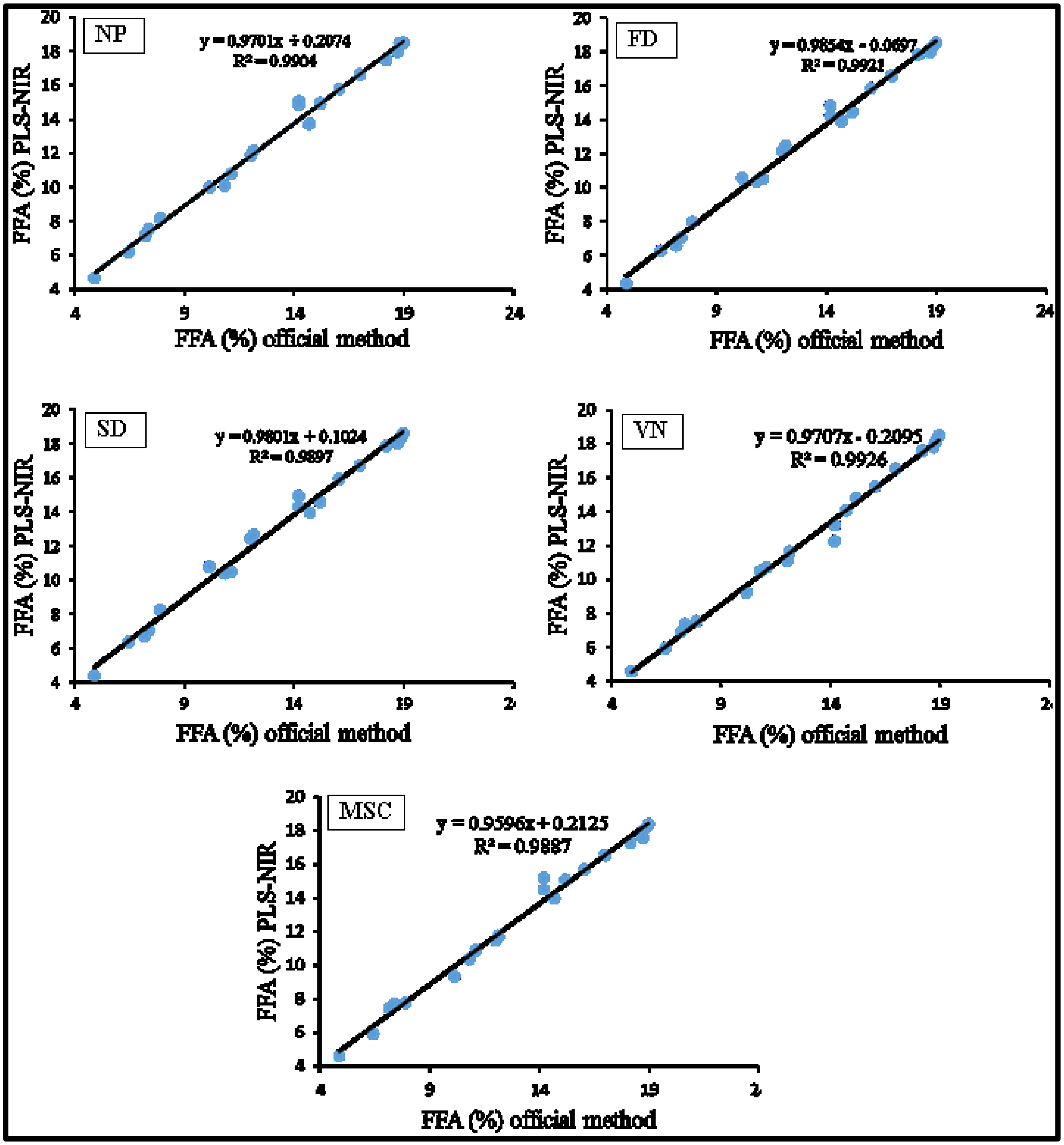

NP - No Preprocessing; FD - First Derivative; SD - Second Derivative; VN - Vector Normalization; MSC - Multiplicative Scatter Correction

Figure 4.5: Plot of predicted vs. true FFA values for the test validation samples

4.4 Conclusion

In this paper, we discussed the influence that FD, SD, MSC and VN pre-processing methods has on the PLS-NIR calibration modeling for the FT-NIR spectroscopy analysis IV and FFA content of AFW and their blends. More robust calibrations were obtained by using real production samples, and variability in the sample data set can be introduced by blending animal fat feedstocks directly in the biodiesel production reactor. The results show that FT-NIR is capable of providing a rapid and accurate measurement of IV and FFA of animal fats and their blends destined for biodiesel production with a proper calibration and a responsive model. Once the calibrations are in place, FT-NIR is a fast and easy to use method for the IV and FFA content measurement in a biodiesel production environment. It drastically reduces the time from routine biodiesel feedstock quality control analysis and does not involve the use of any chemical reagents. FD pre-processing method was found to give a robust and reliable calibration model for both IV and FFA measurement. Conclusively, using FT-NIR spectroscopy as a biodiesel feedstock (AFW and blends) quality control tool for IV and FFA measurement will reduce cost of production and possible chemical hazard in the production environment.

CONNECTING TEXT TO CHAPTER 5

In chapters 3 and 4, the use of conventional and non-destructive techniques for AFW characterization were employed, respectively. Our findings from these two chapters were used to select parameter range of the investigated factors such as molar ratio of waste fat to methanol in Chapter 5 based on the amount of FFA in each of the waste fat samples. This chapter provides a description of data collection and methodology used for enzyme-catalyzed synthesis and kinetic of biodiesel production from waste tallow assisted by ultrasonication. Chapter 5 manuscript was published in Ultrasonics Sonochemistry Journal in May, 2015. The manuscript is co-authored by Drs. Dumont, M.-J., and Ngadi, M. The format of the manuscript has been altered to be consistent with this thesis. All literature cited in this chapter is listed in the references section at the end of this thesis.

Peter Adewale, Marie-Josee Dumont and Michael Ngadi, 2015. Enzyme-catalyzed synthesis of biodiesel from waste tallow assisted by ultrasonication. Ultrasonics Sonochemistry, 27, 1-9; doi:10.1016/j.ultsonch.2015.04.032.

Chapter 5

Enzyme-catalyzed synthesis and kinetic of biodiesel production from waste tallow assisted by ultrasonication

Abstract

The use of ultrasonic processing was evaluated for its ability to achieve adequate mixing while providing sufficient activation energy for the enzymatic transesterification of waste tallow. The effects of ultrasonic parameters (amplitude, cycle and pulse) and major reaction factors (molar ratio and enzyme concentration) on the reaction kinetic of biodiesel generation from waste tallow bio-catalyzed by immobilized lipase [*Candida antarctica* Lipase B (CALB)] were investigated. Three experimental sets namely A, B, and C were conducted. In experiment set A, two factors (ultrasonic amplitude and cycle) were investigated at three levels; in experiment set B, two factors (molar ratio and enzyme concentration) were examined at three levels; and in experiment set C, two factors (ultrasonic amplitude and reaction time) were investigated at five levels. A Ping Pong Bi Bi kinetic model approach was employed to study the effect of ultrasonic amplitude on the enzymatic transesterification. Kinetic constants of transesterification reaction were determined at different ultrasonic amplitudes (30, 35, 40, 45, and 50%) and enzyme concentrations (4, 6, and 8% wt. of fat) at constant molar ratio (fat:methanol); 1:6, and ultrasonic cycle; 5 Hz. Optimal conditions for ultrasound-assisted biodiesel production from waste tallow were fat:methanol molar ratio, 1:4; catalyst level 6% (w/w of fat); reaction time, 20 min (30 times less than conventional batch processes); ultrasonic amplitude 40% at 5 Hz. The kinetic model results reveal interesting features of ultrasound assisted enzyme-catalyzed transesterification (as compared to conventional system): at ultrasonic amplitude 40%, the reaction activities within the system seemed to be steady

after 7 min which means the reaction could proceed with or without ultrasonic mixing. Reversed phase high performance liquid chromatography indicated the biodiesel yield to be 85.6 ± 0.08%.

5.1 Introduction

Energy and mixing requirements of batch reactors commonly employed in biodiesel production are provided by heating systems and mechanical agitators, respectively. However, such production methods are costly in terms of time, reagents, and labour. Indeed, conventional transesterification reactions, particularly those which are enzyme catalyzed are rather time consuming. For example, Lu et al. (2007) reported a biodiesel yield of 87.4% through the synthesis of fatty acid methyl esters (FAME) from lard with immobilized *Candida* sp. 99-125 using reciprocal shaker mixing technique operating at 180 rpm, 40 °C, and a 30 h reaction time. Similarly, Aryee et al. (2011) reported a fatty acid ethyl ester (FAEE) yield of 50% through enzymatic transesterification of fats and oils from animal discards with immobilized *Mucor miehei* (Lipozyme-IM) using shaking water bath mixing technique at 25°C and 96 h of reaction time. In order to further enhance miscibility of substrates during transesterification reaction, application of ultrasonication has been studied as an alternative remedy. Choudhury et al. (2013); Mahamuni and Adewuyi (2009); Teixeira et al. (2009) and Colucci et al. (2005) reported the feasibilities of ultrasound-assisted transesterification of vegetable oils and animal fats using acid and alkaline catalysis.

While ultrasonic-assisted transesterification of different vegetable oils has been widely investigated and reported (Al-Zuhair et al., 2012; Chand et al., 2010; Fan et al., 2010; Hsiao et al., 2010; Kumar et al., 2012; Kumar et al., 2011a; Zou and Lei, 2012), few reports of ultrasonic-assisted transesterification of AFW appear in the literature. In an evaluation of ultrasonic-assisted ethanolysis production of biodiesel from fish oil (Armenta et al., 2007a), the authors examined the effects of different parameters including: ultrasonic device (bath vs. probe), catalyst type (potassium hydroxide vs. sodium ethoxide), catalyst concentration (0.5 vs. 1%), temperature (20°C vs. 60°C), and duration of exposure (10–90 min) on the production process. They concluded that sodium ethoxide was a more efficient catalyst than potassium hydroxide. Comparing biodiesel yield from conventional *vs.* ultrasonic-assisted transesterification of beef tallow, Teixeira et al. (2009) found methanolysis of triglycerides using ultrasonic power to be an efficient, time-saving and economical method of producing biodiesel fuel. However, the authors did not report effects of reaction and ultrasonic parameters on the yield of biodiesel from the feedstock.

Similarly, studies on ultrasound-assisted transesterification of vegetable oils and animal fats using conventional catalysts (acid and base) and their possible reaction kinetic pathways have been extensively reported (Armenta et al., 2007a; Colucci et al., 2005; Elizabeth Grant and Gnaneswar Gude, 2014; Kumar et al., 2012; Kumar et al., 2010; Salamatinia et al., 2013; Teixeira et al., 2009). Enzyme-catalyzed transesterification and esterification reactions were reported to possibly proceed kinetically by Ping Pong Bi Bi mechanism, ternary complex ordered Bi Bi mechanism, or ternary complex random Bi Bi mechanism (Hari Krishna and Karanth, 2001; Shinde and Yadav, 2014; Veny et al., 2014). In ping pong mechanism, one substrate binds to release one product before the second substrate can bind in order to release the second product. For the ternary complex ordered mechanism, substrates bind to the enzyme in a defined sequence that is one substrate must bind before the second substrate can bind and the products are releases in a defined sequence. Ternary complex random mechanism is similar to ordered sequential but there is no defined order in which substrates must bind or products must be released. Most recent kinetic studies of enzymatic transesterification of vegetable oils and fats for the production of biodiesel have been focused on triglycerides (TG) pathway rather than FFA pathway (Al-Zuhair, 2005; Al-Zuhair et al., 2009; Al-Zuhair et al., 2007; Cheirsilp et al., 2008; Salamatinia et al., 2013). Consecutive application of hydrolysis and esterification reactions pathway for the production of biodiesel leads to a product with high acid value due to remnant FFA produced during hydrolysis reaction (Ciudad et al., 2011; Hari Krishna and Karanth, 2001; Talukder et al., 2009). On the contrary, biodiesel production mainly through transesterification reaction pathway tends to contain acid value near the established international biodiesel standards (Cheirsilp et al., 2008).

In the investigation of Azócar et al. (2014) on the reaction kinetic of enzymatic biodiesel production from waste frying oil (WFO) and crude rapeseed oil using co-solvent and an anhydrous medium to improve lipase performance in a semi-continuous reactor, the authors described the reaction mechanism as a Ping Pong Bi Bi model and reported methanol as the competitive inhibitor. Hari Krishna and Karanth (2001) studied lipase-catalyzed synthesis of isoamyl butyrate kinetics using the immobilized lipase Lipozyme IM-20 from *Rhizomucor miehei*. The authors reported the reaction route to be a Ping Pong Bi Bi model and identified isoamyl alcohol and butyric acid as two competitive substrate inhibitors. Similarly, Veny et al. (2014) proposed a kinetic model of lipase catalyzed transesterification of jatropha oil in circulated batch packed bed reactor based on Ping Pong Bi Bi mechanism with reverse inhibition by methanol.

This work seeks to investigate the effects of ultrasound parameters and reaction kinetic of enzyme-catalyzed transesterification pathway assisted by ultrasonication to produce biodiesel from waste tallow. The effects of ultrasonic wave amplitude, ultrasonic cycles, and reaction parameters (e.g. fat:methanol molar ratio, enzyme concentration, duration) on biodiesel yields from waste tallow were examined. Moreover, an acoustic mixing and mechanism of enzyme-catalyzed transesterification pathway were used for the reaction kinetic modeling of biodiesel production from waste tallow assisted by ultrasonication.

5.2 Materials and methods

5.2.1 Materials and equipment

Waste beef tallow was obtained from a biodiesel production company in Canada (Rothsay Biodiesel, Montreal, Canada). Commercially produced immobilized *Candida antarctica* lipase B (CALB) was purchased from CLEA Technologies (Delftechpark, The Netherland). American Chemical Society (ACS) and HPLC grades of methanol were purchased from Fisher Scientific (Ontario, Canada). Saturated and unsaturated FAME standards for calibration curves were purchased from Sigma Aldrich, (Oakville, ON, Canada).

An ultrasonication set-up featuring a Vibra-Cell (VXC 500 series, Sonic and Materials Inc., CT, USA) was employed for the transesterification reaction. The Vibra-Cell device is designed to ensure uniform sonotrode probe amplitude, regardless of the varying loading conditions encountered during the processing cycle. The ultrasonic device operates at 500 W and 20 kHz frequency. The probe amplitude, cycle and pulse are adjustable from 0 to 100%, 0.1 - 1.0 per sec and 0.1 - 1.0 sec, respectively. For the identification and quantification of biodiesel produced, a Varian HPLC equipped with a refractive index (RI) detector and reverse phase (RP) C18 column was used.

5.2.2 Experimental set-up and procedure

The solvent free production of biodiesel from waste tallow involved an immobilized lipase catalyst (CALB), and transesterification with methanol to yield methyl esters. The transesterification of waste tallow using ultrasonication (Vibra-Cell) was carried out in a screw cap bottle (25 mL). The effects of processing and ultrasonic parameters such as amplitude, cycle, reaction time, molar ratio and loaded catalyst (enzyme) were carefully examined. Ultrasound amplitude was varied from low to mild regions (30, 35, 40, 45, and 50%) in order to prevent disintegration of the immobilized enzyme matrix by ultrasound waves. The ultrasonic wave cycle was investigated at 3, 5, and 7 per sec, factorially combined with three levels of ultrasonic amplitudes (30, 40, and 50%). In investigating the transesterification reaction, fat:methanol molar ratios of 1:4, 1:6, and 1:8, were factorially combined with enzyme concentration of 4, 6 and 8% (w/w) of fat. Three sets of experiments namely A, B, and C were conducted which allows us to study the effect of each factor on the yield, as well as the effects of interactions between factors on the biodiesel yield and to identify most important level of each of the factors. In experiment set A, two factors (ultrasonic amplitude and cycle) were investigated at three levels (3^2). Other parameters (molar ratio, enzyme concentration and reaction time) were kept constant. In experiment set B, two factors (Molar ratio and enzyme concentration) were examined at three levels (3^2). Other parameters (ultrasonic amplitude, ultrasonic cycle and reaction time) were kept constant. In experiment set C, two factors (ultrasonic amplitude and reaction time) were investigated at five levels (5^2) (Table 5.1).

Table 5.1: Experimental set, independent variables and levels used in the full factorial design for the enzymatic transesterification assisted by ultrasonication

Experiment set	**Experimental parameter values (constants in bold)**				
	Amplitude (%)	**No.Cycles (Hz)**	**Enzyme Conc. (% w/w of fat)**	**Fat : Methanol ratio**	**Reaction time (min)**
A	30	3	**6**	**1:6**	**30**
	40	5			
	50	7			
B	**40**	**5**	4	1:4	**30**
			6	1:6	
			8	1:8	
C	30	**5**	**6**	**1:6**	10
	35				15
	40				20
	45				25
	50				30

Fat samples stored below -20ºC prior to analysis, were melted in a water bath (50ºC) before sampling. A fat sample (10 g) was then transferred to a 25 mL screw cap bottle and subjected to ultrasound waves for 1 min in order to further break down all possible fat crystals before the addition of other reagents. The mixture of all reagents was introduced, and ultrasound waves applied according to pre-set parameters. With the sonotrode probe submerged and fixed at a depth of 20 mm in the solution, the ultrasonic amplitude, ultrasonic cycle and the reaction time were adjusted using the controller. At each reaction time, a 500 µL aliquot was pipetted into a 2 mL micro centrifuge tube. The reaction was stopped by the addition of 50 µL of glacial acetic acid while 1 mL distilled water was added to wash excess methanol and traces of glycerol from the ester layer. The mixture was vortexed for 3 min before being centrifuged for 10 min at 10,000 × g using an Eppendorf 5415R Micro-centrifuge (Eppendorf Canada Ltd., Mississauga, Ontario) to separate the upper ester and lower aqueous phase. The upper layer is a mixture of esters while the lower layer is a mixture of glycerol, enzyme and aqueous solutions. For the analysis, 100 µL of the ester phase was diluted with acetone to an appropriate concentration before HPLC injection.

To further investigate the effects of ultrasonic parameters on the reaction kinetics of enzyme-catalyzed transesterification of waste tallow, series of experiments were performed at varying ultrasound amplitude in the absence of CALB enzyme, no products were detected in those experiments. But a significant concentrations of intermediate glyceride products mostly monoglyceride, and diglyceride were observed (Data not reported). This confirmed that ultrasonic parameters only assisted in the enzyme-catalyzed transesterification reaction but did not cause the product formation without the presence of CALB enzyme.

5.2.3 Standard calibration curves, biodiesel identification and quantification by HPLC

Calibration curves for FAME standards were developed by injecting six different concentrations (0.5-3.0 mg/mL) of each of the FAME standards expected to elute in the reaction products. The retention time of each of the FAME standards was matched to the corresponding peaks produced by the biodiesel samples. Analysis of the FAME standards and the reaction product were carried out by dissolving the samples in acetone. Some other solvents such as methanol, hexane, chloroform, and toluene were considered but the reaction product showed their greatest solubility in acetone. An external standard quantitation procedure on HPLC was used to develop the FAME standard calibration curves employed in this study. This procedure is a basic quantification approach in which both standard and unknown samples are analysed under the same conditions and the results from the unknown samples are then related to those of the standard samples. The curves were constructed by injecting different known concentrations of the standard solution and measuring the peak area obtained. A regression line of best fit was used to join the points of the curve obtained. All calibration concentration points were ran in triplicate. The best fit regression line gave a correlation coefficient which measured how well the data point's best fit to a straight line. The correlation coefficient equally showed predictability strength of the developed calibration curves to measure the concentrations of the unknown analytes. The developed calibration curves were used to estimate the amount of the desired compounds in the biodiesel aliquot.

The ester phase was analyzed by RP-HPLC which separated the different product components according to their polarity. A Varian HPLC unit equipped with a Varian Prostar 240 pump, a reverse phase (RP) Discovery HS C18, 5 µm, 25 cm × 4.6 mm column (Supelco Analytical, Bellefonte, PA, USA), and a Varian 356-LC refractive index (RI) detector (Varian Inc., Walnut

Creek, CA, USA) was used to analyze and quantify the conversion, the FAME composition and the purity of the ester phase (Chakraborty and Sahu, 2014). For all the experiments, an isocratic mobile phase method was used for the separation and determination of the biodiesel produced by the methanolysis of waste tallow. The system operated at a flow rate of 1 mL/min, with an injection volume of 25 μL, and a sample runtime of 30 minutes.

$$\%\text{Yield (FAME)} = \frac{\sum \text{FAME}}{\sum(\text{TG}+\text{DG}+\text{MG}+\text{FFA}+\sum \text{FAME})} \qquad 5\text{-}1$$

Where, DG and MG are diglycerides, and MG, respectively.

5.2.4 Kinetic model development

In enzyme-catalyzed reaction kinetics, the reaction rate is measured by varying the effects of the reaction conditions (Yang et al., 2005) and monitor how these varying parameters affect the enzyme activities in term of product yields. The kinetic mechanism of enzyme-catalyzed transesterification of beef tallow was developed based on ping pong Bi Bi Cleland nomenclature for two substrates (Meunier et al., 2014a). The substrates bind to the enzyme's active reaction site and then transformed into products through a series of steps known as the enzymatic mechanism.

5.2.4.1 Enzyme kinetics mechanisms

Equation 5.2 represents a typical multi-substrate Bi-Bi enzyme kinetic of transesterification reaction: TG and methanol (M) are the substrates while biodiesel (Bd) and glycerol (G) are the products. In this mechanism, the enzyme (E) must bind the first substrate (TG) to form enzyme-substrate complex [ETG], and then released the first product (Bd) and transformed intermediate enzyme ($E^{'}$). This is followed by binding of second substrate (M) to ($E^{'}$) and breakdown of the transitory complex [$E^{'}$M] to free enzyme (E) and the second product (G) (Cheirsilp et al., 2008; Veny et al., 2014; Yang et al., 2005).

$$\mathrm{TG} + \mathrm{M} \overset{\mathrm{E}}{\leftrightarrow} \mathrm{Bd} + \mathrm{G} \qquad 5\text{-}2$$

The reaction mechanism (Ping Pong Bi Bi) can be described as follows:

$$\mathrm{E} + \mathrm{TG} \underset{\mathrm{k_2}}{\overset{\mathrm{k_1}}{\leftrightarrow}} [\mathrm{ETG}] \overset{\mathrm{k_3}}{\Rightarrow} \mathrm{E'} + \mathrm{Bd} \qquad 5\text{-}3$$

$$\mathrm{E'} + \mathrm{M} \underset{\mathrm{k_5}}{\overset{\mathrm{k_4}}{\leftrightarrow}} [\mathrm{E'M}] \overset{\mathrm{k_6}}{\Rightarrow} \mathrm{E} + \mathrm{G} \qquad 5\text{-}4$$

Equation 5.3 represents the formation of the enzyme–substrate complex with TG [ETG], the release of Bd from this complex and the generation of transformed enzyme (E'). The formation of the transformed enzyme-substrate complex with M [E'M] and the release of the second product (G) and free enzyme (E) is shown in equation 5.4. Rate constants k_1 and k_4 are for the enzyme–substrate complex associations for TG and M, respectively; k_2 and k_5 are rate constants of the enzyme–substrate complex dissociations for TG and M, respectively; k_3 and k_6 are the catalytic rate constants for the formation of products Bd and G, respectively. The rate expressions for the overall reaction mechanism (Equations 5.3 and 5.4) above, without considering possible intermediate glycerides (di- and monoglyceride) are expressed as in Equations. 5.5 – 5.12. Because a much faster reaction occurs with the diglyceride and monoglyceride than the triglyceride, hence the overall reaction can be used to develop a simplified model instead of the all three reaction steps (Azócar et al., 2014).

$$\frac{\mathrm{d(TG)}}{\mathrm{dt}} = -\mathrm{k_1}[\mathrm{TG}][\mathrm{E}] + \mathrm{k_2}[\mathrm{ETG}] \qquad 5\text{-}5$$

$$\frac{\mathrm{d(M)}}{\mathrm{dt}} = -\mathrm{k_4}[\mathrm{M}][\mathrm{E'}] + \mathrm{k_5}[\mathrm{E'M}] \qquad 5\text{-}6$$

$$\frac{\mathrm{d(Bd)}}{\mathrm{dt}} = \mathrm{k_3}[\mathrm{ETG}] \qquad 5\text{-}7$$

$$\frac{d(G)}{dt} = k_6[E'M] \qquad 5\text{-}8$$

$$\frac{d(E)}{dt} = -k_1[TG][E] + k_2[ETG] + k_6[E'M] \qquad 5\text{-}9$$

$$\frac{d(E')}{dt} = -k_4[M][E'] + k_5[E'M] + k_3[ETG] \qquad 5\text{-}10$$

$$\frac{d(ETG)}{dt} = k_1[TG][E] - k_2[ETG] - k_3[ETG] \qquad 5\text{-}11$$

$$\frac{d(E'M)}{dt} = k_4[M][E'] - k_5[E'M] - k_6[E'M] \qquad 5\text{-}12$$

The influence of external and internal mass transfer on the reaction kinetic was assumed negligible due to small volume of the reaction vessel and given that immobilized lipase would be more accessible. A single response that was used to justify possibility of mass transfer was the biodiesel yield from the combination of the independent variables. Based on these assumptions, the reaction kinetics was studied independently of the mass transfer, which made the model to be mass transfer limited.

5.2.4.2 Determination of kinetic parameters

The concentrations of the substrates, free fatty acid and fatty acid methyl ester (biodiesel) at different times were determined experimentally starting with 10 g of waste beef tallow and varied methanol amounts of 1.51, 2.27 and 3.03 g to obtain molar ratios of methanol to beef tallow of 4, 6 and 8, respectively. The effects processing parameters; ultrasonic amplitude (30, 35, 40, 45, and 50%) at varied reaction time (5, 10, 15, 20, 25, and 30 min.) on the reaction rates of enzyme-catalyzed transesterification of waste beef tallow were investigated. This was achieved by fitting the reaction rate differential equations generated based on Ping Pong Bi Bi mechanism to the experimental data. The reaction rate differential equations and variable definitions as generated in equations 5.5 - 5.12 were used to develop kinetic reaction model in Mathematica programming software where they were solved by the NDSolve function to generate model and experimental data time plots. The values of rate constants were estimated at best fitted plot of model and experimental data.

5.2.5 Statistical Analysis

A full factorial design was used for each of the three experimental sets ran independently to verify effects of ultrasound and reaction parameters on the biodiesel yields from waste beef tallow. Statistical analysis was carried out using the procedure of analysis of variance (PROC ANOVA), graphic plot (PROC GPLOT) and Box plot (PROC BOXPLOT) procedures using SAS (Statistical Analysis Systems, Version 9.4, SAS Institute Inc., Cary, NC, USA). Mean comparison of each of the parameters levels and their significant differences were analyzed by Tukey's studentized range test. By definition, Tukey's HSD (honest significant difference) test is a single-step multiple comparison procedure that compares the means of every treatment to the means of every other treatments.

5.3 Results and Discussion

As reported in our previous study (Adewale et al., 2014a; Adewale et al., 2014o), free fatty acid (FFA) content of waste beef tallow was 3.19% according to AOCS (Ca 5a-40). The GC analysis showed the fatty acid (FA) profile of the waste beef tallow to mainly consist of: C16:0 (25.95%), C16:1 (2.84%), C18:0 (17.54%), C18:1 (41.67%), and C18:2 (6.91%) (Adewale et al., 2014a). High percentage of saturated FA results in it being in semi-solid state at room temperature. To effectively use base catalysts with no preprocessing steps, the FFA content in a biodiesel feedstock cannot exceed 1% (w/w). In order to prevent soap formation either enzymatic catalysis can be used or heterogeneous base catalysts (Liu et al., 2007; Mutreja et al., 2011) can be used to neutralize the FFA. In the present study, enzymatic catalysis was used and variables such as molar ratio (fat:methanol), catalyst concentration, reaction time, ultrasound amplitude and cycle were investigated. The FAME profile of biodiesel produced at 40% ultrasound amplitude and 20 min reaction time is shown in Figure 5.1.

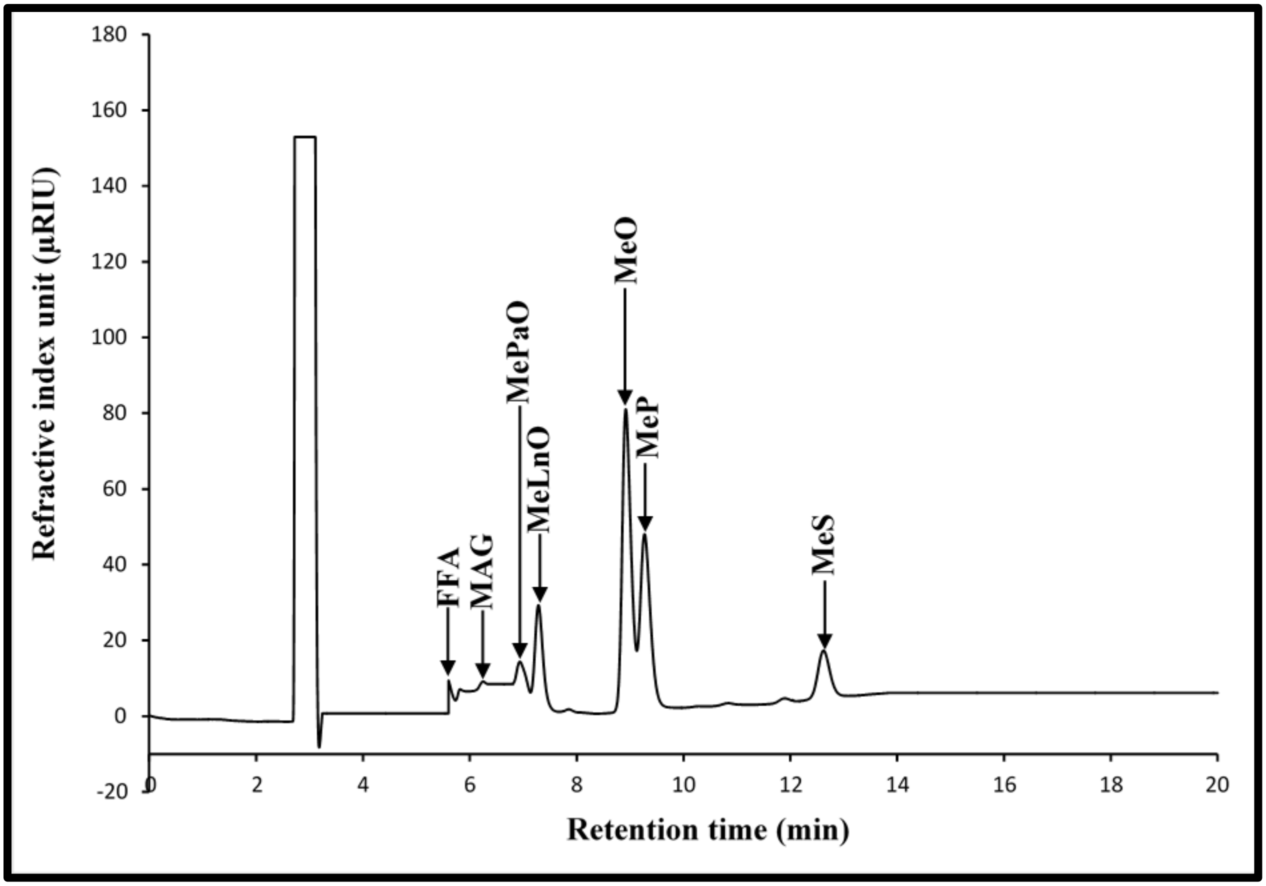

Figure 5.1: HPLC chromatogram of the product biodiesel obtained at 40% ultrasonic amplitude and 20 minutes reaction time showing the characteristic peaks corresponding to different methyl ester

5.3.1 Effect of ultrasonic amplitude and cycle

Three different ultrasonic amplitudes (30, 40, and 50%) were examined to investigate the effect of ultrasonic amplitude on biodiesel yield from waste tallow as shown in experimental set A (Table 5.1). Effect of each of the ultrasonic amplitudes on the biodiesel yield was investigated at three different ultrasonic cycles (3, 5, and 7 per sec), by keeping other reaction conditions the same. In these pre-optimized conditions, more than 85% conversion of waste tallow to biodiesel was obtained at reaction time, 30 min as shown in Figure 5.2. At ultrasonic amplitude 30%, there was no difference in yield between cycles 0.3 and 0.5 (per sec). The biodiesel yield increases with increase in ultrasonic amplitude and cycles but a steady yield was observed between ultrasonic amplitude 40 and 50 at 0.7 ultrasonic cycle. An ANOVA result showed that the effects of ultrasonic amplitude, ultrasonic cycle and the interaction between amplitude and cycle were significant ($P < 0.05$) in the transesterification of waste tallow to produce biodiesel.

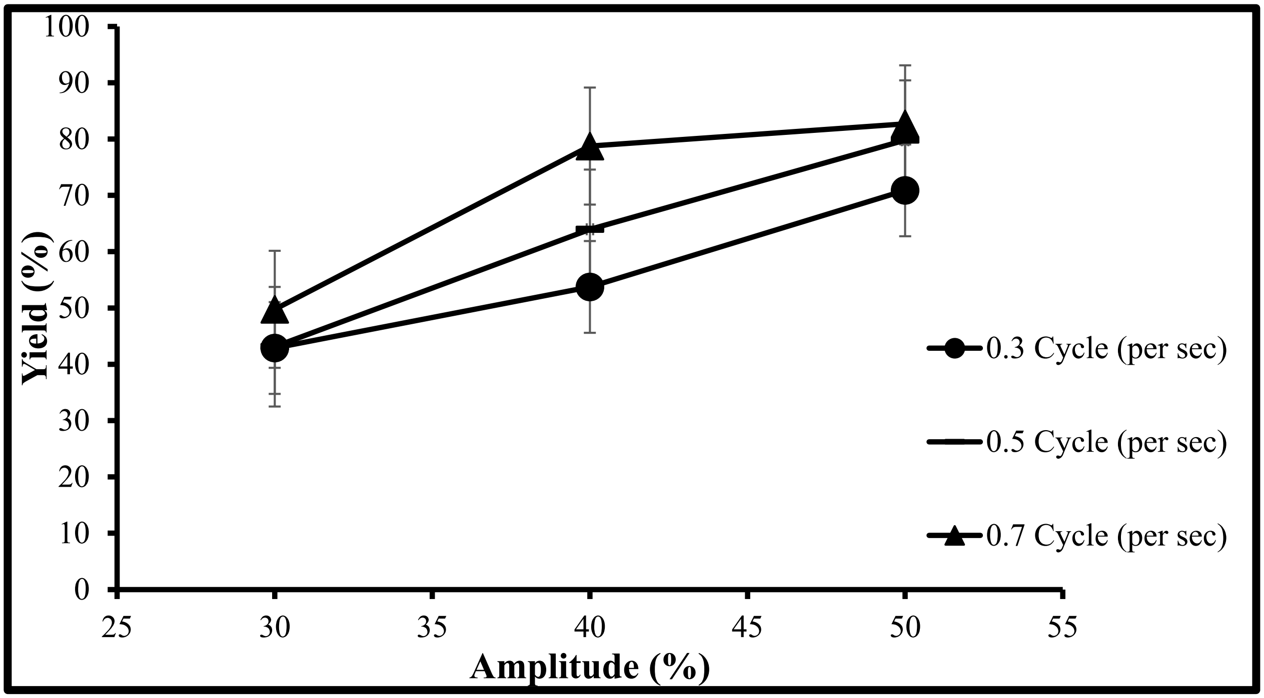

Figure 5.2: Effect of ultrasonic amplitude and cycle of the conversion of waste tallow to biodiesel at enzyme concentration 6 wt.% of fat, reaction time 30 min, and molar ratio (fat:methanol) 1:6.

The distribution plots of biodiesel yield from waste tallow due to ultrasonic amplitude and ultrasonic cycle are shown in Figures 5.3A and B, respectively. For amplitude, the widest range of biodiesel yield occurred with the 40% ultrasonic amplitude (Figure 5.3A), while for cycles per second, the widest range occurred 5 cycle per sec. Differences in biodiesel yield from waste tallow were further investigated by Tukey’s studentized range test HSD (honest significant difference; $p < 0.05$ for multiple comparison of means. The results of the comparison of means showed biodiesel yields at each amplitude and cycle investigated to be significantly different from one another (Table 5.2A and B), confirming the distribution of ultrasonic amplitude and cycle data presented in Figures 5.3A and B, respectively.

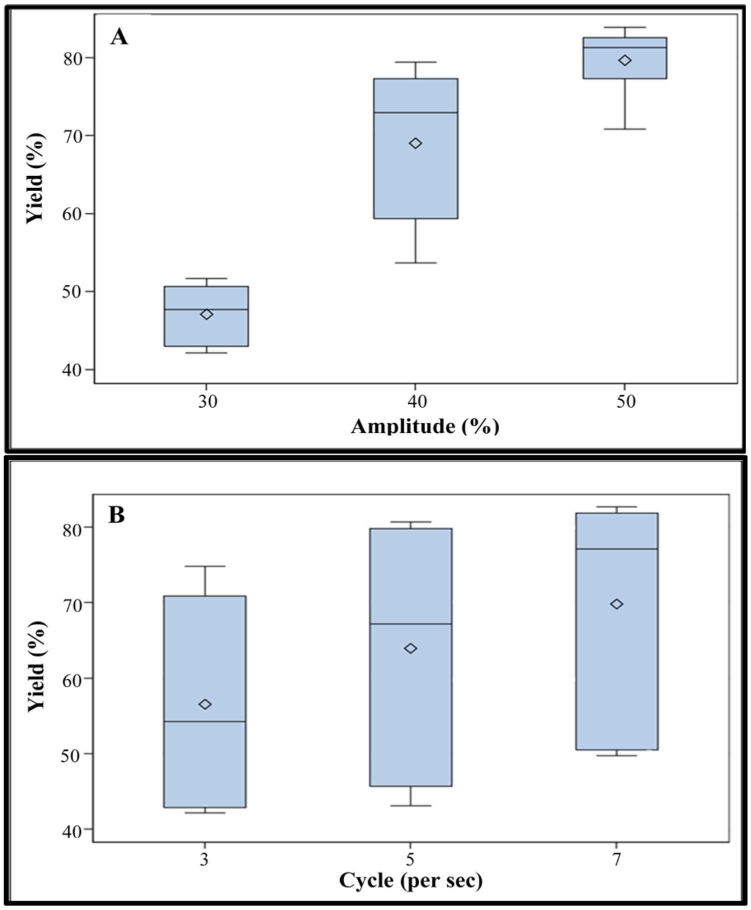

Figure 5.3: ANOVA distribution of biodiesel yield based on: (A) Ultrasonic Amplitude (B) Ultrasonic Cycle.

Table 5.2: Comparison of biodiesel yield based on effect of (A) ultrasonic amplitude and (B) cycle by Tukey's Studentized Range (HSD) Test.

A

Comparisons significant at the 0.05 level are indicated by *.**

Amplitude Comparison	Difference Between Means	Simultaneous 95% Confidence Limits		
50 - 40	12.268	8.913	15.624	***
50 - 30	32.772	29.416	36.127	***
40 - 50	-12.268	-15.624	-8.913	***
40 - 30	20.503	17.148	23.859	***
30 - 50	-32.772	-36.127	-29.416	***
30 - 40	-20.503	-23.859	-17.148	***

B

Comparisons significant at the 0.05 level are indicated by *.**

Cycle Comparison	Difference Between Means	Simultaneous 95% Confidence Limits		
7 - 5	5.902	2.546	9.257	***
7 - 3	13.303	9.948	16.659	***
5 - 7	-5.902	-9.257	-2.546	***
5 - 3	7.402	4.046	10.757	***
3 - 7	-13.303	-16.659	-9.948	***
3 - 5	-7.402	-10.757	-4.046	***

5.3.2 Effect of enzyme concentration

In enzymatic catalysis, where the catalyst is in a different phase to the reactants, ultrasonic dispersion enhances the surface area available for the reactants activities. The occurrence of cavitation in this process increases the efficiency of enzyme activities and allows optimum conversion at lower enzyme levels to be achieved. To assess the effect of enzyme concentration on biodiesel yield at varying molar ratios during transesterification of waste tallow assisted by ultrasonication, experimental set B was used. The lowest biodiesel yield was observed at 4% (w/w of fat) enzyme concentration for all the molar ratios tested (Figure 5.4), indicating an insufficient enzyme concentration to catalyze the reaction completely. No difference in biodiesel yield was apparent between the enzyme concentrations of 6 and 8% (w/w of fat), concurring with the findings of Chen et al. (2006), in their investigation of enzymatic conversion of waste cooking oils (WCO) into alternative fuel-biodiesel. In the ANOVA of biodiesel yields, enzyme concentration had a significant effect ($p < 0.05$) on biodiesel yield from waste tallow.

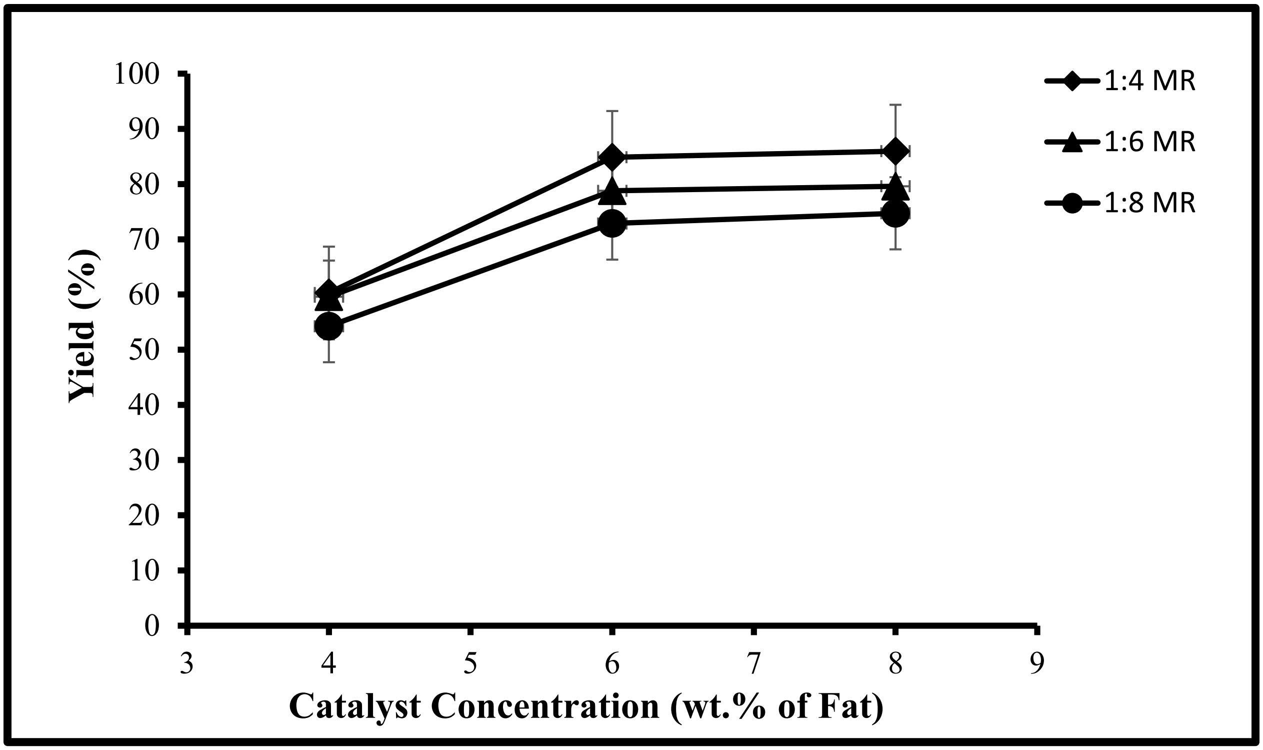

Figure 5.4: Effect of molar ratio and catalyst concentration of the conversion of waste tallow to biodiesel at reaction time 30 min, ultrasonic cycle 5 Hz, and ultrasonic amplitude 40%.

Figure 5.5A shows biodiesel yield distribution under different enzyme concentrations. The widest distribution of biodiesel yield was observed at an enzyme concentration of 6% (w/w of fat). This result showed a substantial reduction in enzyme concentration as compared to reported results using conventional stirring techniques. For example, Xu et al. (2003) reported an enzyme concentration of 30% (w/w of oil), a molar ratio of methyl acetate/oil of 12:1, and reaction time of 10 h as optimum conditions yielding a methyl ester (ME) yield of 92%. Chen et al. (2006) equally reported an enzyme concentration of 30% (w/w of WCO) as optimum in generating a methyl ester yield of 88–90%. In this regard, application of ultrasound for biodiesel production would significantly reduce production reagent costs. The HSD test of biodiesel yield under different enzyme concentrations shows significant difference between all enzyme concentrations except between 6 and 8% (w/w of fat) (Table 5.3B).

Table 5.3: Comparison of biodiesel yield based on effect of (A) molar ratio and (B) enzyme concentration by Tukey's Studentized Range (HSD) Test

A

Comparisons significant at the 0.05 level are indicated by *.**

Molar ratio Comparison	Difference Between Means	Simultaneous 95% Confidence Limits		
4 - 6	4.702	0.954	8.449	***
4 - 8	9.723	5.976	13.471	***
6 - 4	-4.702	-8.449	-0.954	***
6 - 8	5.022	1.274	8.769	***
8 - 4	-9.723	-13.471	-5.976	***
8 - 6	-5.022	-8.769	-1.274	***

B

Comparisons significant at the 0.05 level are indicated by *.**

Enzyme Comparison	Difference Between Means	Simultaneous 95% Confidence Limits		
8 - 6	1.647	-2.101	5.394	
8 - 4	21.273	17.526	25.021	***
6 - 8	-1.647	-5.394	2.101	
6 - 4	19.627	15.879	23.374	***
4 - 8	-21.273	-25.021	-17.526	***
4 - 6	-19.627	-23.374	-15.879	***

5.3.3 Effect of molar ratio

The molar ratio of alcohol to fats/oils in transesterification reaction has been known to be one of the most important variables affecting the yield of biodiesel. To study the effect of molar ratio on the yield of biodiesel at varying catalyst concentration, experimental set B was used. The relationship between molar ratios and yield was investigated under different catalyst concentrations, over a constant reaction time of 30 min, ultrasonic amplitude of 40%, and cycle of 5 Hz (Figure 5.4). Yield was found to increase with increase in enzyme catalyst concentration, but decrease with increase in molar ratio. Biodiesel yield remained constant at enzyme concentrations exceeding 6% (w/w) of fat. The ANOVA of biodiesel yield based on molar ratios, enzyme concentrations, and interaction between molar ratio and enzyme concentration showed molar ratio and enzyme concentration to be significant ($p < 0.05$) for the biodiesel yield from waste tallow, however, their interaction was not. The lack of interaction might due to the good stability of immobilized CALB against methanol (Mendes et al., 2011). The HSD test of biodiesel yield differences with molar ratio shows significant difference ($p < 0.05$) between all molar ratios investigated (Table 5.3A). Figures 5.5A and 5.5B show biodiesel yield distribution under different enzyme concentrations and under different molar ratios, respectively. The molar ratio with widest ANOVA distribution of biodiesel yield was observed at 1:4 (fat:methanol).

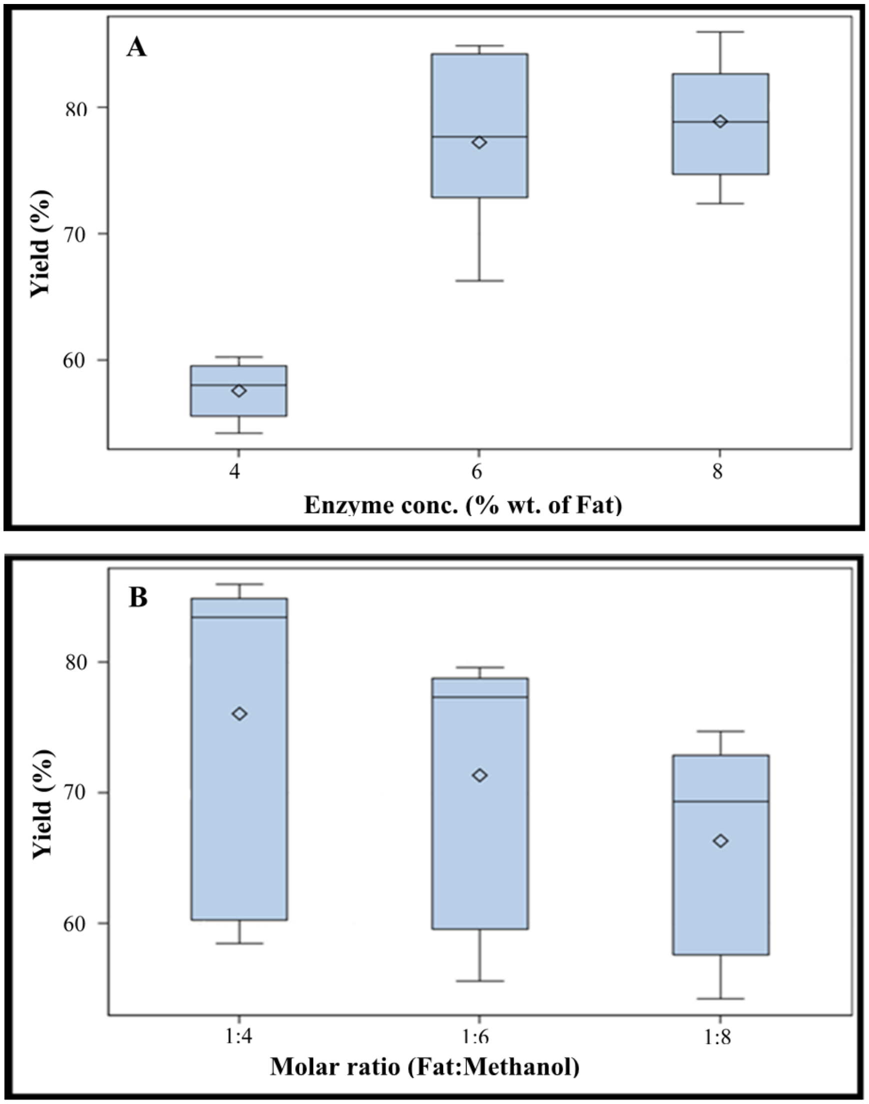

Figure 5.5: ANOVA distribution of biodiesel yield based on: (A) Enzyme Concentration (B) Molar Ratio (Fat:Methanol)

5.3.4 Effect of reaction time and amplitude

The effect of reaction time on biodiesel yield from waste tallow was assessed at various reaction times as shown in Table 5.1, experimental set C. Figure 5.8, showing biodiesel yield at different reaction times over varying amplitudes (30, 35, 40, 45, and 50%), illustrates how biodiesel yield increases as reaction time extended. Above an amplitude of 35%, the yield increases up to a reaction time of 20 min, but remains largely constant thereafter. The effects of reaction time and ultrasonic amplitude under pre-optimized conditions [e.g. molar ratio (fat:methanol) (1:6), and enzyme concentration (6% w/w of fat)] were significant, as was their interaction. Figure 5.6 shows biodiesel yield distribution due to reaction time. In this figure, biodiesel yield distribution between 15 and 20 min seems to be similar but in the HSD test for comparison of means (Table 5.4) both are significantly difference ($p < 0.05$). Comparatively, Fan et al. (2010), who studied ultrasonically-assisted production of biodiesel from crude cottonseed oil, found no significant differences for biodiesel yield at shorter reaction times (10 sec to 5 min), but did find differences at longer reaction time (30–60 min). Processing time by conventional batch methods are in the range of 12-24 h for biodiesel production, where with sonication these times are reduced to less than 30 min.

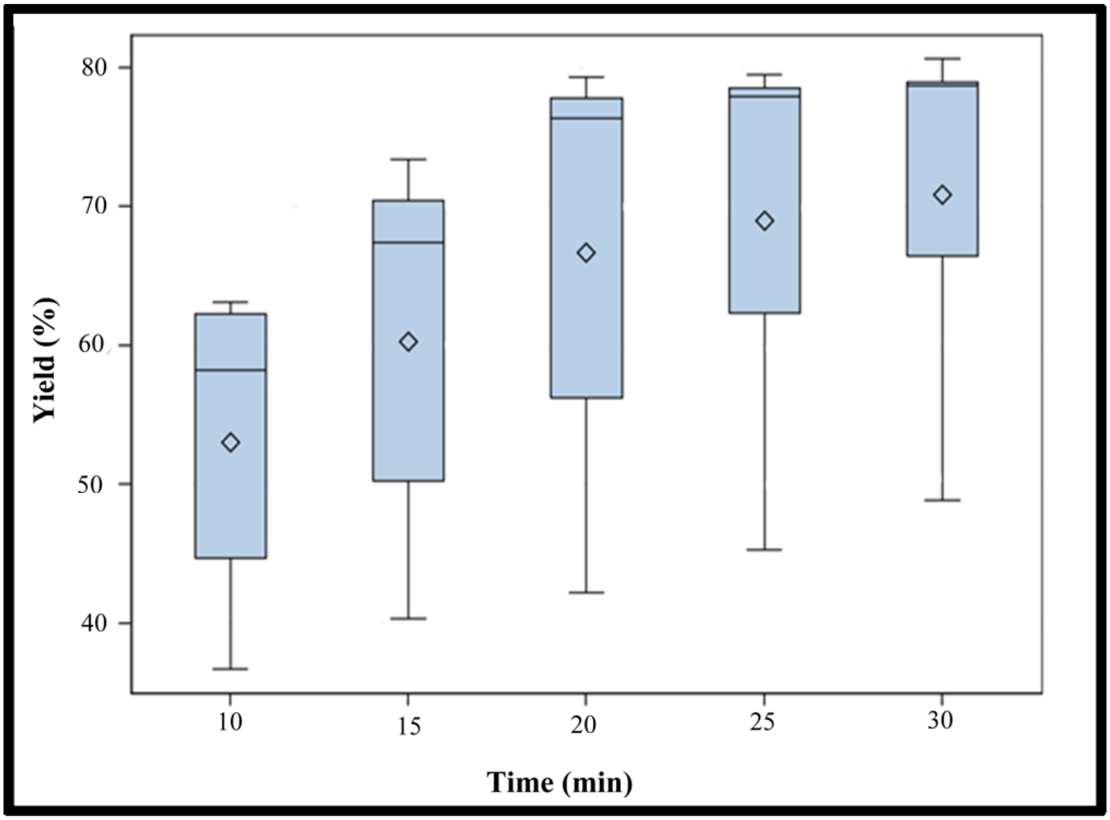

Figure 5.6: ANOVA distribution of biodiesel yield based on: reaction time

Table 5.4: Comparison of biodiesel yield based on effect of reaction time by Tukey's Studentized Range (HSD) Test

Comparisons significant at the 0.05 level are indicated by *.**

Time Comparison	**Difference Between Means**	**Simultaneous 95% Confidence Limits**		
30 - 25	1.8700	0.4213	3.3187	***
30 - 20	4.1410	2.6923	5.5897	***
30 - 15	10.5470	9.0983	11.9957	***
30 - 10	17.8050	16.3563	19.2537	***
25 - 30	-1.8700	-3.3187	-0.4213	***
25 - 20	2.2710	0.8223	3.7197	***
25 - 15	8.6770	7.2283	10.1257	***
25 - 10	15.9350	14.4863	17.3837	***
20 - 30	-4.1410	-5.5897	-2.6923	***
20 - 25	-2.2710	-3.7197	-0.8223	***
20 - 15	6.4060	4.9573	7.8547	***
20 - 10	13.6640	12.2153	15.1127	***
15 - 30	-10.5470	-11.9957	-9.0983	***
15 - 25	-8.6770	-10.1257	-7.2283	***
15 - 20	-6.4060	-7.8547	-4.9573	***
15 - 10	7.2580	5.8093	8.7067	***
10 - 30	-17.8050	-19.2537	-16.3563	***
10 - 25	-15.9350	-17.3837	-14.4863	***
10 - 20	-13.6640	-15.1127	-12.2153	***
10 - 15	-7.2580	-8.7067	-5.8093	***

5.3.5 Enzyme-catalyzed kinetic model

The enzyme-catalyzed kinetics for the production of biodiesel from waste tallow using immobilized CALB and a Ping Pong model was based on simultaneous hydrolysis and esterification of triglyceride mechanism as reported by Al-Zuhair et al. (2007), and Cheirsilp et al. (2008). Transesterification pathway mechanism was reported to be more accurate and generate high quality product by assuming that transesterification takes place by direct alcoholysis of the triglyceride than two consecutive steps of hydrolysis and esterification (Azócar et al., 2014; Belafi Bako et al., 2002), rather the two consecutive steps occur simultaneously. Figure 5.7 shows the Cleland nomenclature of enzyme-catalyzed transesterification of waste tallow mechanism. The E binds with TG to form the enzyme-substrate complex [E.TG], after which transformation to Bd and E′ complex [E′.Bd] occurs. Based on Ping Pong model, the first product (Bd) emanates leaving E′ which further binds with the second substrate (M) to form [E′.M] complex. The complex is transformed to E and G complex [E.G] to synthesis second product (G) and E. This mechanism limits the production of water due to simultaneous hydrolysis and esterification reactions, water generated during esterification is usually consumed during hydrolysis process (Belafi Bako et al., 2002). One step esterification reaction occurs at the beginning of the process due to the FFA content of waste tallow.

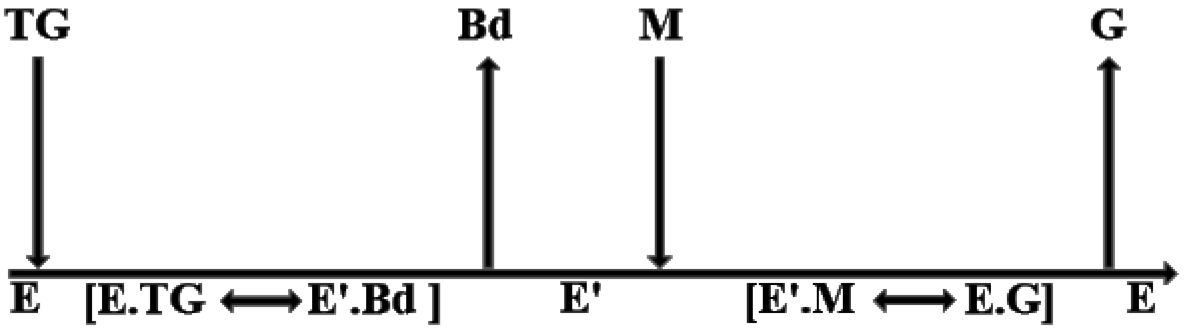

Figure 5.7: Cleland nomenclature of Ping Pong Bi-Bi mechanism for enzyme-catalyzed transesterification of waste tallow

As shown in Figure 5.8, the Ping Pong Bi Bi kinetic model presumably predicted reaction performance enzyme-catalyzed transesterification of waste tallow assisted by ultrasonication, indicating that all the reaction rate constants were duly estimated. At ultrasonic amplitudes (30 and 35%), TG conversion did not show a sigmoidal (S-shaped) pattern. This could be attributed to the low reaction rate due to miscibility issue of waste tallow and methanol and the formation of intermediate substrates complexes with enzyme. Ultrasound amplitude above 40% showed TG conversion to be sigmoidal pattern with limited concentration of intermediate substrates complexes. This result confirmed the assumed mechanism that the reaction would be in transesterification pathway where both hydrolysis and esterification reactions occurred simultaneously. This indicated that in the presence of methanol, the triglycerides were more easily yielded to FAME through methanolysis reaction rather than to FFA through hydrolysis reaction (Azócar et al., 2011; Cheirsilp et al., 2008). Similarly, above 40% ultrasonic amplitudes, activities within the reaction system occur below 20 min of the studied reaction time. Which means, effects of ultrasonic amplitude after this reaction time was limited because the reaction could proceed without mixing.

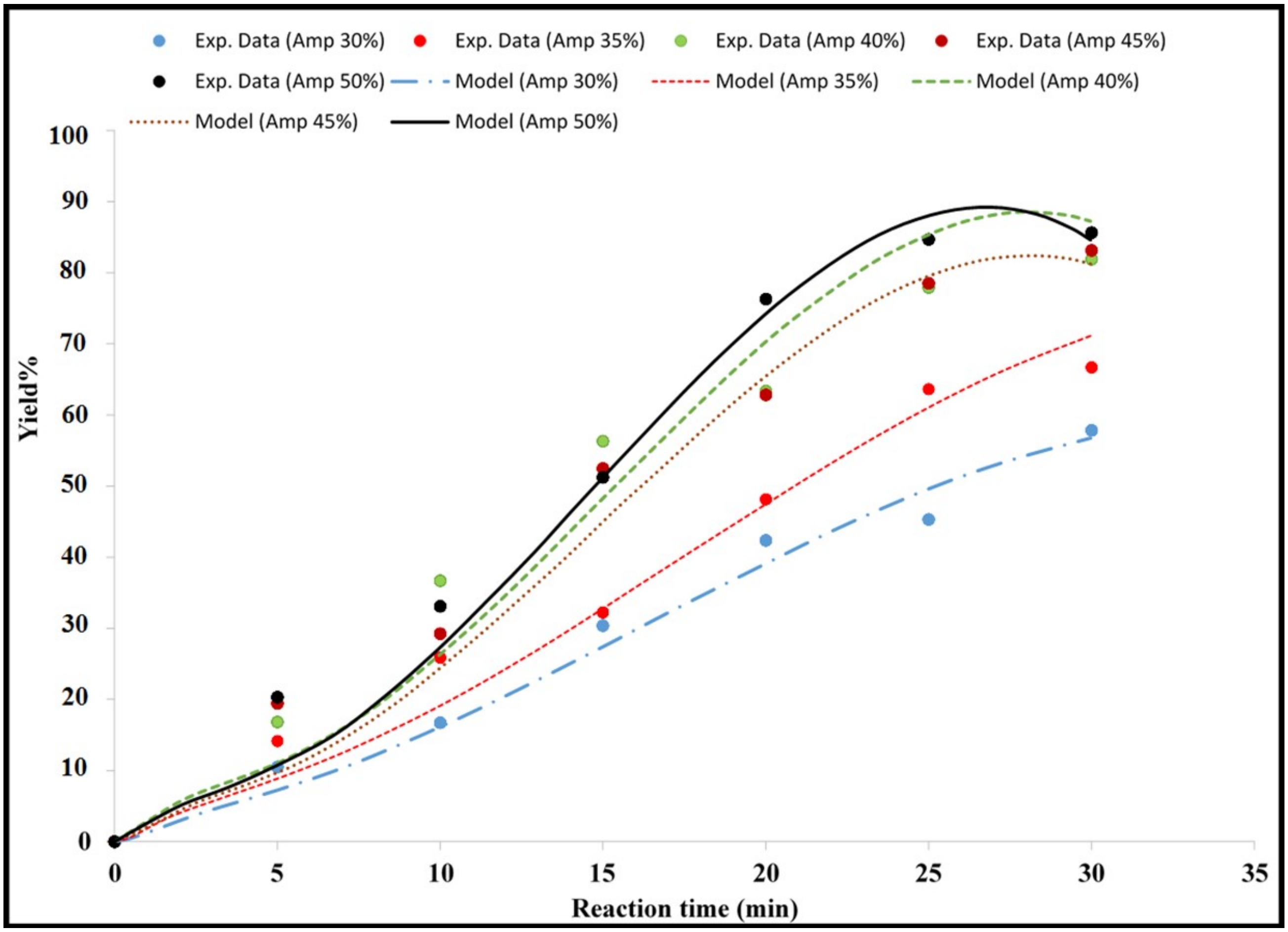

Figure 5.8: Plots of experimental data and model of biodiesel production at varying reaction times and ultrasonic amplitudes at constant enzyme conc. 6% (w/w) of fat, molar ratio (fat:methanol) 1:6, and ultrasonic amplitude 40%.

5.3.6 Effects of ultrasonic amplitude on the reaction rate constants

Experimental setup at varying ultrasonic amplitudes and reaction times were carried out to investigate the effects of ultrasonic amplitude on the reaction rate constants. The enzyme concentration and fat/methanol molar ration were kept at 6% (w/w) of fat and 1:6, respectively. Ultrasound amplitudes were run at 5, 10, 15, 20, 25, and 30 min reaction time. Based on the experimental results, the reaction rate constants were estimated by the procedure presented in section 2.5. Figure 5.9 shows the plots of reaction rate constants evaluated at each of the ultrasonic amplitudes studied. The values of the reaction rate constants, k_1 to k_6 change significantly at different ultrasonic amplitude. A rapid increase in the forward reaction rate constants (k_1, k_3, k_4, and k_6) and decrease in reverse reaction rate constants (k_2 and k_5) was observed at 40% ultrasonic amplitude. There is no significant difference ($P > 0.05$) in reaction rate constants (k_1 - k_6) between ultrasonic amplitudes 30 and 35%. The rate constant (k_2) for the dissociation of enzyme-TG complex was highest at ultrasound amplitude 30% while the lowest was at ultrasound amplitude 40%. This might be due to weak binding of enzyme and TG at 30% amplitude. The rate constant (k_3) that is responsible for the formation of biodiesel was highest at ultrasound amplitude 40% and lowest at 30%. This result confirms ultrasound amplitude 40% to be optimum amplitude for the production of biodiesel as earlier reported in this study. Across all the ultrasound amplitudes, the reaction rate (k_6) for the association of biodiesel and glycerol to form the reactants was negative. This indicated that possibility of glycerol combining with biodiesel is limited during ultrasonication treatment of transesterification reaction.

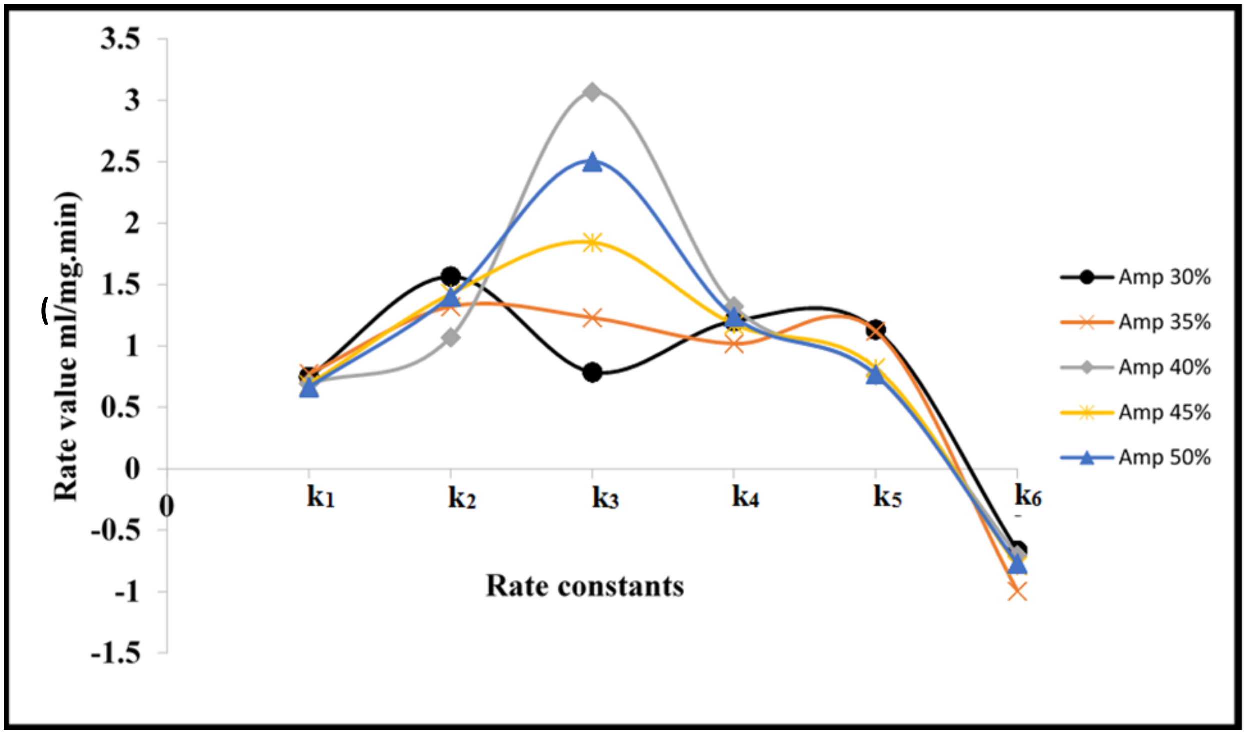

Figure 5.9: Plots of reaction rate constant values of the ultrasonic amplitudes

5.4 Conclusion

Enzymatic catalysis of waste tallow transesterification for the production of biodiesel and the effects of reaction factors such as molar ratio (fat:methanol), catalyst concentration, reaction time, ultrasound amplitude and cycle on biodiesel yield were successfully investigated. The reaction kinetics of an ultrasound assisted enzyme-catalyzed transesterification of waste tallow with methanol for biodiesel production were successfully modeled using reaction rate expressions by varying ultrasonic amplitude parameter. The biodiesel yield was found to increase with increase in enzyme catalyst concentration, but decrease with increase in molar ratio. The interaction between molar ratio and enzyme catalyst concentration was not significant for the production of biodiesel from waste tallow. The model results supported the assumption made in this study that the two reactions of hydrolysis and methanolysis would occur simultaneously rather than by the stepwise hydrolysis followed by esterification. There was no significant ($P > 0.05$) change in the reaction rate constants between ultrasonic amplitudes 45 and 50%. Moreover, a rapid increase in the forward reaction rate constants (k_1, k_3, k_4, and k_6) and decrease in reverse reaction rate constants (k_2 and k_5) was observed at 40% ultrasonic amplitude and above. There was no significant difference ($P > 0.05$) in reaction rate constants, k_1 to k_6 between ultrasonic amplitudes 30 and 35%. A better understanding of the reaction rates with respect to individual reactants and system parameters will be beneficial for the design and construction of the biodiesel reactors using ultrasonication mixing. Application of this mixing technique for transesterification reaction would drastically reduce the reaction time and amount of methanol require for the production of biodiesel which would directly affect cost of production in terms of amount reagents, production time, and indirectly energy use.

CONNECTING TEXT TO CHAPTER 6

In chapters 3 and 4, the use of conventional and non-destructive techniques for AFW characterization were employed, respectively. Our findings from these two chapters were used to select a range of parameters for the investigated factors such as molar ratio of waste fat to methanol in Chapter 6 based on the amount of FFA in each of the waste fat samples. This chapter provides a description of data collection and methodology used for enzyme-catalyzed synthesis and kinetic of biodiesel production from waste lard assisted by ultrasonication. Chapter 6 manuscript was prepared and submitted to the Chemical Engineering Journal in February, 2015. It is currently under review. The manuscript is co-authored by Drs. Dumont, M.-J., and Ngadi, M. The format of the manuscript has been altered to be consistent with this thesis. All literature cited in this chapter is listed in the references section at the end of this thesis.

Chapter 6

Enzyme-catalyzed synthesis and kinetic of biodiesel production from waste lard assisted by Ultrasonication

Abstract

In this study, the effects of ultrasonic parameters (amplitude, cycle and pulse) and major reaction factors (molar ratio and enzyme concentration) on the reaction kinetics of biodiesel generation from waste lard bio-catalyzed by immobilized lipase [*Candida antarctica Lipase B* (CALB)] were investigated. A Ping Pong Bi Bi kinetic model approach was employed to study the effect of ultrasonic amplitude on the enzymatic transesterification. Kinetic constants of transesterification reaction were determined at different ultrasonic amplitudes (30, 35, 40, 45, and 50%) and enzyme concentrations (4, 6, and 8% wt. of fat) at constant molar ratio (fat:methanol); 1:6, and ultrasonic cycle; 5 Hz. Parametric effects on the yield were studied using three sets of experiments namely A, B, and C. In experiment set A, two factors (ultrasonic amplitude and cycle) were investigated at three levels; in experiment set B, two factors (molar ratio and enzyme concentration) were examined at three levels; and in experiment set C, two factors (ultrasonic amplitude and reaction time) were investigated at five levels. A yield of 96.8% was attained in 20 min at an ultrasonic amplitude (40%) at 5 Hz, fat:methanol molar ratio (1:4) and catalyst level 6% (wt/wt of fat). The fitted curves of the kinetic mechanism showed a sigmoidal curve due to mass transfer limitations which controlled the process at the beginning of the reaction. The kinetic model results also revealed interesting features of ultrasound assisted enzyme-catalyzed transesterification: at ultrasonic amplitude 40%, the reaction activities within the system seemed to be steady after 20 min which means the reaction could proceed with or without ultrasonic mixing. The kinetic model approach employed describes the whole methanolysis process accurately.

6.1 Introduction

The use of non-edible feedstocks as cheap raw materials for biodiesel production is a key point towards economic competitiveness with petro-diesel. Another advantage of utilizing non-edible vegetable oils (e.g. Jatropha oil, Polanga oil) or AFW (e.g. lard, tallow) feedstocks for biodiesel production is that they do not face the ‘food vs fuel’ dilemma which has been a serious food security concern (Canakci and Van Gerpen, 2001; Gerpen, 2005; Srinivasan, 2009). However, suitable production technique to maximize biodiesel yield from these feedstocks is a challenge due to their physicochemical properties (Adewale et al., 2014a; Adewale et al., 2014o). In conventional batch reactors, energy and mixing requirements for biodiesel production are provided by heating systems and mechanical agitators, respectively. These production methods are labour intensive and costly in terms of time and reagents involved. In fact, enzyme-catalyzed transesterification methods are more time consuming when using conventional techniques. For instance, Kumar et al. (2013) studied effectiveness of enzymatic transesterification of beef tallow using experimental enzyme Ns88001 with methanol and hexane. The authors reported that the highest conversion yield of biodiesel (71.94%) was obtained at an oil:alcohol molar ratio of 1:4, 16 h reaction time and 45°C reaction temperature using a reciprocal shaking bath at 200 rpm. Huang et al. (2010) optimized lipase-catalyzed transesterification of lard for biodiesel production on a reciprocal shaker using response surface methodology. The authors reported the optimal reaction conditions as: 0.04 of amount of lipase/oil (w/w), 0.49 of proportion of Novozym435/total lipases (w/w), and 20 h of reaction time, which yielded 97.2% of fatty acid methyl ester (FAME). To further enhance substrates miscibility during transesterification reaction, application of ultrasonication has been reported as a reliable alternative (Deshmane and Adewuyi, 2013; Mahamuni and Adewuyi, 2009).

Recently, Choudhury et al. (2013); Michelin et al. (2015) and Teixeira et al. (2009) demonstrated the effectiveness of ultrasound-assisted transesterification of vegetable oils and animal fats for the production of biodiesel. In an evaluation of ultrasonic-assisted ethanolysis production of biodiesel from fish oil, Armenta et al. (2007a) examined the effects of different parameters including: ultrasonic device (bath vs. probe), catalyst type (potassium hydroxide vs. sodium ethoxide), catalyst concentration (0.5 vs. 1%), temperature (20°C vs. 60°C), and duration of exposure (10–90 min) on the production process. They concluded that sodium ethoxide was a more efficient catalyst than potassium hydroxide. Comparing biodiesel yield from conventional *vs.* ultrasonic-assisted transesterification of fishmeal plant waste oil, Maghami et al. (2015) reported optimal conditions for the biodiesel production to be 1% KOH, 55°C temperature, 6:1 alcohol to oil molar ratio and the yields were 79.6% at 30 min reaction time and 78% at 1h reaction time for the ultrasonic and conventional methods respectively.

Similarly, studies on ultrasound-assisted transesterification of vegetable oils and animal fats using an acid or an alkaline catalyst and their possible reaction kinetic pathways have been extensively reported (Armenta et al., 2007a; Elizabeth Grant and Gnaneswar Gude, 2014; Kumar et al., 2012; Maghami et al., 2015; Michelin et al., 2015; Salamatinia et al., 2013; Sánchez et al., 2015). Enzyme-catalyzed transesterification and esterification reactions were reported to possibly proceed kinetically by Ping Pong Bi Bi mechanism, ternary complex ordered Bi Bi mechanism, or ternary complex random Bi Bi mechanism (Shinde and Yadav, 2014; Veny et al., 2014). Cheirsilp et al. (2008) studied the impact of transesterification mechanisms on the kinetic modeling of biodiesel production using immobilized lipase by fitting experimental data of the transesterification of palm oil with various ethanol concentrations to estimate the reaction kinetic parameters. A good agreement between experimental results and those predicted proposed model equations by the authors was reported. In the investigation of Azócar et al. (2014) on the reaction kinetic of enzymatic biodiesel production from waste frying oil and crude rapeseed oil using co-solvent and an anhydrous medium to improve lipase performance in a semi-continuous reactor, the authors described the reaction mechanism as a Ping Pong Bi Bi model and reported methanol as the competitive inhibitor. Similarly, Veny et al. (2014) proposed a kinetic model of lipase catalyzed transesterification of *jatropha* oil in circulated batch packed bed reactor based on Ping Pong Bi Bi mechanism with reverse inhibition by methanol. In a recent study of Michelin et al. (2015) on the kinetics of ultrasound-assisted enzymatic biodiesel production from Macauba coconut oil, the authors investigated evaluate the effects of temperature (40 – 70°C), enzyme (5 - 20 wt%) concentration, oil to ethanol molar ratio (1:3 - 1:10) and output irradiation power (40 - 70 % of the maximum supply value) on the reaction yield. They concluded that ultrasound-assisted lipase-catalyzed transesterification of Macauba coconut oil in a solvent-free system might be a potential alternative route to conventional alkali-catalyzed and/or traditional enzymatic methods.

The effects of ultrasound parameters and reaction kinetic of enzyme-catalyzed transesterification pathway assisted by ultrasonication to produce biodiesel from waste lard were investigated in this study. Moreover, parametric effects of ultrasonic wave amplitude, ultrasonic cycles, and reaction parameters (e.g. fat:methanol molar ratio, enzyme concentration, duration) on biodiesel yields from waste lard were examined. An acoustic mixing and mechanism of enzyme-catalyzed transesterification pathway were used for the reaction kinetic modeling of biodiesel production from waste lard assisted by ultrasonication.

6.2 Materials and methods

6.2.1 Materials and equipment

Waste lard was obtained from a biodiesel production company in Canada (Rothsay Biodiesel, Montreal, Canada). Commercially produced immobilized *Candida antarctica* lipase B (CALB) was purchased from CLEA Technologies (Delftechpark, The Netherland). American Chemical Society (ACS) and HPLC grades of methanol were purchased from Fisher Scientific (Ontario, Canada). Saturated and unsaturated FAME standards for calibration curves were purchased from Sigma Aldrich, (Oakville, ON, Canada).

An ultrasonication set-up featuring a Vibra-Cell (VXC 500 series, Sonic and Materials Inc., CT, USA) was employed for the transesterification reaction. The Vibra-Cell device is designed to ensure uniform sonotrode probe amplitude, regardless of the varying loading conditions encountered during the processing cycle. The ultrasonic device operates at 500 W and 20 kHz frequency. The probe amplitude, cycle and pulse are adjustable from 0 to 100%, 0.1 - 1.0 per sec and 0.1 - 1.0 sec, respectively. For the identification and quantification of biodiesel produced, a Varian HPLC equipped with a refractive index (RI) detector and reverse phase (RP) C18 column was used.

6.2.2 Experimental set-up and procedure

The solvent free production of biodiesel from waste lard involved an immobilized lipase catalyst (CALB), and transesterification with methanol to yield methyl esters. The transesterification of waste lard using ultrasonication (Vibra-Cell) was carried out in a screw cap bottle (25 mL). The effects of processing and ultrasonic parameters such as amplitude, cycle, reaction time, molar ratio and loaded catalyst (enzyme) were carefully examined. Ultrasound amplitude was varied from low to mild regions (30, 35, 40, 45, and 50%) in order to prevent disintegration of the immobilized enzyme matrix by ultrasound waves. The ultrasonic wave cycle was investigated at 3, 5, and 7 per sec, factorially combined with three levels of ultrasonic amplitudes (30, 40, and 50%). To study the transesterification reaction, fat:methanol molar ratios of 1:4, 1:6, and 1:8, were factorially combined with enzyme concentration of 4, 6 and 8% (w/w) of fat. Three sets of experiments namely A, B, and C were conducted in order to study the effect of each factor on the biodiesel yield, as well as the effects of interactions between factors on the biodiesel yield and to identify most important level of each of the factors. In experiment set A, two factors (ultrasonic amplitude and cycle) were investigated at three levels (3^2). Other parameters (molar ratio, enzyme concentration and reaction time) were kept constant. In experiment set B, two factors (Molar ratio and enzyme concentration) were examined at three levels (3^2). Other parameters (ultrasonic amplitude, ultrasonic cycle and reaction time) were kept constant. In experiment set C, two factors (ultrasonic amplitude and reaction time) were investigated at five levels (5^2) (Table 5.1).

Fat samples stored below -20ºC prior to analysis, were melted in a water bath (50ºC) before sampling. A fat sample (10 g) was then transferred to a 25 mL screw cap bottle and subjected to ultrasound waves for 1 min in order to further break down all possible fat crystals before the addition of other reagents. The mixture of all reagents was introduced, and ultrasound waves applied according to pre-set parameters. With the sonotrode probe submerged and fixed at a depth of 20 mm in the solution, the ultrasonic amplitude, ultrasonic cycle and the reaction time were adjusted using the controller. At each reaction time, a 500 µL aliquot was pipetted into a 2 mL micro centrifuge tube. The reaction was stopped by the addition of 50 µL of glacial acetic acid while 1 mL distilled water was added to wash excess methanol and traces of glycerol from the ester layer. The mixture was vortexed for 3 min before being centrifuged for 10 min at 10,000 × g using an Eppendorf 5415R Micro-centrifuge (Eppendorf Canada Ltd., Mississauga, Ontario) to separate the upper ester and lower aqueous phase. The upper layer is a mixture of esters while the lower layer is a mixture of glycerol, enzyme and aqueous solutions. For the analysis, 100 µL of the ester phase was diluted with acetone to an appropriate concentration before HPLC injection.

6.2.3 Standard calibration curves, biodiesel identification and quantification by HPLC

Calibration curves for FAME standards were developed by injecting six different concentrations (0.5-3.0 mg/mL) of each of the FAME standards expected to elute in the reaction products. The retention time of each of the FAME standards was matched to the corresponding peaks produced by the biodiesel samples. Analysis of the FAME standards and the reaction product were carried out by dissolving the samples in acetone. Some other solvents such as methanol, hexane, chloroform, and toluene were considered but the reaction product showed their greatest solubility in acetone. An external standard quantitation procedure on HPLC was used to develop the FAME standard calibration curves employed in this study. This procedure is a basic quantification approach in which both standard and unknown samples are analysed under the same conditions and the results from the unknown samples are then related to those of the standard samples. The curves were constructed by injecting different known concentrations of the standard solution and measuring the peak area obtained. A regression line of best fit was used to join the points of the curve obtained. All calibration concentration points were ran in triplicate. The best fit regression line gave a correlation coefficient which measured how well the data point's best fit to a straight line. The correlation coefficient equally showed predictability strength of the developed calibration curves to measure the concentrations of the unknown analytes. The developed calibration curves were used to estimate the amount of the desired compounds in the biodiesel aliquot.

The ester phase was analyzed by RP-HPLC which separated the different product components according to their polarity. A Varian HPLC unit equipped with a Varian Prostar 240 pump, a reverse phase (RP) Discovery HS C18, 5 µm, 25 cm × 4.6 mm column (Supelco Analytical, Bellefonte, PA, USA), and a Varian 356-LC refractive index (RI) detector (Varian Inc., Walnut Creek, CA, USA) was used to analyze and quantify the conversion, the FAME composition and the purity of the ester phase (Chakraborty and Sahu, 2014). For all the experiments, an isocratic mobile phase method was used for the separation and determination of the biodiesel produced by the methanolysis of waste lard. The system operated at a flow rate of 1 mL/min, with an injection volume of 25 µL, and a sample runtime of 30 minutes.

6.2.4 Kinetic model development

In enzyme-catalyzed reaction kinetics, the reaction rate is measured by varying the effects of the reaction conditions (Yang et al., 2005) and monitor how these varying parameters affect the enzyme activities in term of product yields. The kinetic mechanism of enzyme-catalyzed transesterification of lard was developed based on ping pong Bi Bi Cleland nomenclature for two substrates (Meunier et al., 2014b). The substrates bind to the enzyme's active reaction site and then transformed into products through a series of steps known as the enzymatic mechanism.

6.2.4.1 Enzyme kinetics mechanisms

Equation 5.2 represents a typical multi-substrate Bi-Bi enzyme kinetic of transesterification reaction: TG and methanol (M) are the substrates while biodiesel (Bd) and glycerol (G) are the products. In this mechanism, the enzyme (E) must bind the first substrate (TG) to form enzyme-substrate complex [ETG], and then released the first product (Bd) and transformed intermediate enzyme (E'). This is followed by binding of second substrate (M) to (E') and breakdown of the transitory complex [E$'$M] to free enzyme (E) and the second product (G) (Cheirsilp et al., 2008; Veny et al., 2014; Yang et al., 2005). Equation 5.3 represents the formation of the enzyme–substrate complex with TG [ETG], the release of Bd from this complex and the generation of transformed enzyme (E$'$). The formation of the transformed enzyme-substrate complex with M [E$'$M] and the release of the second product (G) and free enzyme (E) is shown in equation 5.4. Rate constants k_1 and k_4 are for the enzyme–substrate complex associations for TG and M, respectively; k_2 and k_5 are rate constants of the enzyme–substrate complex dissociations for TG and M, respectively; k_3 and k_6 are the catalytic rate constants for the formation of products Bd and G, respectively. The rate expressions for the overall reaction mechanism (Eqns. 5.3 and 5.4) above, without considering possible intermediate glycerides (di- and monoglyceride) are expressed as in equations 5.5 – 5.12. Because a much faster reaction occurs with the diglyceride and monoglyceride than the triglyceride, hence the overall reaction can be used to develop a simplified model instead of the all three reaction steps (Azócar et al., 2014). The influence of external and internal mass transfer on the reaction kinetic was assumed negligible due to the small volume of the reaction vessel (25 ml) and given that immobilized lipase would be more accessible. A single response that was used to justify possibility of mass transfer was the biodiesel yield from the combination of the independent variables. Based on these assumptions, the reaction kinetics was studied independently of the mass transfer, which made the model to be mass transfer limited.

6.2.5 Determination of kinetic parameters

The concentrations of the substrates, FAME (biodiesel) at different times were determined experimentally starting with 10 g of waste lard and varied methanol amounts of 1.51, 2.27 and 3.03 g to obtain molar ratios of methanol to lard of 4, 6 and 8, respectively. The effects processing parameters; ultrasonic amplitude (30, 35, 40, 45, and 50%) at varied reaction time (5, 10, 15, 20, 25, and 30 min.) on the reaction rates of enzyme-catalyzed transesterification of waste lard were investigated. This was achieved by fitting the reaction rate differential equations generated based on Ping Pong Bi Bi mechanism to the experimental data. The reaction rate differential equations and variable definitions as generated in equations 5.5 – 5.12 were used to develop kinetic reaction model in Mathematica programming software where they were solved by the NDSolve function to generate model and experimental data time plots. The values of rate constants were estimated at best fitted plot of model and experimental data.

6.2.6 Statistical Analysis

A Full factorial design was used for each of the three experimental sets ran independently to verify effects of ultrasound and reaction parameters on the biodiesel yields from waste lard. Statistical analysis was carried out using the procedure of analysis of variance (PROC ANOVA), graphic plot (PROC GPLOT) and Box plot (PROC BOXPLOT) procedures using SAS (Statistical Analysis Systems, Version 9.4, SAS Institute Inc., Cary, NC, USA). Mean comparison of each of the parameters levels and their significant differences were analyzed by Tukey's studentized range test. By definition, Tukey's HSD (honest significant difference) test is a single-step multiple comparison procedure that compares the means of every treatment to the means of every other treatments.

6.3 Results and Discussion

The free fatty acid (FFA) content of waste lard was 10.03% according to AOCS (Ca 5a-40) as reported in our previous study (Adewale et al., 2014a; Adewale et al., 2014o). The GC analysis showed the fatty acid (FA) profile of the waste lard to mainly consist of: C16:0 (25.69%), C16:1 (2.82%), C18:0 (14.50%), C18:1 (40.88%), and C18:2 (12.93%) (Adewale et al., 2014a). To effectively use base catalysts with no preprocessing steps, the FFA content in a biodiesel feedstock cannot exceed 1% (w/w) (Canakci and Van Gerpen, 2001). FFA can be neutralized to prevent soap formation by either enzymatic catalysis or heterogeneous base catalysts (Liu et al., 2007; Mutreja et al., 2011). In this study, enzymatic catalysis was used and variables such as molar ratio (fat:methanol), catalyst concentration, reaction time, ultrasound amplitude and cycle were investigated.

6.3.1 Effect of enzyme concentration

The occurrence of cavitation in ultrasonic process increases the efficiency of enzyme activities and allows optimum conversion at lower enzyme levels to be achieved (Michelin et al., 2015). To investigate the effect of enzyme concentration on biodiesel yield at varying molar ratios during transesterification of waste lard assisted by ultrasonication, experimental set B was used (Table 5.1). The lowest biodiesel yield was observed at 4% (w/w of fat) enzyme concentration for all the molar ratios tested (Figure 6.1), indicating an insufficient enzyme concentration to catalyze the reaction completely. No significant difference ($p < 0.05$) in biodiesel yield was apparent between the enzyme concentrations of 6 and 8% (w/w of fat).

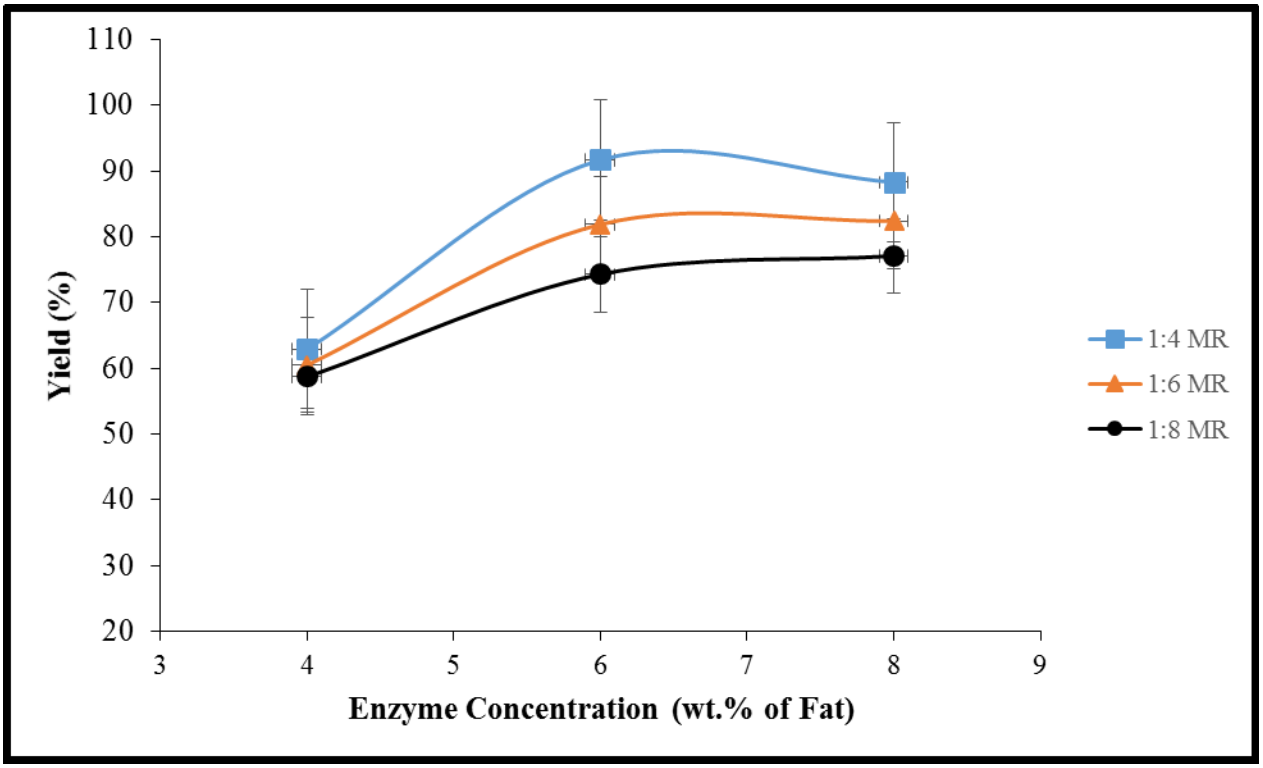

Figure 6.1: Effect of molar ratio and catalyst concentration of the conversion of waste lard to biodiesel at reaction time 30 min, ultrasonic cycle 5 Hz, and ultrasonic amplitude

Figure 6.2A shows biodiesel yield distribution under different enzyme concentrations. The widest distribution of biodiesel yield was observed at an enzyme concentration of 6% (w/w of fat). This enzyme concentration was considerably reduced to the reported results using conventional stirring techniques. For example, Xu et al. (2003) studied a novel enzymatic route for biodiesel production from renewable oils in a solvent-free medium. The authors reported the optimum conditions as: an enzyme concentration of 30% (w/w of oil), a molar ratio of methyl acetate/oil of 12:1, reaction time of 10 h as optimum conditions and yielded 92% of methyl esters (ME). Similarly, Chen et al. (2006) reported an enzyme concentration of 30% (w/w of waste cooking oil) as optimum in generating a methyl ester yield of 88–90%. In this regard, application of ultrasound for biodiesel production would significantly reduce production reagent costs. The HSD test of biodiesel yield under different enzyme concentrations shows significant difference between all enzyme concentrations except between 6 and 8% (w/w of fat) (Table 6.1B).

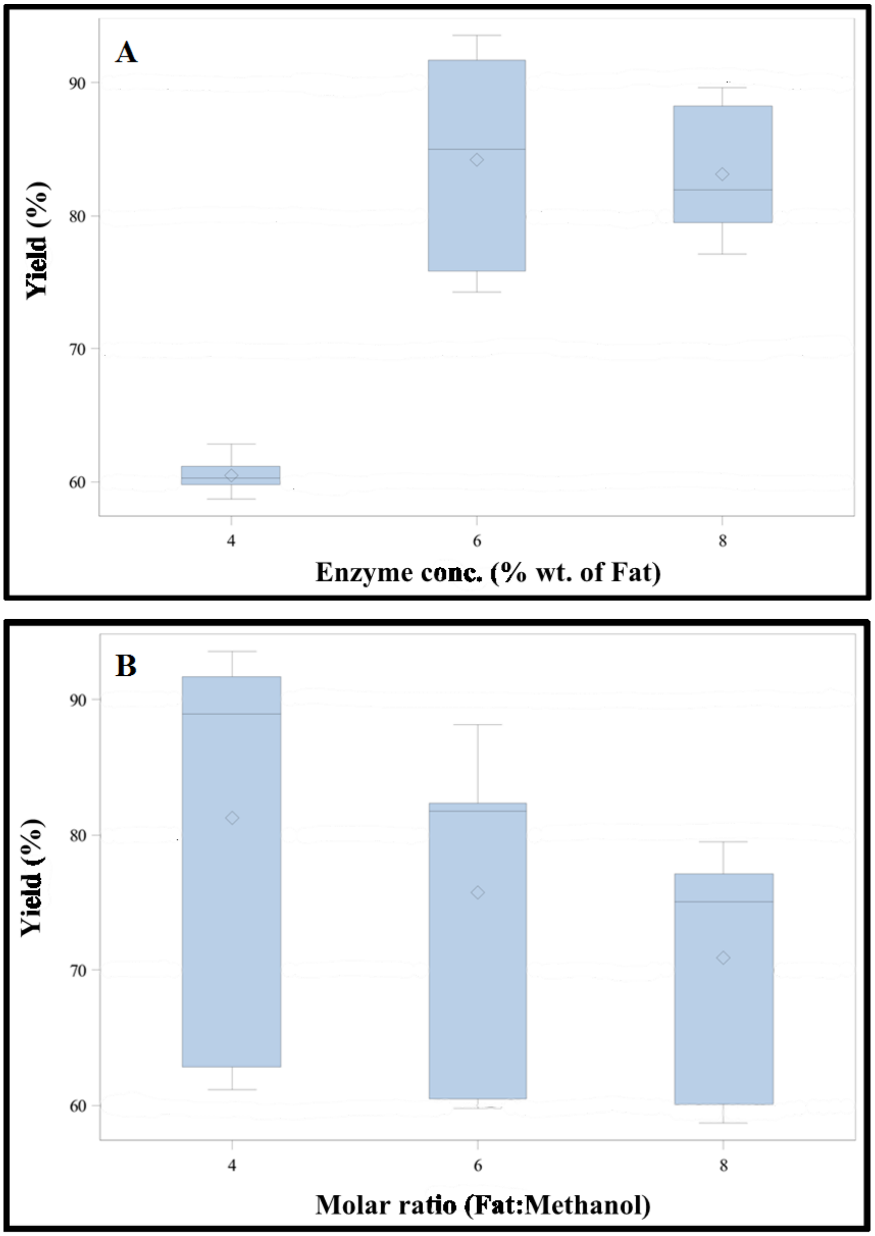

Figure 6.2: ANOVA distribution of biodiesel yield based on: (A) Enzyme Concentration (B) Molar Ratio (Fat:Methanol)

6.3.2 Effect of molar ratio

To study the effect of molar ratio on the yield of biodiesel at varying catalyst concentration, experimental set B was used. The relationship between molar ratios and yield was investigated under different catalyst concentrations, over a constant reaction time of 30 min, ultrasonic amplitude of 40%, and cycle of 5 Hz (Figure 6.1). Yield was found to increase with increase in enzyme catalyst concentration, but decrease with increase in molar ratio. There is no significant effect of enzyme on biodiesel yield when enzyme concentrations exceed 6% (w/w) of fat. The ANOVA of biodiesel yield based on molar ratios, enzyme concentrations, and interaction between molar ratio and enzyme concentration showed molar ratio and enzyme concentration to be significant ($p < 0.05$) for the biodiesel yield from waste lard, however, their interaction was not. The lack of interaction might due to the good stability of immobilized CALB against methanol (Mendes et al., 2011). Table 6.1A shows the HSD test results of molar ratio effects on biodiesel yield with significant difference ($p < 0.05$) between all molar ratios investigated. Figure 6.2B shows biodiesel yield distribution at different levels of molar ratios. The molar ratio with widest ANOVA distribution of biodiesel yield was observed at 1:4 (fat:methanol).

Table 6.1: Comparison of biodiesel yield based on effect of (A) molar ratio and (B) enzyme concentration by Tukey's Studentized Range (HSD) Test

A

Comparisons significant at the 0.05 level are indicated by *.**

Molar ratio Comparison	Difference Between Means	Simultaneous 95% Confidence Limits		
4 - 6	5.500	2.568	8.432	***
4 - 8	10.300	7.368	13.232	***
6 - 4	-5.500	-8.432	-2.568	***
6 - 8	4.800	1.868	7.732	***
8 - 4	-10.300	-13.232	-7.368	***
8 - 6	-4.800	-7.732	-1.868	***

B

Comparisons significant at the 0.05 level are indicated by *.**

Enzyme Comparison	Difference Between Means	Simultaneous 95% Confidence Limits		
6 - 8	1.167	-1.765	4.099	
6 - 4	23.733	20.801	26.665	***
8 - 6	-1.167	-4.099	1.765	
8 - 4	22.567	19.635	25.499	***
4 - 6	-23.733	-26.665	-20.801	***
4 - 8	-22.567	-25.499	-19.635	***

6.3.3 Effect of ultrasonic amplitude and cycle

Three levels of ultrasonic amplitudes (30, 40, and 50%) were examined for the effect of ultrasonic amplitude on biodiesel yield from waste lard as shown in experimental set A (Table 5.1). Effect of amplitude on the biodiesel yield was investigated at three levels ultrasonic cycles (3, 5, and 7 per sec), by keeping other reaction conditions the same. At ultrasonic amplitudes 30% and 50%, there was no significant difference ($P < 0.05$) in yield between cycles 0.3 and 0.5 (per sec), respectively. In these pre-optimized conditions, more than 96% conversion of waste lard to biodiesel was obtained at reaction time, 30 min as shown in Figure 6.3. The effects of ultrasonic amplitude, ultrasonic cycle and the interaction between amplitude and cycle were statistically significant ($P < 0.05$) in the transesterification of waste lard to produce biodiesel.

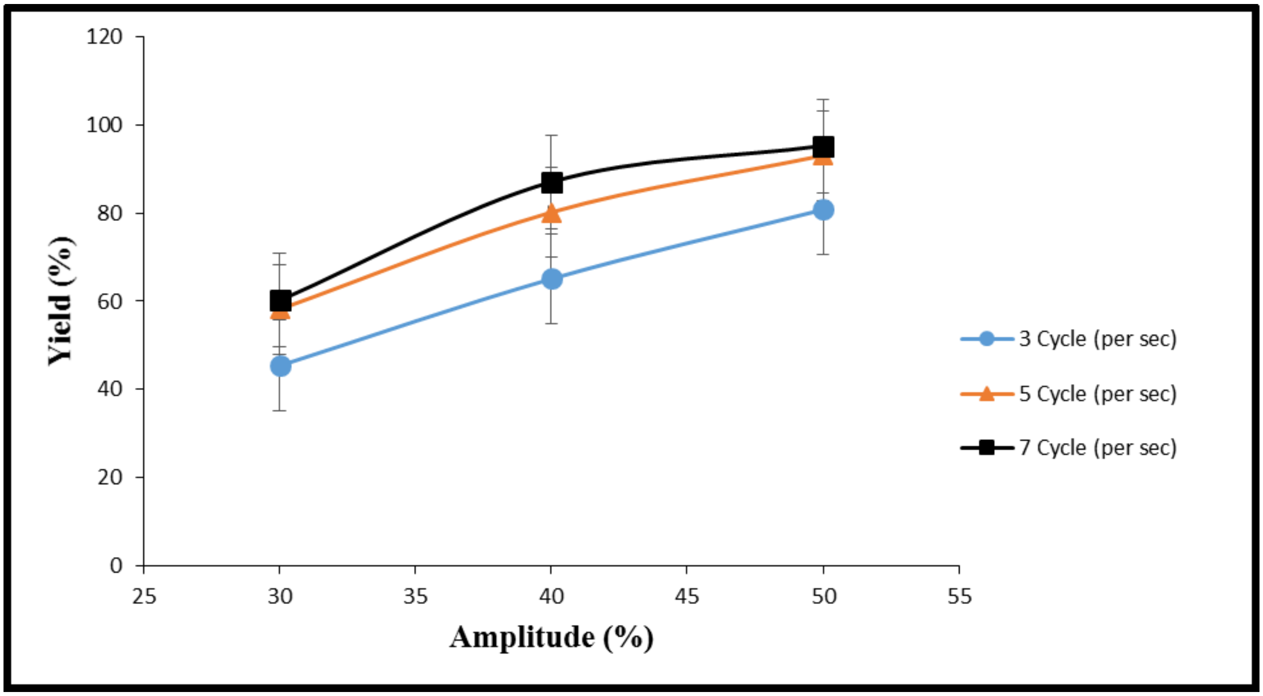

Figure 6.3: Effect of ultrasonic amplitude and cycle of the conversion of waste lard to biodiesel at enzyme conc. 6 wt.% of fat, reaction time 30 min, and molar ratio (fat:methanol) 1:6

Figures 6.4A and 6.4B show the distribution plots of biodiesel yield from waste lard due to ultrasonic amplitude and ultrasonic cycle, respectively. For amplitude, the widest range of biodiesel yield occurred with the 40% ultrasonic amplitude (Figure 6.4A), while for cycles per second, the widest range was observed at 7 cycle per sec (Figure 6.4B). Differences in biodiesel yield from waste lard were further investigated by Tukey's honest significant difference (HSD) test; $p < 0.05$ for multiple comparison of means. The results of the comparison of means showed biodiesel yields at each amplitude investigated to be significantly different from one another (Table 6.2A), confirming the distribution of ultrasonic amplitude and cycle data presented in Figure 6.4A. On the other hand, the results of the comparison of means showed biodiesel yields at each ultrasonic cycle investigated to be not significantly different between 5 and 7 cycles (Table 6.2B).

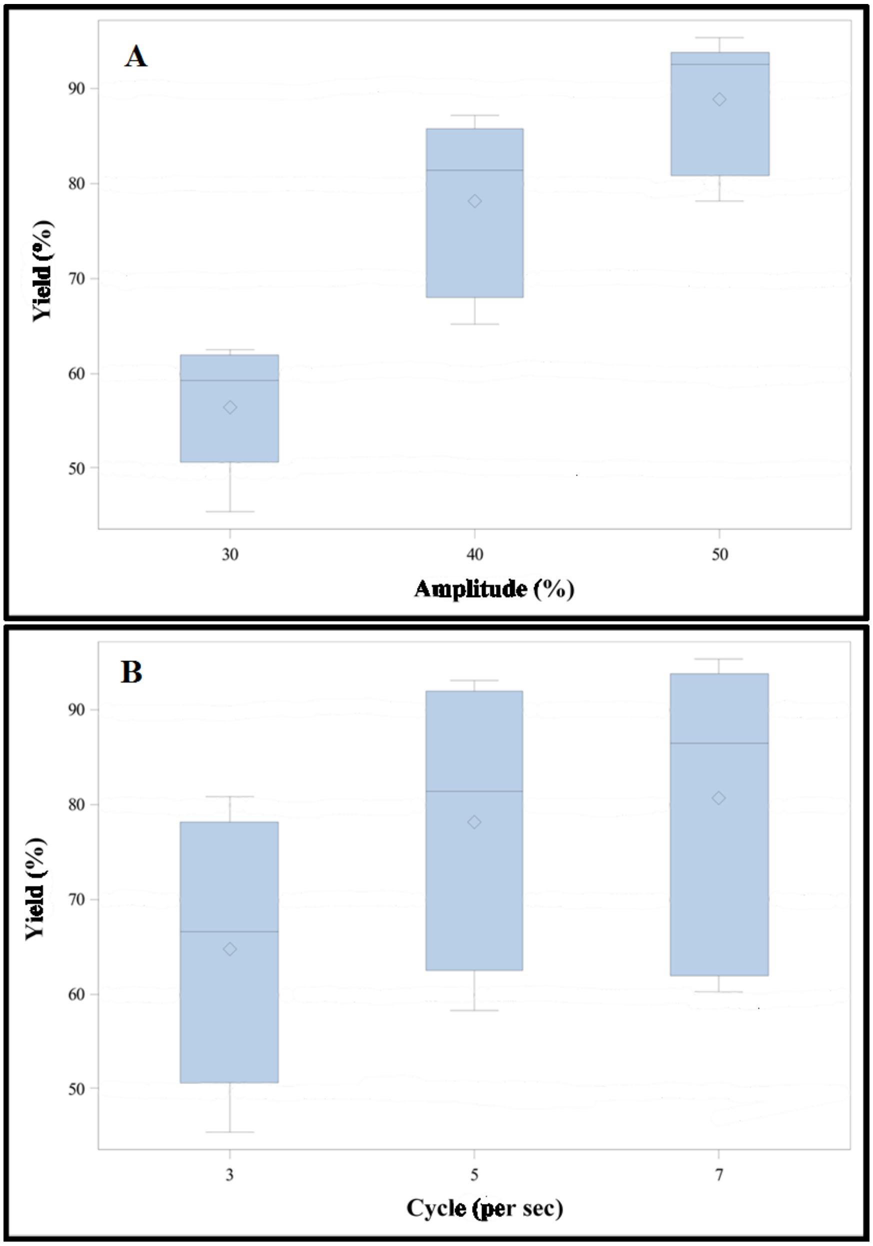

Figure 6.4: ANOVA distribution of biodiesel yield based on: (A) Ultrasonic Amplitude (B) Ultrasonic Cycle

Table 6.2: Comparison of biodiesel yield based on effect of (A) ultrasonic amplitude and (B) cycle by Tukey's Studentized Range (HSD) Test

A

Comparisons significant at the 0.05 level are indicated by *.**

Amplitude Comparison	Difference Between Means	Simultaneous 95% Confidence Limits		
50 - 40	10.750	7.466	14.034	***
50 - 30	32.367	29.083	35.650	***
40 - 50	-10.750	-14.034	-7.466	***
40 - 30	21.617	18.333	24.900	***
30 - 50	-32.367	-35.650	-29.083	***
30 - 40	-21.617	-24.900	-18.333	***

B

Comparisons significant at the 0.05 level are indicated by *.**

Cycle Comparison	Difference Between Means	Simultaneous 95% Confidence Limits		
7 - 5	2.617	-0.667	5.900	
7 - 3	16.000	12.716	19.284	***
5 - 7	-2.617	-5.900	0.667	
5 - 3	13.383	10.100	16.667	***
3 - 7	-16.000	-19.284	-12.716	***
3 - 5	-13.383	-16.667	-10.100	***

6.3.4 Effect of reaction time and amplitude

Figure 6.6 shows the biodiesel yield at different reaction times over varying amplitudes (30, 35, 40, 45, and 50%). It illustrates how biodiesel yield increases as reaction time extended. Above an amplitude of 30%, the yield increases up to a reaction time of 20 min, but remains largely constant thereafter. The effects of reaction time and ultrasonic amplitude under pre-optimized conditions [e.g. molar ratio (fat:methanol) (1:6), and enzyme concentration (6% w/w of fat)] were significant ($P < 0.05$), as was their interaction. Figure 6.5 shows the biodiesel yield distribution based on reaction time. In this figure, the biodiesel yield distribution at 15 min reaction time was observed to be slightly wider than others and with the closest mean and median. Differences in biodiesel yield from waste lard were further investigated by Tukey's honest significant difference (HSD) test; $p < 0.05$ for multiple comparison of means. The results of the comparison of means showed biodiesel yields at each reaction time investigated to be significantly different from one another (Table 6.3). Comparatively, Fan et al. (2010), who studied ultrasonically-assisted production of biodiesel from crude cottonseed oil, found no significant differences for biodiesel yield at shorter reaction times (10 sec to 5 min), but did find differences at longer reaction time (30–60 min). Processing time by enzyme-catalyzed conventional batch methods are in the range of 12-24 h for biodiesel production, where with sonication these times are reduced to less than 30 min.

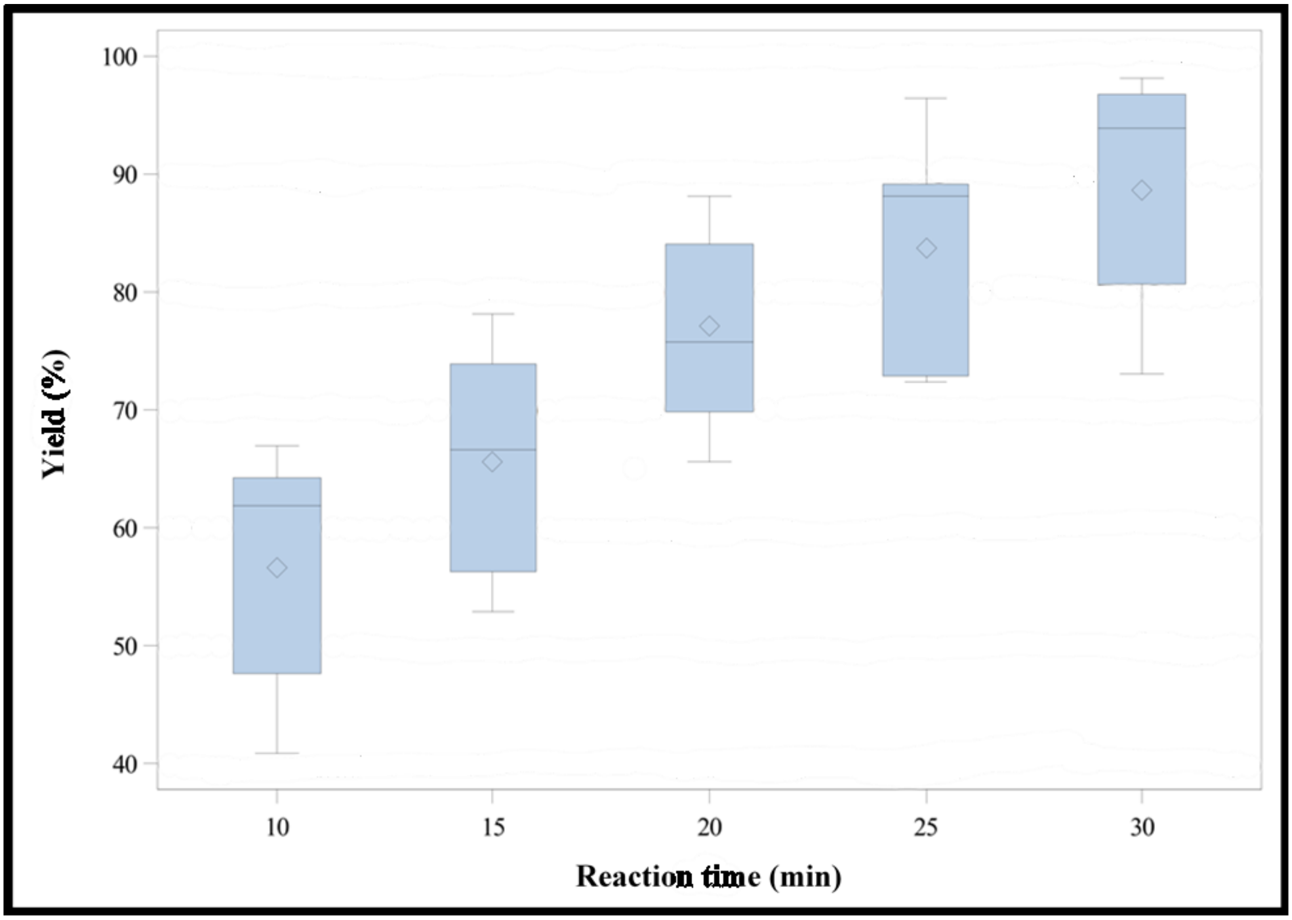

Figure 6.5: ANOVA distribution of biodiesel yield based on: reaction time

Table 6.3: Comparison of biodiesel yield based on effect of reaction time by Tukey's Studentized Range (HSD) Test

Comparisons significant at the 0.05 level are indicated by ***.				
Time Comparison	**Difference Between Means**	**Simultaneous 95% Confidence Limits**		
30 - 25	4.8900	2.8993	6.8807	***
30 - 20	11.5200	9.5293	13.5107	***
30 - 15	22.9800	20.9893	24.9707	***
30 - 10	31.9900	29.9993	33.9807	***
25 - 30	-4.8900	-6.8807	-2.8993	***
25 - 20	6.6300	4.6393	8.6207	***
25 - 15	18.0900	16.0993	20.0807	***
25 - 10	27.1000	25.1093	29.0907	***
20 - 30	-11.5200	-13.5107	-9.5293	***
20 - 25	-6.6300	-8.6207	-4.6393	***
20 - 15	11.4600	9.4693	13.4507	***
20 - 10	20.4700	18.4793	22.4607	***
15 - 30	-22.9800	-24.9707	-20.9893	***
15 - 25	-18.0900	-20.0807	-16.0993	***
15 - 20	-11.4600	-13.4507	-9.4693	***
15 - 10	9.0100	7.0193	11.0007	***
10 - 30	-31.9900	-33.9807	-29.9993	***
10 - 25	-27.1000	-29.0907	-25.1093	***
10 - 20	-20.4700	-22.4607	-18.4793	***
10 - 15	-9.0100	-11.0007	-7.0193	***

6.3.5 Enzyme-catalyzed kinetic model

To further investigate the effects of ultrasonic parameters on the reaction kinetics of enzyme-catalyzed transesterification of waste lard, series of experiments were performed at varying ultrasound amplitude in the absence of CALB enzyme. No product was detected in those experiments but a significant concentrations of intermediate glyceride products mostly monoglyceride, and diglyceride were observed (Data not reported). This confirmed that ultrasonic parameters only assisted in the enzyme-catalyzed transesterification reaction but did not cause the product formation without the presence of CALB enzyme. The Cleland nomenclature of enzyme-catalyzed transesterification of waste lard mechanism is shown in Figure 5.7. In this mechanism, E binds with TG to form the enzyme-substrate complex [E.TG], after which transformation to Bd and E′ complex [E′.Bd] occurs. Based on Ping Pong model, the first product (Bd) emanates leaving E′ which further binds with the second substrate (M) to form [E′.M] complex. The complex is transformed to E and G complex [E.G] to synthesis second product (G) and E. This mechanism limits the production of water due to simultaneous hydrolysis and esterification reactions, water generated during esterification is usually consumed during hydrolysis process (Belafi Bako et al., 2002). One step esterification reaction occurs at the beginning of the process due to the FFA content of waste lard. The enzyme-catalyzed kinetics for the production of biodiesel from waste lard using immobilized CALB and a Ping Pong model was based on simultaneous hydrolysis and esterification of triglyceride mechanism as reported by Al-Zuhair et al. (2007), and Cheirsilp et al. (2008). Transesterification pathway mechanism was reported to be more accurate and generate high quality product by assuming that transesterification takes place by direct alcoholysis of the triglyceride than two consecutive steps of hydrolysis and esterification (Azócar et al., 2014; Belafi Bako et al., 2002), rather the two consecutive steps occur simultaneously. The Ping Pong Bi Bi kinetic model prediction of the reaction performance of enzyme-catalyzed transesterification of waste lard assisted by ultrasonication was shown in Figure 6.6. At ultrasonic amplitude of 30%, the TG conversion did not show a sigmoidal (S-shaped) pattern. This could be attributed to the low reaction rate due to miscibility issue of waste lard and methanol and the formation of intermediate substrates complexes with enzyme. Ultrasound amplitude above 35% showed TG conversion to be sigmoidal pattern with limited concentration of intermediate substrates complexes. This result confirmed the assumed mechanism that the reaction would be in transesterification pathway where both hydrolysis and esterification reactions occurred simultaneously. This indicated that in the presence of methanol, the triglycerides were more easily yielded to FAME through methanolysis reaction rather than to FFA through hydrolysis reaction (Azócar et al., 2011; Cheirsilp et al., 2008). Similarly, above 40% ultrasonic amplitudes, activities within the reaction system occur below 20 min of the studied reaction time. Which means, effects of ultrasonic amplitude after this reaction time was limited since the reaction could proceed without mixing.

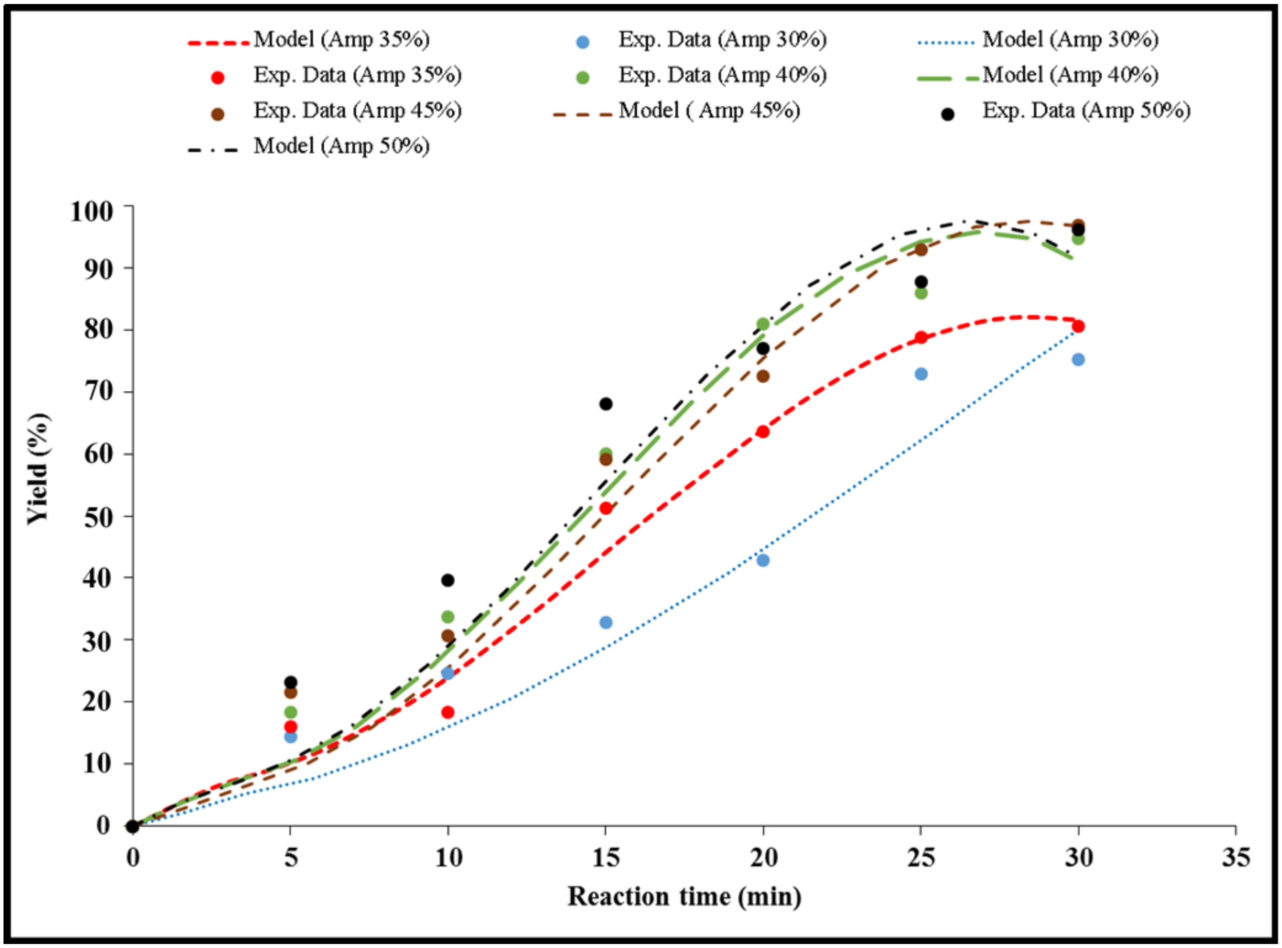

Figure 6.6: Plots of experimental data and model of biodiesel production at varying reaction times and ultrasonic amplitudes at constant enzyme conc. 6% (w/w) of fat, molar ratio (fat:methanol) 1:6, and ultrasonic amplitude 40%

6.3.6 Effects of ultrasonic amplitude on the reaction rate constants

Experimental setup at varying ultrasonic amplitudes and reaction times were carried out to investigate the effects of ultrasonic amplitude on the reaction rate constants. The enzyme concentration and fat:methanol molar ratio were kept at 6% (w/w) of fat and 1:6, respectively. Ultrasound amplitudes were run at 5, 10, 15, 20, 25, and 30 min reaction time. Based on the experimental results, the reaction rate constants were estimated by the procedure presented in section 2.5. Figure 6.7 shows the plots of reaction rate constants evaluated at each of the ultrasonic amplitudes studied. The values of the reaction rate constants, k_1 to k_6 change significantly at different ultrasonic amplitude. The rate constant (k_2) for the dissociation of enzyme-TG complex was highest at ultrasound amplitude 30% while the lowest was at ultrasound amplitudes 40% and 50%. This might be due to weak binding of enzyme and TG at 30% amplitude. The rate constant (k_3) that is responsible for the formation of biodiesel was highest at ultrasound amplitude 40% and lowest at 30%. This result confirms ultrasound amplitude of 40% to be a reliable amplitude for the production of biodiesel as earlier reported in this study. The graphical pattern of amplitude 30% in Figure 6.7 did not conform to other amplitudes. This confirmed the reason for deviation in amplitude 30% model curve as observed in Figure 6.6. Across all the ultrasound amplitudes, the reaction rate (k_6) for the association of biodiesel and glycerol to form the reactants was negative. This indicated that possibility of glycerol combining with biodiesel is limited during ultrasonication treatment of transesterification reaction. Similarly, the reaction rate (k_5) for the dissociation of E' and M was negative. This indicated that the possibility of disintegration of $E'M$ complex is limited during ultrasonication treatment of transesterification reaction which might be responsible to the substantial yield (more than 96%) observed.

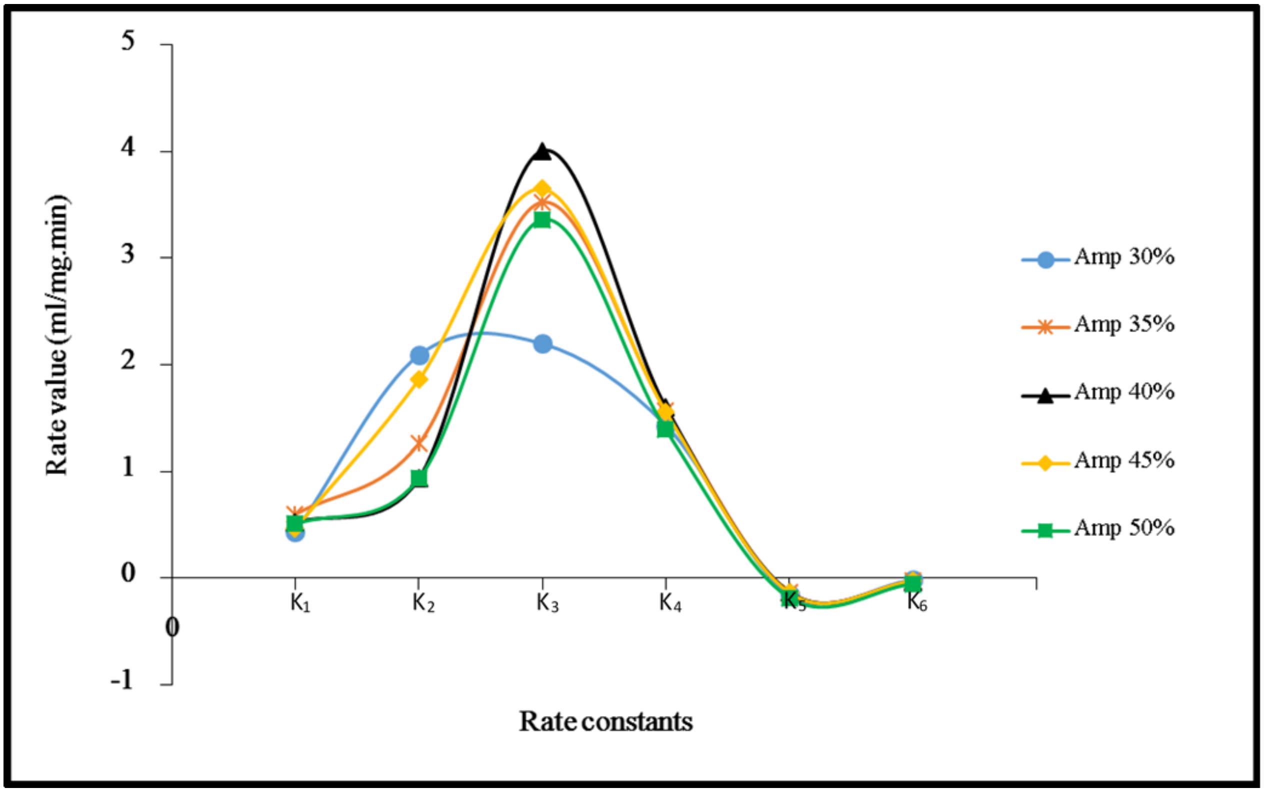

Figure 6.7: Plots of reaction rate constant values of the ultrasonic amplitudes

6.4 Conclusions

The reaction kinetics of an ultrasound assisted enzyme-catalyzed transesterification of waste lard with methanol for biodiesel production were successfully modeled using reaction rate expressions by varying ultrasonic amplitude parameter. The effects of reaction factors such as molar ratio (fat:methanol), catalyst concentration, reaction time, ultrasound amplitude and cycle on biodiesel yield were successfully investigated. The biodiesel yield was found to increase with increase in enzyme catalyst concentration, but decrease with increase in molar ratio. The kinetic model developed demonstrate reaction activities of enzyme-catalyzed methanolysis of waste lard for biodiesel production. A rapid increase in the forward reaction rate constants (k_1, k_3, k_4, and k_6) and decrease in reverse reaction rate constants (k_2 and k_5) was observed at 35% ultrasonic amplitude and above. The results of this study give a better understanding of the reaction rates with respect to individual reactants and system parameters which is a great advantage for design and construction of the biodiesel reactors using ultrasonication mixing.

CONNECTING TEXT TO CHAPTER 7

In chapters 3 and 4, the use of conventional and non-destructive techniques for AFW characterization were employed, respectively. Our findings from these two chapters were used to select parameter range of the investigated factors such as molar ratio of waste fat to methanol in Chapter 7 based on the amount of FFA in each of the waste fat samples. This chapter provides a description of data collection and methodology used for enzyme-catalyzed synthesis and kinetic of biodiesel production from waste choice white grease assisted by Ultrasonication. Chapter 7 manuscript was prepared and submitted to Energy and Fuel journal. The manuscript is co-authored by Drs. Dumont, M.-J., and Ngadi, M. The format of the manuscript has been altered to be consistent with this thesis. All literature cited in this chapter is listed in the references section at the end of this thesis.

Chapter 7

Enzyme-catalyzed synthesis and kinetic of biodiesel production from waste choice white grease assisted by ultrasonication

Abstract

In this study, the effects of ultrasonic parameters (amplitude, cycle and pulse) and major reaction factors (molar ratio and enzyme concentration) on the reaction kinetics of biodiesel generation from waste CWG bio-catalyzed by immobilized lipase [*Candida antarctica* Lipase B (CALB)] were investigated. A Ping Pong Bi Bi kinetic model approach was employed to study the effect of ultrasonic amplitude on the enzymatic transesterification. Kinetic constants of transesterification reaction were determined at different ultrasonic amplitudes (30, 35, 40, 45, and 50%) and enzyme concentrations (4, 6, and 8% wt. of fat) at constant molar ratio (fat:methanol); 1:6, and ultrasonic cycle; 5 Hz. Parametric effects on the yield were studied using three sets of experiments namely A, B, and C. In experiment set A, two factors (ultrasonic amplitude and cycle) were investigated at three levels; in experiment set B, two factors (molar ratio and enzyme concentration) were examined at three levels; and in experiment set C, two factors (ultrasonic amplitude and reaction time) were investigated at five levels. A yield of 98.2% was attained in 20 min at an ultrasonic amplitude (40%) at 5 Hz, fat:methanol molar ratio (1:4) and catalyst level 6% (w/w of fat). The fitted curves of the kinetic mechanism showed a sigmoidal curve due to mass transfer limitations which controlled the process at the beginning of the reaction. The kinetic model results also revealed interesting features of ultrasound assisted enzyme-catalyzed transesterification. The kinetic model approach described the whole methanolysis process accurately. At the ultrasonic

amplitude of 40%, the reaction activities within the system seemed to have steadied after 20 min which means the reaction could proceed with or without ultrasonic mixing.

7.1 Introduction

The production of biodiesel has increased significantly over the last decades with its global acceptance as a suitable substitute for fossil diesel. This trend is expected to increase even more in nearest future. The use of non-edible feedstocks as cheap raw materials for biodiesel production is a key point towards economic competitiveness with petro-diesel. Most of these non-edible feedstocks such as non-edible vegetable oils (e.g. Jatropha oil, Polanga oil) or AFW (e.g. Chicken fat, CWG) are characterized with high free fatty acids (FFA) and water (Adewale et al., 2014a, 2015; Canakci and Van Gerpen, 2001; Gerpen, 2005). The most widely used method for biodiesel production (alkali-catalyzed transesterification) is a challenge for these feedstocks due to their physicochemical properties (Adewale et al., 2014a; Adewale et al., 2014o). In fact, conventional approach of enzyme-catalyzed transesterification method which has been reported as a suitable technique for these types of feedstocks are more time consuming (Mata et al., 2011; Mata et al., 2012). For instance, Zago et al. (2014) studied the synthesis of ethylic esters for biodiesel purposes using lipases naturally immobilized in a fermented solid produced using *Rhizopus* microspores. The authors reported best conversion to be 91% at 48 h reaction time, obtained at 44 °C, with a molar ratio of ethanol/oil of 3:1 using a rotary shaker at 180 rpm. Sharma et al. (2013) quantified alkyl ester generated by biocatalysis employing different alcohols using new proton nuclear magnetic resonance-based derivation. The authors reported alkyl ester yield by butanol, pentanol, hexanol, and octanol as 67%, 76%, 66%, and 56%, respectively for 36 h reaction duration using a magnetic stirrer at 30°C. To further enhance substrates miscibility during transesterification reaction, application of ultrasonication has been reported as a reliable alternative (Deshmane and Adewuyi, 2013; Mahamuni and Adewuyi, 2009).

Recently, Choudhury et al. (2013); Mahamuni and Adewuyi (2009); Mahamuni and Adewuyi (2010); Michelin et al. (2015) and Teixeira et al. (2009) demonstrated the effectiveness of ultrasound-assisted transesterification of vegetable oils and animal fats for the production of biodiesel. Enzyme-catalyzed transesterification and esterification reactions were reported to possibly proceed kinetically by Ping Pong Bi Bi mechanism, ternary complex ordered Bi Bi mechanism, or ternary complex random Bi Bi mechanism (Shinde and Yadav, 2014). Veny et al. (2014) proposed a kinetic model of lipase catalyzed transesterification of jatropha oil in circulated batch packed bed reactor based on Ping Pong Bi Bi mechanism with reverse inhibition by methanol. In the investigation of Azócar et al. (2014) on the reaction kinetic of enzymatic biodiesel production from waste frying oil and crude rapeseed oil using co-solvent and an anhydrous medium to improve lipase performance in a semi-continuous reactor, the authors described the reaction mechanism as a Ping Pong Bi Bi model and reported methanol as the competitive inhibitor.

Cheirsilp et al. (2008) studied the impact of transesterification mechanisms on the kinetic modeling of biodiesel production using immobilized lipase by fitting experimental data of the transesterification of palm oil with various ethanol concentrations to estimate the reaction kinetic parameters. In a recent study of Michelin et al. (2015) on the kinetics of ultrasound-assisted enzymatic biodiesel production from Macauba coconut oil, the authors concluded that ultrasound-assisted lipase-catalyzed transesterification of Macauba coconut oil in a solvent-free system might be a potential alternative route to conventional alkali-catalyzed and/or traditional enzymatic methods. The objectives of this study were to investigate the parametric effects of ultrasonic wave amplitude, ultrasonic cycles, and reaction parameters (e.g. fat:methanol molar ratio, enzyme concentration, duration) on biodiesel yields from waste CWG and the effects of acoustic mixing on the kinetic modeling of enzyme-catalyzed transesterification pathway for biodiesel production from waste CWG.

7.2 Materials and methods

7.2.1 Materials and equipment

Waste CWG was obtained from a biodiesel production company in Canada (Rothsay Biodiesel, Montreal, Canada). Commercially produced immobilized *Candida antarctica* lipase B (CALB) was purchased from CLEA Technologies (Delftechpark, The Netherland). American Chemical Society (ACS) and HPLC grades of methanol were purchased from Fisher Scientific (Ontario, Canada). Saturated and unsaturated fatty acid methyl ester (FAME) standards for calibration curves were purchased from Sigma Aldrich, (Oakville, ON, Canada).

An ultrasonication set-up featuring a Vibra-Cell (VXC 500 series, Sonic and Materials Inc., CT, USA) was employed for the transesterification reaction. The Vibra-Cell device is designed to ensure uniform sonotrode probe amplitude, regardless of the varying loading conditions encountered during the processing cycle. The ultrasonic device operates at 500 W and 20 kHz frequency. The probe amplitude, cycle and pulse are adjustable from 0 to 100%, 0.1 - 1.0 per sec and 0.1 - 1.0 sec, respectively. For the identification and quantification of biodiesel produced, a Varian HPLC equipped with a refractive index (RI) detector and reverse phase (RP) C18 column was used.

7.2.2 Experimental set-up and procedure

The solvent free production of biodiesel from waste CWG involved an immobilized lipase catalyst (CALB), and transesterification with methanol to yield methyl esters. The transesterification of waste CWG using ultrasonication (Vibra-Cell) was carried out in a screw cap bottle (25 mL). The effects of processing and ultrasonic parameters such as amplitude, cycle, reaction time, molar ratio and loaded catalyst (enzyme) were carefully examined. Ultrasound amplitude was varied from low to mild regions (30, 35, 40, 45, and 50%) in order to prevent disintegration of the immobilized enzyme matrix by ultrasound waves. The ultrasonic wave cycle was investigated at 3, 5, and 7 per sec, factorially combined with three levels of ultrasonic amplitudes (30, 40, and 50%). To study the transesterification reaction, fat:methanol molar ratios of 1:4, 1:6, and 1:8, were factorially combined with enzyme concentration of 4, 6 and 8% (w/w) of fat. Three sets of experiments namely A, B, and C were conducted in order to study the effect of each factor on the biodiesel yield, as well as the effects of interactions between factors on the biodiesel yield and to identify most important level of each of the factors. In experiment set A, two factors (ultrasonic amplitude and cycle) were investigated at three levels (3^2). Other parameters (molar ratio, enzyme concentration and reaction time) were kept constant. In experiment set B, two factors (Molar ratio and enzyme concentration) were examined at three levels (3^2). Other parameters (ultrasonic amplitude, ultrasonic cycle and reaction time) were kept constant. In experiment set C, two factors (ultrasonic amplitude and reaction time) were investigated at five levels (5^2) (Table 5.1). Ultrasound amplitude was varied from low to mild regions (30, 35, 40, 45, and 50%) in order to prevent disintegration of the immobilized enzyme matrix by ultrasound waves. The ultrasonic wave cycle was investigated at 3, 5, and 7 Hz, factorially combined with three levels of ultrasonic amplitudes (30, 40, and 50%). To study the transesterification reaction, fat:methanol molar ratios of 1:4, 1:6, and 1:8, were factorially combined with enzyme concentration of 4, 6 and 8% (w/w) of fat.

Fat samples stored below -20ºC prior to analysis, were melted in a water bath (50ºC) before sampling. A fat sample (10 g) was then transferred to a 25 mL screw cap bottle and subjected to ultrasound waves for 1 min in order to further break down all possible fat crystals before the addition of other reagents. The mixture of all reagents was introduced, and ultrasound waves applied according to pre-set parameters. With the sonotrode probe submerged and fixed at a depth of 20 mm in the solution, the ultrasonic amplitude, ultrasonic cycle and the reaction time were adjusted using the controller. At each reaction time, a 500 µL aliquot was pipetted into a 2 mL micro centrifuge tube. The reaction was stopped by the addition of 50 µL of glacial acetic acid while 1 mL distilled water was added to wash excess methanol and traces of glycerol from the ester layer. The mixture was vortexed for 3 min before being centrifuged for 10 min at 10,000 × g using an Eppendorf 5415R Micro-centrifuge (Eppendorf Canada Ltd., Mississauga, Ontario) to separate the upper ester and lower aqueous phase. The upper layer is a mixture of esters while the lower layer is a mixture of glycerol, enzyme and aqueous solutions. For the analysis, 100 µL of the ester phase was diluted with acetone to an appropriate concentration before HPLC injection.

7.2.3 Chemical analysis

Calibration curves for FAME standards were developed by injecting six different concentrations (0.5-3.0 mg/mL) of each of the FAME standards expected to elute in the reaction products. The retention time of each of the FAME standards was matched to the corresponding peaks produced by the biodiesel samples. Analysis of the FAME standards and the reaction product were carried out by dissolving the samples in acetone. Some other solvents such as methanol, hexane, chloroform, and toluene were considered but the reaction product showed their greatest solubility in acetone. An external standard quantitation procedure on HPLC was used to develop the FAME standard calibration curves employed in this study. This procedure is a basic quantification approach in which both standard and unknown samples are analysed under the same conditions and the results from the unknown samples are then related to those of the standard samples. The curves were constructed by injecting different known concentrations of the standard solution and measuring the peak area obtained. A regression line of best fit was used to join the points of the curve obtained. All calibration concentration points were ran in triplicate. The best fit regression line gave a correlation coefficient which measured how well the data point's best fit to a straight line. The correlation coefficient equally showed predictability strength of the developed calibration curves to measure the concentrations of the unknown analytes. The developed calibration curves were used to estimate the amount of the desired compounds in the biodiesel aliquot.

The ester phase was analyzed by RP-HPLC which separated the different product components according to their polarity. A Varian HPLC unit equipped with a Varian Prostar 240 pump, a reverse phase (RP) Discovery HS C18, 5 µm, 25 cm × 4.6 mm column (Supelco Analytical, Bellefonte, PA, USA), and a Varian 356-LC refractive index (RI) detector (Varian Inc., Walnut Creek, CA, USA) was used to analyze and quantify the conversion, the FAME composition and the purity of the ester phase (Chakraborty and Sahu, 2014). For all the experiments, an isocratic mobile phase method was used for the separation and determination of the biodiesel produced by the methanolysis of waste CWG. The system operated at a flow rate of 1 mL/min, with an injection volume of 25 µL, and a sample runtime of 30 minutes.

7.2.4 Kinetic model development

In enzyme-catalyzed reaction kinetics, the reaction rate is measured by varying the effects of the reaction conditions (Yang et al., 2005) and monitor how these varying parameters affect the enzyme activities in term of product yields. The kinetic mechanism of enzyme-catalyzed transesterification of CWG was developed based on ping pong Bi Bi Cleland nomenclature for two substrates (Meunier et al., 2014b). The substrates bind to the enzyme's active reaction site and then transformed into products through a series of steps known as the enzymatic mechanism.

7.2.4.1 Enzyme kinetics mechanisms

Equation 5.2 represents a typical multi-substrate Bi-Bi enzyme kinetic of transesterification reaction: TG and methanol (M) are the substrates while biodiesel (Bd) and glycerol (G) are the products. In this mechanism, the enzyme (E) must bind the first substrate (TG) to form enzyme-substrate complex [ETG], and then released the first product (Bd) and transformed intermediate enzyme (E'). This is followed by binding of second substrate (M) to (E') and breakdown of the transitory complex [$E'M$] to free enzyme (E) and the second product (G) (Cheirsilp et al., 2008; Veny et al., 2014; Yang et al., 2005).

Equation 5.3 represents the formation of the enzyme–substrate complex with TG [ETG], the release of Bd from this complex and the generation of transformed enzyme (E'). The formation of the transformed enzyme-substrate complex with M [$E'M$] and the release of the second product (G) and free enzyme (E) is shown in equation 5.4. Rate constants k_1 and k_4 are for the enzyme–substrate complex associations for TG and M, respectively; k_2 and k_5 are rate constants of the enzyme–substrate complex dissociations for TG and M, respectively; k_3 and k_6 are the catalytic rate constants for the formation of products Bd and G, respectively. The rate expressions for the overall reaction mechanism (Equations 5.3 and 5.4) above, without considering possible intermediate glycerides (di- and monoglyceride) are expressed as in Equations 5.5 – 5.12. Because a much faster reaction occurs with the diglyceride and monoglyceride than the triglyceride, hence the overall reaction can be used to develop a simplified model instead of the all three reaction steps (Azócar et al., 2014). The influence of external and internal mass transfer on the reaction kinetic was assumed negligible due to the small volume of the reaction vessel (25 ml) and given that immobilized lipase would be more accessible. A single response that was used to justify possibility of mass transfer was the biodiesel yield from the combination of the independent variables. Based on these assumptions, the reaction kinetics was studied independently of the mass transfer, which made the model to be mass transfer limited.

7.2.5 Determination of kinetic parameters

The concentrations of the substrates, FAME (biodiesel) at different times were determined experimentally starting with 10 g of waste CWG and varied methanol amounts of 1.51, 2.27 and 3.03 g to obtain molar ratios of methanol to CWG of 4, 6 and 8, respectively. The effects processing parameters; ultrasonic amplitude (30, 35, 40, 45, and 50%) at varied reaction time (5, 10, 15, 20, 25, and 30 min.) on the reaction rates of enzyme-catalyzed transesterification of waste CWG were investigated. This was achieved by fitting the reaction rate differential equations generated based on Ping Pong Bi Bi mechanism to the experimental data. The reaction rate differential equations and variable definitions as generated in equations 5-12 were used to develop kinetic reaction model in Mathematica programming software where they were solved by the NDSolve function to generate model and experimental data time plots. The values of rate constants were estimated at best fitted plot of model and experimental data.

7.2.6 Statistical Analysis

A full factorial design was used for each of the three experimental sets ran independently to verify effects of ultrasound and reaction parameters on the biodiesel yields from waste CWG. Statistical analysis was carried out to investigate factor effect leverage and desirability using JMP$^{®}$ 11.2.0 (Statistical Analysis Systems, SAS Institute Inc., Cary, NC, USA). Leverage Plot reports the effect of each factor on the response variable and gives insight on possible multicollinearity observations. Desirability functions was used to find the optimal value for each factor.

7.3 Results and Discussion

The free fatty acid (FFA) content of waste CWG was 19.26% according to AOCS (Ca 5a-40) as reported in our previous study (Adewale et al., 2014a; Adewale et al., 2014o). The GC analysis showed the fatty acid (FA) profile of the waste CWG to mainly consist of: C16:0 (22.39%), C16:1 (3.40%), C18:0 (9.15%), C18:1 (44.14%), and C18:2 (11.90%) (Adewale et al., 2014a). In this study, enzymatic catalysis was used and variables such as molar ratio (fat:methanol), catalyst concentration, reaction time, ultrasound amplitude and cycle were investigated.

7.3.1 Effect of enzyme concentration and molar ratio

In the investigation of the effect of enzyme concentration on biodiesel yield at varying molar ratios during transesterification of waste CWG assisted by ultrasonication, experimental set B (Table 5.1) was used. Figure 7.1 shows the relationship between molar ratios and yield under different enzyme concentrations, over a constant reaction time of 30 min, ultrasonic amplitude of 40%, and cycle of 5 Hz. As shown in the Figure, the lowest biodiesel yield was observed at 4% (w/w of fat) enzyme concentration for all the molar ratios tested, indicating an insufficient enzyme concentration to catalyze the reaction completely. Biodiesel yield was found to decrease with increase in molar ratio. Figures 7.2A-F show the effects leverage and desirability plots of biodiesel yield from waste CWG based on molar ratio (fat:methanol) and enzyme concentration. The plot of actual versus predicted values, which shows the observed data of biodiesel yield against the predicted data of the yield is shown in Figure 7.2A. The figure shows the leverage plot for the whole model with regression coefficient $R^2 = 0.83$, and root mean square error (RMSE) = 6.6067 ($p < 0.05$). The residual plot shows a random pattern around horizontal axis, indicating a good fit of the model (Figure 7.2E). The effect leverage plot, Figure 7.2C shows enzyme concentration to be significant ($p < 0.05$) for the production of biodiesel from waste CWG. Interaction between enzyme concentration and molar ratio (Figure 7.2D), is found to be statistically insignificant ($p > 0.05$). This could be attributed to less inhibitive effect of methanol on immobilized enzyme (CLEA) (Lu et al., 2007; Luković et al., 2011). The desirable value for enzyme concentration is 6% (w/w of fat) as shown in desirability profiler with a corresponding desirable value for biodiesel yield to be 92.6% (Figure 7.2F).

This enzyme concentration (6% w/w of fat) was considerably reduced to the reported results using conventional stirring techniques. For instance, Xie and Wang (2014) investigated enzymatic production of biodiesel from soybean oil by using immobilized lipase on Fe_3O_4/Poly (styrene-methacrylic acid) magnetic microsphere as a biocatalyst. The authors reported 50% enzyme concentration (based on the oil mass) as the suitable amount of the bound lipase chosen to conduct the transesterification reaction with highest conversion of 86% at 24 h reaction time. Shah et al. (2004) and Kumari et al. (2007) used 10% enzyme concentration (w/w of oil) in the lipase-catalyzed production of biodiesel from jatropha oil and high FFA containing oil from *Madhuca indica*, respectively. Similarly, Xu et al. (2003) studied a novel enzymatic route for biodiesel production from renewable oils in a solvent-free medium. The authors reported the optimum conditions as: an enzyme concentration of 30% (w/w of oil), a molar ratio of methyl acetate/oil of 12:1, reaction time of 10 h as optimum conditions and yielded 92% of methyl esters (ME). In this regard, application of ultrasound for biodiesel production would significantly reduce production reagent costs. The effect leverage plot, Figure 7.2B shows molar ratio as a significant factor ($p < 0.05$) for the production of biodiesel from waste CWG, however, interaction between enzyme concentration and molar ratio is not significant. Molar ratio desirable value is 1:4 (fat:methanol) as depicted in desirability profiler with a corresponding desirable value for biodiesel yield to be 92.6% (Figure 7.2F).

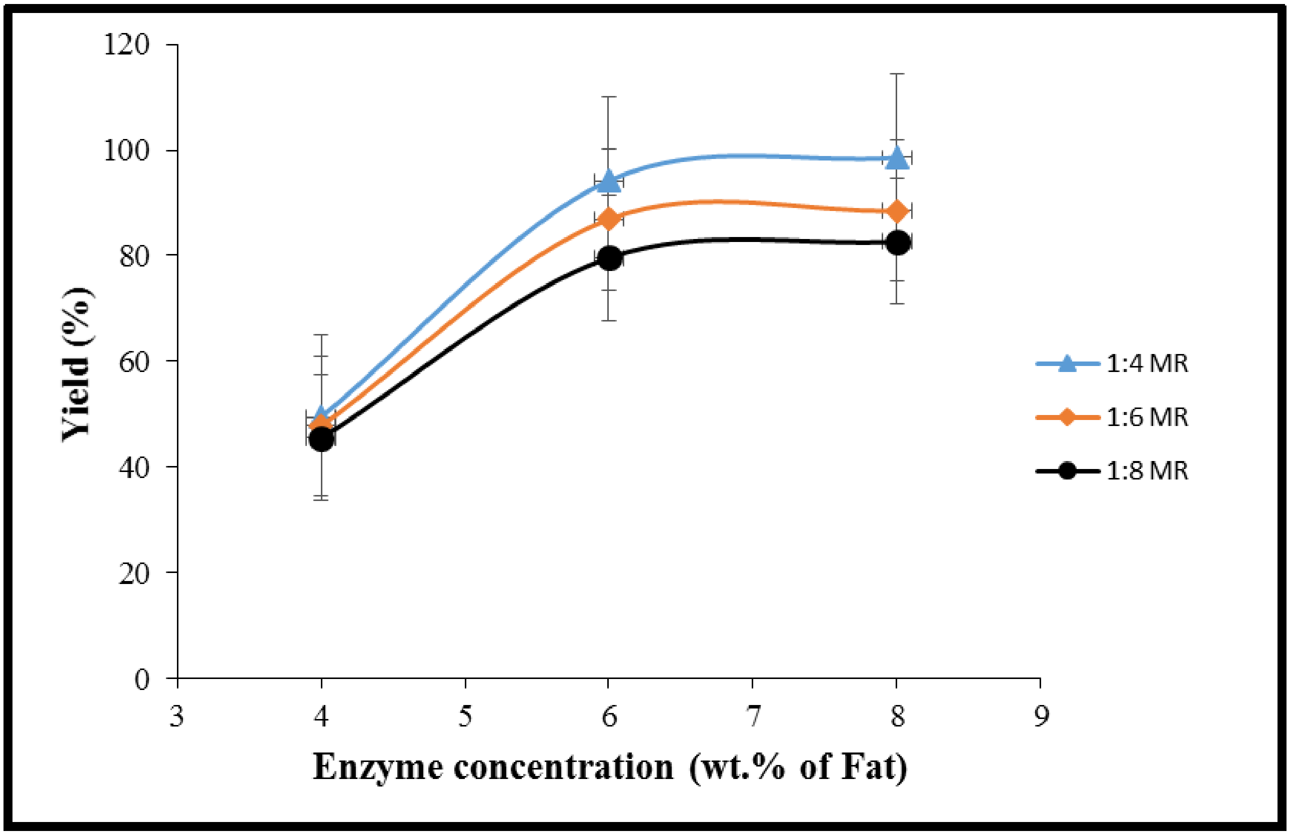

Figure 7.1: Effect of molar ratio and catalyst concentration of the conversion of waste CWG to biodiesel at reaction time 30 min, ultrasonic cycle 5 Hz, and ultrasonic amplitude

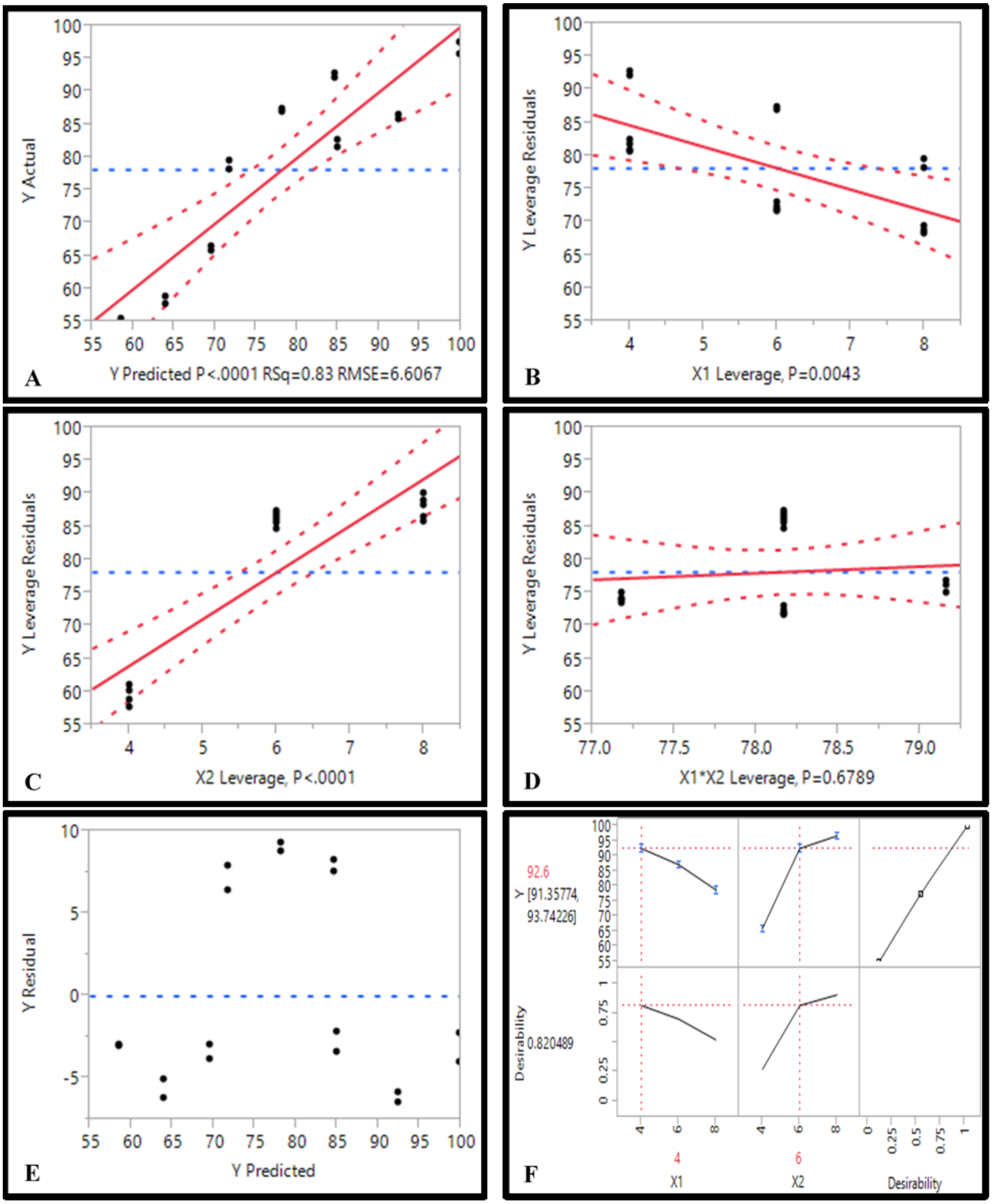

Figure 7.2: Effects leverage and desirability plots of biodiesel yield based on: (A) Yield Prediction (B) Molar Ratio (fat:methanol) (C) Enzyme concentration (D) Factors interaction (E) Yield residual plot (F) Desirability of factors

7.3.2 Effect of ultrasonic amplitude and cycle

Three levels of ultrasonic amplitudes (30, 40, and 50%) were examined for the effect of ultrasonic amplitude on biodiesel yield from waste CWG as shown in experimental set A (Table 5.1). The amplitude effect on the biodiesel yield was investigated at three levels ultrasonic cycles (3, 5, and 7 per sec), by keeping other reaction conditions the same. Increase in both ultrasonic amplitude and cycle leads to increase in biodiesel yield from waste CWG (Figure 7.3). In the pre-optimized conditions above, more than 98% conversion of waste CWG to biodiesel was obtained at 30 min reaction time. This high yield could be related to low viscosity of CWG as compared to other AFW (Adewale et al., 2014a), which would give less resistance to acoustic wave generated by the ultrasound machine. The plot of actual versus predicted values, which shows the observed data of biodiesel yield against the predicted data of the yield is shown in Figure 7.4A. The figure shows the leverage plot for the whole model with regression coefficient $R^2 = 0.91$, and RMSE = 5.9975 ($p < 0.05$). The residual plot shows a random pattern around horizontal axis, indicating a good fit of the model (Figure 7.4E). The effect leverage plot, Figures 7.4B and C show ultrasonic cycle and amplitude to significantly ($p < 0.05$) influence the production of biodiesel from waste CWG. Interaction between ultrasonic amplitude and cycle is not insignificant ($p > 0.05$) as shown in Figure 7.4D. This can be ascribed to the physicochemical properties of CWG which was found to have least viscosity and viscoelasticity out of the AWFs studied in our previous investigation (Adewale et al., 2014a). CWG was found to have least viscosity among the AFW considered in the study. From the results of a further statistical test carried out to investigate the actual effect of these factors using desirability function. The desirable values for ultrasonic amplitude and cycle are 40% and 7 Hz, respectively with a corresponding desirable value for biodiesel yield to be 95.8% (Figure 7.4F).

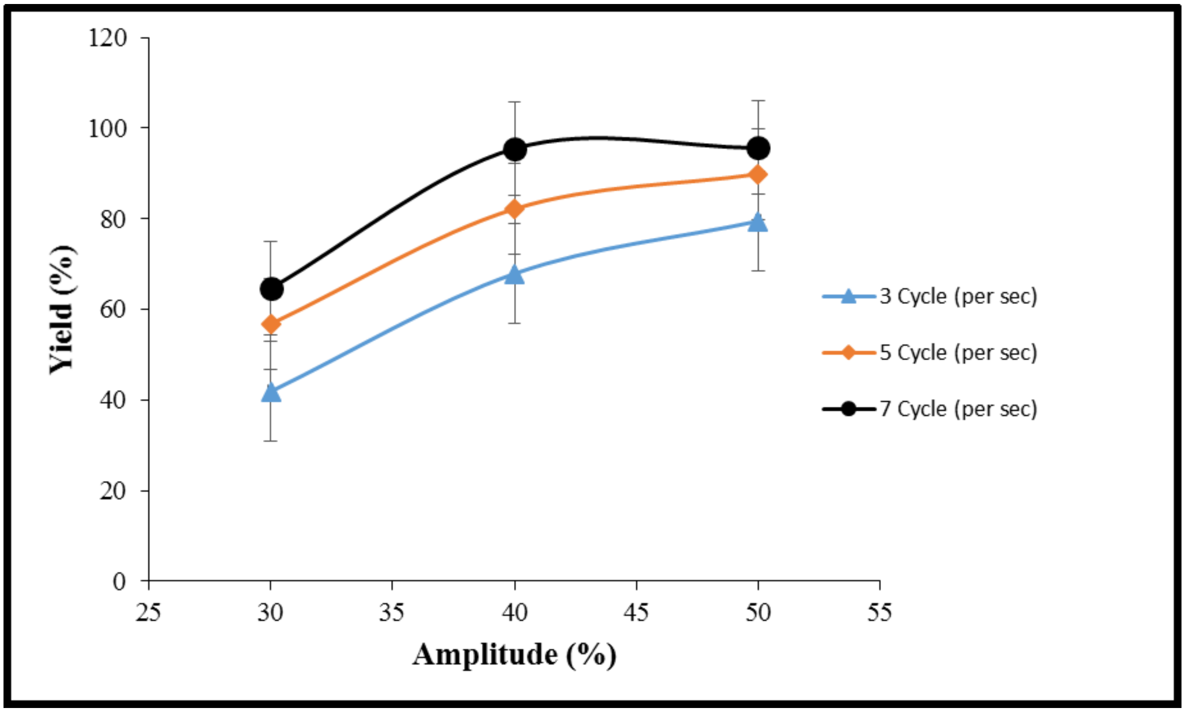

Figure 7.3: Effect of ultrasonic amplitude and cycle of the conversion of waste CWG to biodiesel at enzyme conc. 6 wt.% of fat, reaction time 30 min, and molar ratio (fat:methanol) 1:6

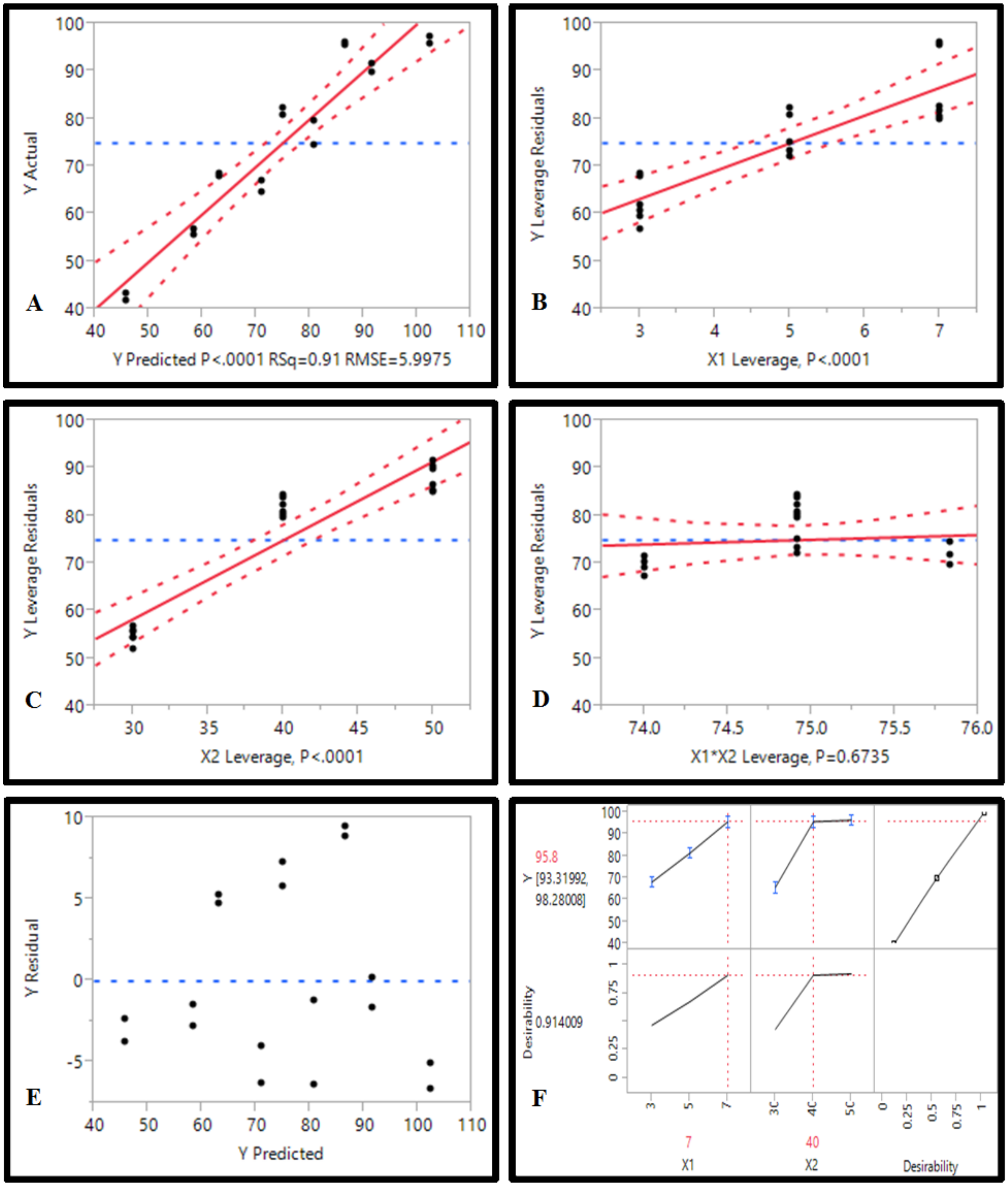

Figure 7.4: Effects leverage and desirability plots of biodiesel yield based on: (A) Yield prediction (B) Ultrasonic cycle (C) Ultrasonic amplitude (D) Factors interaction (E) Yield residual plot (F) Factors desirability

7.3.3 Effect of reaction time and amplitude

Figures 7.5A-F show the effects leverage and desirability plots of biodiesel yield from waste CWG based on ultrasonic amplitude and reaction time. The plot of actual by predicted values, which shows the observed data of biodiesel yield against the predicted data of the yield is shown in Figure 7.5A. The figure shows the leverage plot for the whole model with regression coefficient $R^2 = 0.90$, and RMSE = 5.8259 ($p < 0.05$). The residual plot against predicted values of biodiesel yield shows a random pattern around horizontal axis, indicating a good fit of the model (Figure 7.5E). Illustrations of how biodiesel yield increases as reaction time extended at different reaction times over varying amplitudes (30, 35, 40, 45, and 50%) is shown in Figure 7.6. The effects of reaction time and ultrasonic amplitude under pre-optimized conditions [e.g. molar ratio (fat:methanol) (1:6), and enzyme concentration (6% w/w of fat)] were significant ($P < 0.05$), as well as their interaction (Figures 7.5B and C). The desirable value for reaction time and ultrasonic amplitude as shown in desirability profiler (Figure 7.5F), are 20 min, and 40%, respectively. In a relative findings, Noipin and Kumar (2015) optimized ethyl ester production from refined palm oil assisted by ultrasonic power, reported that the ethyl ester yield was around 80% within 5 min of the reaction time and it reached equilibrium in a short reaction time of 20 min. Similarly, Fan et al. (2010), who studied ultrasonically-assisted production of biodiesel from crude cottonseed oil, found no significant differences for biodiesel yield at shorter reaction times (10 sec to 5 min), but did find differences at longer reaction time (30–60 min). Processing time by enzyme-catalyzed conventional batch methods are in the range of 12-24 h for biodiesel production while sonication process reaction times are reduced drastically to less than 30 min.

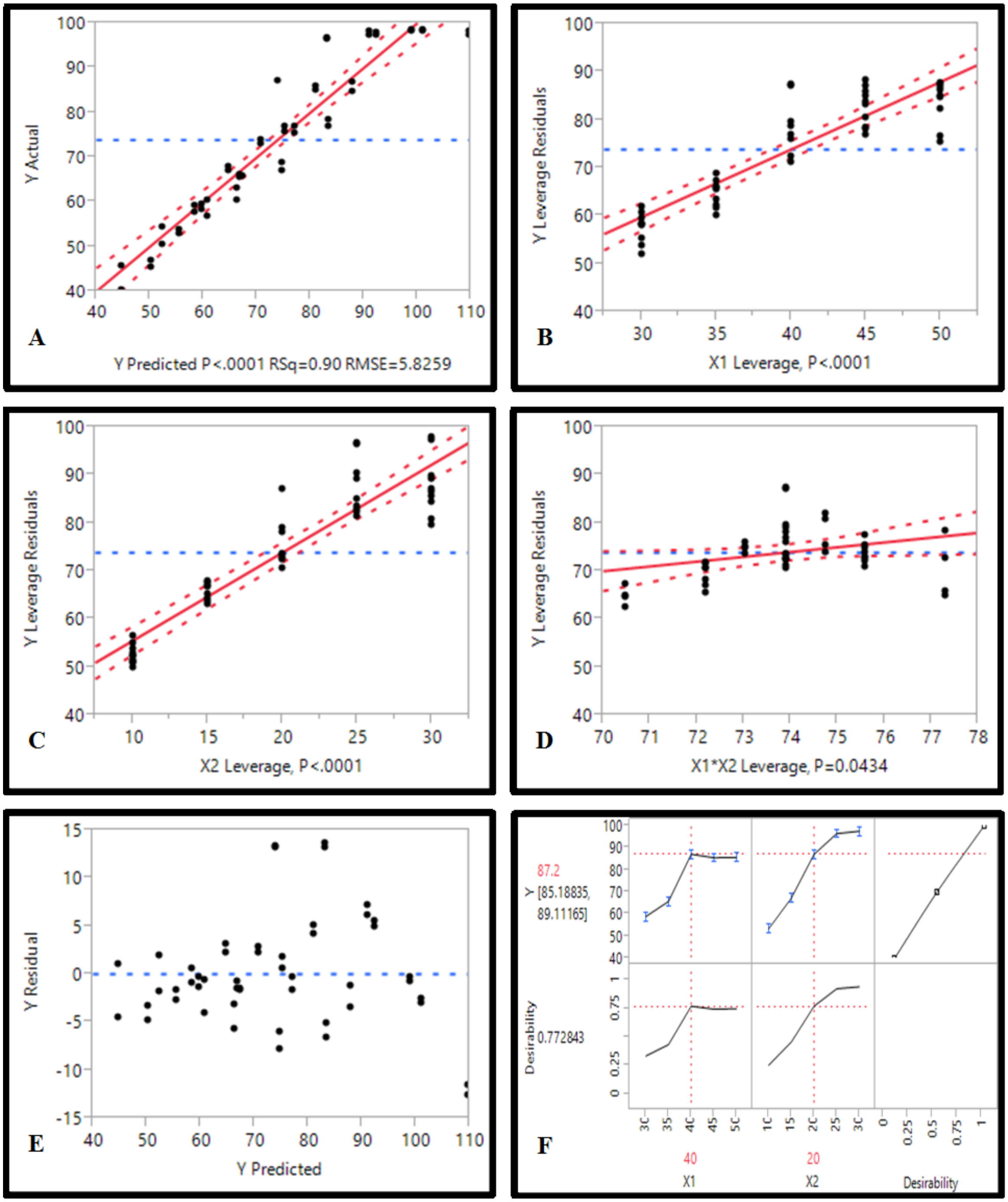

Figure 7.5: Effects leverage and desirability plots of biodiesel yield based on: (A) Yield Prediction (B) Ultrasonic amplitude (C) Reaction time (D) Factors interaction (E) Yield residual plot (F) Desirability of factors

7.3.4 Enzyme-catalyzed kinetic model

The Cleland nomenclature of enzyme-catalyzed transesterification of waste CWG mechanism is shown in Figure 5.7. In this mechanism, E binds with TG to form the enzyme-substrate complex [E.TG], after which transformation to Bd and E′ complex [E′.Bd] occurs. Based on Ping Pong model, the first product (Bd) emanates leaving E′ which further binds with the second substrate (M) to form [E′.M] complex. The complex is transformed to E and G complex [E.G] to synthesis second product (G) and E. This mechanism limits the production of water due to simultaneous hydrolysis and esterification reactions, water generated during esterification is usually consumed during hydrolysis process (Belafi Bako et al., 2002). One step esterification reaction occurs at the beginning of the process due to the FFA content of waste CWG. The enzyme-catalyzed kinetics for the production of biodiesel from waste CWG using immobilized CALB and a Ping Pong model was based on simultaneous hydrolysis and esterification of triglyceride mechanism as reported by Al-Zuhair et al. (2007), and Cheirsilp et al. (2008). Transesterification pathway mechanism was reported to be more accurate and generate high quality product by assuming that transesterification takes place by direct alcoholysis of the triglyceride than two consecutive steps of hydrolysis and esterification (Azócar et al., 2014; Belafi Bako et al., 2002), rather the two consecutive steps occur simultaneously. The Ping Pong Bi Bi kinetic model prediction of the reaction performance of enzyme-catalyzed transesterification of waste CWG assisted by ultrasonication was shown in Figure 7.6.

At ultrasonic amplitude of 30%, the TG conversion did not show a sigmoidal (S-shaped) pattern. This could be attributed to the low reaction rate due to miscibility issue of waste CWG and methanol. Ultrasound amplitude above 35% showed TG conversion to be sigmoidal pattern with limited concentration of intermediate substrates complexes. This result confirmed the assumed mechanism that the reaction would be in transesterification pathway where both hydrolysis and esterification reactions occurred simultaneously. This indicated that in the presence of methanol, the triglycerides were more easily yielded to FAME through methanolysis reaction rather than to FFA through hydrolysis reaction (Azócar et al., 2011; Cheirsilp et al., 2008). Similarly, above 40% ultrasonic amplitudes, activities within the reaction system occur below 20 min of the studied reaction time. Which means, effects of ultrasonic amplitude after this reaction time was limited since the reaction could proceed without mixing. Different sets of experiments were performed to further investigate the effects of ultrasonic parameters on the reaction kinetics of enzyme-catalyzed transesterification of waste CWG at varying ultrasound amplitude in the absence of CALB enzyme. Very minute traces of FAMEs were detected in those experiments but a significant concentrations of intermediate glyceride products mostly monoglyceride, and diglyceride were observed (Data not reported). This confirmed that ultrasonic parameters only assisted in the enzyme-catalyzed transesterification reaction but did not cause the product formation without the presence of CALB enzyme.

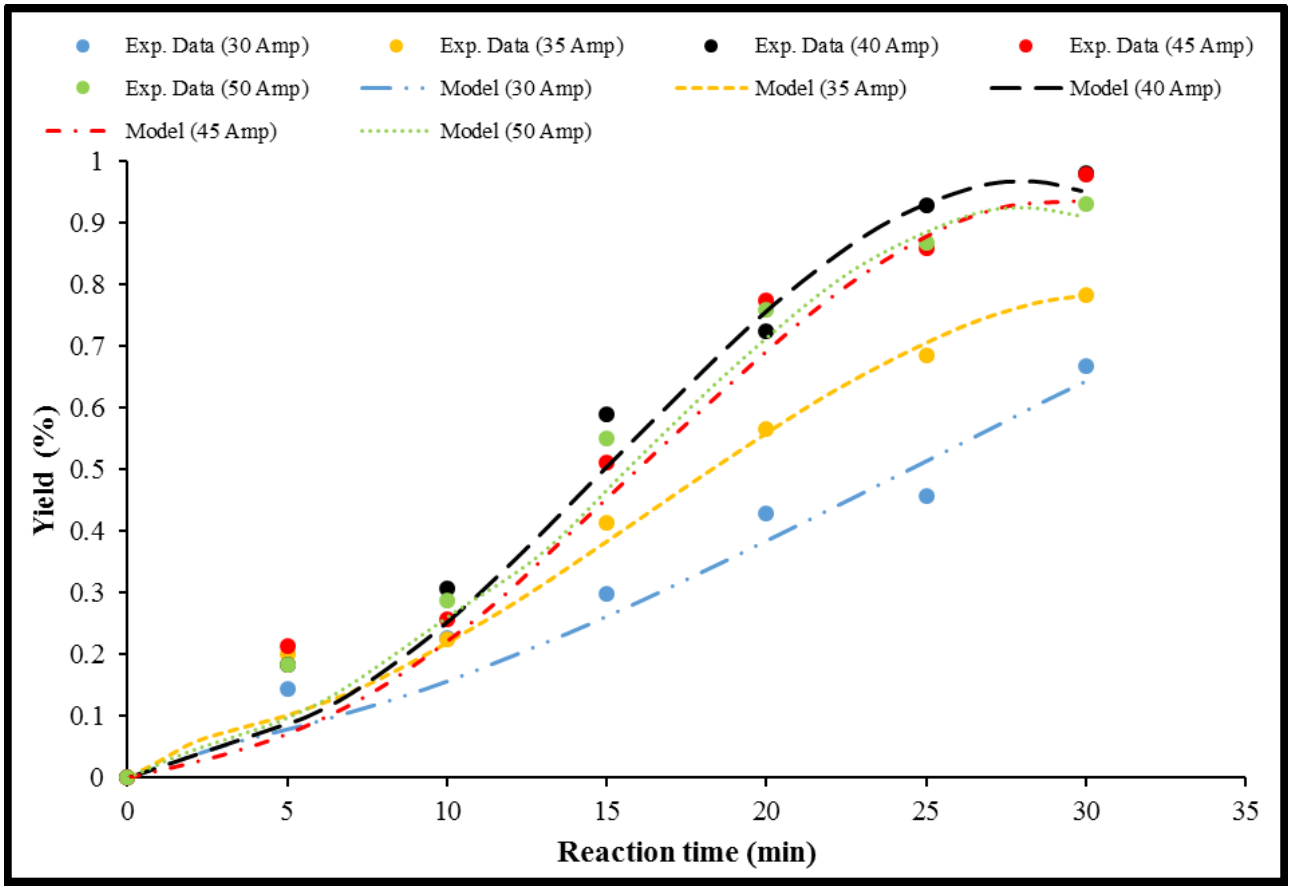

Figure 7.6: Plots of experimental data and model of biodiesel production at varying reaction times and ultrasonic amplitudes at constant enzyme conc. 6% (w/w) of fat, molar ratio (fat:methanol) 1:6, and ultrasonic amplitude 40%

7.3.5 Effects of ultrasonic amplitude on the reaction rate constants

Experimental setup at varying ultrasonic amplitudes and reaction times were carried out to investigate the effects of ultrasonic amplitude on the reaction rate constants. The enzyme concentration and molar ratio (fat:methanol) were kept at 6% (w/w) of fat and 1:6, respectively. Ultrasound amplitudes were run at 5, 10, 15, 20, 25, and 30 min reaction time. Based on the experimental results, the reaction rate constants were estimated by the procedure presented in section 2.5. Figure 7.7 shows the plots of reaction rate constants evaluated at each of the ultrasonic amplitudes studied. The values of the reaction rate constants, k_1 to k_4 change significantly at different ultrasonic amplitude while between k_4 and k_6 limited activities were observed. The rate constant (k_2) for the dissociation of enzyme-TG complex was highest at ultrasound amplitude 30% while the lowest was at ultrasound amplitudes 40%. This might be due to weak binding of enzyme and TG at 30% amplitude. The rate constant (k_3) that is responsible for the formation of biodiesel was highest at ultrasound amplitude 40% and lowest at 30%. This result confirms ultrasound amplitude of 40% to be a reliable amplitude for the production of biodiesel as earlier reported in this study. Across all the ultrasound amplitudes, the reaction rate (k_6) for the association of biodiesel and glycerol to form the reactants was negative. This indicated that possibility of glycerol combining with biodiesel is limited during ultrasonication treatment of transesterification reaction. Similarly, the reaction rate (k_5) for the dissociation of E' and M was negative. This indicated that the possibility of disintegration of $E'M$ complex is limited during ultrasonication treatment of transesterification reaction which might be responsible to the substantial yield (more than 98%) observed.

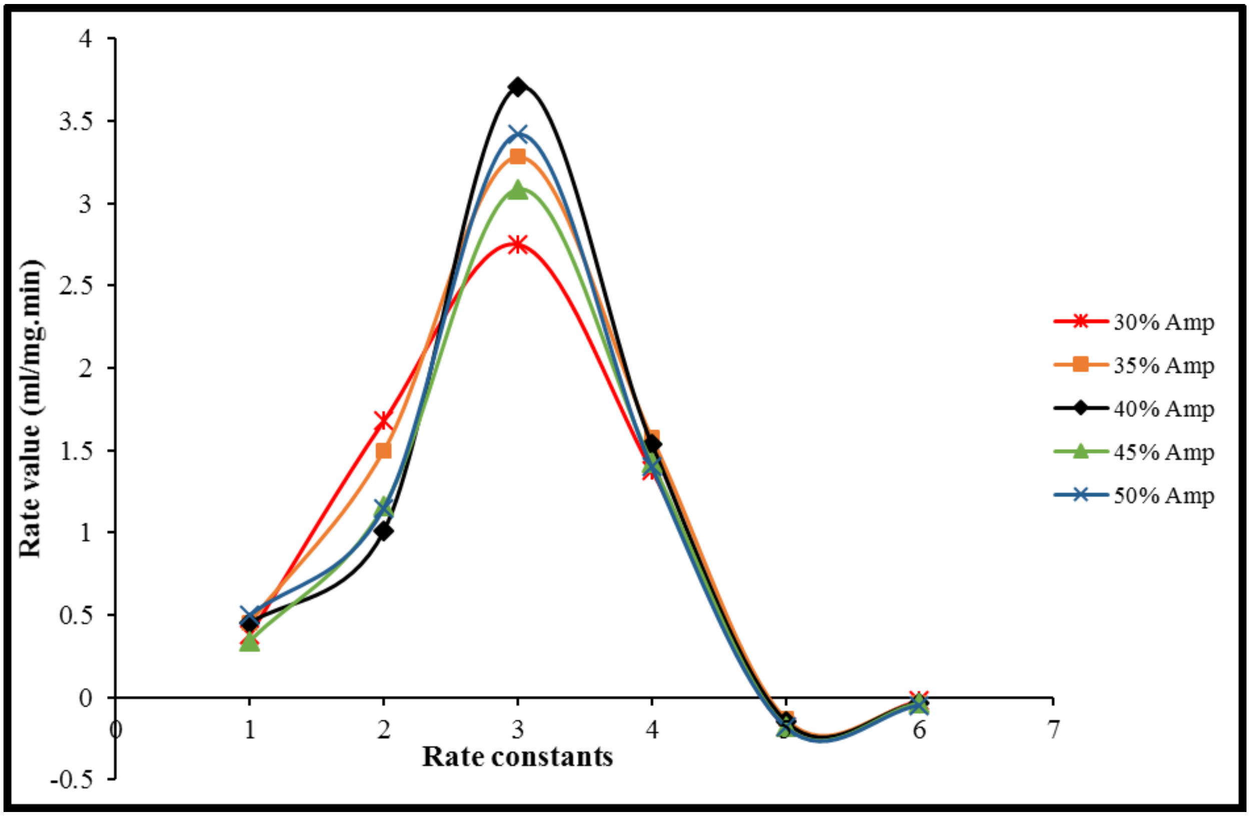

Figure 7.7: Plots of reaction rate constant values of the ultrasonic amplitudes

7.4 Conclusions

The reaction kinetics of an ultrasound assisted enzyme-catalyzed transesterification of waste CWG with methanol for biodiesel production were successfully modeled using reaction rate expressions by varying ultrasonic amplitude parameter. The effects of reaction factors such as molar ratio (fat:methanol), catalyst concentration, reaction time, ultrasound amplitude and cycle on biodiesel yield were successfully investigated. The time required (less than 30 min) to achieve 98.2 % yield of biodiesel from waste CWG was substantially reduced by ultrasonic mixing vs. conventional mixing. The biodiesel yield was found to increase with increase in enzyme catalyst concentration, but decrease with increase in molar ratio. A rapid increase in the forward reaction rate constants (k_1, k_3, k_4, and k_6) and decrease in reverse reaction rate constants (k_2 and k_5) was observed at 35% ultrasonic amplitude and above. Application of this mixing technique for transesterification reaction would drastically reduce the reaction time and amount of methanol require for the production of biodiesel which would directly affect cost of production in terms of amount reagents, production time, and indirectly energy use. The results of this study give a better understanding of the reaction rates with respect to individual reactants and system parameters which is a very good advantage for design and construction of the biodiesel reactors using ultrasonication mixing.

Chapter 8

General Summary and Conclusions

The main objective of this research was to investigate the impact of ultrasonic mixing processes on the enhancement of enzyme catalyzed biodiesel production from waste animal fats. Four different types of animal fats (tallow, lard, CWG, and YG) were examined. Rheometer was employed to determine the viscosity and viscoelasticity of the waste animal fats at varying temperature and time. Thermal and physicochemical properties (such as melting point, crystallization temperature, iodine value, free fatty acid contents, fatty acids profile etc.) of the AWFs were determined by DSC, and GC-FID, respectively. A non-destructive method to characterize AWFs was developed using FT-NIR. The parametric effects of ultrasonic waves as a mixing phenomenon during enzyme-catalyzed transesterification of AWFs were elucidated. Reaction kinetics modeling to determine the reaction rate constants of methanol and AWFs enzyme-catalyzed transesterification assisted by ultrasonication were estimated. The research described in this thesis had four distinct objectives: (i). to evaluate physicochemical and thermal properties of waste animal fats destined for the production of biodiesel. (ii). to develop non-destructive determination of physicochemical properties of waste animal fats destined for the production of biodiesel. (iii). to determine parametric effects of ultrasonic mixing on the yield of biodiesel produced from AFW. (iv). Reaction kinetics modeling of ultrasonic mixing processes on transesterification of AFW for the production of biodiesel.

The following conclusions are drawn from this research:

I. The thermal and rheological behavioral pattern at different shear rate and temperature were established for each of the samples. The transesterification operating temperature for each sample must be above the temperature at which the viscosity becomes steady. Steady viscosity equally exists at shear rate above which increase in shear rate has no effect on the sample viscosity. Which that means if the agitation is lowered or stopped when this shear rate is achieved, the transesterification reaction will proceed without loss of biodiesel yield. This will reduce wear and tear, more so production cost. It is necessary to reduce the FFA level of the fats by using acid pretreatment or enzyme catalyzed transesterification. It was established that animal fat waste impurities had effect on their rheological and thermal properties, but did not show any significant effect on the fatty acid profile except differ percentage compositions between PL and lard.

II. The influence that FD, SD, MSC and VN pre-processing methods has on the PLS-NIR calibration modeling for the FT-NIR spectroscopy analysis IV and FFA content of AFW and their blends were established. More robust calibrations were obtained by using real production samples, and variability in the sample data set can be introduced by blending animal fat feedstocks directly in the biodiesel production reactor. The results showed that FT-NIR is capable of providing a rapid and accurate measurement of IV and FFA of animal fats and their blends destined for biodiesel production with a proper calibration and a responsive model. FD pre-processing method was found to give a robust and reliable calibration model for both IV and FFA measurement. Conclusively, using FT-NIR spectroscopy as a biodiesel feedstock (AFW and blends) quality control tool for IV and FFA measurement will reduce cost of production and possible chemical hazard in the production environment.

III. The effects of reaction factors such as molar ratio (fat:methanol), catalyst concentration, reaction time, ultrasound amplitude and cycle on biodiesel yield from enzyme catalyzed waste tallow, lard and CWG were successfully investigated. The biodiesel yield was found to increase with increase in enzyme catalyst concentration, but decreased with an increase in molar ratio. The interaction between molar ratio and enzyme catalyst concentration was not significant for the production of biodiesel from waste tallow and lard with the exception of CWG. Application of ultrasonics mixing technique for transesterification reaction would drastically reduce the reaction time and amount of methanol require for the production of biodiesel which would directly affect the cost of production in terms of amount of reagents, production time, and indirectly energy use.

IV. The reaction kinetics of an ultrasound assisted enzyme-catalyzed transesterification of waste tallow, lard, and CWG with methanol for biodiesel production were successfully modeled using reaction rate expressions by varying ultrasonic amplitude parameter. The kinetic model developed demonstrate activities of enzyme-catalyzed methanolysis of waste lard for biodiesel production. A rapid increase in the forward reaction rate constants (k_1, k_3, k_4, and k_6) and decrease in reverse reaction rate constants (k_2 and k_5) was observed at 35% ultrasonic amplitude and above. The results of this study give a better understanding of the reaction rates with respect to individual reactants and system parameters which is a great advantage for the design and the construction of the biodiesel reactors using ultrasonication mixing.

Chapter 9

Contributions to Knowledge and Recommendations for Further Research.

9.1 Contributions to Knowledge

The presence of a high content in FFA in AFW has been seen as a challenge, especially when synthesized by alkaline-catalyzed transesterification. Enzyme-based production techniques are suitable for overcoming the limitations of chemical-based production techniques and have the advantages of overcoming the specific limitations of base or acid transesterification technology (e.g. need for feedstock extremely low in FFA content and moisture) through an enzyme-catalyzed transesterification process. The impacts of ultrasonic mixing on the yield of biodiesel from enzyme catalyzed transesterification of AFW are not well understood, and the modeling of reaction kinetics of enzymatic mechanism in this regards have not been well elucidated. More also, determination of two major physicochemical properties of AFW by a non-destructive approach has not been well developed. Furthermore, a comprehensive evaluation of rheological, thermal, and physicochemical properties of AFW were depicted in this study. Therefore, this study made an attempt to overcome the above limitations. This thesis thus contributes to the knowledge of biodiesel production from AFW in the following respects:

a) A non-destructive technique was developed for quantifying the FFA and IV of AFW using FT-NIR. The developed model can quantify the FFA and IV of other animal fats successfully. This is a suitable technique for industrial purpose in order to reduce production time and the require time for quality control in any biodiesel production plant.

b) This research also demonstrated the effects of the various rheological, thermal and physicochemical parameters of AFW on the corresponding associated production techniques.

c) Ultrasound parametric effects on enzyme catalyzed transesterification of AFW showed reliable yield of biodiesel which tends to reduce the reaction time and reagents which would indirectly affect the overall production cost.

d) A novel technique was employed to determine the rate constants of the enzyme catalyzed biodiesel production from AFW. The results gave a better understanding of the reaction rates with respect to individual reactants and system parameters. Which is beneficial for the design and construction of the biodiesel reactors using ultrasonication mixing.

9.2 Recommendations for Further Research

The following areas of further research were identified in this study:

I. The use of some other non-destructive techniques such as FT-IR, FT-MIR to develop models for the determination of FFA and IV of AFW is recommended. This would provide a room for robustness and comparison of techniques.

II. To investigate the behavior of other enzymes during transesterification of AFW assisted by ultrasonication to further investigated.

III. Enzyme mechanistic behavior and ultrasonics energy consumed should be further examined.

IV. Higher capacity reaction chamber that would give an opportunity for mass transfer in the reaction system and possibility of scale up should be considered.

Chapter 10 Bibliography

Abdul Azis, A., Mohamud, Y., Roselina, K., Che Man, Y.B., Boo, H.C., Nyuk, L.C., 2011. Rheological, chemical and DSC thermal characteristics of different types of palm oil/palm stearin-based shortenings. Int. Food Res. J. International Food Research Journal 18, 189-200.

Adebanjo, A.O., Dalai, A.K., Bakhshi, N.N., 2005. Production of Diesel-Like Fuel and Other Value-Added Chemicals from Pyrolysis of Animal Fat. Energy and Fuels 19, 1735-1741.

Adewale, P., Dumont, M.-J., Ngadi, M., 2014a. Rheological, Thermal, and Physicochemical Characterization of Animal Fat Wastes for use in Biodiesel Production. Energy Technology 2, 634-642.

Adewale, P., Dumont, M.-J., Ngadi, M., 2015o. Recent trends of biodiesel production from animal fat wastes and associated production techniques. Renewable and Sustainable Energy Reviews 45, 574-588.

Adewale, P., Mba, O., Dumont, M.-J., Ngadi, M., Cocciardi, R., 2014. Determination of the iodine value and the free fatty acid content of waste animal fat blends using FT-NIR. Vibrational Spectroscopy 72, 72-78.

Aguirre-Mandujano, E., Lobato-Calleros, C., Beristain, C.I., Garcia, H.S., Vernon-Carter, E.J., 2009. Microstructure and viscoelastic properties of low-fat yoghurt structured by monoglyceride gels. LWT - Food Science and Technology 42, 938-944.

Akoh, C.C., Chang, S.-W., Lee, G.-C., Shaw, J.-F., 2007. Enzymatic Approach to Biodiesel Production. Journal of Agricultural and Food Chemistry 55, 8995-9005.

Al-Zuhair, S., 2005. Production of Biodiesel by Lipase-Catalyzed Transesterification of Vegetable Oils: A Kinetics Study. Biotechnology Progress 21, 1442-1448.

Al-Zuhair, S., Dowaidar, A., Kamal, H., 2009. Dynamic modeling of biodiesel production from simulated waste cooking oil using immobilized lipase. Biochemical Engineering Journal 44, 256-262.

Al-Zuhair, S., Hussein, A., Al-Marzouqi, A.H., Hashim, I., 2012. Continuous production of biodiesel from fat extracted from lamb meat in supercritical CO2 media. Biochemical Engineering Journal 60, 106-110.

Al-Zuhair, S., Ling, F.W., Jun, L.S., 2007. Proposed kinetic mechanism of the production of biodiesel from palm oil using lipase. Process Biochemistry 42, 951-960.

Alencar, J.W., Alves, P.B., Craveiro, A.A., 1983. Pyrolysis of tropical vegetable oils. Journal of Agricultural and Food Chemistry 31, 1268-1270.

Alptekin, E., Canakci, M., 2010. Optimization of pretreatment reaction for methyl ester production from chicken fat. Fuel 89, 4035-4039.

Alptekin, E., Canakci, M., 2011. Optimization of transesterification for methyl ester production from chicken fat. Fuel 90, 2630-2638.

Alptekin, E., Canakci, M., Sanli, H., 2012. Evaluation of leather industry wastes as a feedstock for biodiesel production. Fuel 95, 214-220.

Anand, K., Sharma, R., Mehta, P.S., 2011. A comprehensive approach for estimating thermo-physical properties of biodiesel fuels. Applied Thermal Engineering 31, 235-242.

Anitescu, G., Bruno, T.J., 2012a. Biodiesel Fuels from Supercritical Fluid Processing: Quality Evaluation with the Advanced Distillation Curve Method and Cetane Numbers. Energy and Fuels 26, 5256-5264.

Anitescu, G., Bruno, T.J., 2012b. Fluid properties needed in supercritical transesterification of triglyceride feedstocks to biodiesel fuels for efficient and clean combustion – A review. The Journal of Supercritical Fluids 63, 133-149.

AOAC, 1999. The official methods and recommended practices of the Association of Analytical Communities. Official Method 993.20: Iodine Value.

AOCS, 2009. The official methods and recommended practices of the American Oil Chemists' Society. Official Method Ca 5a-40: acid value.

AOCS, 2013. The AOCS Lipid Library: Animal Fats. http://lipidlibrary.aocs.org.

Armenta, R.E., Vinatoru, M., Burja, A.M., Kralovec, J.A., Barrow, C.J., 2007. Transesterification of fish oil to produce fatty acid ethyl esters using ultrasonic energy. Journal of the American Oil Chemists' Society 84, 1045-1052.

Armenta, S., Garrigues, S., de la Guardia, M., 2007. Determination of edible oil parameters by near infrared spectrometry. Analytica Chimica Acta 596, 330-337.

Aryee, A.N.A., Simpson, B.K., Cue, R.I., Phillip, L.E., 2011. Enzymatic transesterification of fats and oils from animal discards to fatty acid ethyl esters for potential fuel use. Biomass and Bioenergy 35, 4149-4157.

Asomaning, J., Mussone, P., Bressler, D.C., 2014. Two-stage thermal conversion of inedible lipid feedstocks to renewable chemicals and fuels. Bioresource Technology 158, 55-62.

Atabani, A.E., Silitonga, A.S., Ong, H.C., Mahlia, T.M.I., Masjuki, H.H., Badruddin, I.A., Fayaz, H., 2013. Non-edible vegetable oils: A critical evaluation of oil extraction, fatty acid compositions, biodiesel production, characteristics, engine performance and emissions production. Renewable and Sustainable Energy Reviews 18, 211-245.

Aydın, S., Kaushik-Basu, N., Özbaş-Turan, S., Akbuğa, J., Mega Tiber, P., Orun, O., R

Gurukumar, K., Basu, A., Güniz Küçükgüzel, Ş., 2014. Synthesis of 1-aroyl-3, 5-dimethyl-1H-pyrazoles as Anti-HCV and Anticancer Agents. Letters in Drug Design & Discovery 11, 121-131.

Azizian, H., Kramer, J.K., 2005. A rapid method for the quantification of fatty acids in fats and oils with emphasis on trans fatty acids using Fourier transform near infrared spectroscopy (FT-NIR). Lipids 40, 855-867.

Azizian, H., Kramer, J.K., Mossoba, M.M., 2010. Progression to Fatty Acid Profiling of Edible Fats and Oils Using Vibrational Spectroscopy. Handbook of Vibrational Spectroscopy.

Azócar, L., Ciudad, G., Heipieper, H.J., Muñoz, R., Navia, R., 2011. Lipase-catalyzed process in an anhydrous medium with enzyme reutilization to produce biodiesel with low acid value. Journal of Bioscience and Bioengineering 112, 583-589.

Azócar, L., Navia, R., Beroiz, L., Jeison, D., Ciudad, G., 2014. Enzymatic biodiesel production kinetics using co-solvent and an anhydrous medium: a strategy to improve lipase performance in a semi-continuous reactor. New Biotechnology 31, 422-429.

Badday, A.S., Abdullah, A.Z., Lee, K.-T., 2013. Optimization of biodiesel production process from Jatropha oil using supported heteropolyacid catalyst and assisted by ultrasonic energy. Renewable Energy 50, 427-432.

Balat, M., 2011. Potential alternatives to edible oils for biodiesel production–A review of current work. Energy Conversion and Management 52, 1479-1492.

Bamgboye, A., Hansen, A., 2008. Prediction of cetane number of biodiesel fuel from the fatty acid methyl ester (FAME) composition. International Agrophysics 22, 21.

Baptista, P., Felizardo, P., Menezes, J.C., Neiva Correia, M.J., 2008. Multivariate near infrared spectroscopy models for predicting the iodine value, CFPP, kinematic viscosity at 40 C and density at 15 C of biodiesel. Talanta 77, 144-151.

Behçet, R., 2011. Performance and emission study of waste anchovy fish biodiesel in a diesel engine. Fuel Processing Technology 92, 1187-1194.

Belafi Bako, K., Kovacs, F., Gubicza, L., Hancsok, J., 2002. Enzymatic biodiesel production from sunflower oil by Candida antarctica lipase in a solvent-free system. Biocatal Biotransform 20, 437 - 439.

Bell, A., Gordon, M.H., Jirasubkunakorn, W., Smith, K.W., 2007. Effects of composition on fat rheology and crystallisation. Food Chemistry 101, 799-805.

Ben Hassen-Trabelsi, A., Kraiem, T., Naoui, S., Belayouni, H., 2014. Pyrolysis of waste animal fats in a fixed-bed reactor: Production and characterization of bio-oil and bio-char. Waste Management 34, 210-218.

Bender, M., 1999. Economic feasibility review for community-scale farmer cooperatives for biodiesel. Bioresource Technology 70, 81-87.

Bernal, J.M., Lozano, P., García-Verdugo, E., Burguete, M.I., Sánchez-Gómez, G., López-López, G., Pucheault, M., Vaultier, M., Luis, S.V., 2012. Supercritical synthesis of biodiesel. Molecules 17, 8696-8719.

Berrios, M., Gutiérrez, M., Martín, M., Martín, A., 2009. Application of the factorial design of experiments to biodiesel production from lard. Fuel Processing Technology 90, 1447-1451.

Bhatti, H.N., Hanif, M.A., Qasim, M., Ata ur, R., 2008. Biodiesel production from waste tallow. Fuel 87, 2961-2966.

Bianchi, C., Boffito, D., Pirola, C., Ragaini, V., 2010. Low temperature de-acidification process of animal fat as a pre-step to biodiesel production. Catalysis Letters 134, 179-183.

Birur, D.K., Hertel, T.W., Tyner, W.E., 2007. The biofuels boom: implications for world food markets. The Food Economy, 61.

Boffito, D.C., Mansi, S., Leveque, J.M., Pirola, C., Bianchi, C.L., Patience, G.S., 2013. Ultrafast Biodiesel Production Using Ultrasound in Batch and Continuous Reactors. ACS Sustainable Chemistry and Engineering 1, 1432-1439.

Borges, M., Díaz, L., 2012. Recent developments on heterogeneous catalysts for biodiesel production by oil esterification and transesterification reactions: a review. Renewable and Sustainable Energy Reviews 16, 2839-2849.

Bousbaa, H., Sary, A., Liazid, A., Tazerout, M., 2012. Investigations on a Compression Ignition Engine Using Animal Fats and Vegetable Oil as Fuels. Journal of Energy Resources Technology 134, 022202-11.

Bowling, J.J., Anderson, J.B., Armbrust, K.L., Hamann, M.T., 2014. Evaluation of potential biodiesel feedstock production from oleaginous insect *Solenopsis* sp. Fuel 117, Part A, 5-7.

Büning-Pfaue, H., 2003. Analysis of water in food by near infrared spectroscopy. Food Chemistry 82, 107-115.

Canakci, M., 2007. The potential of restaurant waste lipids as biodiesel feedstocks. Bioresource Technology 98, 183-190.

Canakci, M., Sanli, H., 2008. Biodiesel production from various feedstocks and their effects on the fuel properties. Journal of industrial microbiology & biotechnology 35, 431-441.

Canakci, M., Van Gerpen, J., 1999. Biodiesel production via acid catalysis. Transactions of the ASAE-American Society of Agricultural Engineers 42, 1203-1210.

Canakci, M., Van Gerpen, J., 2001. Biodiesel production from oils and fats with high free fatty acids. Transactions-American Society of Agricultural Engineers 44, 1429-1436.

Canakci, M., Van Gerpen, J., 2003. A pilot plant to produce biodiesel from high free fatty acid feedstocks. Transactions of the ASAE 46, 945-954.

Canoira, L., Rodríguez-Gamero, M., Querol, E., Alcántara, R.n., Lapuerta, M.n., Oliva, F.n., 2008. Biodiesel from Low-Grade Animal Fat: Production Process Assessment and Biodiesel Properties Characterization. Industrial & Engineering Chemistry Research 47, 7997-8004.

Çaylı, G., Küsefoğlu, S., 2008. Increased yields in biodiesel production from used cooking oils by a two step process: Comparison with one step process by using TGA. Fuel processing technology 89, 118-122.

Cen, H., He, Y., 2007. Theory and application of near infrared reflectance spectroscopy in determination of food quality. Trends in Food Science and Technology 18, 72-83.

Chakraborty, R., Sahu, H., 2014. Intensification of biodiesel production from waste goat tallow using infrared radiation: Process evaluation through response surface methodology and artificial neural network. Applied Energy 114, 827-836.

Chand, P., Chintareddy, V.R., Verkade, J.G., Grewell, D., 2010. Enhancing Biodiesel Production from Soybean Oil Using Ultrasonics. Energy and Fuels 24, 2010-2015.

Che Man, Y.B., Setiowaty, G., Voort, F.R., 1999. Determination of iodine value of palm oil by fourier transform infrared spectroscopy. Journal of the American Oil Chemists' Society 76, 693-699.

Cheirsilp, B., H-Kittikun, A., Limkatanyu, S., 2008. Impact of transesterification mechanisms on the kinetic modeling of biodiesel production by immobilized lipase. Biochemical Engineering Journal 42, 261-269.

Chen, G., Ying, M., Li, W., 2006. Enzymatic conversion of waste cooking oils into alternative fuel—biodiesel. Applied biochemistry and biotechnology 132, 911-921.

Chesterfield, D.M., Rogers, P.L., Al-Zaini, E.O., Adesina, A.A., 2012. Production of biodiesel via ethanolysis of waste cooking oil using immobilised lipase. Chemical Engineering Journal 207–208, 701-710.

Choudhury, H.A., Malani, R.S., Moholkar, V.S., 2013. Acid catalyzed biodiesel synthesis from Jatropha oil: Mechanistic aspects of ultrasonic intensification. Chemical Engineering Journal 231, 262-272.

Christopher, L.P., Kumar, H., Zambare, V.P., 2014. Enzymatic biodiesel: Challenges and opportunities. Applied Energy 119, 497-520.

Ciudad, G., Reyes, I., Jorquera, M., Azócar, L., Wick, L., Navia, R., 2011. Novel three-phase bioreactor concept for fatty acid alkyl ester production using R. oryzae as whole cell catalyst. World J Microbiol Biotechnol 27, 2505-2512.

Colak, S., Zengin, G., ÖZGÜNAY, H., SARI, Ö., YÜCEER, H.S.L., 2006. A New and environmental friendly method for utilization of leather industry fleshings: Biodiesel, IULTCS Euro-congress, Istanbul, Turkey.

Colak, S., Zengin, G., Ozgunay, H., Sarikahya, H., Sari, O., Yuceer, L., 2005. Utilization of leather industry prefleshings in biodiesel production. Journal of the American Leather Chemists Association 100, 137-141.

Colucci, J., Borrero, E., Alape, F., 2005. Biodiesel from an alkaline transesterification reaction of soybean oil using ultrasonic mixing. Journal of the American Oil Chemists' Society 82, 525-530.

Costa, J., Almeida, M., Alvim-Ferraz, M., Dias, J., 2013. Biodiesel production using oil from fish canning industry wastes. Energy Conversion and Management 74, 17-23.

Couvreur, S., Hurtaud, C., Lopez, C., Delaby, L., Peyraud, J.L., 2006. The Linear Relationship Between the Proportion of Fresh Grass in the Cow Diet, Milk Fatty Acid Composition, and Butter Properties. Journal of Dairy Science 89, 1956-1969.

Cox, R., Lebrasseur, J., Michiels, E., Buijs, H., Li, H., Voort, F.R., Ismail, A.A., Sedman, J., 2000. Determination of iodine value with a fourier transform-near infrared based global calibration using disposable vials: An international collaborative study. Journal of the American Oil Chemists' Society 77, 1229-1234.

Cullen, P.J., 2009. Food Mixing: Principles and Applications. Wiley Online Library.

Da Cunha, M.E., Krause, L.C., Moraes, M.S.A., Faccini, C.S., Jacques, R.A., Almeida, S.R., Rodrigues, M.R.A., Caramão, E.B., 2009. Beef tallow biodiesel produced in a pilot scale. Fuel Processing Technology 90, 570-575.

Da Rós, P., Silva, G.A., Mendes, A.A., Santos, J.C., de Castro, H.F., 2010. Evaluation of the catalytic properties of Burkholderia cepacia lipase immobilized on non-commercial matrices to be used in biodiesel synthesis from different feedstocks. Bioresource Technology 101, 5508-5516.

Da Rós, P.C., de Castro, H.F., Carvalho, A.K., Soares, C.M., de Moraes, F.F., Zanin, G.M., 2012. Microwave-assisted enzymatic synthesis of beef tallow biodiesel. Journal of Industrial Microbiology and Biotechnology 39, 529-536.

Dale, N., 1992. True metabolizable energy of feather meal. The Journal of Applied Poultry Research 1, 331-334.

Darnoko, D., Cheryan, M., 2000. Kinetics of palm oil transesterification in a batch reactor. Journal of the American Oil Chemists' Society 77, 1263-1267.

De Paola, M.G., Ricca, E., Calabrò, V., Curcio, S., Iorio, G., 2009. Factor analysis of transesterification reaction of waste oil for biodiesel production. Bioresource Technology 100, 5126-5131.

Demirbas, A., 2009a. Biodiesel from waste cooking oil via base-catalytic and supercritical methanol transesterification. Energy Conversion and Management 50, 923-927.

Demirbas, A., 2009c. Potential resources of non-edible oils for biodiesel. Energy Sources, Part B 4, 310-314.

Demirbas, M.F., 2008. Pyrolysis of vegetable oils and animal fats for the production of renewable fuels. Energy Education Science and Technology 22, 59-67.

Deshmane, V.G., Adewuyi, Y.G., 2013. Synthesis and kinetics of biodiesel formation via calcium methoxide base catalyzed transesterification reaction in the absence and presence of ultrasound. Fuel 107, 474-482.

Di Serio, M., Tesser, R., Pengmei, L., Santacesaria, E., 2007. Heterogeneous Catalysts for Biodiesel Production. Energy and Fuels 22, 207-217.

Dias, J.M., Alvim-Ferraz, M., Almeida, M.F., 2009. Production of biodiesel from acid waste lard. Bioresource Technology 100, 6355-6361.

Dias, J.M., Alvim-Ferraz, M., Almeida, M.F., Méndez Díaz, J.D., Polo, M.S., Utrilla, J.R., 2012. Selection of heterogeneous catalysts for biodiesel production from animal fat. Fuel 94, 418-425.

Dias, J.M., Alvim-Ferraz, M.C.M., Almeida, M.F., 2008a. Mixtures of Vegetable Oils and Animal Fat for Biodiesel Production: Influence on Product Composition and Quality. Energy and Fuels 22, 3889-3893.

Dias, J.M., Ferraz, C.A., Almeida, M.F., 2008c. Using Mixtures of Waste Frying Oil and Pork

Lard to produce Biodiesel. Proceedings of World Academy of Science: Engineering and Technology 46.

Dizge, N., Keskinler, B., 2008. Enzymatic production of biodiesel from canola oil using immobilized lipase. Biomass and Bioenergy 32, 1274-1278.

Du, R., Lai, K., Xiao, Z., Shen, Y., Wang, X., Huang, Y., 2012. Evaluation of the Quality of Deep Frying Oils with Fourier Transform Near-infrared and Mid-infrared Spectroscop. Journal of Food Science 77, C261-C266.

Elizabeth Grant, G., Gnaneswar Gude, V., 2014. Kinetics of ultrasonic transesterification of waste cooking oil. Environmental Progress and Sustainable Energy 33, 1051-1058.

Encinar, J.M., Sánchez, N., Martínez, G., García, L., 2011. Study of biodiesel production from animal fats with high free fatty acid content. Bioresource Technology 102, 10907-10914.

Evans, B., Gray, R., 2013. Canada Biofuels Annual. USDA Foreign Agricultural Service: Global Agricultural Information Network CA13034, 1-40.

Fan, X., Wang, X., Chen, F., 2010. Ultrasonically assisted production of biodiesel from crude cottonseed oil. International Journal of Green Energy 7, 117-127.

Franklin, S., Somanchi, A., Wee, J., Rudenko, G., Moseley, J.L., Rakitsky, W., Zhao, X., Bhat, R., 2014. Tailored oils produced from recombinant oleaginous microorganisms. Google Patents.

Gedye, R.N., Smith, F.E., Westaway, K.C., 1988. The rapid synthesis of organic compounds in microwave ovens. Canadian Journal of Chemistry 66, 17-26.

Geller, D.P., Adams, T.T., Goodrum, J.W., Pendergrass, J., 2008. Storage stability of poultry fat and diesel fuel mixtures: Specific gravity and viscosity. Fuel 87, 92-102.

Gerpen, J.V., 2005. Biodiesel processing and production. Fuel Processing Technology 86, 1097-

1107.

Ghazavi, M.A., Fallahipanah, M., Jeshvaghani, H.S., 2013. A feasibility study on beef tallow conversion to some esters for biodiesel production. International Journal Of Recycling of Organic Waste in Agriculture 2, 2.

Ghoreishi, S.M., Moein, P., 2013. Biodiesel synthesis from waste vegetable oil via transesterification reaction in supercritical methanol. The Journal of Supercritical Fluids 76, 24-31.

Gog, A., Roman, M., Toşa, M., Paizs, C., Irimie, F.D., 2012. Biodiesel production using enzymatic transesterification – Current state and perspectives. Renewable Energy 39, 10-16.

Goodrum, J.W., Geller, D.P., Adams, T.T., 2003. Rheological characterization of animal fats and their mixtures with# 2 fuel oil. Biomass and Bioenergy 24, 249-256.

Graboski, M.S., McCormick, R.L., 1998. Combustion of fat and vegetable oil derived fuels in diesel engines. Progress in Energy and Combustion Science 24, 125-164.

Grompone, M., Moyna, P., 1983. Characteristics of uruguayan beef tallow1. J Am Oil Chem Soc 60, 1331-1332.

Guadixz, A., Guadix, E.M., 2013. Biodiesel Production from Fish Oil. Utilization of Fish Waste, 193.

Gui, M.M., Lee, K., Bhatia, S., 2008. Feasibility of edible oil vs. non-edible oil vs. waste edible oil as biodiesel feedstock. Energy 33, 1646-1653.

Gürü, M., Artukoğlu, B.D., Keskin, A., Koca, A., 2009. Biodiesel production from waste animal fat and improvement of its characteristics by synthesized nickel and magnesium additive. Energy Conversion and Management 50, 498-502.

Gürü, M., Koca, A., Can, Ö., Çınar, C., Şahin, F., 2010. Biodiesel production from waste chicken fat based sources and evaluation with Mg based additive in a diesel engine. Renewable Energy 35, 637-643.

Hari Krishna, S., Karanth, N.G., 2001. Lipase-catalyzed synthesis of isoamyl butyrate: A kinetic study. Biochimica et Biophysica Acta (BBA) - Protein Structure and Molecular Enzymology 1547, 262-267.

Harold, S., 1997. Industrial Vegetable Oils: Opportunities Within the European Biodiesel and Lubricant Markets. Part 2. Market Characteristics. Lipid Technology 9, 67-70.

Hendl, O., Howell, J.A., Lowery, J., Jones, W., 2001. A rapid and simple method for the determination of iodine values using derivative Fourier transform infrared measurements. Analytica Chimica Acta 427, 75-81.

Hill, J., 2007. Environmental costs and benefits of transportation biofuel production from food- and lignocellulose-based energy crops. A review. Agronomy for Sustainable Development 27, 1-12.

Hsiao, M.-C., Lin, C.-C., Chang, Y.-H., 2011. Microwave irradiation-assisted transesterification of soybean oil to biodiesel catalyzed by nanopowder calcium oxide. Fuel 90, 1963-1967.

Hsiao, M.-C., Lin, C.-C., Chang, Y.-H., Chen, L.-C., 2010. Ultrasonic mixing and closed microwave irradiation-assisted transesterification of soybean oil. Fuel 89, 3618-3622.

Hsu, A.-F., Jones, K., Marmer, W., Foglia, T., 2001. Production of alkyl esters from tallow and grease using lipase immobilized in a phyllosilicate sol-gel. Journal of the American Oil Chemists' Society 78, 585-588.

Huang, H., Yu, H., Xu, H., Ying, Y., 2008. Near infrared spectroscopy for on/in-line monitoring of quality in foods and beverages: A review. Journal of Food Engineering 87, 303-313.

Huang, Y., Zheng, H., Yan, Y., 2010. Optimization of lipase-catalyzed transesterification of lard for biodiesel production using response surface methodology. Applied biochemistry and biotechnology 160, 504-515.

Huong, L.T.T., Tan, P.M., Hoa, T.T.V., 2011. Biodiesel Production from Fat of Tra Catfish via Heterogeneous Basic-Catalyzed Transesterification Using Ultrasonic Mixing. e-Journal of Surface Science and Nanotechnology 9, 477-481.

İşler, A., Sundu, S., Tüter, M., Karaosmanoğlu, F., 2010. Transesterification reaction of the fat originated from solid waste of the leather industry. Waste management 30, 2631-2635.

Ito, T., Sakurai, Y., Kakuta, Y., Sugano, M., Hirano, K., 2012. Biodiesel production from waste animal fats using pyrolysis method. Fuel Processing Technology 94, 47-52.

Ivanov, I.B., Kralchevsky, P.A., 1997. Stability of emulsions under equilibrium and dynamic conditions. Colloids and Surfaces A: Physicochemical and Engineering Aspects 128, 155-175.

Izida, T., Bussler, L., Silva, J.R., Andrade, L.H.C., Simionatto, E., Simionatto, E.L., Scharf, D.R., Lima, S.M., 2015. On-line in situ monitoring of the soybean oil and ethanol transesterification reaction by fluorescence spectroscopy. Fuel 145, 109-115.

Jacobson, K., Gopinath, R., Meher, L.C., Dalai, A.K., 2008. Solid acid catalyzed biodiesel production from waste cooking oil. Applied Catalysis B: Environmental 85, 86-91.

Jadhav, S.H., Gogate, P.R., 2014a. Intensification in the Activity of Lipase Enzyme Using Ultrasonic Irradiation and Stability Studies. Industrial & Engineering Chemistry Research 53, 1377-1385.

Jadhav, S.H., Gogate, P.R., 2014b. Ultrasound assisted enzymatic conversion of non edible oil to methyl esters. Ultrasonics Sonochemistry 21, 1374-1381.

Jasen, P., Marchetti, J.M., 2012. Kinetic study of the esterification of free fatty acid and ethanol in the presence of triglycerides using solid resins as catalyst. International Journal of Low-Carbon Technologies.

Jayasinghe, P., Hawboldt, K., 2012. A review of bio-oils from waste biomass: Focus on fish processing waste. Renewable and Sustainable Energy Reviews 16, 798-821.

Jayasinghe, P., Hawboldt, K., 2013. Biofuels from fish processing plant effluents–waste characterization and oil extraction and quality. Sustainable Energy Technologies and Assessments 4, 36-44.

Kaieda, M., Samukawa, T., Kondo, A., Fukuda, H., 2001. Effect of methanol and water contents on production of biodiesel fuel from plant oil catalyzed by various lipases in a solvent-free system. J Biosci Bioeng 91, 12 - 15.

Kaieda, M., Samukawa, T., Matsumoto, T., Ban, K., Kondo, A., Shimada, Y., Noda, H., Nomoto, F., Ohtsuka, K., Izumoto, E., Fukuda, H., 1999. Biodiesel fuel production from plant oil catalyzed by Rhizopus oryzae lipase in a water-containing system without an organic solvent. J Biosci Bioeng 88, 627 - 631.

Kalva, A., Sivasankar, T., Moholkar, V.S., 2008. Physical Mechanism of Ultrasound-Assisted Synthesis of Biodiesel. Industrial & Engineering Chemistry Research 48, 534-544.

Karmakar, A., Karmakar, S., Mukherjee, S., 2010. Properties of various plants and animals feedstocks for biodiesel production. Bioresource Technology 101, 7201-7210.

Kerihuel, A., Senthil Kumar, M., Bellettre, J., Tazerout, M., 2005. Use of animal fats as CI engine fuel by making stable emulsions with water and methanol. Fuel 84, 1713-1716.

Kerihuel, A., Senthil Kumar, M., Bellettre, J., Tazerout, M., 2006. Ethanol animal fat emulsions as a diesel engine fuel – Part 1: Formulations and influential parameters. Fuel 85, 2640-2645.

Khattab, R.Y., Eskin, M.N., Thiyam-Hollander, U., 2014. Production of Canolol from Canola Meal Phenolics via Hydrolysis and Microwave-Induced Decarboxylation. Journal of the American Oil Chemists' Society 91, 89-97.

Kim, H., Kang, B., Kim, M., Park, Y., Kim, D., Lee, J., Lee, K., 2004. Transesterification of vegetable oil to biodiesel using heterogeneous base catalyst. Catal Today 93-95, 315 - 320.

Kim M., DiMaggio C., Yan S., Wang H., Salley S. O., Simon Ng K. Y., 2011. Performance of heterogeneous ZrO2 supported metaloxide catalysts for brown grease esterification and sulfur removal. Bioresource Technology 102, 2380-2386.

Knothe, G., 2002. Structure indices in FA chemistry. How relevant is the iodine value? Journal of the American Oil Chemists' Society 79, 847-854.

Knothe, G., 2005. Dependence of biodiesel fuel properties on the structure of fatty acid alkyl esters. Fuel processing technology 86, 1059-1070.

Knothe, G., 2007. Some aspects of biodiesel oxidative stability. Fuel Processing Technology 88, 669-677.

Knothe, G., Van Gerpen, J.H., Krahl, J., 2005. The biodiesel handbook. AOCS press Champaign, IL.

Kondamudi, N., Strull, J., Misra, M., Mohapatra, S.K., 2009. A Green Process for Producing Biodiesel from Feather Meal. Journal of Agricultural and Food Chemistry 57, 6163-6166.

Kulkarni, M.G., Dalai, A.K., 2006. Waste Cooking OilAn Economical Source for Biodiesel: A Review. Industrial & Engineering Chemistry Research 45, 2901-2913.

Kumar, D., Kumar, G., Johari, R., Kumar, P., 2012. Fast, easy ethanomethanolysis of Jatropha curcus oil for biodiesel production due to the better solubility of oil with ethanol in reaction mixture assisted by ultrasonication. Ultrasonics Sonochemistry 19, 816-822.

Kumar, D., Kumar, G., Poonam, Singh, C.P., 2010. Fast, easy ethanolysis of coconut oil for biodiesel production assisted by ultrasonication. Ultrasonics Sonochemistry 17, 555-559.

Kumar, G., Kumar, D., Poonam, Johari, R., Singh, C.P., 2011a. Enzymatic transesterification of Jatropha curcas oil assisted by ultrasonication. Ultrasonics Sonochemistry 18, 923-927.

Kumar, G.R., Ravi, R., Chadha, A., 2011. Kinetic Studies of Base-Catalyzed Transesterification Reactions of Non-edible Oils to Prepare Biodiesel: The Effect of Co-solvent and Temperature. Energy and Fuels 25, 2826-2832.

Kumar, M.S., Kerihuel, A., Bellettre, J., Tazerout, M., 2005. A Comparative Study of Different Methods of Using Animal Fat as a Fuel in a Compression Ignition Engine. Journal of Engineering for Gas Turbines and Power 128, 907-914.

Kumar, M.S., Kerihuel, A., Bellettre, J., Tazerout, M., 2006. Ethanol animal fat emulsions as a diesel engine fuel–part 2: engine test analysis. Fuel 85, 2646-2652.

Kumar, R., Ravi Kumar, G., Chandrashekar, N., 2011. Microwave assisted alkali-catalyzed transesterification of Pongamia pinnata seed oil for biodiesel production. Bioresource Technology 102, 6617-6620.

Kumar, S., Ghaly, A., Brooks, M., Budge, S., Dave, D., 2013. Effectiveness of Enzymatic Transesterification of Beef tallow Using Experimental Enzyme ns88001 with Methanol and Hexane. Enz Eng 2, 2.

Kumari, A., Mahapatra, P., Garlapati, V., Banerjee, R., 2009. Enzymatic transesterification of Jatropha oil. Biotechnology for Biofuels 2, 1.

Kumari, V., Shah, S., Gupta, M.N., 2007. Preparation of Biodiesel by Lipase-Catalyzed Transesterification of High Free Fatty Acid Containing Oil from Madhuca indica. Energy and Fuels 21, 368-372.

Kusdiana, D., Saka, S., 2001. Kinetics of transesterification in rapeseed oil to biodiesel fuel as treated in supercritical methanol. Fuel 80, 693-698.

Lai, O., Ghazali, H., Cho, F., Chong, C., 2000. Physical properties of lipase-catalyzed transesterified blends of palm stearin and anhydrous milk fat. Food Chemistry 70, 215-219.

Lam, M.K., Lee, K.T., Mohamed, A.R., 2010. Homogeneous, heterogeneous and enzymatic catalysis for transesterification of high free fatty acid oil (waste cooking oil) to biodiesel: A review. Biotechnology Advances 28, 500-518.

Lee, J.H., Akoh, C.C., Himmelsbach, D.S., Lee, K.-T., 2008. Preparation of Interesterified Plastic Fats from Fats and Oils Free of Trans Fatty Acid. Journal of Agricultural and Food Chemistry 56, 4039-4046.

Lee, K.-T., Foglia, T.A., Chang, K.-S., 2002. Production of alkyl ester as biodiesel from fractionated lard and restaurant grease. Journal of the American Oil Chemists' Society 79, 191-195.

Leung, D.Y.C., Wu, X., Leung, M.K.H., 2010. A review on biodiesel production using catalyzed transesterification. Applied Energy 87, 1083-1095.

Li, H., Van De Voort, F., Ismail, A., Cox, R., 2000. Determination of peroxide value by Fourier transform near-infrared spectroscopy. Journal of the American Oil Chemists' Society 77, 137-142.

Li, H., Voort, F.R., Sedman, J., Ismail, A.A., 1999. Rapid determination of cis and trans content, iodine value, and saponification number of edible oils by fourier transform near-infrared spectroscopy. Journal of the American Oil Chemists' Society 76, 491-497.

Lidström, P., Tierney, J., Wathey, B., Westman, J., 2001. Microwave assisted organic synthesis—a review. Tetrahedron 57, 9225-9283.

Lima, D.G., Soares, V.C.D., Ribeiro, E.B., Carvalho, D.A., Cardoso, É.C.V., Rassi, F.C., Mundim, K.C., Rubim, J.C., Suarez, P.A.Z., 2004. Diesel-like fuel obtained by pyrolysis of vegetable oils. Journal of Analytical and Applied Pyrolysis 71, 987-996.

Lin, C.-Y., Li, R.-J., 2009. Engine performance and emission characteristics of marine fish-oil biodiesel produced from the discarded parts of marine fish. Fuel Processing Technology 90, 883-888.

Liu, C., Yang, M., Huang, F., 2012. Influence of Extraction Processing on Rheological Properties of Rapeseed Oils. Journal of the American Oil Chemists' Society 89, 73-78.

Liu, H., Xu, X.M., Guo, S.D., 2008. Comparison of full-fat and low-fat cheese analogues with or without pectin gel through microstructure, texture, rheology, thermal and sensory analysis. International Journal of Food Science & Technology 43, 1581-1592.

Liu, Y., Lotero, E., Goodwin Jr, J.G., Mo, X., 2007. Transesterification of poultry fat with methanol using Mg–Al hydrotalcite derived catalysts. Applied Catalysis A: General 331, 138-148.

Lotero, E., Liu, Y., Lopez, D.E., Suwannakarn, K., Bruce, D.A., Goodwin, J.G., 2005. Synthesis of biodiesel via acid catalysis. Industrial & engineering chemistry research 44, 5353-5363.

Lu, J., Nie, K., Xie, F., Wang, F., Tan, T., 2007. Enzymatic synthesis of fatty acid methyl esters from lard with immobilized Candida sp. 99-125. Process Biochemistry 42, 1367-1370.

Luković, N., Z. Knežević-Jugović, and D. Bezbradica. Biodiesel Fuel Production by Enzymatic Transesterification of Oils: Recent Trends, Challenges and Future Perspectives, Alternative Fuel. ISBN (2011): 978-953.

Ma, F., Clements, L., Hanna, M., 1998. The Effects of Catalyst, Free Fatty Acids, and Water on

Transecterification of Beef Tallow. Transactions of the ASAE-American Society of Agricultural Engineers 41(5), 1261-1264

Ma, F., Clements, L.D., Hanna, M.A., 1999. The effect of mixing on transesterification of beef tallow. Bioresource Technology 69, 289-293.

Ma, F., Hanna, M.A., 1999. Biodiesel production: a review. Bioresource Technology 70, 1-15. Madras, G., Kolluru, C., Kumar, R., 2004. Synthesis of biodiesel in supercritical fluids. Fuel 83, 2029-2033.

Maghami, M., Sadrameli, S., Ghobadian, B., 2015. Production of biodiesel from fishmeal plant waste oil using ultrasonic and conventional methods. Applied Thermal Engineering 75, 575-579.

Mahamuni, N.N., Adewuyi, Y.G., 2009. Optimization of the synthesis of biodiesel via ultrasound-enhanced base-catalyzed transesterification of soybean oil using a multifrequency ultrasonic reactor. Energy and Fuels 23, 2757-2766.

Mahamuni, N.N., Adewuyi, Y.G., 2010. Application of Taguchi Method to Investigate the Effects of Process Parameters on the Transesterification of Soybean Oil Using High Frequency Ultrasound. Energy and Fuels 24, 2120-2126.

Mandolesi de Araújo, C.D., de Andrade, C.C., de Souza e Silva, E., Dupas, F.A., 2013. Biodiesel production from used cooking oil: A review. Renewable and Sustainable Energy Reviews 27, 445-452.

Marulanda, V.F., Anitescu, G., Tavlarides, L.L., 2009. Biodiesel Fuels through a Continuous Flow Process of Chicken Fat Supercritical Transesterification. Energy and Fuels 24, 253-260.

Marulanda, V.F., Anitescu, G., Tavlarides, L.L., 2010. Investigations on supercritical transesterification of chicken fat for biodiesel production from low-cost lipid feedstocks. The Journal of Supercritical Fluids 54, 53-60.

Mata, T., Martins, A., Caetano, N., 2013. Valorization of Waste Frying Oils and Animal Fats for Biodiesel Production, in: Lee, J.W. (Ed.), Advanced Biofuels and Bioproducts. Springer New York, pp. 671-693.

Mata, T.M., Cardoso, N., Ornelas, M., Neves, S., Caetano, N.S., 2011. Evaluation of Two Purification Methods of Biodiesel from Beef Tallow, Pork Lard, and Chicken Fat. Energy and Fuels 25, 4756-4762.

Mata, T.M., Sousa, I.R.B.G., Vieira, S.S., Caetano, N.S., 2012. Biodiesel Production from Corn Oil via Enzymatic Catalysis with Ethanol. Energy and Fuels 26, 3034-3041.

McClure, W.F., 1994. Near-infrared spectroscopy. The giant is running strong. Analytical chemistry 66, 43A-53A.

Meher, L.C., Vidya Sagar, D., Naik, S.N., 2006. Technical aspects of biodiesel production by transesterification—a review. Renewable and Sustainable Energy Reviews 10, 248-268.

Melero, J., Bautista, L., Iglesias, J., Morales, G., Sánchez-Vázquez, R., 2012. Zr-SBA-15 acid catalyst: optimization of the synthesis and reaction conditions for biodiesel production from low-grade oils and fats. Catalysis Today 195, 44-53.

Mendes, A.A., Giordano, R.C., Giordano, R.L.C., de Castro, H.F., 2011. Immobilization and stabilization of microbial lipases by multipoint covalent attachment on aldehyde-resin affinity: application of the biocatalysts in biodiesel synthesis. Journal of Molecular Catalysis B: Enzymatic 68, 109-115.

Meunier, S.M., Rajabzadeh, A.R., Legge, R.L., 2014. Kinetic modelling of the production of methyl oleate by Celite® supported lipase sol–gels. Biochemical Engineering Journal 85, 63-70.

Michelin, S., Penha, F.M., Sychoski, M.M., Scherer, R.P., Treichel, H., Valério, A., Di Luccio, M., de Oliveira, D., Oliveira, J.V., 2015. Kinetics of ultrasound-assisted enzymatic biodiesel production from Macauba coconut oil. Renewable Energy 76, 388-393.

Mondal, P., Basu, M., Balasubramanian, N., 2008. Direct use of vegetable oil and animal fat as alternative fuel in internal combustion engine. Biofuels, Bioproducts and Biorefining 2, 155-174.

Moraes, M.S.A., Krause, L.C., da Cunha, M.E., Faccini, C.S., de Menezes, E.W., Veses, R.C., Rodrigues, M.R.A., Caramão, E.B., 2008. Tallow Biodiesel: Properties Evaluation and Consumption Tests in a Diesel Engine. Energy and Fuels 22, 1949-1954.

Moritz, J., Latshaw, J., 2001. Indicators of nutritional value of hydrolyzed feather meal. Poultry Science 80, 79-86.

Mrad, N., Varuvel, E.G., Tazerout, M., Aloui, F., 2012. Effects of biofuel from fish oil industrial residue–diesel blends in diesel engine. Energy 44, 955-963.

Mutreja, V., Singh, S., Ali, A., 2011. Biodiesel from mutton fat using KOH impregnated MgO as heterogeneous catalysts. Renewable Energy 36, 2253-2258.

Natsuga, M., Kawamura, S., 2006. Visible and near-infrared reflectance spectroscopy for determining physicochemical properties of rice. Transactions of the ASABE 49, 1069-1076.

Nelson, L., Foglia, T., Marmer, W., 1996. Lipase-catalyzed production of biodiesel. Journal of the American Oil Chemists' Society 73, 1191-1195.

Ngo, H.L., Vanselous, H., Strahan, G.D., Haas, M., 2013. Esterification of Fatty Acids in Greases to Fatty Acid Methyl Esters with Highly Active Diphenylamine Salts. Journal of the American Oil Chemists' Society 90, 563-570.

Ngo, H.L.F., T. A. Zafiropoulos, N. A. Samulski, E. T. Lin, W., 2008. Efficient two-step synthesis of biodiesel from greases. Energy and Fuels 22, 626-634.

Ngo, H.L.F., T. A. Zafiropoulos, N. A. Samulski, E. T. Lin, W., 2010. Mesoporous silica-supported diarylammonium catalysts for esterification of free fatty acids in greases. Journal of the American Oil Chemists' Society 87, 445-452.

Nielsen, P.M., Brask, J., Fjerbaek, L., 2008. Enzymatic biodiesel production: Technical and economical considerations. European Journal of Lipid Science and Technology 110, 692-700.

Noipin, K., Kumar, S., 2015. Optimization of ethyl ester production assisted by ultrasonic irradiation. Ultrasonics Sonochemistry 22, 548-558.

Noureddini, H., Gao, X., Philkana, R., 2005. Immobilized Pseudomonas cepacia lipase for biodiesel fuel production from soybean oil. Bioresource Technology 96, 769-777.

Noureddini, H., Zhu, D., 1997. Kinetics of transesterification of soybean oil. Journal of the American Oil Chemists' Society 74, 1457-1463.

Nurfitri, I., Maniam, G.P., Hindryawati, N., Yusoff, M.M., Ganesan, S., 2013. Potential of feedstock and catalysts from waste in biodiesel preparation: A review. Energy Conversion and Management 74, 395-402.

Olsen, E.F., Baustad, C., Egelandsdal, B., Rukke, E.-O., Isaksson, T., 2010. Long-term stability of a Raman instrument determining iodine value in pork adipose tissue. Meat Science 85, 1-6.

Öner, C., Altun, Ş., 2009. Biodiesel production from inedible animal tallow and an experimental investigation of its use as alternative fuel in a direct injection diesel engine. Applied Energy 86, 2114-2120.

Ong, L.K., Kurniawan, A., Suwandi, A.C., Lin, C.X., Zhao, X.S., Ismadji, S., 2013. Transesterification of leather tanning waste to biodiesel at supercritical condition: Kinetics and thermodynamics studies. The Journal of Supercritical Fluids 75, 11-20.

Ozgunay, H., Colak, S., Mutlu, M., Akyuz, F., 2007. Characterization of Leather Industry Wastes. Polish Journal of Environmental Studies 16.

Parkar, P.A., Choudhary, H.A., Moholkar, V.S., 2012. Mechanistic and kinetic investigations in ultrasound assisted acid catalyzed biodiesel synthesis. Chemical Engineering Journal 187, 248-260.

Patil, P.D., Gude, V.G., Camacho, L.M., Deng, S., 2009. Microwave-Assisted Catalytic Transesterification of Camelina Sativa Oil. Energy and Fuels 24, 1298-1304.

Pérez-Juan, M., Afseth, N.K., González, J., Díaz, I., Gispert, M., Furnols, M.F.i., Oliver, M.A., Realini, C.E., 2010. Prediction of fatty acid composition using a NIRS fibre optics probe at two different locations of ham subcutaneous fat. Food Research International 43, 1416-1422.

Pérez-Marín, D., Garrido-Varo, A., De Pedro, E., Guerrero-Ginel, J.E., 2007. Chemometric utilities to achieve robustness in liquid NIRS calibrations: Application to pig fat analysis. Chemometrics and Intelligent Laboratory Systems 87, 241-246.

Pinzi, S., Garcia, I.L., Lopez-Gimenez, F.J., Luque de Castro, M.D., Dorado, G., Dorado, M.P., 2009. The Ideal Vegetable Oil-based Biodiesel Composition: A Review of Social, Economical and Technical Implications. Energy and Fuels 23, 2325-2341.

Pinzi, S., Leiva, D., López-García, I., Redel-Macías, M.D., Dorado, M.P., 2014. Latest trends in feedstocks for biodiesel production. Biofuels, Bioproducts and Biorefining 8, 126-143.

Poljanšek, I., Likozar, B., 2011. Influence of Mass Transfer and Kinetics on Biodiesel Production Process. Multiphase Systems and its Applications, InTech, 433-458.

Prieto, N., Dugan, M.E.R., López-Campos, O., McAllister, T.A., Aalhus, J.L., Uttaro, B., 2012. Near infrared reflectance spectroscopy predicts the content of polyunsaturated fatty acids and biohydrogenation products in the subcutaneous fat of beef cows fed flaxseed. Meat Science 90, 43-51.

Raita, M., Kiatkittipong, W., Laosiripojana, N., Champreda, V., 2015. Kinetic study on esterification of palmitic acid catalyzed by glycine-based crosslinked protein coated microcrystalline lipase. Chemical Engineering Journal 278, 19-23

Ramadhas, A.S., Jayaraj, S., Muraleedharan, C., 2005. Biodiesel production from high FFA rubber seed oil. Fuel 84, 335-340.

Ramírez-Verduzco, L.F., Rodríguez-Rodríguez, J.E., Jaramillo-Jacob, A.d.R., 2012. Predicting cetane number, kinematic viscosity, density and higher heating value of biodiesel from its fatty acid methyl ester composition. Fuel 91, 102-111.

Rodrigues, R.C., Fernandez-Lafuente, R., 2010. Lipase from Rhizomucor miehei as a biocatalyst in fats and oils modification. Journal of Molecular Catalysis B: Enzymatic 66, 15-32.

Ross, K.A., Pyrak-Nolte, L.J., Campanella, O.H., 2006. The effect of mixing conditions on the material properties of an agar gel—microstructural and macrostructural considerations. Food Hydrocolloids 20, 79-87.

Saka, S., Isayama, Y., Ilham, Z., Jiayu, X., 2010. New process for catalyst-free biodiesel production using subcritical acetic acid and supercritical methanol. Fuel 89, 1442-1446.

Sakthivel, G., Nagarajan, G., Ilangkumaran, M., 2013. Experimental investigations of the performance, emission and combustion characteristics of a biodiesel (ethyl ester of fish oil) fuelled direct–injection diesel engine. International Journal of Vehicle Performance 1, 137-156.

Salamatinia, B., Mootabadi, H., Hashemizadeh, I., Abdullah, A.Z., 2013. Intensification of biodiesel production from vegetable oils using ultrasonic-assisted process: Optimization and kinetic. Chemical Engineering and Processing: Process Intensification 73, 135-143.

Samukawa, T., Kaieda, M., Matsumoto, T., Ban, K., Kondo, A., Shimada, Y., Noda, H., Fukuda, H., 2000. Pretreatment of immobilized Candida antarctica lipase for biodiesel fuel production from plant oil. J Biosci Bioeng 90, 180 - 183.

Samyn, P., Van Nieuwkerke, D., Schoukens, G., Vonck, L., Stanssens, D., Van den Abbeele, H., 2012. Quality and Statistical Classification of Brazilian Vegetable Oils Using Mid-Infrared and Raman Spectroscopy. Applied Spectroscopy 66, 552-565.

Sánchez, M., Marchetti, J.M., El Boulifi, N., Aracil, J., Martínez, M., 2015. Kinetics of Jojoba oil methanolysis using a waste from fish industry as catalyst. Chemical Engineering Journal 262, 640-647.

Sanli, H., Canakci, M., Alptekin, E., 2013. Predicting the higher heating values of waste frying oils as potential biodiesel feedstock. Fuel.

SAS, 2013. SAS/STAT 9.4 user's guide. SAS Institute Inc., Cary, NC, USA.

Sato, K., 2001. Crystallization behaviour of fats and lipids — a review. Chemical Engineering Science 56, 2255-2265.

Schörken, U., Kempers, P., 2009. Lipid biotechnology: Industrially relevant production processes. European Journal of Lipid Science and Technology 111, 627-645.

Schwab, A., Nielsen, H., Brooks, D., Pryde, E., 1983. Triglyceride/aqueous ethanol/1-butanol microemulsions. Journal of Dispersion Science and Technology 4, 1-17.

Schwab, A.W., Bagby, M.O., Freedman, B., 1987. Preparation and properties of diesel fuels from vegetable oils. Fuel 66, 1372-1378.

Semwal, S., Arora, A.K., Badoni, R.P., Tuli, D.K., 2011. Biodiesel production using heterogeneous catalysts. Bioresource Technology 102, 2151-2161.

Senthil Kumar, M., Kerihuel, A., Bellettre, J., Tazerout, M., 2005. Experimental investigations on the use of preheated animal fat as fuel in a compression ignition engine. Renewable Energy 30, 1443-1456.

Shah, S., Gupta, M., 2007. Lipase catalyzed preparation of biodiesel from Jatropha oil in a solvent-free system. Process Biochem 42, 409 - 414.

Shah, S., Sharma, S., Gupta, M.N., 2004. Biodiesel Preparation by Lipase-Catalyzed Transesterification of Jatropha Oil. Energy and Fuels 18, 154-159.

Sharma, A., Verma, A., Luxami, V., Melo, J.S., D'Souza, S.F., Prakash, N.T., Prakash, R., 2013. New Proton Nuclear Magnetic Resonance-Based Derivation for Quantification of Alkyl Esters Generated Using Biocatalysis. Energy and Fuels 27, 2660-2664.

Shin, H.-Y., An, S.-H., Sheikh, R., Park, Y.H., Bae, S.-Y., 2012. Transesterification of used vegetable oils with a Cs-doped heteropolyacid catalyst in supercritical methanol. Fuel 96, 572-578.

Shin, H.-Y., Lee, S.-H., Ryu, J.-H., Bae, S.-Y., 2012c. Biodiesel production from waste lard using supercritical methanol. The Journal of Supercritical Fluids 61, 134-138.

Shinde, S.D., Yadav, G.D., 2014. Microwave Irradiated Immobilized Lipase Catalyzed Synthesis of Alkyl Benzoate Esters by Transesterification: Mechanism and Kinetic Modeling. Industrial & Engineering Chemistry Research 53, 8706-8713.

Silitonga, A.S., Masjuki, H.H., Mahlia, T.M.I., Ong, H.C., Atabani, A.E., Chong, W.T., 2013. A global comparative review of biodiesel production from jatropha curcas using different homogeneous acid and alkaline catalysts: Study of physical and chemical properties. Renewable and Sustainable Energy Reviews 24, 514-533.

Singh, A.K., Fernando, S.D., Hernandez, R., 2007. Base-Catalyzed Fast Transesterification of Soybean Oil Using Ultrasonication. Energy and Fuels 21, 1161-1164.

Smith, F.E., Arsenault, E.A., 1996. Microwave-assisted sample preparation in analytical chemistry. Talanta 43, 1207-1268.

Soldi, R.A., Oliveira, A.R.S., Ramos, L.P., César-Oliveira, M.A.F., 2009. Soybean oil and beef tallow alcoholysis by acid heterogeneous catalysis. Applied Catalysis A: General 361, 42-48.

Srinivasan, S., 2009. The food v. fuel debate: A nuanced view of incentive structures. Renewable Energy 34, 950-954.

Stamenković, O.S., Lazić, M.L., Todorović, Z.B., Veljković, V.B., Skala, D.U., 2007. The effect of agitation intensity on alkali-catalyzed methanolysis of sunflower oil. Bioresource Technology 98, 2688-2699.

Stamenković, O.S., Todorović, Z.B., Lazić, M.L., Veljković, V.B., Skala, D.U., 2008. Kinetics of sunflower oil methanolysis at low temperatures. Bioresource Technology 99, 1131-1140.

Stefanov, I., Baeten, V., Abbas, O., Vlaeminck, B., De Baets, B., Fievez, V., 2013. Evaluation of FT-NIR and ATR-FTIR Spectroscopy Techniques for Determination of Minor Odd- and Branched-Chain Saturated and trans Unsaturated Milk Fatty Acids. Journal of Agricultural and Food Chemistry 61, 3403-3413.

Taher, H., Al-Zuhair, S., AlMarzouqui, A., Hashim, I., 2011. Extracted fat from lamb meat by supercritical CO2 as feedstock for biodiesel production. Biochemical Engineering Journal 55, 23-31.

Talukder, M.M.R., Wu, J.C., Van Nguyen, T.B., Fen, N.M., Melissa, Y.L.S., 2009. Novozym 435 for production of biodiesel from unrefined palm oil: Comparison of methanolysis methods. Journal of Molecular Catalysis B: Enzymatic 60, 106-112.

Tan, C., Che Man, Y., 2000. Differential scanning calorimetric analysis of edible oils: Comparison of thermal properties and chemical composition. Journal of the American Oil Chemists' Society 77, 143-155.

Tan, C., Che Man, Y., 2002. Differential scanning calorimetric analysis of palm oil, palm oil based products and coconut oil: effects of scanning rate variation. Food Chemistry 76, 89-102.

Tang, D., Marangoni, A., 2006. Microstructure and fractal analysis of fat crystal networks. Journal of the American Oil Chemists' Society 83, 377-388.

Tanwar, D., Tanwar, A., Sharma, D., Mathur, Y.P., Khatri, K.K., Soni, S.L., Gupta, R., 2013. Production and Characterization of Fish Oil Methyl Ester. IJITR 1, 209-217.

Taravus, S., Temur, H., Yartasi, A., 2009. Alkali-Catalyzed Biodiesel Production from Mixtures of Sunflower Oil and Beef Tallow. Energy and Fuels 23, 4112-4115.

Tateno, T., Sasaki, T., 2004. Process for producing fatty acid esters and fuels comprising fatty acid ester. Google Patents.

Taufiq-Yap, Y.H., Lee, H.V., Yunus, R., Juan, J.C., 2011. Transesterification of non-edible Jatropha curcas oil to biodiesel using binary Ca–Mg mixed oxide catalyst: Effect of stoichiometric composition. Chemical Engineering Journal 178, 342-347.

Teixeira, L.S.G., Assis, J.C.R., Mendonça, D.R., Santos, I.T.V., Guimarães, P.R.B., Pontes, L.A.M., Teixeira, J.S.R., 2009. Comparison between conventional and ultrasonic preparation of beef tallow biodiesel. Fuel Processing Technology 90, 1164-1166.

Tong, D., Hu, C., Jiang, K., Li, Y., 2011. Cetane number prediction of biodiesel from the composition of the fatty acid methyl esters. Journal of the American Oil Chemists' Society 88, 415-423.

Varma, R.S., 2001. Solvent-free accelerated organic syntheses using microwaves. Pure and Applied Chemistry 73, 193-198.

Veljković, V.B., Avramović, J.M., Stamenković, O.S., 2012. Biodiesel production by ultrasound-assisted transesterification: State of the art and the perspectives. Renewable and Sustainable Energy Reviews 16, 1193-1209.

Venkat Reddy, C.R., Oshel, R., Verkade, J.G., 2006. Room-Temperature Conversion of Soybean Oil and Poultry Fat to Biodiesel Catalyzed by Nanocrystalline Calcium Oxides. Energy and Fuels 20, 1310-1314.

Veny, H., Aroua, M.K., Sulaiman, N.M.N., 2014. Kinetic study of lipase catalyzed transesterification of jatropha oil in circulated batch packed bed reactor. Chemical Engineering Journal 237, 123-130.

Wang, L., He, H., Xie, Z., Yang, J., Zhu, S., 2007a. Transesterification of the crude oil of rapeseed with NaOH in supercritical and subcritical methanol. Fuel Processing Technology 88, 477-481.

Wang, L., Yang, J., 2007. Transesterification of soybean oil with nano-MgO or not in supercritical and subcritical methanol. Fuel 86, 328-333.

Wang, R., Hanna, M.A., Zhou, W.-W., Bhadury, P.S., Chen, Q., Song, B.-A., Yang, S., 2011.

Production and selected fuel properties of biodiesel from promising non-edible oils: *Euphorbia lathyris* L., *Sapium sebiferum* L. and *Jatropha curcas* L. Bioresource technology 102, 1194-1199.

Wang, T., Briggs, J.L., 2002. Rheological and thermal properties of soybean oils with modified FA compositions. Journal of the American Oil Chemists' Society 79, 831-836.

Wang, Y., Liu, P., Ou, S., Zhang, Z., 2007b. Preparation of biodiesel from waste cooking oil via two-step catalyzed process. Energy Conversion and Management 48, 184-188.

Wiggers, V., Wisniewski Jr, A., Madureira, L., Barros, A., Meier, H., 2009. Biofuels from waste fish oil pyrolysis: Continuous production in a pilot plant. Fuel 88, 2135-2141.

Williams, P.C., 2001. Implementation of near-infrared technology. Near-infrared technology in the agricultural and food industries 2, 143.

Wisniewski Jr, A., Wiggers, V.R., Simionatto, E.L., Meier, H.F., Barros, A.A.C., Madureira, L.A.S., 2010. Biofuels from waste fish oil pyrolysis: Chemical composition. Fuel 89, 563-568.

Wyatt, V.T., Hess, M.A., Dunn, R.O., Foglia, T.A., Haas, M.J., Marmer, W.N., 2005. Fuel properties and nitrogen oxide emission levels of biodiesel produced from animal fats. Journal of the American Oil Chemists' Society 82, 585-591.

Xie, W., Wang, J., 2014. Enzymatic Production of Biodiesel from Soybean Oil by Using Immobilized Lipase on Fe3O4/Poly(styrene-methacrylic acid) Magnetic Microsphere as a Biocatalyst. Energy and Fuels 28, 2624-2631.

Xu, Y., Du, W., Liu, D., Zeng, J., 2003. A novel enzymatic route for biodiesel production from renewable oils in a solvent-free medium. Biotechnology Letters 25, 1239-1241.

Yagiz, F., Kazan, D., Akin, A.N., 2007. Biodiesel production from waste oils by using lipase immobilized on hydrotalcite and zeolites. Chemical Engineering Journal 134, 262-267.

Yang, C.-R., Shapiro, B.E., Mjolsness, E.D., Hatfield, G.W., 2005. An enzyme mechanism language for the mathematical modeling of metabolic pathways. Bioinformatics 21, 774-780.

Yılmaz, M.T., Karakaya, M., Aktaş, N., 2010. Composition and thermal properties of cattle fats. European Journal of Lipid Science and Technology 112, 410-416.

Yin, J.-Z., Ma, Z., Shang, Z.-Y., Hu, D.-P., Xiu, Z.-L., 2012. Biodiesel production from soybean oil transesterification in subcritical methanol with K3PO4 as a catalyst. Fuel 93, 284-287.

Zago, E., Botton, V., Alberton, D., Córdova, J., Yamamoto, C.I., Côcco, L.C., Mitchell, D.A., Krieger, N., 2014. Synthesis of Ethylic Esters for Biodiesel Purposes Using Lipases Naturally Immobilized in a Fermented Solid Produced Using Rhizopus microsporus. Energy and Fuels 28, 5197-5203.

Zhang, X., Yan, S., Tyagi, R.D., Drogui, P., Surampalli, R.Y., 2014. Ultrasonication assisted lipid extraction from oleaginous microorganisms. Bioresource Technology 158, 253-261

Zheng, S., Kates, M., Dubé, M.A., McLean, D.D., 2006. Acid-catalyzed production of biodiesel from waste frying oil. Biomass and Bioenergy 30, 267-272.

Zou, H., Lei, M., 2012. Optimum process and kinetic study of Jatropha curcas oil pre-esterification in ultrasonical field. Journal of the Taiwan Institute of Chemical Engineers 43, 730-735.